frontiers | Research Topics

Advances in tooth development and regeneration: The importance of cytodifferentiation and mineralization processes

Edited by
Guohua Yuan, Shuo Chen, Q. Adam Ye and Huan Liu

Published in
Frontiers in Physiology

ISSN 1664-8714
ISBN 978-2-88976-646-8
DOI 10.3389/978-2-88976-646-8

About Frontiers

Frontiers is more than just an open access publisher of scholarly articles: it is a pioneering approach to the world of academia, radically improving the way scholarly research is managed. The grand vision of Frontiers is a world where all people have an equal opportunity to seek, share and generate knowledge. Frontiers provides immediate and permanent online open access to all its publications, but this alone is not enough to realize our grand goals.

Frontiers journal series

The Frontiers journal series is a multi-tier and interdisciplinary set of open-access, online journals, promising a paradigm shift from the current review, selection and dissemination processes in academic publishing. All Frontiers journals are driven by researchers for researchers; therefore, they constitute a service to the scholarly community. At the same time, the *Frontiers journal series* operates on a revolutionary invention, the tiered publishing system, initially addressing specific communities of scholars, and gradually climbing up to broader public understanding, thus serving the interests of the lay society, too.

Dedication to quality

Each Frontiers article is a landmark of the highest quality, thanks to genuinely collaborative interactions between authors and review editors, who include some of the world's best academicians. Research must be certified by peers before entering a stream of knowledge that may eventually reach the public - and shape society; therefore, Frontiers only applies the most rigorous and unbiased reviews. Frontiers revolutionizes research publishing by freely delivering the most outstanding research, evaluated with no bias from both the academic and social point of view. By applying the most advanced information technologies, Frontiers is catapulting scholarly publishing into a new generation.

What are Frontiers Research Topics?

Frontiers Research Topics are very popular trademarks of the *Frontiers journals series*: they are collections of at least ten articles, all centered on a particular subject. With their unique mix of varied contributions from Original Research to Review Articles, Frontiers Research Topics unify the most influential researchers, the latest key findings and historical advances in a hot research area.

Find out more on how to host your own Frontiers Research Topic or contribute to one as an author by contacting the Frontiers editorial office: frontiersin.org/about/contact

Advances in tooth development and regeneration: The importance of cytodifferentiation and mineralization processes

Topic editors

Guohua Yuan — Wuhan University, China

Shuo Chen — The University of Texas Health Science Center at San Antonio, United States

Q. Adam Ye — Massachusetts General Hospital, Harvard Medical School, United States

Huan Liu — Wuhan University, China

Citation

Yuan, G., Chen, S., Ye, Q. A., Liu, H., eds. (2023). *Advances in tooth development and regeneration: The importance of cytodifferentiation and mineralization processes*. Lausanne: Frontiers Media SA. doi: 10.3389/978-2-88976-646-8

Table of contents

05 Microenvironment Influences Odontogenic Mesenchymal Stem Cells Mediated Dental Pulp Regeneration
Xiaoyao Huang, Zihan Li, Anqi Liu, Xuemei Liu, Hao Guo, Meiling Wu, Xiaoxue Yang, Bing Han and Kun Xuan

16 Epithelial Bone Morphogenic Protein 2 and 4 Are Indispensable for Tooth Development
Haibin Mu, Xin Liu, Shuoshuo Geng, Dian Su, Heran Chang, Lili Li, Han Jin, Xiumei Wang, Ying Li, Bin Zhang and Xiaohua Xie

25 Novel Molecule Nell-1 Promotes the Angiogenic Differentiation of Dental Pulp Stem Cells
Mengyue Li, Qiang Wang, Qi Han, Jiameng Wu, Hongfan Zhu, Yixuan Fang, Xiuting Bi, Yue Chen, Chao Yao and Xiaoying Wang

34 Enamel Defects Associated With Dentin Sialophosphoprotein Mutation in Mice
Tian Liang, Qian Xu, Hua Zhang, Suzhen Wang, Thomas G. H. Diekwisch, Chunlin Qin and Yongbo Lu

46 Connexin 43-Mediated Gap Junction Communication Regulates Ameloblast Differentiation *via* ERK1/2 Phosphorylation
Aya Yamada, Keigo Yoshizaki, Masaki Ishikawa, Kan Saito, Yuta Chiba, Emiko Fukumoto, Ryoko Hino, Seira Hoshikawa, Mitsuki Chiba, Takashi Nakamura, Tsutomu Iwamoto and Satoshi Fukumoto

60 Cells at the Edge: The Dentin–Bone Interface in Zebrafish Teeth
Joana T. Rosa, Paul Eckhard Witten and Ann Huysseune

73 Mechanosensitive Piezo1 in Periodontal Ligament Cells Promotes Alveolar Bone Remodeling During Orthodontic Tooth Movement
Yukun Jiang, Yuzhe Guan, Yuanchen Lan, Shuo Chen, Tiancheng Li, Shujuan Zou, Zhiai Hu and Qingsong Ye

83 Facilitating Reparative Dentin Formation Using Apigenin Local Delivery in the Exposed Pulp Cavity
Yam Prasad Aryal, Chang-Yeol Yeon, Tae-Young Kim, Eui-Seon Lee, Shijin Sung, Elina Pokharel, Ji-Youn Kim, So-Young Choi, Hitoshi Yamamoto, Wern-Joo Sohn, Youngkyun Lee, Seo-Young An, Chang-Hyeon An, Jae-Kwang Jung, Jung-Hong Ha and Jae-Young Kim

93 Operation of the Atypical Canonical Bone Morphogenetic Protein Signaling Pathway During Early Human Odontogenesis
Xiaoxiao Hu, Chensheng Lin, Ningsheng Ruan, Zhen Huang, Yanding Zhang and Xuefeng Hu

103 circKLF4 Upregulates *Klf4* and *Endoglin* to Promote Odontoblastic Differentiation of Mouse Dental Papilla Cells *via* Sponging miRNA-1895 and miRNA-5046
Yue Zhang, Hao Zhang, Guohua Yuan and Guobin Yang

111 Odontogenic MSC Heterogeneity: Challenges and Opportunities for Regenerative Medicine
Yuan Chen, Zhaoyichun Zhang, Xiaoxue Yang, Anqi Liu, Shiyu Liu, Jianying Feng and Kun Xuan

frontiers in Physiology

REVIEW
published: 22 April 2021
doi: 10.3389/fphys.2021.656588

Microenvironment Influences Odontogenic Mesenchymal Stem Cells Mediated Dental Pulp Regeneration

Xiaoyao Huang[1,2,3†], Zihan Li[1,2,3†], Anqi Liu[1,2,3], Xuemei Liu[1,2,3], Hao Guo[1,2,3], Meiling Wu[1,2,3], Xiaoxue Yang[1,2,3], Bing Han[1,2,3] and Kun Xuan[1,2,3]*

[1] State Key Laboratory of Military Stomatology, Fourth Military Medical University, Xi'an, China, [2] National Clinical Research Center for Oral Diseases, Fourth Military Medical University, Xi'an, China, [3] Shaanxi Clinical Research Center for Oral Diseases, Department of Preventive Dentistry, School of Stomatology, Fourth Military Medical University, Xi'an, China

Dental pulp as a source of nutrition for the whole tooth is vulnerable to trauma and bacterial invasion, which causes irreversible pulpitis and pulp necrosis. Dental pulp regeneration is a valuable method of restoring the viability of the dental pulp and even the whole tooth. Odontogenic mesenchymal stem cells (MSCs) residing in the dental pulp environment have been widely used in dental pulp regeneration because of their immense potential to regenerate pulp-like tissue. Furthermore, the regenerative abilities of odontogenic MSCs are easily affected by the microenvironment in which they reside. The natural environment of the dental pulp has been proven to be capable of regulating odontogenic MSC homeostasis, proliferation, and differentiation. Therefore, various approaches have been applied to mimic the natural dental pulp environment to optimize the efficacy of pulp regeneration. In addition, odontogenic MSC aggregates/spheroids similar to the natural dental pulp environment have been shown to regenerate well-organized dental pulp both in preclinical and clinical trials. In this review, we summarize recent progress in odontogenic MSC-mediated pulp regeneration and focus on the effect of the microenvironment surrounding odontogenic MSCs in the achievement of dental pulp regeneration.

Keywords: odontogenic MSCs, cell aggregate/spheroids, dental pulp regeneration, microenvironment, pulp regeneration approaches

OPEN ACCESS

Edited by:
Guohua Yuan,
Wuhan University, China

Reviewed by:
Alastair James Sloan,
University of Melbourne, Australia
Anne Poliard,
Université Paris Descartes, France

***Correspondence:**
Kun Xuan
xuankun@fmmu.edu.cn

† These authors have contributed equally to this work

Specialty section:
This article was submitted to Craniofacial Biology and Dental Research, a section of the journal Frontiers in Physiology

Received: *21 January 2021*
Accepted: *23 March 2021*
Published: *22 April 2021*

Citation:
Huang X, Li Z, Liu A, Liu X, Guo H, Wu M, Yang X, Han B and Xuan K (2021) Microenvironment Influences Odontogenic Mesenchymal Stem Cells Mediated Dental Pulp Regeneration. Front. Physiol. 12:656588. doi: 10.3389/fphys.2021.656588

INTRODUCTION

Being the source of nutrition for the whole tooth, the dental pulp is the residence of a large number of odontogenic mesenchymal stem cells (MSCs), which play an important role in the process of tooth development and injury repair (Lambrichts et al., 2017). However, the dental pulp is prone to traumas and infections, which ultimately lead to the development of irreversible pulpitis or necrosis, because its nutrition is supplied by a tiny apical foramen. The traditional treatment for pulpitis is root canal therapy, which requires removing all the pulp and filling the canals with bioinert synthetic materials. However, it permanently deprives nutrition from teeth, which may increase the friability of the residual tissue of the tooth and arrest the root development of immature permanent teeth (Lu et al., 2019). Therefore, maintaining pulp vitality is necessary to save the whole tooth. Subsequently, approaches to restore the pulp viability of immature permanent

teeth have been established, such as partial pulpotomy and apexification, which make use of pulp cells in the residual dental pulp tissue to repair injured pulp, and made great progress in promoting the root development of immature permanent teeth (Garcia-Godoy and Murray, 2012). Meanwhile, odontogenic MSCs were separated from postnatal dental pulp tissue and developing tooth tissues successively and showed the immense potential to regenerate pulp-like tissues (Gronthos et al., 2000; Miura et al., 2003). Consequently, odontogenic MSCs based dental pulp regeneration has been proposed to maintain teeth vitality. It has made great progress in regenerating a complete dental pulp containing blood vessels, nerves, and newly formed dentin both in ectopic and *in situ* regeneration (Itoh et al., 2018; Xuan et al., 2018; Meng et al., 2020). Most importantly, it has been demonstrated that exogenous odontogenic MSC transplantation regenerated functional dental pulp, which showed a response to clinical tests similar to those of normal dental pulp (Nakashima and Iohara, 2017; Nakashima et al., 2017; Xuan et al., 2018). The regenerated pulp tissue contained normal structures such as an odontoblast layer, connective tissue, blood vessels, and nervous tissue in histologic examination (Xuan et al., 2018). Therefore, odontogenic MSC based dental pulp regeneration could potentially become a valuable method to restore vital teeth in clinical practice.

The environment of the dental pulp is essential for the regulation of odontogenic MSC homeostasis, proliferation, and differentiation (Smith et al., 2015). When the dental pulp environment is invaded by trauma or bacteria, the MSCs residing in the dental pulp are prone to odontogenic differentiation to repair the dental pulp, but this results in local or total calcification of the pulp tissue rather than the original well-organized connective tissue (Zhang et al., 2017c). Therefore, rebuilding an environment similar to that of the natural dental pulp is inevitable to induce odontogenic MSCs to regenerate pulp tissue containing normal structures. Various approaches have been applied to mimic the natural dental pulp environment, including its complex mechanical, chemical, and biological properties. The use of cytokines, scaffold materials, and cell aggregates/spheroids is mainstream in current studies and has made great progress both in preclinical studies and clinical trials (Nakashima and Iohara, 2017; Nakashima et al., 2017; Itoh et al., 2018; Xuan et al., 2018; He et al., 2019; Meng et al., 2020). In this review, we summarize recent progress in odontogenic MSC-mediated pulp regeneration, concentrating on the effect of the microenvironment surrounding odontogenic MSCs in the achievement of well-organized functional dental pulp regeneration.

ODONTOGENIC MSCs AND DENTAL PULP REGENERATION

The dental pulp is a well-organized soft connective tissue in the root canal, with bundles of blood vessels and nerves and a layer of odontoblasts lining along the chamber that can generate the mineralized dentin (Linde, 1985). Regenerating dental pulp containing these well-organized structures is crucial to maintain the function of the dental pulp and to restore the vitality of the whole tooth. Odontogenic MSCs separated from dental pulp and dental apical papilla with immense potential to form pulp-like tissues with blood vessels, nerves, and mineralized dentin was applied for functional dental pulp regeneration. In addition, their ability to regenerate the original well-organized dental pulp is easily affected by the microenvironment in which they are located, and a dental pulp microenvironment that has been changed by infection invasion and root canal preparation is unsuitable for odontogenic MSC-mediated dental pulp regeneration.

MSCs From Dental Pulp Applied in Dental Pulp Regeneration

The odontogenic MSCs from dental pulp show typical MSC features, including colony formation, expression of specific surface markers, and multi-directional differentiation (Morsczeck and Reichert, 2018). Under physiological conditions, these MSCs reside in the surrounding neurovascular bundle in the dental pulp and act as a reservoir for stem cells capable of differentiating into the various types of cells required for dental pulp maintenance and repair (Zhao et al., 2014). The odontogenic MSCs separated from dental pulp were demonstrated to form blood vessels, nerves, and mineralized dentin, which are regarded as indispensable for functional dental pulp regeneration (Hilkens et al., 2017; Yang et al., 2019) (**Figure 1**). Hence, the odontogenic MSCs residing in the dental pulp were applied in dental pulp regeneration.

Dental pulp stem cells (DPSCs), the first odontogenic MSCs isolated from dental pulp, have been shown to have the capacity to form mineralized tissue, blood vessels, and nerve tissues. It has been shown that DPSCs can form dentin/pulp-like structures in ectopic transplantation with hydroxyapatite/tricalcium phosphate (Gronthos et al., 2000). In addition, DPSCs have also been shown to be effective in regenerating functional dental pulp with nerves, vasculature, and newly formed dentin in *in situ* pulp regeneration (Iohara et al., 2014; Nakashima et al., 2017). Stem cells from human exfoliated teeth (SHED), another type of stem cell from dental pulp, were isolated and showed a higher proliferation rate and a higher number of population doublings than DPSCs (Miura et al., 2003). SHED also showed the capacity to differentiate into odontoblasts, generate dentin, and form blood vessels and nerve tissues (Miura et al., 2003; Xuan et al., 2018), and were able to regenerate pulp-like tissues with odontoblasts capable of generating new tubular dentin after being injected into the roots of human premolars with scaffolds (Puramatrix^{TM} or rhCollagen) in ectopic transplantation experiments (Rosa et al., 2013). Furthermore, SHED has been reported to regenerate functional dental pulp with blood vessels, sensory nerves, and the odontoblast layer in injured immature permanent teeth (Xuan et al., 2018).

Other Odontogenic MSCs in Dental Pulp Regeneration

In addition to odontogenic MSCs from dental pulp, odontogenic MSCs also include MSCs separated from periodontal tissue

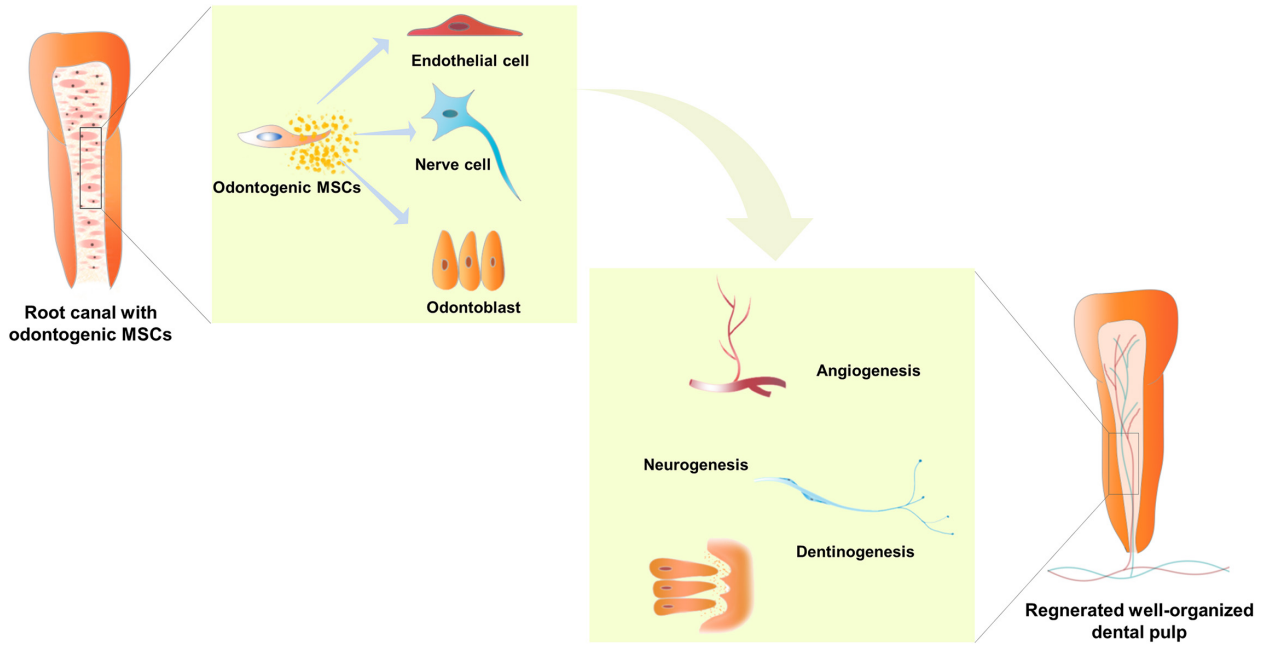

FIGURE 1 | Odontogenic mesenchymal stem cells (MSCs) located in a suitable root canal environment were able to differentiate into endothelial cells, nerve cells, and odontoblasts, and secrete a group of cytokines to mediate angiogenesis, neurogenesis, and dentinogenesis. Hence, well-organized dental pulp with bundles of blood vessels and nerves and a layer of odontoblasts lining along the chamber, which can generate mineralized dentin, is regenerated in injured teeth. In addition, the flared root canal of the injured immature permanent tooth shows lengthened root, thickened root canal wall, and narrowed apical foramen.

and developing tooth tissues such as the apical papilla and dental follicle. According to research, the odontogenic MSCs from periodontal tissue and dental follicle mainly repair and regenerate periodontal tissue because of the capacity to generate a cementum/periodontal ligament-like structure (Seo et al., 2004). However, stem cells from the apical papilla (SCAPs) isolated from the apical papilla, which was confirmed to develop dental pulp tissue in the early stage of tooth development, were also applied in dental pulp regeneration, and they showed high proliferative potential and were more likely to differentiate into odontoblasts than DPSCs (Sonoyama et al., 2008). It has been demonstrated that SCAPs have a dramatic ability to form dentin, blood vessels, and nerve tissue (Sonoyama et al., 2008; Hilkens et al., 2017), and can regenerate dental pulp with well-established vascularity and a layer of odontoblast-like cells that are able to form dentin-like tissue in ectopic transplantation experiments (Na et al., 2016). However, SCAPs are hardly widely used because they are derived from developing teeth that are scarcely discarded in clinical practice. In general, DPSCs and SHED separated from dental pulp are common odontogenic MSCs for dental pulp regeneration because of their biological properties and extensive sources.

Pulp Regeneration Ability of Odontogenic MSCs Impaired by the Damaged Pulp Microenvironment

The natural dental pulp tissue is vulnerable to bacteria and traumas, which cause cell death among odontoblasts and other cells in the dental pulp and distort the collagen arrangement in the pulp matrix. Then, the odontogenic MSCs residing in the dental pulp will be subsequently recruited to the injured site by a cascade of signal molecules to differentiate into odontoblasts and form reparative dentin, which is a type of calcified tissue diffused in the root canal rather than the original soft connective tissue (Colombo et al., 2014; Zhang et al., 2017c). If the infection persists, the dental pulp is prone to develop irreversible pulpitis or necrosis, that is, the natural dental pulp microenvironment is damaged, and bacteria, necrotic tissue, toxins, and dead cells, etc. will remain in the root canal, which are unfavorable for maintaining the biological properties of odontogenic MSCs to regenerate dental pulp. Even when the root canal was cleaned before pulp regeneration, the bacteria and inflammation cannot be cleaned due to the complexity of the root canal system.

Research on dental pulp regeneration in animal models has shown that residual bacteria remain in the root canal after traditional root canal preparation and disinfection, and empty space or necrotic tissue was found between residual bacteria and revitalized tissue (Verma et al., 2017). Meanwhile, lipopolysaccharide (LPS), a glycolipid in the outer membrane of gram-negative bacteria, was reported to increase the levels of inflammatory mediators, such as IL-1β and TNF-α (Yuan et al., 2018), and interfere with dentinogenesis of DPSCs (Hozhabri et al., 2015). In addition, DPSCs with repeated LPS stimulation induced DNA double-strand breaks and DNA damage responses, which had a significant influence on cell proliferation and apoptosis (Feng et al., 2014; Huang et al., 2018). Moreover, the root canal is under an ischemic condition when dental pulp is

removed, which means there is no oxygen or nutrients in the root canal. Agata et al. (2008) have shown that ischemia has a significantly negative influence on dental pulp cell survival and differentiation. Similarly, it has been reported that hypoxia decreases cell viability and increases cleaved caspase-3 and poly ADP-ribose polymerase in human dental pulp cells, indicating that it induces apoptotic cell death in these cells (Park et al., 2018). It has also been shown that cells die in the center of large-sized DPSCs spheroids due to the ischemic environment in the center (Xiao et al., 2014), which is similar to the condition that MSCs confront in the root canal.

Overall, the potential of odontogenic MSCs to regenerate well-organized dental pulp tissue is mediated by the microenvironment in which they reside, and the dental pulp microenvironment damaged by infection, and the prepared root canals with inflammatory and ischemic conditions are unfavorable for odontogenic MSCs to regenerate original well-organized connective pulp tissue. Optimizing the external environment of odontogenic MSCs is crucial for promoting the effect of pulp regeneration.

MIMIC THE NATURAL PULP MICROENVIRONMENT TO IMPROVE THE PULP REGENERATION EFFICACY

The natural dental pulp microenvironment is crucial for the maintenance of a stem cell phenotype that is suitable for downstream pulp regeneration applications (Smith et al., 2015). Therefore, it is feasible to mimic the physiological natural pulp microenvironment to maintain the regeneration ability of odontogenic MSCs when the environment is changed due to bacterial invasion and root canal preparation. Based on this, researchers have found some methods to improve the efficacy of dental pulp regeneration by maintaining the regeneration ability of odontogenic MSCs that reside in the inflammatory and ischemic microenvironment.

Cytokine Application

Cooper et al. (2014) have reviewed that the body can produce various types of cytokines that can promote the migration, proliferation, and differentiation of MSCs to maintain dental pulp homeostasis under physiological conditions. It is widely believed that cytokines have the potential to recruit endogenous MSCs to repair damaged tissue, which is defined as cell homing and applied in dental pulp regeneration (Kim et al., 2010).

Stromal cell-derived factor 1 (SDF-1), a member of the CXC chemokine subfamily, was reported to regenerate pulp-like tissue in pulpectomy mature teeth of dogs (Iohara et al., 2011). And researchers have found that SDF-1 can recruit odontogenic MSCs via SDF-1/C-X-C chemokine receptor type 4 (CXCR4) pathway (Yang et al., 2016; Xiao et al., 2019); mediate mineralization tissue formation by activation of Smads and Erk (Liu et al., 2015; Xiao et al., 2019) and promote vascularization through autophagy (Yang et al., 2015). In addition, granulocyte-colony stimulating factor (G-CSF) which was allowed for clinical application was also reported to have migratory efficacy on pulp stem cells (Iohara et al., 2008) and was shown to regenerate total pulp with pulp stem cells in the pulpectomized teeth of dogs (Iohara et al., 2013). Murakami et al. (2013) found that DPSCs with migratory response to G-CSF (MDPSCs) showed enhanced migration and immunomodulatory abilities and expressed higher stem cell markers Oct3/4, Nanog, Rex1, GDF3 compared to DPSCs, which means a better regeneration ability. A pilot clinical study demonstrated that MDPSCs transplantation showed excellent clinical efficacy in patients with Pulpitis. In addition, multiple growth factors were applied to recruit odontogenic MSCs and promote nerve, blood vessels, and mineralized tissue formation. Nerve growth factor (NGF) plays a role in attracting nerve fiber growth into the root canal and has been reported to mediate the proliferative differentiation and survival of odontogenic MSCs (Mitsiadis et al., 2017) and promote mineralized tissue formation (Xiao et al., 2018).

Fibroblast growth factor (FGF) expressed in enamel knots during primary dentinogenesis has been reported to induce dentin regeneration on amputated pulp (Ishimatsu et al., 2009). Platelet-derived growth factor (PDGF) and vascular endothelial growth factor (VEGF) play a major role in angiogenesis and were shown to generate highly vascularized dental pulp-like connective tissue (Kim et al., 2010; Zhang et al., 2017a). Furthermore, stem cell factor (Pan et al., 2013), tumor necrosis factor-a (TNF-α) (Shi et al., 2017), interferon-γ (IFN-γ) (He et al., 2017b), and BMP (Kim et al., 2010) have also been reported to promote dental pulp regeneration by increasing odontogenic MSCs migration and differentiation. To achieve satisfactory regeneration efficacy, these cytokines are usually applied in combination with other cytokines, scaffolds, and MSCs. It has been reported that combinations of SDF-1, bFGF, and BMP7 in collagen scaffolds were efficient in regenerating pulp-like tissues in endodontically treated human root canals subcutaneously implanted in rats (Suzuki et al., 2011).

Scaffold Material Application

It has been proven that signals from extracellular matrix (ECM) microenvironments significantly affect stem cell migration, proliferation, and differentiation (Cosgrove et al., 2016). Scaffold materials act as odontogenic MSC ECM in the regeneration of dental pulp, and changes in their mechanical properties, composition, and structure will affect the biological properties of MSCs (Shafiq et al., 2015; Rahman et al., 2018; Huang et al., 2019). As recently reviewed by Moussa and Aparicio (2019), the scaffold materials applied for dental pulp regeneration mainly include: (1) naturally derived polymeric scaffolds like collagen, fibrin, decellularized dental pulp tissue (Alqahtani et al., 2018; Bakhtiar et al., 2020), and treated dentin matrix (TDM) (Yang et al., 2012; Meng et al., 2020); (2) synthetically engineered polymeric scaffolds such as polylactic acid, polyglycolic acid, and ceramic scaffolds; and (3) composite scaffolds that balance the advantages and disadvantages of individual material, improving the overall material performance (Moussa and Aparicio, 2019).

These scaffold materials rebuild a suitable environment for odontogenic MSCs to regenerate dental pulp tissue by changing mechanical properties, composition, and structure and combining them with cytokines and other scaffold materials.

In order to prevent the growth of residual endodontic bacteria, chitosan was applied as a scaffold material (Ducret et al., 2019). In addition, the nanofibrous engineered matrix with fibrous topography similar to dental pulp matrix was proved to induce odontoblastic differentiation of DPSCs through Wnt/β-catenin signaling (Rahman et al., 2018). Remarkably, naturally derived materials showed a better capability of maintaining dental pulp stem cell viability and forming pulp-like tissue compared with all synthetic materials. Decellularized dental pulp tissue containing collagen type I, dentin matrix protein 1, dentin sialoprotein, Von Willebrand factor, TGF-β, VEGF, and bFGF was showed an increased induction of DPSCs proliferation, migration, and multidirectional differentiation (Alqahtani et al., 2018; Li et al., 2020). And more convincing, the decellularized tooth buds seeded with stem cells were able to regenerate well-developed teeth after implanted into the jawbone of mini-pigs (Zhang et al., 2017b). Furthermore, TDM comprised of hydroxyapatite and ECM was reported to be the reservoir of bioactive protein necessary for dentinogenesis (Li et al., 2011). Thus, researchers found that TMD can release dentinogenic factors and growth factors to improve the attachment, growth, and viability of odontogenic MSCs and induce DPSCs to form dentin pulp-like tissue (Meng et al., 2020). This proves that similar scaffold materials mimic the natural pulp environment and that the more similar they are, the better the dental pulp regeneration.

Extracellular Vesicles Application

Extracellular vesicles (EVs) are particles secreted from cells and composed of a lipid bilayer carrying bioactive molecules like mRNA, micoRNA, and cytokines, etc. (Zhang et al., 2020a). The biological function of EVs is dominated by the contents of EVs and varied according to the tissue they are derived from. Thus, EVs generated from the dental pulp cells residing in the relatively closed root canal were demonstrated to have advantageous proangiogenic, antiapoptotic, anti-inflammatory, and immunomodulatory abilities when applied in tissue regeneration (Jarmalavičiūtė et al., 2015; Pivoraitė et al., 2015; Xian et al., 2018; Hu et al., 2019).

Recently, odontogenic MSCs derived EVs have drawn attention in the field of dental pulp regeneration. Huang et al. (2016) demonstrated that DPSC derived EVs mediated the odontogenic differentiation of DPSCs through the P38 MAPK pathway and regenerated pulp-like tissue when composited with collagen membrane in a tooth root slice model. Besides, Zhang et al. (2020a) proved that EVs from DPSCs can promote angiogenesis and induce collagen deposition along neovasculature in an injectable hydrogel *in vitro*, which indicates the initiation of pulp-like tissue formation (Zhang et al., 2020a). More importantly, Zhang et al. (2020b) presented that EVs generated by Hertwig's epithelial root sheath cells which exist in the developing period of teeth can trigger lineage-specific differentiation of dental papilla cells and regenerate dentin-pulp like tissue which is composed of dentin-like hard tissue and soft tissue containing blood vessels and neurons (Zhang et al., 2020b). In general, EVs derived from dental pulp cells can provide proper microenvironments that mimic the process of angiogenesis, dentin formation, and epithelia-mesenchyme interactions in tooth development, which means that EVs from dental pulp are a favorable choice for dental pulp regeneration.

Since the contents of EVs are abundant and varied according to the environment, further research should be carried out to optimize the contents of EVs, making them more suitable for dental pulp regeneration. In addition, suitable scaffold materials must be picked out to maintain the biologic function of EVs and facilitate them applied into root canals, and *in situ* dental pulp regeneration experiments and clinical research are required to verify the efficacy and safety of EVs in dental pulp regeneration.

Cell Aggregates/Spheroids Application

Cell aggregates and spheroids have been demonstrated to consist of high-density stem cells with a self-produced, tissue-specific ECM, multiple cytokines, and large amounts of extracellular vesicles (Tsai et al., 2015; Sjöqvist et al., 2019; Sui et al., 2019b). Besides, cell aggregates/spheroids were reported to show enhanced abilities anti-inflammatory and anti-ischemic abilities compared to regular cultured cells (Tsai et al., 2015; Sukho et al., 2018; Cheng et al., 2020), which means cell aggregates/spheroids are suitable for the inflammatory and ischemic environment of the root canal.

Cell aggregates/spheroids have been proven to promote the anti-inflammatory phenotype differentiation of macrophages and express more anti-inflammatory signaling molecules including CXCR4, prostaglandin E2 (PGE-2), and interleukin 6 (IL-6) when compared to regular cultured cells, which means cells in cell aggregates/spheroids have better cell migration and anti-inflammatory abilities (Tsai et al., 2015; Sukho et al., 2018). Other studies have shown that the center of cell aggregates/spheroids is in an ischemic and hypoxia condition, thus cell aggregates/spheroids contain more trophic factors and pro-angiogenic factors (like VEGF, FGF-F, and HGF) and have great pro-angiogenesis capabilities (Bhang et al., 2011; Zhang et al., 2012; Cheng et al., 2020). Based on this, cell aggregates/spheroids have been proven to be the reservoir of the cytokines that are essential for odontogenic MSCs to migrate, proliferate, differentiate and regenerate dental pulp. Furthermore, compared to regular cultured cells, cell aggregates express more ECM protein like COLI, integrinβ1, and fibronectin which are crucial for cell signaling transmission and biological property maintenance (Yang et al., 2012; Yavropoulou and Yovos, 2016). Studies have shown that DPSC aggregate-derived ECM (DPM) preserved the important fibrous portions of dental pulp tissue-derived ECM and showed a similar 3D structure of dental pulp, and the DPM provides a microenvironment to balance the replication and mineralization of the behaviors of DPSCs in a way similar to a natural dental pulp microenvironment (Zhang et al., 2017c). The comparison of gene expression among SCAP cell aggregates, SCAPs, and apical papilla tissues, which generate pulp and dentin during tooth development, showed that SCAP cell aggregates can recover some gene expression in the apical papilla niche compared to SCAPs (Diao et al., 2017).

Therefore, odontogenic MSC aggregates/spheroids are considered fantastic martial to realize dental pulp regeneration. It has been shown that after implant a human tooth root canal which was filled with DPSC spheroids into immunodeficient mice

subcutaneously, pulp-like tissues with blood vessel ingrowths were observed in the human root canal (Itoh et al., 2018). Similarly, implanted SCAP aggregates into immunodeficient mice with human treated dentin matrix fragments, the root space was found to be filled completely with dental pulp-like tissue with well-organized vascularity and a continuous layer of newly formed dentin-like tissue along the existing dentin (Na et al., 2016). Furthermore, our clinical trial found that the implantation of SHED aggregates induces the regeneration of functional pulp tissue with blood vessels and sensory nerves in immature permanent teeth with pulp necrosis after dental trauma (Xuan et al., 2018).

PROGRESS OF DENTAL PULP REGENERATION

Dental pulp regeneration methods, including pulp revascularization, cytokine combined with scaffold transplantation, and exogenous odontogenic MSC transplantation were put into practice *in situ* dental pulp regeneration in animals or patients, based on approaches put forward to optimize the surrounding microenvironment of odontogenic MSCs involved in the pulp regeneration process. The first two methods are claimed to recruit endogenous MSCs by cytokines and without the application of exogenous odontogenic MSCs, while the latter method applies exogenous odontogenic MSCs alone or with cytokines and scaffold materials and has demonstrated dramatic efficacy of functional dental pulp regeneration both in preclinical animal studies and clinical trials (**Figure 2**).

Pulp Revascularization

Pulp revascularization has been practiced clinically in the past decade (Wigler et al., 2013; Gaviño Orduña et al., 2020). In this method, an optimized microenvironment was built in the disinfected root canal system with endodontic instrument-induced blood clots (Yang et al., 2016). It is believed that oxygen, nutrients, and endogenous cytokines, and MSCs are brought into the root canal by blood clots (He et al., 2017a), and there is no need for exogenous cytokines or stem cells.

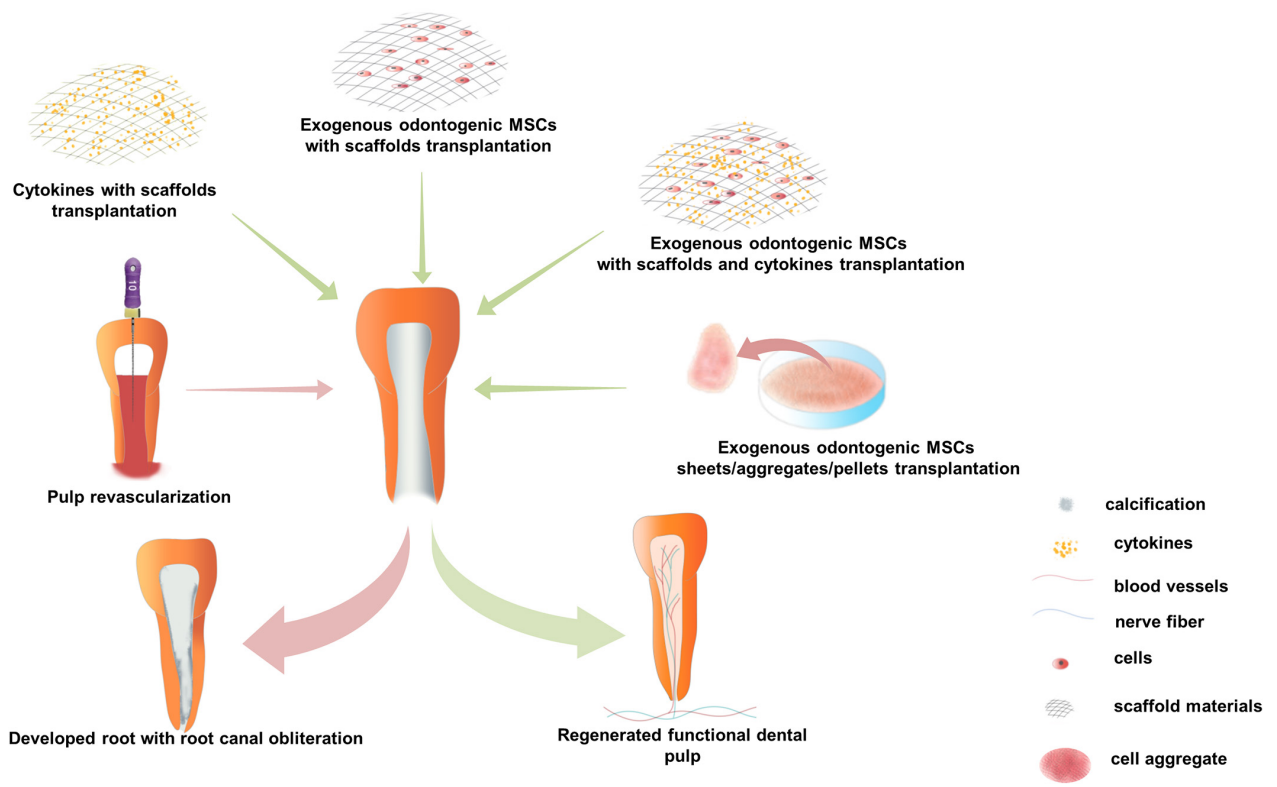

FIGURE 2 | Current strategies for *in situ* dental pulp regeneration practiced in preclinical and clinical settings. There are three major operation strategies: (1) Pulp revascularization, nutrition, oxygen, endogenous cytokines, and mesenchymal stem cells (MSCs) were brought into the root canal by instrument-induced blood. During the follow-up process, it usually shows lengthened root, thickened root canal wall, and narrowed apical foramen in immature permanent teeth with calcification in the root canal but not in the dental pulp. (2) Cytokines composite with scaffold materials transplantation, various kinds of cytokines, and scaffold materials are transplanted into treated root canal in a combination; functional pulp tissue is regenerated in preclinical animal models, but there is no evidence to prove functional pulp tissue regeneration in clinical trials. (3) Exogenous odontogenic MSCs transplantation, mainly include three application methods: (1) co-transplantation with scaffold materials and cytokines, (2) co-transplantation with scaffold materials, and (3) scaffold-free odontogenic MSC sheets/aggregates/pellets transplantation. Functional dental pulp equipped with blood vessels and sensory nerves is regenerated by exogenous odontogenic MSCs transplantation, both in clinical and preclinical experiments.

Some cases of pulp revascularization have shown sensitivity to cold or electric stimuli in the clinical examination of pulp vitality (He et al., 2017a), while some cases showed no response to thermal or electric stimuli during long-term follow-up. Radiographic examination revealed that the root was lengthened, the wall of the root canal was thickened, and the apical foramen was narrowed in some cases of immature permanent teeth (Nagata et al., 2015; Peng et al., 2017). However, histological studies have shown that most of the tissues generated in pulp revascularization cases were finally turned into non-pulp-like tissues including cementum, periodontal, and bone-like tissues because endogenous MSCs and cytokines brought in by blood clots are uncontrollable and MSCs from the periodontal ligament and bone marrow might be brought into root canals (Peng et al., 2017) (**Figure 2**). Therefore, the formation of pulp-like tissues requires further studies, and multiple exogenous cytokines and odontogenic MSCs should be applied in dental pulp regeneration.

Cytokines Combined With Scaffold Transplantation

Cytokines can induce odontogenic MSCs to migrate, proliferate, and differentiate, while scaffold materials can not only influence the biological properties of odontogenic MSCs but also provide attachment for cells (Kim et al., 2010; Moussa and Aparicio, 2019). Therefore, exogenous cytokines are usually transplanted with scaffold materials, creating an environment to induce endogenous stem cells to regenerate dental pulp tissue (**Figure 2**). It has been proven that the delivery of bFGF, VEGF, or PDGF with a basal set of NGF and BMP7 in collagen scaffolds regenerated dental-pulp-like tissue in the entire root canal in an ectopic transplantation animal model (Kim et al., 2010). Similar studies have shown that a combination of Wnt3a, BMP7, and collagen gel delivered into the root canal of mini-pigs yielded pulp-dentin-like structures with obvious dentinal tubules (He et al., 2019). Furthermore, many blood-derived scaffold materials containing rich growth factors are used in clinical pulp therapy, such as platelet-rich plasma (PRP), concentrated growth factors, and platelet-rich fibrin, and showed a much better influence on cell proliferation, viability, apoptosis, and mineralization of human dental pulp cells than traditional materials such as $Ca(OH)_2$, mineral trioxide aggregate, and iRoot BP (Dou et al., 2020). Moreover, Jadhav et al. (2012) proved that PRP showed a better treatment effect in periapical healing, apical closure, and dentinal wall thickening compared to blood clots in regenerative endodontic tissue. However, histological evidence showed that there was no difference in the average percentage of apical closure, new tissue formation, and pulp-like tissue formation between PRP and blood clots in regenerative endodontic treatment of animal models (Zhang et al., 2014).

It is claimed that the regenerated pulp-like tissue in the root canal and the better treatment effect of blood-derived scaffold materials were due to the endogenous stem cells recruited by exogenous cytokines (Kim et al., 2010; Suzuki et al., 2011; Zhujiang and Kim, 2016). However, there is no direct evidence to prove that the pulp-like tissue was regenerated by recruited endogenous MSCs, and no clinical trials or research to confirm the functional *in situ* pulp regeneration with exogenous cell-free approaches (Sui et al., 2019a), while clinical trials have achieved functional dental pulp regeneration in injured immature permanent teeth and permanent teeth with pulpitis by exogenous odontogenic MSC transplantation (Nakashima and Iohara, 2017; Nakashima et al., 2017; Xuan et al., 2018). In summary, exogenous stem cell implantation can be considered a promising approach for dental pulp regeneration.

Exogenous Odontogenic MSCs Transplantation

The application of exogenous odontogenic MSCs in *in situ* pulp regeneration has been practiced in preclinical animal models and clinical patients. Since the external microenvironment is crucial for the maintenance of the biological properties of odontogenic MSCs (Smith et al., 2015) to promote their capacity to regenerate dental pulp tissue, various methods have been applied to maintain the external microenvironment of transplanted odontogenic MSCs, such as scaffolds and cytokines, and applied in the form of cell aggregates/spheroids.

Exogenous odontogenic MSCs transplanted with scaffold materials and cytokines were proven feasible both in preclinical and clinical trials. Studies on animals have shown that side populations of DPSCs transplanted with cytokines (G-CSF and SDF-1) into the treated root canal of dogs regenerated pulp *in situ*, including nerves and vasculature, and new dentin deposition along the dentinal wall (Iohara et al., 2011, 2014) (**Figure 2**). Furthermore, clinical trials have also proved that autologous DPSC subsets transplanted with G-CSF and atelocollagen into pulpectomized teeth regenerated pulp tissue, which showed a robust positive response to the electric pulp test (EPT), showed the similar signal intensity of magnetic resonance imaging to that of the normal dental pulp, demonstrated functional dentin formation in cone-beam computed tomography (CBCT) test, and showed no adverse events or toxicity in the clinical and laboratory evaluations (Nakashima and Iohara, 2017; Nakashima et al., 2017). Meanwhile, transplantation of exogenous odontogenic MSC aggregates was also proven to be effective in preclinical studies and clinical trials. It has been demonstrated that the transplantation of the side populations of DPSCs cell aggregates into an *in vivo* model of amputated pulp and pulp tissue with capillaries and nerves was regenerated (Iohara et al., 2009). Furthermore, our recent study of mini-pigs demonstrated that the transplantation of pig DPSC aggregates into endodontically treated pig teeth regenerated functional dental pulp with blood vessels and nerves (**Figure 2**). Meanwhile, we carried out a randomized clinical trial with autologous SHED aggregate transplantation in patients with tooth trauma. Thirty-six patients with pulp necrosis after dental trauma were included, with 26 patients in the SHED aggregate transplantation group and 10 patients in the traditional apexification treatment group. After a 12-month follow-up, the SHED aggregate transplantation group showed regeneration of well-organized pulp tissue with blood

vessels and sensory nerve ingrowth histologically, and clinical examination showed robust positive results in the EPT, increased vascular formation in laser Doppler flowmetry, and increased length of the root and closed apical foramen in CBCT. Furthermore, there were no adverse events at the 24-month follow-up (Xuan et al., 2018). These studies suggest that exogenous odontogenic MSC implantation may be an effective approach to regenerate functional dental pulp, and the application of odontogenic MSC aggregates may be a promising method for future regenerative endodontics in clinical settings.

DISCUSSION

The efficacy of dental pulp regeneration depends on the biological properties of the odontogenic MSCs involved in the regeneration process, and the natural dental pulp microenvironment of odontogenic MSCs is essential to regulate their homeostasis, proliferation, and differentiation; thus, mimicking the natural pulp microenvironment is the key to realizing pulp regeneration.

By summarizing recent achievements in pulp regeneration, we found that exogenous odontogenic MSC transplantation has made dramatic progress both in preclinical research and clinical trials (Nakashima and Iohara, 2017; Nakashima et al., 2017; Xuan et al., 2018). In addition, odontogenic MSC aggregates show immense potential to regenerate well-organized pulp (Iohara et al., 2009; Na et al., 2016; Itoh et al., 2018; Xuan et al., 2018; Meng et al., 2020). This is likely because the ECM of odontogenic MSCs was similar to that of dental pulp tissue-derived ECM (Zhang et al., 2017c). Furthermore, the dental pulp regenerated by the transplantation of cell aggregates into treated root canals is similar to the process of pulp-dentin complex development. Before the regeneration procedure, the root canal was routinely treated with ethylene diamine tetra-acetic acid, which was been proven to expose the dentin tubules, loosen the intertubular and peritubular dentin, and promote the release of dentin growth factors. These structure and growth factors not only play important roles in inducing MSC proliferation and differentiation but also offer a scaffold to form dentin tissues and control mineralization during dentin regeneration (Li et al., 2011). Cell aggregates have been shown to preserve the normal cellular junctions and endogenous ECM similar to their natural microenvironment, and to mimic the mechanical, chemical, and biological properties of the natural microenvironment (Diao et al., 2017). When cell aggregates were implanted into the root canal, the interaction between cell aggregates and the treated dentin is similar to that between the newly formed dentin and the apical papilla, which is the aggregate of odontogenic MSCs in the early stage of tooth development. Therefore, we hypothesize it may be possible that transplantation of cell aggregates into treated root canals simulated the microenvironment of the pulp-dentin complex development and initiated the process of pulp-dentin complex development. Meanwhile, recent research has demonstrated that Alx3, a transcription factor highly expressed in developing teeth, regenerated parenchymal and stromal tissue of the tooth. Wnt3a, as Alx3's direct target delivered in endodontically prepared root canals, was shown to regenerate both the parenchyma and stroma in adult teeth (He et al., 2019). From this, we can see that signals from the development microenvironment of teeth play a pivotal role in dental pulp regeneration. Therefore, mimicking the development of the microenvironment of the pulp-dentin complex will probably become a feasible and effective approach in dental pulp regeneration.

CONCLUSION

In conclusion, the microenvironment surrounding odontogenic MSCs can easily influence the biological properties of odontogenic MSCs and affect the efficacy of dental pulp regeneration. Methods mimicking the natural dental pulp microenvironment are effective in regenerating well-organized functional dental pulp by maintaining homeostasis, proliferation, and differentiation of the odontogenic MSCs. Moreover, simulating the development of the microenvironment of the pulp-dentin complex may be a more effective approach to regenerate dental pulp.

AUTHOR CONTRIBUTIONS

XH, ZL, and AL conceptualized the review. XH, HG, and XL prepared the figures. ZL and XH revised the manuscript. KX supervised the work. All authors contributed to writing the manuscript and approved the submitted version.

FUNDING

This work was supported by the National Natural Science Foundation of China (Grant Nos. 82071075 and 81900957).

ACKNOWLEDGMENTS

Thanks to KX for the choice of authors and for bringing them together to complete this manuscript. XH would like to thank KX, AL, XL, HG, and MW for their guidance and encouragement.

REFERENCES

Agata, H., Kagami, H., Watanabe, N., and Ueda, M. (2008). Effect of ischemic culture conditions on the survival and differentiation of porcine dental pulp-derived cells. *Differentiation* 76, 981–993. doi: 10.1111/j.1432-0436.2008.00282.x

Alqahtani, Q., Zaky, S. H., Patil, A., Beniash, E., Ray, H., and Sfeir, C. (2018). Decellularized swine dental pulp tissue for regenerative root

canal therapy. *J. Dent. Res.* 97, 1460–1467. doi: 10.1177/00220345187 85124

Bakhtiar, H., Pezeshki-Modaress, M., Kiaipour, Z., Shafiee, M., Ellini, M. R., Mazidi, A., et al. (2020). Pulp ECM-derived macroporous scaffolds for stimulation of dental-pulp regeneration process. *Dent. Mater.* 36, 76–87. doi: 10.1016/j.dental. 2019.10.011

Bhang, S. H., Cho, S. W., La, W. G., Lee, T. J., Yang, H. S., Sun, A. Y., et al. (2011). Angiogenesis in ischemic tissue produced by spheroid grafting of human adipose-derived stromal cells. *Biomaterials* 32, 2734–2747. doi: 10.1016/ j.biomaterials.2010.12.035

Cheng, N. C., Tu, Y. K., Lee, N. H., and Young, T. H. (2020). Influence of human platelet lysate on extracellular matrix deposition and cellular characteristics in adipose-derived stem cell sheets. *Front. Cell Dev. Biol.* 8:558354. doi: 10.3389/ fcell.2020.558354

Colombo, J. S., Moore, A. N., Hartgerink, J. D., and D'souza, R. N. (2014). Scaffolds to control inflammation and facilitate dental pulp regeneration. *J. Endod.* 40, S6–S12. doi: 10.1016/j.joen.2014.01.019

Cooper, P. R., Holder, M. J., and Smith, A. J. (2014). Inflammation and regeneration in the dentin-pulp complex: a double-edged sword. *J. Endod.* 40, S46–S51. doi: 10.1016/j.joen.2014.01.021

Cosgrove, B. D., Mui, K. L., Driscoll, T. P., Caliari, S. R., Mehta, K. D., Assoian, R. K., et al. (2016). N-cadherin adhesive interactions modulate matrix mechanosensing and fate commitment of mesenchymal stem cells. *Nat. Mater.* 15, 1297–1306. doi: 10.1038/nmat4725

Diao, S., Lin, X., Wang, L., Dong, R., Du, J., Yang, D., et al. (2017). Analysis of gene expression profiles between apical papilla tissues, stem cells from apical papilla and cell sheet to identify the key modulators in MSCs niche. *Cell Prolif.* 50:e12337. doi: 10.1111/cpr.12337

Dou, L., Yan, Q., and Yang, D. (2020). Effect of five dental pulp capping agents on cell proliferation, viability, apoptosis and mineralization of human dental pulp cells. *Exp. Ther. Med.* 19, 2377–2383. doi: 10.3892/etm.2020. 8444

Ducret, M., Montembault, A., Josse, J., Pasdeloup, M., Celle, A., Benchrih, R., et al. (2019). Design and characterization of a chitosan-enriched fibrin hydrogel for human dental pulp regeneration. *Dent. Mater.* 35, 523–533. doi: 10.1016/j. dental.2019.01.018

Feng, X., Feng, G., Xing, J., Shen, B., Tan, W., Huang, D., et al. (2014). Repeated lipopolysaccharide stimulation promotes cellular senescence in human dental pulp stem cells (DPSCs). *Cell Tissue Res.* 356, 369–380. doi: 10.1007/s00441-014-1799-7

Garcia-Godoy, F., and Murray, P. E. (2012). Recommendations for using regenerative endodontic procedures in permanent immature traumatized teeth. *Dent. Traumatol.* 28, 33–41. doi: 10.1111/j.1600-9657.2011.01044.x

Gaviño Orduña, J. F., García García, M., Dominguez, P., Caviedes Bucheli, J., Martin Biedma, B., Abella Sans, F., et al. (2020). Successful pulp revascularization of an autotransplantated mature premolar with fragile fracture apicoectomy and plasma rich in growth factors: a 3-year follow-up. *Int. Endod. J.* 53, 421–433. doi: 10.1111/iej.13230

Gronthos, S., Mankani, M., Brahim, J., Robey, P. G., and Shi, S. (2000). Postnatal human dental pulp stem cells (DPSCs) *in vitro* and in vivo. *Proc. Natl. Acad. Sci. U.S.A.* 97, 13625–13630. doi: 10.1073/pnas.240309797

He, L., Kim, S. G., Gong, Q., Zhong, J., Wang, S., Zhou, X., et al. (2017a). Regenerative endodontics for adult patients. *J. Endod.* 43, S57–S64. doi: 10. 1016/j.joen.2017.06.012

He, L., Zhou, J., Chen, M., Lin, C. S., Kim, S. G., Zhou, Y., et al. (2019). Parenchymal and stromal tissue regeneration of tooth organ by pivotal signals reinstated in decellularized matrix. *Nat. Mater.* 18, 627–637. doi: 10.1038/s41563-019-0368-6

He, X., Jiang, W., Luo, Z., Qu, T., Wang, Z., Liu, N., et al. (2017b). IFN-γ regulates human dental pulp stem cells behavior via NF-κB and MAPK signaling. *Sci. Rep.* 7:40681. doi: 10.1038/srep40681

Hilkens, P., Bronckaers, A., Ratajczak, J., Gervois, P., Wolfs, E., and Lambrichts, I. (2017). The angiogenic potential of DPSCs and SCAPs in an *In Vivo* model of dental pulp regeneration. *Stem Cells Int.* 2017:2582080. doi: 10.1155/2017/ 2582080

Hozhabri, N. S., Benson, M. D., Vu, M. D., Patel, R. H., Martinez, R. M., Nakhaie, F. N., et al. (2015). Decreasing NF-κB expression enhances odontoblastic differentiation and collagen expression in dental pulp stem cells exposed to inflammatory cytokines. *PLoS One* 10:e0113334. doi: 10.1371/journal.pone. 0113334

Hu, X., Zhong, Y., Kong, Y., Chen, Y., Feng, J., and Zheng, J. (2019). Lineage-specific exosomes promote the odontogenic differentiation of human dental pulp stem cells (DPSCs) through TGFβ1/smads signaling pathway via transfer of microRNAs. *Stem Cell Res. Ther.* 10:170. doi: 10.1186/s13287-019-1278-x

Huang, C. C., Narayanan, R., Alapati, S., and Ravindran, S. (2016). Exosomes as biomimetic tools for stem cell differentiation: applications in dental pulp tissue regeneration. *Biomaterials* 111, 103–115. doi: 10.1016/j.biomaterials.2016. 09.029

Huang, R., Wang, J., Chen, H., Shi, X., Wang, X., Zhu, Y., et al. (2019). The topography of fibrous scaffolds modulates the paracrine function of Ad-MSCs in the regeneration of skin tissues. *Biomater. Sci.* 7, 4248–4259. doi: 10.1039/ c9bm00939f

Huang, Y., Qiao, W., Wang, X., Gao, Q., Peng, Y., Bian, Z., et al. (2018). Role of Ku70 in the apoptosis of inflamed dental pulp stem cells. *Inflamm. Res.* 67, 777–788. doi: 10.1007/s00011-018-1167-2

Iohara, K., Imabayashi, K., Ishizaka, R., Watanabe, A., Nabekura, J., Ito, M., et al. (2011). Complete pulp regeneration after pulpectomy by transplantation of CD105+ stem cells with stromal cell-derived factor-1. *Tissue Eng. Part A* 17, 1911–1920. doi: 10.1089/ten.TEA.2010.0615

Iohara, K., Murakami, M., Nakata, K., and Nakashima, M. (2014). Age-dependent decline in dental pulp regeneration after pulpectomy in dogs. *Exp. Gerontol.* 52, 39–45. doi: 10.1016/j.exger.2014.01.020

Iohara, K., Murakami, M., Takeuchi, N., Osako, Y., Ito, M., Ishizaka, R., et al. (2013). A novel combinatorial therapy with pulp stem cells and granulocyte colony-stimulating factor for total pulp regeneration. *Stem Cells Transl. Med.* 2, 521–533. doi: 10.5966/sctm.2012-0132

Iohara, K., Zheng, L., Ito, M., Ishizaka, R., Nakamura, H., Into, T., et al. (2009). Regeneration of dental pulp after pulpotomy by transplantation of CD31(−)/CD146(−) side population cells from a canine tooth. *Regen. Med.* 4, 377–385. doi: 10.2217/rme.09.5

Iohara, K., Zheng, L., Wake, H., Ito, M., Nabekura, J., Wakita, H., et al. (2008). A novel stem cell source for vasculogenesis in ischemia: subfraction of side population cells from dental pulp. *Stem Cells* 26, 2408–2418. doi: 10.1634/ stemcells.2008-0393

Ishimatsu, H., Kitamura, C., Morotomi, T., Tabata, Y., Nishihara, T., Chen, K. K., et al. (2009). Formation of dentinal bridge on surface of regenerated dental pulp in dentin defects by controlled release of fibroblast growth factor-2 from gelatin hydrogels. *J. Endod.* 35, 858–865. doi: 10.1016/j.joen.2009.03.049

Itoh, Y., Sasaki, J. I., Hashimoto, M., Katata, C., Hayashi, M., and Imazato, S. (2018). Pulp regeneration by 3-dimensional dental pulp stem cell constructs. *J. Dent. Res.* 97, 1137–1143. doi: 10.1177/0022034518772260

Jadhav, G., Shah, N., and Logani, A. (2012). Revascularization with and without platelet-rich plasma in nonvital, immature, anterior teeth: a pilot clinical study. *J. Endod.* 38, 1581–1587. doi: 10.1016/j.joen.2012.09.010

Jarmalavičiūtė, A., Tunaitis, V., Pivoraitė, U., Venalis, A., and Pivoriūnas, A. (2015). Exosomes from dental pulp stem cells rescue human dopaminergic neurons from 6-hydroxy-dopamine-induced apoptosis. *Cytotherapy* 17, 932–939. doi: 10.1016/j.jcyt.2014.07.013

Kim, J. Y., Xin, X., Moioli, E. K., Chung, J., Lee, C. H., Chen, M., et al. (2010). Regeneration of dental-pulp-like tissue by chemotaxis-induced cell homing. *Tissue Eng. Part A* 16, 3023–3031. doi: 10.1089/ten.TEA.2010.0181

Lambrichts, I., Driesen, R. B., Dillen, Y., Gervois, P., Ratajczak, J., Vangansewinkel, T., et al. (2017). Dental pulp stem cells: their potential in reinnervation and angiogenesis by using scaffolds. *J. Endod.* 43, S12–S16. doi: 10.1016/j.joen.2017. 06.001

Li, J., Rao, Z., Zhao, Y., Xu, Y., Chen, L., Shen, Z., et al. (2020). A Decellularized matrix hydrogel derived from human dental pulp promotes dental pulp stem cell proliferation, migration, and induced multidirectional differentiation *In Vitro*. *J. Endod.* 46, 1438–1447.e5. doi: 10.1016/j.joen.2020. 07.008

Li, R., Guo, W., Yang, B., Guo, L., Sheng, L., Chen, G., et al. (2011). Human treated dentin matrix as a natural scaffold for complete human dentin tissue regeneration. *Biomaterials* 32, 4525–4538. doi: 10.1016/j.biomaterials.2011. 03.008

Linde, A. (1985). The extracellular matrix of the dental pulp and dentin. *J. Dent. Res.* 64, 523–529. doi: 10.1177/002203458506400405

Liu, J. Y., Chen, X., Yue, L., Huang, G. T., and Zou, X. Y. (2015). CXC chemokine receptor 4 is expressed paravascularly in apical papilla and coordinates with stromal cell-derived factor-1α during transmigration of stem cells from apical papilla. *J. Endod.* 41, 1430–1436. doi: 10.1016/j.joen.2015.04.006

Lu, J., Li, Z., Wu, X., Chen, Y., Yan, M., Ge, X., et al. (2019). iRoot BP Plus promotes osteo/odontogenic differentiation of bone marrow mesenchymal stem cells via MAPK pathways and autophagy. *Stem Cell Res. Ther.* 10:222. doi: 10.1186/s13287-019-1345-3

Meng, H., Hu, L., Zhou, Y., Ge, Z., Wang, H., Wu, C. T., et al. (2020). A sandwich structure of human dental pulp stem cell sheet, treated dentin matrix, and matrigel for tooth root regeneration. *Stem Cells Dev.* 29, 521–532. doi: 10.1089/scd.2019.0162

Mitsiadis, T. A., Magloire, H., and Pagella, P. (2017). Nerve growth factor signalling in pathology and regeneration of human teeth. *Sci. Rep.* 7:1327. doi: 10.1038/s41598-017-01455-3

Miura, M., Gronthos, S., Zhao, M., Lu, B., Fisher, L. W., Robey, P. G., et al. (2003). SHED: stem cells from human exfoliated deciduous teeth. *Proc. Natl. Acad. Sci. U.S.A.* 100, 5807–5812. doi: 10.1073/pnas.0937635100

Morsczeck, C., and Reichert, T. E. (2018). Dental stem cells in tooth regeneration and repair in the future. *Expert. Opin. Biol. Ther.* 18, 187–196. doi: 10.1080/14712598.2018.1402004

Moussa, D. G., and Aparicio, C. (2019). Present and future of tissue engineering scaffolds for dentin-pulp complex regeneration. *J. Tissue Eng. Regen. Med.* 13, 58–75. doi: 10.1002/term.2769

Murakami, M., Horibe, H., Iohara, K., Hayashi, Y., Osako, Y., Takei, Y., et al. (2013). The use of granulocyte-colony stimulating factor induced mobilization for isolation of dental pulp stem cells with high regenerative potential. *Biomaterials* 34, 9036–9047. doi: 10.1016/j.biomaterials.2013.08.011

Na, S., Zhang, H., Huang, F., Wang, W., Ding, Y., Li, D., et al. (2016). Regeneration of dental pulp/dentine complex with a three-dimensional and scaffold-free stem-cell sheet-derived pellet. *J. Tissue Eng. Regen. Med.* 10, 261–270. doi: 10.1002/term.1686

Nagata, J. Y., Rocha-Lima, T. F., Gomes, B. P., Ferraz, C. C., Zaia, A. A., Souza-Filho, F. J., et al. (2015). Pulp revascularization for immature replanted teeth: a case report. *Aust. Dent. J.* 60, 416–420. doi: 10.1111/adj.12342

Nakashima, M., and Iohara, K. (2017). Recent progress in translation from bench to a pilot clinical study on total pulp regeneration. *J. Endod.* 43, S82–S86. doi: 10.1016/j.joen.2017.06.014

Nakashima, M., Iohara, K., Murakami, M., Nakamura, H., Sato, Y., Ariji, Y., et al. (2017). Pulp regeneration by transplantation of dental pulp stem cells in pulpitis: a pilot clinical study. *Stem Cell Res. Ther.* 8:61. doi: 10.1186/s13287-017-0506-5

Pan, S., Dangaria, S., Gopinathan, G., Yan, X., Lu, X., Kolokythas, A., et al. (2013). SCF promotes dental pulp progenitor migration, neovascularization, and collagen remodeling - potential applications as a homing factor in dental pulp regeneration. *Stem Cell Rev. Rep.* 9, 655–667. doi: 10.1007/s12015-013-9442-7

Park, S. Y., Sun, E. G., Lee, Y., Kim, M. S., Kim, J. H., Kim, W. J., et al. (2018). Autophagy induction plays a protective role against hypoxic stress in human dental pulp cells. *J. Cell Biochem.* 119, 1992–2002. doi: 10.1002/jcb.26360

Peng, C., Zhao, Y., Wang, W., Yang, Y., Qin, M., and Ge, L. (2017). Histologic findings of a human immature revascularized/regenerated tooth with symptomatic irreversible pulpitis. *J. Endod.* 43, 905–909. doi: 10.1016/j.joen.2017.01.031

Pivoraitė, U., Jarmalavičiūtė, A., Tunaitis, V., Ramanauskaitė, G., Vaitkuvienė, A., Kašėta, V., et al. (2015). Exosomes from human dental pulp stem cells suppress carrageenan-induced acute inflammation in mice. *Inflammation* 38, 1933–1941. doi: 10.1007/s10753-015-0173-6

Rahman, S. U., Oh, J. H., Cho, Y. D., Chung, S. H., Lee, G., Baek, J. H., et al. (2018). Fibrous topography-potentiated canonical wnt signaling directs the odontoblastic differentiation of dental pulp-derived stem cells. *ACS Appl. Mater. Interfaces* 10, 17526–17541. doi: 10.1021/acsami.7b19782

Rosa, V., Zhang, Z., Grande, R. H., and Nör, J. E. (2013). Dental pulp tissue engineering in full-length human root canals. *J. Dent. Res.* 92, 970–975. doi: 10.1177/0022034513505772

Seo, B. M., Miura, M., Gronthos, S., Bartold, P. M., Batouli, S., Brahim, J., et al. (2004). Investigation of multipotent postnatal stem cells from human periodontal ligament. *Lancet* 364, 149–155. doi: 10.1016/s0140-6736(04)16627-0

Shafiq, M., Jung, Y., and Kim, S. H. (2015). In situ vascular regeneration using substance P-immobilised poly(L-lactide-co-ε-caprolactone) scaffolds: stem cell recruitment, angiogenesis, and tissue regeneration. *Eur. Cell Mater.* 30, 282–302. doi: 10.22203/ecm.v030a20

Shi, L., Fu, S., Fahim, S., Pan, S., Lina, H., Mu, X., et al. (2017). TNF-alpha stimulation increases dental pulp stem cell migration in vitro through integrin alpha-6 subunit upregulation. *Arch. Oral. Biol.* 75, 48–54. doi: 10.1016/j.archoralbio.2016.12.005

Sjöqvist, S., Ishikawa, T., Shimura, D., Kasai, Y., Imafuku, A., Bou-Ghannam, S., et al. (2019). Exosomes derived from clinical-grade oral mucosal epithelial cell sheets promote wound healing. *J. Extracell Vesicles* 8:1565264. doi: 10.1080/20013078.2019.1565264

Smith, J. G., Smith, A. J., Shelton, R. M., and Cooper, P. R. (2015). Dental pulp cell behavior in biomimetic environments. *J. Dent. Res.* 94, 1552–1559. doi: 10.1177/0022034515599767

Sonoyama, W., Liu, Y., Yamaza, T., Tuan, R. S., Wang, S., Shi, S., et al. (2008). Characterization of the apical papilla and its residing stem cells from human immature permanent teeth: a pilot study. *J. Endod.* 34, 166–171. doi: 10.1016/j.joen.2007.11.021

Sui, B., Chen, C., Kou, X., Li, B., Xuan, K., Shi, S., et al. (2019a). Pulp stem cell-mediated functional pulp regeneration. *J. Dent. Res.* 98, 27–35. doi: 10.1177/0022034518808754

Sui, B. D., Zhu, B., Hu, C. H., Zhao, P., and Jin, Y. (2019b). Reconstruction of regenerative stem cell niche by cell aggregate engineering. *Methods Mol. Biol.* 2002, 87–99. doi: 10.1007/7651_2018_186

Sukho, P., Hesselink, J. W., Kops, N., Kirpensteijn, J., Verseijden, F., and Bastiaansen-Jenniskens, Y. M. (2018). Human mesenchymal stromal cell sheets induce macrophages predominantly to an anti-inflammatory phenotype. *Stem Cells Dev.* 27, 922–934. doi: 10.1089/scd.2017.0275

Suzuki, T., Lee, C. H., Chen, M., Zhao, W., Fu, S. Y., Qi, J. J., et al. (2011). Induced migration of dental pulp stem cells for *in vivo* pulp regeneration. *J. Dent. Res.* 90, 1013–1018. doi: 10.1177/0022034511408426

Tsai, A. C., Liu, Y., Yuan, X., and Ma, T. (2015). Compaction, fusion, and functional activation of three-dimensional human mesenchymal stem cell aggregate. *Tissue Eng. Part A* 21, 1705–1719. doi: 10.1089/ten.TEA.2014.0314

Verma, P., Nosrat, A., Kim, J. R., Price, J. B., Wang, P., Bair, E., et al. (2017). Effect of residual bacteria on the outcome of pulp regeneration *In Vivo*. *J. Dent. Res.* 96, 100–106. doi: 10.1177/0022034516671499

Wigler, R., Kaufman, A. Y., Lin, S., Steinbock, N., Hazan-Molina, H., and Torneck, C. D. (2013). Revascularization: a treatment for permanent teeth with necrotic pulp and incomplete root development. *J. Endod.* 39, 319–326. doi: 10.1016/j.joen.2012.11.014

Xian, X., Gong, Q., Li, C., Guo, B., and Jiang, H. (2018). Exosomes with highly angiogenic potential for possible use in pulp regeneration. *J. Endod.* 44, 751–758. doi: 10.1016/j.joen.2017.12.024

Xiao, L., Kumazawa, Y., and Okamura, H. (2014). Cell death, cavitation and spontaneous multi-differentiation of dental pulp stem cells-derived spheroids *in vitro*: a journey to survival and organogenesis. *Biol. Cell* 106, 405–419. doi: 10.1111/boc.201400024

Xiao, M., Yao, B., Zhang, B. D., Bai, Y., Sui, W., Wang, W., et al. (2019). Stromal-derived Factor-1α signaling is involved in bone morphogenetic protein-2-induced odontogenic differentiation of stem cells from apical papilla via the Smad and Erk signaling pathways. *Exp. Cell Res.* 381, 39–49. doi: 10.1016/j.yexcr.2019.04.036

Xiao, N., Yu, W. Y., and Liu, D. (2018). Glial cell-derived neurotrophic factor promotes dental pulp stem cell migration. *J. Tissue Eng. Regen. Med.* 12, 705–714. doi: 10.1002/term.2490

Xuan, K., Li, B., Guo, H., Sun, W., Kou, X., He, X., et al. (2018). Deciduous autologous tooth stem cells regenerate dental pulp after implantation into injured teeth. *Sci. Transl. Med.* 10:eaaf3227. doi: 10.1126/scitranslmed.aaf3227

Yang, B., Chen, G., Li, J., Zou, Q., Xie, D., Chen, Y., et al. (2012). Tooth root regeneration using dental follicle cell sheets in combination with a dentin matrix - based scaffold. *Biomaterials* 33, 2449–2461. doi: 10.1016/j.biomaterials.2011.11.074

Yang, J., Yuan, G., and Chen, Z. (2016). Pulp regeneration: current approaches and future challenges. *Front. Physiol.* 7:58. doi: 10.3389/fphys.2016.00058

Yang, J. W., Zhang, Y. F., Wan, C. Y., Sun, Z. Y., Nie, S., Jian, S. J., et al. (2015). Autophagy in SDF-1α-mediated DPSC migration and pulp regeneration. *Biomaterials* 44, 11–23. doi: 10.1016/j.biomaterials.2014.12.006

Yang, X., Ma, Y., Guo, W., Yang, B., and Tian, W. (2019). Stem cells from human exfoliated deciduous teeth as an alternative cell source in bio-root regeneration. *Theranostics* 9, 2694–2711. doi: 10.7150/thno.31801

Yavropoulou, M. P., and Yovos, J. G. (2016). The molecular basis of bone mechanotransduction. *J. Musculoskelet Neuronal Interact* 16, 221–236.

Yuan, H., Zhao, H., Wang, J., Zhang, H., Hong, L., Li, H., et al. (2018). MicroRNA let-7c-5p promotes osteogenic differentiation of dental pulp stem cells by inhibiting lipopolysaccharide-induced inflammation via HMGA2/PI3K/Akt signal blockade. *Clin. Exp. Pharmacol. Physiol.* 46, 389–397. doi: 10.1111/1440-1681.13059

Zhang, D. D., Chen, X., Bao, Z. F., Chen, M., Ding, Z. J., and Zhong, M. (2014). Histologic comparison between platelet-rich plasma and blood clot in regenerative endodontic treatment: an animal study. *J. Endod.* 40, 1388–1393. doi: 10.1016/j.joen.2014.03.020

Zhang, M., Jiang, F., Zhang, X., Wang, S., Jin, Y., Zhang, W., et al. (2017a). The effects of platelet-derived growth factor-bb on human dental pulp stem cells mediated dentin-pulp complex regeneration. *Stem Cells Transl. Med.* 6, 2126–2134. doi: 10.1002/sctm.17-0033

Zhang, Q., Nguyen, A. L., Shi, S., Hill, C., Wilder-Smith, P., Krasieva, T. B., et al. (2012). Three-dimensional spheroid culture of human gingiva-derived mesenchymal stem cells enhances mitigation of chemotherapy-induced oral mucositis. *Stem Cells Dev.* 21, 937–947. doi: 10.1089/scd.2011.0252

Zhang, S., Thiebes, A. L., Kreimendahl, F., Ruetten, S., Buhl, E. M., Wolf, M., et al. (2020a). Extracellular vesicles-loaded fibrin gel supports rapid neovascularization for dental pulp regeneration. *Int. J. Mol. Sci.* 21:4226. doi: 10.3390/ijms21124226

Zhang, S., Yang, Y., Jia, S., Chen, H., Duan, Y., Li, X., et al. (2020b). Exosome-like vesicles derived from Hertwig's epithelial root sheath cells promote the regeneration of dentin-pulp tissue. *Theranostics* 10, 5914–5931. doi: 10.7150/thno.43156

Zhang, W., Vazquez, B., Oreadi, D., and Yelick, P. C. (2017b). Decellularized tooth bud scaffolds for tooth regeneration. *J. Dent. Res.* 96, 516–523. doi: 10.1177/0022034516689082

Zhang, X., Li, H., Sun, J., Luo, X., Yang, H., Xie, L., et al. (2017c). Cell-derived micro-environment helps dental pulp stem cells promote dental pulp regeneration. *Cell Prolif.* 50:e12361. doi: 10.1111/cpr.12361

Zhao, H., Feng, J., Seidel, K., Shi, S., Klein, O., Sharpe, P., et al. (2014). Secretion of shh by a neurovascular bundle niche supports mesenchymal stem cell homeostasis in the adult mouse incisor. *Cell Stem Cell* 14, 160–173. doi: 10.1016/j.stem.2013.12.013

Zhujiang, A., and Kim, S. G. (2016). Regenerative endodontic treatment of an immature necrotic molar with arrested root development by using recombinant human platelet-derived growth factor: a case report. *J. Endod.* 42, 72–75. doi: 10.1016/j.joen.2015.08.026

Conflict of Interest: The authors declare that the research was conducted in the absence of any commercial or financial relationships that could be construed as a potential conflict of interest.

frontiers in Physiology

ORIGINAL RESEARCH
published: 16 August 2021
doi: 10.3389/fphys.2021.660644

Epithelial Bone Morphogenic Protein 2 and 4 Are Indispensable for Tooth Development

Haibin Mu[1,2], Xin Liu[1], Shuoshuo Geng[1], Dian Su[1], Heran Chang[1], Lili Li[3], Han Jin[2], Xiumei Wang[1], Ying Li[2], Bin Zhang[2,4] and Xiaohua Xie[1,2]**

[1] Department of Stomatology, The Second Affiliated Hospital of Harbin Medical University, Harbin, China, [2] Institute of Hard Tissue Development and Regeneration, The Second Affiliated Hospital of Harbin Medical University, Harbin, China, [3] Department of Stomatology, The First Affiliated Hospital of Harbin Medical University, Harbin, China, [4] Heilongjiang Academy of Medical Sciences, Harbin, China

OPEN ACCESS

Edited by:
Guohua Yuan,
Wuhan University, China

Reviewed by:
Yiping Chen,
Tulane University, United States
Xiaoying Wang,
Shandong University, China

***Correspondence:**
Bin Zhang
zhangbin@hrbmu.edu.cn
Xiaohua Xie
xiexiaohua@hrbmu.edu.cn

Specialty section:
This article was submitted to Craniofacial Biology and Dental Research, a section of the journal Frontiers in Physiology

Received: 29 January 2021
Accepted: 16 June 2021
Published: 16 August 2021

Citation:
Mu H, Liu X, Geng S, Su D, Chang H, Li L, Jin H, Wang X, Li Y, Zhang B and Xie X (2021) Epithelial Bone Morphogenic Protein 2 and 4 Are Indispensable for Tooth Development. Front. Physiol. 12:660644. doi: 10.3389/fphys.2021.660644

The *Bmp2* and *Bmp4* expressed in root mesenchyme were essential for the patterning and cellular differentiation of tooth root. The role of the epithelium-derived Bmps in tooth root development, however, had not been reported. In this study, we found that the double abrogation of *Bmp2* and *Bmp4* from mouse epithelium caused short root anomaly (SRA). The *K14-cre;Bmp2*$^{f/f}$*;Bmp4*$^{f/f}$ mice exhibited a persistent Hertwig's Epithelial Root Sheath (HERS) with the reduced cell death, and the down-regulated BMP-Smad4 and Erk signaling pathways. Moreover, the *Shh* expression in the HERS, the Shh-Gli1 signaling, and *Nfic* expression in the root mesenchyme of the *K14-cre;Bmp2*$^{f/f}$*;Bmp4*$^{f/f}$ mice were also decreased, indicating a disrupted epithelium- mesenchyme interaction between HERS and root mesenchyme. Such disruption suppressed the *Osx* and *Dspp* expression in the root mesenchyme, indicating an impairment on the differentiation and maturation of root odontoblasts. The impaired differentiation and maturation of root odontoblasts could be rescued partially by transgenic *Dspp*. Therefore, although required in a low dosage and with a functional redundancy, the epithelial Bmp2 and Bmp4 were indispensable for the HERS degeneration, as well as the differentiation and maturation of root mesenchyme

Keywords: tooth root, bone morphogenic protein, short root anomaly (SRA), Hertwig's Epithelial Root Sheath (HERS), epithelial-mesenchymal interaction

INTRODUCTION

Although the mammalian tooth is putatively regarded as an intact organ to fulfill physiological functions, the enamel-covered tooth crown and the cementum-covered tooth root actually undergo separated developmental processes which are regulated by different genetic mechanisms (Steele-Perkins et al., 2003). The development of tooth crown is divided into laminar, bud, cap, and bell stages according to the morphology of the epithelial-derived enamel organ (Luder et al., 2015). In the tooth germs of bell stage, the enamel organ differentiates into outer enamel epithelium (OEE),

satellite reticulum, stratum intermediate, and inner enamel epithelium (IEE) from the external to internal side. At the apical edge of the enamel organ, OEE and IEE meet together to form a bilayer epithelium which elongates into Hertwig's Epithelial Root Sheath (HERS). HERS induces not only the apical dental mesenchymal cells into the root odontoblasts which secret root dentin (Ten Cate, 1996), but also the dental follicle cells into cementoblasts to produce cementum (Kim et al., 2013). Eventually, the HERS degenerates and disappears in the erupted tooth, instead of differentiating into the enamel-secreting ameloblasts as the IEE does in the crown (Huang et al., 2009). A number of studies demonstrated that both the formation and degeneration of HERS were key to the length, shape, and number of tooth root, as well as the cementum and periodontal ligament (Bosshardt et al., 2015).

The initiation of tooth root, namely, the formation of HERS, starts almost at the late morphogenesis of the tooth crown. However, the reciprocal interactions between dental epithelium and the underlying mesenchyme, which are essential for the development of tooth crown (Chai et al., 2006), are also required during the development of tooth root (Huang et al., 2010). The induction of root odontoblasts and cementoblasts by HERS requires the direct contacts of HERS to root mesenchyme and dental follicle cells (Xiong et al., 2013). A lot of growth factors, such as BMPs, TGFβ, and SHH, were secreted by HERS to activate the pivotal transcription factor, *Nuclear Factor I C* (*Nfic*), in the root mesenchyme (Lee et al., 2009). Although *Nfic* transcription can be detected in both the crown and root odontoblasts, the *Nfic* null mice only showed the short tooth roots without overt HERS defects (Park et al., 2007), which indicated that the genetic network in root development was different from that in tooth crown.

Taking the advantages of the genetic animal models, a number of growth factors, transcription factors, and signaling pathways have proven to be involved in root development (Ono et al., 2016). During tooth root development, *Bmp2,3,4,* and *7* were expressed only in the root mesenchyme or pre-odontoblasts, as opposed to HERS (Yamashiro et al., 2003). The BMP ligands emanated from root mesenchyme are believed to activate *Sonic Hedgehog* (*Shh)* expression in HERS through Msx2 or BMP/Smad4 signaling (Li et al., 2015). Then, Shh secreted from HERS activates the transcription of *Nfic* in root mesenchyme through Gli1 (Li et al., 2015). Further, NFIC activates *Osterix* (*OSX*) in the precursors of pre-odontoblasts to promote the differentiation by enhancing *Dentin sialophosphoprotein* (*Dspp*) and *Dental Matrix Protein 1* (*Dmp1*) expression (Zhang et al., 2015). Inactivation of *Smad4* in mouse ectoderm and abrogating *Bmp Receptor IA* (*Bmpr1a*) by inducible *K14-cre* resulted in the complete loss of root and the short root anomaly (SRA), respectively (Huang et al., 2010), indicating that the BMP/Smad4 signaling in the ectoderm-derived HERS was essential for tooth root development.

Up to now, the transcription of *Bmp2,3,4,* and *7* has not been detected in HERS. However, when *Bmp2* and *Bmp4* were both inactivated by *K14-cre*, the mice exhibited not only the compromised amelogenesis (Xie et al., 2016), but also the shorter tooth roots. In this study, we generated *K14-cre;Bmp2*$^{f/f}$*;Bmp4*$^{f/f}$ mouse to address if the BMP/Smad4 signaling in HERS is thoroughly contributed to by the mesenchymal BMP ligands, and the role of epithelial BMP ligands in tooth root development.

MATERIALS AND METHODS

Mouse Lines

The *K14-cre* transgenic (Stock NO. 016230), *Bmp2*$^{f/f}$ (Stock NO. 016878), and *Bmp4*$^{f/f}$ (Stock NO. 018964) knock-in mice were obtained from Jackson Laboratory. The *Dspp* transgenic line was gifted by Dr. Chunlin Qin in Texas A&M College of Dentistry (Jani et al., 2016). To generate *K14-cre;Bmp2*$^{f/f}$*;Bmp4*$^{f/f}$ mice referred to as "*K14-Cre*-mediated double conditional knockout" (dcKO), the *Bmp2*$^{f/f}$*;Bmp4*$^{f/f}$ mice were crossbred with *K14-cre;Bmp2*$^{f/+}$*;Bmp4*$^{f/+}$ mice. To generate *K14-cre;Bmp2*$^{f/f}$*; Bmp4*$^{f/f}$*;Dspp*^{Tg} mice (referred to as dcKO;*Dspp*^{Tg}), the *Bmp2*$^{f/f}$*;Bmp4*$^{f/f}$*;Dspp*^{Tg} mice were crossbred with *K14-cre;Bmp2*$^{f/+}$*;Bmp4*$^{f/+}$ mice. The genotyping procedures and primer sequences were described previously (Xie et al., 2016). All the mouse lines were bred and expanded in the Laboratory Animal Center at The Second Affiliated Hospital of Harbin Medical University. All the animal protocols (KY2016-087 and SYDW2019-2) were in accordance with the guidelines and approved by the research committee at The Second Affiliated Hospital of Harbin Medical University.

Plain X-Ray Radiography and Micro-Computed Tomography

The mandibles dissected from the 3-week-old *Bmp2*$^{f/f}$*; Bmp4*$^{f/f}$(as normal control),*K14-cre; Bmp2*$^{f/+}$*;Bmp4*$^{f/+}$, *K14-cre;Bmp2*$^{f/f}$*;Bmp4*$^{f/+}$, *K14-cre; Bmp2*$^{f/+}$*;Bmp4*$^{f/f}$, and *K14-cre; Bmp2*$^{f/f}$*;Bmp4*$^{f/f}$ (dcKO) mice were fixed in 4% paraformaldehyde (PFA) for 48 h at 4°C and then dehydrated to 70% ethanol gradually. Similarly, the mandibles from 3-week-old *Bmp2*$^{f/f}$*;Bmp4*$^{f/f}$*;Dspp*^{Tg} (as control), *K14-cre;Bmp2*$^{f/+}$*; Bmp4*$^{f/+}$*;Dspp*^{Tg}, *K14-cre; Bmp2*$^{f/f}$*; Bmp4*$^{f/+}$*;Dspp*^{Tg}, *K14-cre; Bmp2*$^{f/+}$*;Bmp4*$^{f/f}$*;Dspp*^{Tg}, and *K14-cre;Bmp2*$^{f/f}$*;Bmp4*$^{f/f}$*; Dspp*^{Tg} (dcKO;*Dspp*^{Tg}) mice were treated in the same procedures. Four pairs of jaws of each genotype (n = 4) were utilized for plain X-ray radiography by Faxitron MX-20 (Faxitron Bioptics, Tucson, AZ, United States). For micro-CT analysis, μCT35 (Scanco Medical, Brüttisellen, Switzerland) was applied for morphological observations with 3.5 μm slice increment. For mineral density and thickness of root dentin or cementum, 200 slices centered on the cut-through of the mesial root in the first molar were analyzed.

Decalcified Paraffin Sections and Hematoxylin and Eosin (H&E) Staining

The mouse mandibles were dissected and fixed in 4% PFA and then decalcified in 15% ethylenediaminetetracetic acid (EDTA) solution at 4°C for 1–2 weeks. The mandibles were dehydrated with gradient alcohols and degreased with xylene for paraffin embedding. Serial sections were prepared in the thickness of

5 μm for hematoxylin and eosin (H&E) staining, PCNA assay, TUNEL assay, or immunohistochemistry (IHC) staining.

Quantitative PCR

To evaluate the *Bmp2* and *Bmp4* abrogation in the dcKO HERS, the HERS was dissected from the P0 dcKO and WT first molars. Meanwhile, the oral mucosa of the P0 WT mice was also collected as negative control. The total RNA of the HERS and oral mucosa were extracted using RNeasy Kit (Qiagen) according to the manufacturer's instructions. The complementary DNA (cDNA) was synthesized with the SuperScript^{TM} VILO^{TM} Master Mix (Invitrogen). The quantitative PCR was performed using SYBR Select Master Mix (Applied Biosystems, CA, United States) and the Quant Studio 6 Flux PCR System (Applied Biosystems). The *Bmp2* primers were 5′-GGGACCCGCTGTCTTCTAGT-3′ (forward) and 5′-TCAACTCAAATTCGCTGAGGAC-3′ (reverse); the Bmp4 primers were 5′-ATTCCTGGTAACCGAATGCTG-3′ (forward) and 5′-CCGGTCTCAGGTATCAAACTAGC-3′ (reverse).

Cell Proliferation and Apoptosis Assay

The antibodies against PCNA (A0264, ABclonal) and Caspase 3 (96625, Cell signaling Technology) were applied to examine the cell proliferation and cell death in the molar roots. The paraffin sections were rehydrated with gradient alcohols after being de-paraffinized in xylene. Then, the sections were treated with 3% H_2O_2 and boiled citrate buffer for antigen retrieval. Prior to the overnight incubation with the antibodies against PCNA and Caspase 3, 3% bovine serum albumin was applied onto the section for 1 h in order to decrease the non-specific reactions. The combined secondary antibody and DAB kit (PV-6001, Zhongshan Golden Bridge Inc.) was used for the color development of the immuno-staining. Eventually, the sections were dehydrated with gradient alcohols and counter-stained with methyl green.

Immunohistochemistry (IHC)

The decalcified paraffin sections for IHC eliminated the endogenous peroxidase activity with 3% H_2O_2 and retrieved antigens with boiled citrate buffer. Then, the sections were treated with 3% bovine serum albumin and 10% normal goat or rabbit serum to reduce non-specific immunoreactions. The sections were incubated with rabbit polyclonal primary antibodies against p-Smad1/5/8, p-Erk1/2, p-Junk, p-p38, DSP from Santa Cruz (Santa Cruz Biotechnology, Inc., Dallas, TX, United States), and rabbit polyclonal primary antibodies against Shh, Gli1, Nfic, OSX from Abcam (Abcam, Cambridge, MA, United States) overnight at 4°C and then the biotinylated-conjugated secondary antibodies (goat anti-rabbit antibodies) at room temperature for 1 h. The immunopositive loci were detected by the ABC kit and the DAB kit (Vector Laboratories, Burlingame, CA, United States) following the manufacturer's instructions.

In situ Hybridization (ISH)

The dissected mandibles were fixed in diethylpyrocarbonate (DEPC)-treated 4% PFA overnight and decalcified in DEPC-treated 15% EDTA solution at 4°C for 10 days. The mandibles were processed for paraffin serial section in the thickness of 10 μm. The DIG-labeled antisense RNA probe for mouse *Dentin sialophosphate protein* (*Dspp*) transcripts (Zhang et al., 2018) was prepared with DIG RNA labeling kit as per the manufacturer's instruction (Roche, Indianapolis, IN, United States). An alkaline-conjugated antibody against DIG was used to detect RNA probes (Roche, Indianapolis, IN, United States) and the BM purple (VectorLaboratories, Burlingame, CA, United States) was used to develop positive signals. All the sections were counterstained with nuclear fast red. The detailed protocol of ISH was described previously (Zhang et al., 2018).

Statistical Analyses

The measurements of the dentin thickness and the root length, the counting of the positive nuclear numbers in PCNA and Caspase 3, as well as the quantification of the immuno-staining intensity were all performed by Image J (version 1.46r, National Institutes of Health). The outcomes from Image J were statistically analyzed with student *T*-test by GraphPad Prism v8.2.1.441. All the statistical results were present in the mean with standard derivation (SD), which was regarded as significant only when the p value was less than 0.05.

RESULTS

Double Abrogation of *Bmp2* and *Bmp4* in Ectoderm Led to SRA

Our previous study showed that, although suffering from a severe Amelogenesis Imperfecta, the *K14-cre;Bmp2$^{f/f}$;Bmp4$^{f/f}$* mice (dcKO) could survive after weaning (Xie et al., 2016). Further investigation showed that both the mandibular bone and the molars were smaller than those of the normal littermates (**Figures 1A,B**). Consistently, the dcKO molar roots were dramatically shorter than the control molar roots. However, the ratio of root length to full tooth length in the dcKO molars was also significantly reduced compared to that of control molars (**Figure 1C**). The relative expression of *Bmp2* and *Bmp4* in the newborn dcKO HERS was also remarkably decreased compared to the WT counterparts (**Figure 1D**). These results suggested that the shortened dcKO molar roots resulted primarily from the impaired root development and the abrogated *Bmp2* and *Bmp4* expression, instead of secondarily to the decreased molar size. Additionally, the thickness of the root dentin in the dcKO molars was also obviously reduced (**Figures 1E,F**), though the density of the root dentin seemed little impacted (**Figure 1G**). Moreover, the SRA in dcKO molars was not detected in the *K14-cre;Bmp2$^{f/+}$;Bmp4$^{f/+}$*, *K14-cre;Bmp2$^{f/f}$;Bmp4$^{f/+}$*, or *K14-cre;Bmp2$^{f/+}$;Bmp4$^{f/f}$* molars (**Supplementary Figures 1A,B**). Thus, only the double inactivation of *Bmp2* and *Bmp4* alleles in the epithelium could cause SRA in mouse molars.

Reduced Cell Death Resulted in the Persistent HERS in dcKO Molar

Since SRA was usually associated with the persistent HERS (Balic et al., 2019), a series of histological sections were prepared

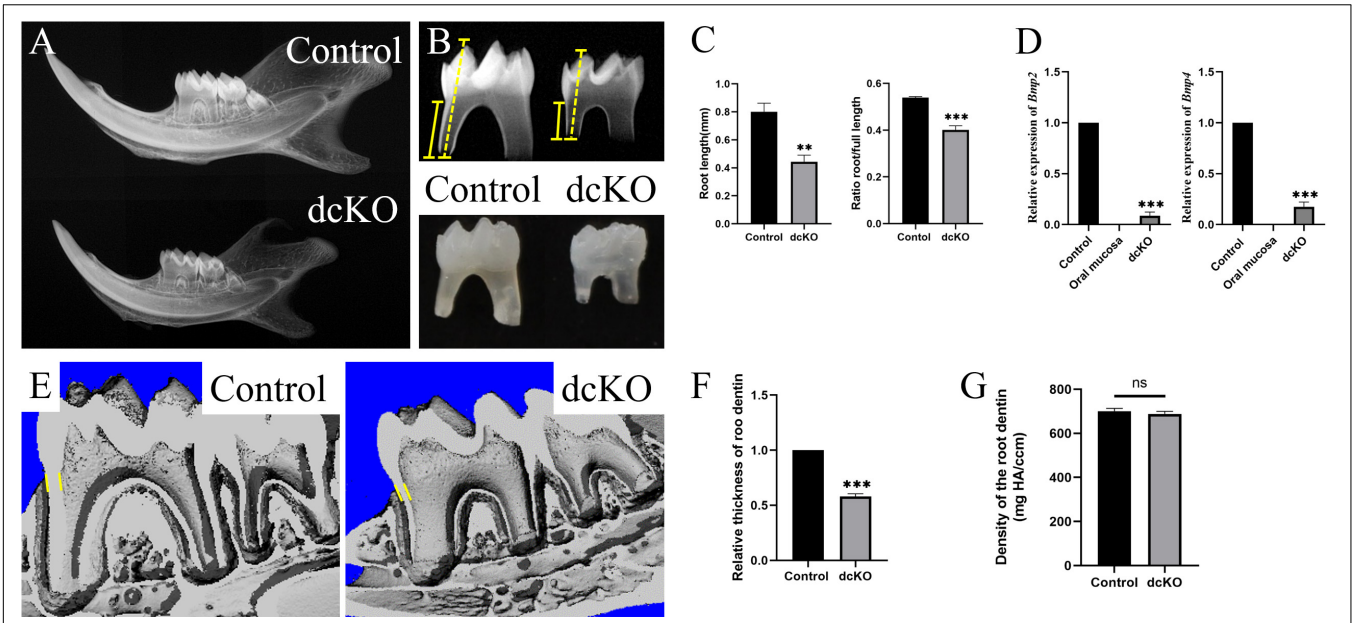

FIGURE 1 | SRA in the dcKO molar. **(A)** The plain X-ray images of the P3W WT and dcKO mandibles. **(B)** The plain X-ray images of the P3W WT and dcKO first molars. **(C)** The statistical analysis of the root lengths of the P3W WT (0.802 ± 0.049 cm) and dcKO first molars (0.443 ± 0.038 cm; $p = 0.0012$). The ratios of root length to full length of the P3W WT (0.539 ± 0.004) and dcKO first molars (0.400 ± 0.014; $p = 0.0002$). **(D)** The quantitative PCR of the P0 HERS from dcKO and WT first molars. Compared to the WT controls, the relative expression of *Bmp2* was 0.08605 ± 0.03078 ($p < 0.0001$), and *Bmp4* 0.17603 ± 0.03775 ($p < 0.0001$). The P0 WT oral mucosa was used as a negative control. **(E)** The micro-CT images of the P3W WT and dcKO first molars. **(F)** The statistical analysis of the relative thicknesses of the dcKO first molar roots (0.54 ± 0.021; $p < 0.001$) to that of P3W WT molar roots. **(G)** Micro-CT scanning showed the gradient density of the P3W WT (700.40 ± 11.67 mg/ccm) and dcKO first molars (688.38 ± 10.23 mg/ccm; $p = 0.0012$). (The yellow dashed lines in panel **B** indicated the height of molar, and the yellow solid lines for the root height; the yellow lines in panels **E**,**F** delineated the measuring thickness of roots; $^{**}p < 0.01$; $^{***}p < 0.001$; $^{ns}p > 0.05$).

to examine the HERS morphology in the dcKO molars. H&E staining showed that at P6, when the control HERS of the 1st molar started to degenerate (**Figure 2A**), the dcKO HERS in the 1st molar stayed intact (**Figure 2B**). Such persistence of the dcKO HERS became more evident at P8 when the control HERS in the 1st molar exhibited an obvious degeneration (**Figures 2C,D**). At P12, there was almost no HERS detected in the control molar roots (**Figure 2E**), while the HERS in the dcKO 1st molar was still intact and kept the long-curved morphology (**Figure 2F**). To verify the persistence of the epithelium-derived HERS in the dcKO molars, the antibody against Keratin 14 was applied in the immunohistochemistry. The Keratin 14-positive cell band labeled an intact and long HERS in the dcKO 1st molar root even at P6 (**Figure 2H**), however, there was a short HERS with the Keratin 14 staining in the control molar roots at the same stage (**Figure 2G**). The persistent K14 positive cells could even be detected in the P10W periodontal ligaments (**Supplementary Figure 2**), confirming the persistent dcKO HERS. To explore how the HERS persisted, the cell proliferation and survival in the dcKO molar roots were examined. In the P8 1st molars, the PCNA densities in both the root mesenchyme and HERS showed no difference between the dcKO and control groups (**Figures 2I–K**). In contrast, although there was almost no difference in the root mesenchyme between the control and dcKO 1st molar, the Caspase3 assay displayed a decreased cell death in the HERS of the P8 dcKO 1st molar compared to the control counterpart (**Figures 2L–N**). Therefore, the persistent HERS in the dcKO molar most likely resulted from the decreased epithelial cell death, which was implicated to count for the SRA.

Suppressed BMP Signaling Pathways in the HERS of dcKO Molar

To confirm the abrogation of *Bmp2* and *Bmp4* in the epithelium-derived HERS of dcKO molar, the Smad-dependent and independent BMP signaling pathways were checked. The intensity of p-Smad1/5/8 was significantly down-regulated in the persistent HERS of the P8 dcKO molar compared to the control molar HERS (**Figures 3A,B**). Moreover, the p-Smad1/5/8 intensity in the dcKO root mesenchyme was also reduced (**Figures 3A,B**), suggesting that the epithelial deletion of *Bmp2* and *Bmp4* also impacted root mesenchyme via epithelial-mesenchymal interactions. Similarly, both the p-Erk1/2 and p-Junk exhibited the decreased intensities in the HERS and root mesenchyme of the dcKO molars compared to the controls (**Figures 3C–F**). However, neither the intensity nor the distribution of the p-p38 in the dcKO molar differed from those in the control molars (**Figures 3G,H**).

The Shh-Gli1-Nfic Interaction Was Disrupted in the dcKO Molar Root

Previous studies demonstrated that the Bmp/Smad4 signaling in HERS controlled tooth root development by activating *Shh*

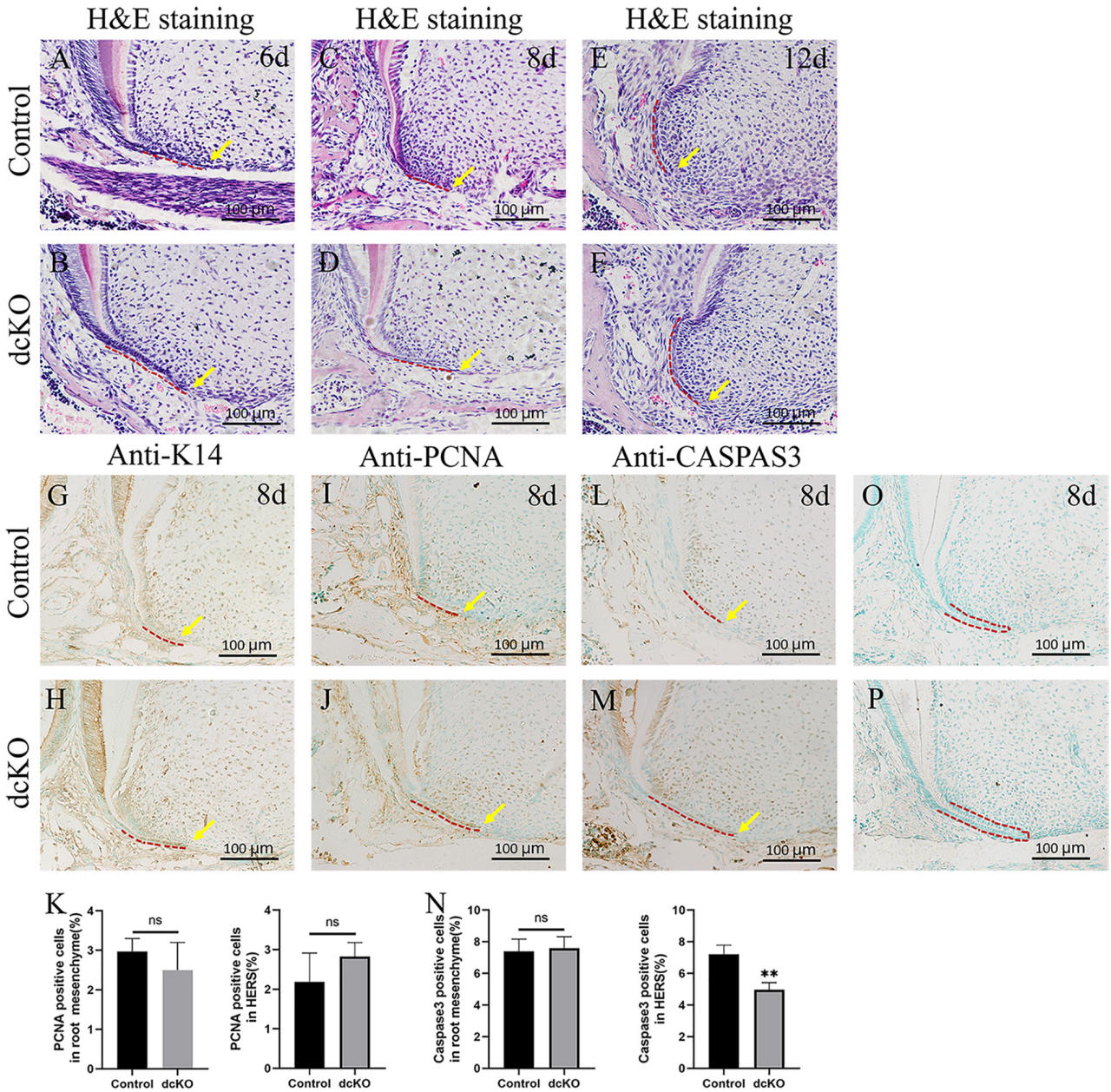

FIGURE 2 | The cell proliferation and death in the persistent HERS of the dcKO molar root. **(A)** The H&E staining of the 1st molar root of P6 WT mouse. **(B)** The H&E staining of the 1st molar root of P6 dcKO mouse. **(C)** The H&E staining of the 1st molar root of P8 WT mouse. **(D)** The H&E staining of the 1st molar root of P8 dcKO mouse. **(E)** The H&E staining of the 1st molar root of P12 WT mouse. **(F)** The H&E staining of the 1st molar root of P12 dcKO mouse. **(G)** The K14 staining in the 1st molar root of P8 WT mouse. **(H)** The K14 staining in the 1st molar root of P8 dcKO mouse. **(I)** The PCNA staining in the 1st molar root of P8 WT mouse. **(J)** The PCNA staining in the 1st molar root of P8 dcKO mouse. **(K)** The statistical analysis of PCNA densities in the root mesenchyme and HERS. **(L)** The Caspase 3 staining in the 1st molar root of P8 WT mouse. **(M)** The Caspase 3 staining in the 1st molar root of P8 dcKO mouse. **(N)** The statistical analysis of Caspase 3 densities in the root mesenchyme and HERS. **(O)** Negative control for the anti-K14 immunostaining in the 1st molar root of P8 WT mouse. **(P)** Negative control for the anti-K14 immunostaining in the 1st molar root of P8 dcKO mouse. (The dashed red lines indicated the HERS; the yellow arrows delineated the end of HERS; $^{**}p < 0.01$; $^{ns}p > 0.05$).

expression in HERS (Huang et al., 2010), which then activated *Nfic* expression in the root mesenchyme (Liu et al., 2015). Compared to the control molar (**Figure 4A**), the *Shh* expression became obviously faint in the persistent HERS of the P8 dcKO molar (**Figure 4B**). Consistent with the reduced *Shh* expression, the numbers of the Gli1 positive cells were also reduced in both the P8 dcKO HERS and the root mesenchyme (**Figures 4C,D**). Similarly, as a down-stream target of Gli1, the expression of *Nfic* in the P8 dcKO molar was also detected in fewer mesenchymal cells compared to the control (**Figures 4E,F**).

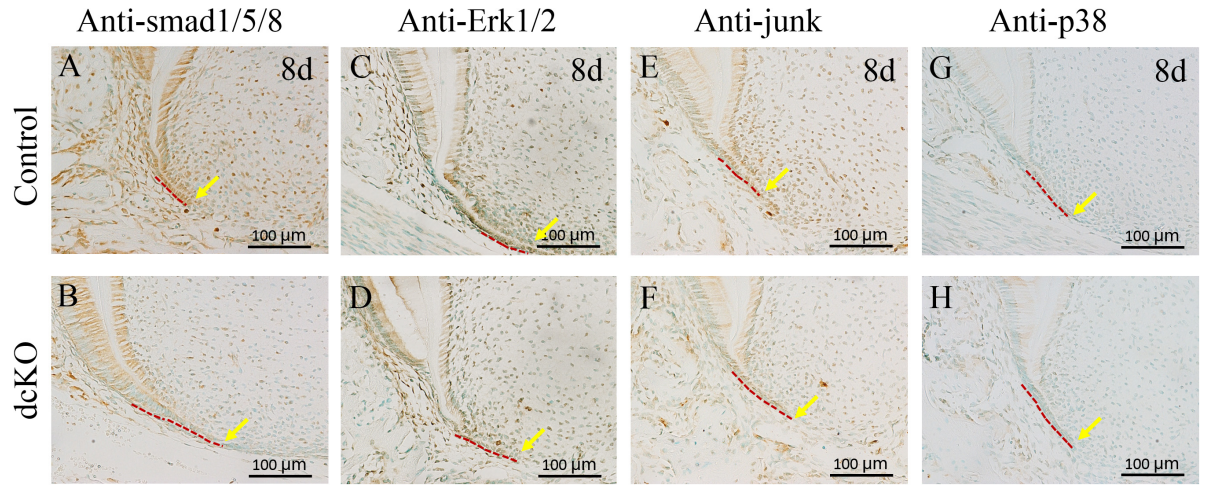

FIGURE 3 | Smad-dependent and independent BMP signaling pathways in the dcKO molar root. **(A)** The immunohistochemistry with antibody against p-Smad1/5/8 in the 1st molar root of P8 WT mouse. **(B)** The immunohistochemistry with antibody against p-Smad1/5/8 in the 1st molar root of P8 dcKO mouse. **(C)** The immunohistochemical staining of p-Erk1/2 in the 1st molar root of P8 WT mouse. **(D)** The immunohistochemical staining of p-Erk1/2 in the 1st molar root of P8 dcKO mouse. **(E)** The p-Junk immunohistochemical staining in the 1st molar root of P8 WT mouse. **(F)** The p-Junk immunohistochemical staining in the 1st molar root of P8 dcKO mouse. **(G)** The immunohistochemistry with antibody against p-p38 in the 1st molar root of P8 WT mouse. **(H)** The immunohistochemistry with antibody against p-p38 in the 1st molar root of P8 dcKO mouse. (The dashed red lines indicated the HERS; the yellow arrows delineated the end of HERS).

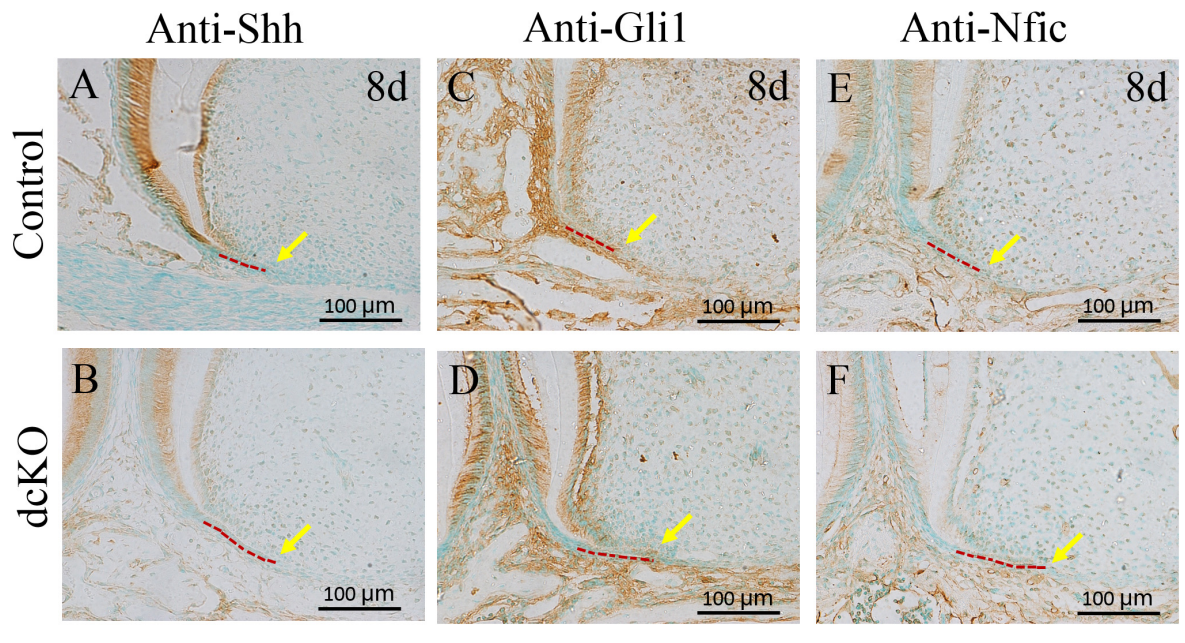

FIGURE 4 | The immunohistochemical staining of the markers involved in tooth root development. **(A)** The Shh immunohistochemical staining in the 1st molar root of P8 WT mouse. **(B)** The Shh immunohistochemical staining in the 1st molar root of P8 dcKO mouse. **(C)** The immunohistochemical staining of Gli1 in the 1st molar root of P8 WT mouse. **(D)** immunohistochemical staining of Gli1 in the 1st molar root of P8 dcKO mouse. **(E)** The immunohistochemistry with antibody against Nfic in the 1st molar root of P8 WT mouse. **(F)** The immunohistochemistry with antibody against Nfic in the 1st molar root of P8 dcKO mouse. (The dashed red lines indicated the HERS; the yellow arrows delineated the end of HERS).

Dspp Transgene Partially Rescued the SRA in the dcKO Roots

As the pivotal transcription factor in tooth root development, Nfic played an essential role in the differentiation and maturation of root mesenchyme (Kim et al., 2015). To explore the odontogenic differentiation and maturation of the dcKO root mesenchyme, the expression of OSX and *Dspp* was examined. The immunohistochemical staining showed the OSX positive nucleus lining in the P16 control root odontoblast layer (**Figure 5A**), but only the sporadic OSX positive nucleus in the P16 dcKO

root odontoblasts (**Figure 5B**). The DSP staining in the dcKO molar root was also much weaker than that of control molar (**Figures 5C,D**). The *in situ* hybridization with the *Dspp* anti-sense RNA probe further confirmed the reduced *Dspp* expression in the dcKO root odontoblasts (**Figures 5E,F**). To address if the SRA in the dcKO molars resulted from the impaired odontogenic differentiation and maturation, the molar roots of dcKO;*Dspp*^{Tg} mice were compared to those of control and dcKO mice. The micro-CT scanning showed that although still shorter and thinner than control root dentin, the root dentin of the P18 dcKO;*Dspp*^{Tg} molar was significantly longer, thicker, and larger than that of the dcKO molar (**Figures 5G,H**), indicating a partial rescue of the SRA in the dcKO molar by transgenic *Dspp*.

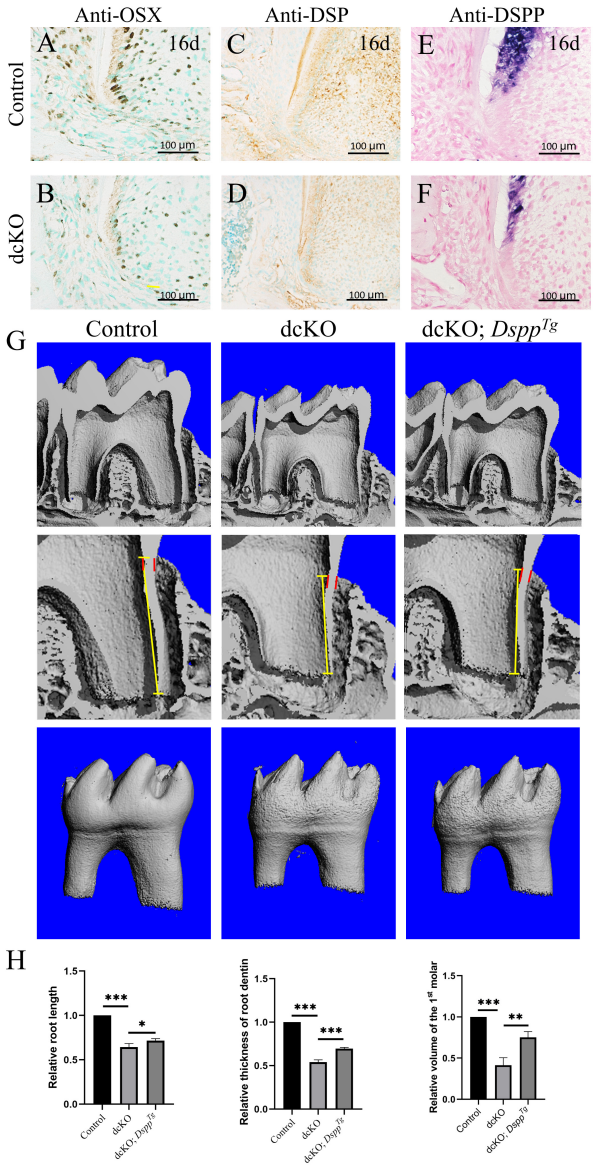

FIGURE 5 | Expression of the odontogenic maturation markers and the morphology of the dcKO; *Dspp*^{Tg} molar root. **(A)** The immunohistochemistry with antibody against OSX in the 1st molar root of P16 WT mouse. **(B)** The immunohistochemistry with antibody against OSX in the 1st molar root of P16 dcKO mouse. **(C)** The immunohistochemistry staining of DSP in the 1st molar root of P16 WT mouse. **(D)** The immunohistochemistry staining of DSP in the 1st molar root of P16 dcKO mouse. **(E)** The *in situ* hybridization with *Dspp* anti-sense RNA probe in the 1st molar root of P16 WT mouse. **(F)** The *in situ* hybridization with *Dspp* anti-sense RNA probe in the 1st molar root of P16 dcKO mouse. **(G)** The micro-CT images of the molar root dentin in the P18 WT, dcKO, and dcKO; *Dspp*^{Tg} mice. **(H)** The statistical analysis of the root dentin length, thickness and volume in the P18 WT, dcKO, and dcKO; *Dspp*^{Tg} mice. (The dashed red lines indicated the HERS; the yellow arrows delineated the end of HERS; ***$p < 0.001$; **$p < 0.01$; *$p < 0.05$).

DISCUSSION

Short root anomaly is the most common phenotype in tooth root defects. In humans, the prevalence of SRA varies from 0.6 to 2.4% in different populations (Puranik et al., 2015). Genetically, the etiology of SRA could arrange from root mesenchyme to epithelial HERS (Huang et al., 2012). With regards to the role of BMP signaling in root development, previous studies demonstrated that *Bmps* were dominantly expressed in the root mesenchyme (Yamashiro et al., 2003), which was essential for the activation and maintenance of *Nfic* expression by activating Smad-dependent BMP signaling in HERS (Huang et al., 2010). However, up to now, there was no report on the involvement of HERS-derived BMPs in tooth root development. In this study, we reported that the deficiency of *Bmp2* and *Bmp4* in the epithelial HERS also resulted in SRA, which extends the insight of BMPs in tooth root development, as well as the etiological knowledge of SRA.

Different from the tooth root defects caused by the single deletion of *Bmp2* or *Bmp4* in the root mesenchyme (Torres et al., 2008; Guo et al., 2015), only the combined abrogation of *Bmp2* and *Bmp4* in ectoderm could result in SRA. The single deletion of *Bmp2* or *Bmp4* in ectoderm, or the double heterozygous of *Bmp2* and *Bmp4* deletion in ectoderm, or even the *K14-cre;Bmp2*$^{f/f}$*;Bmp4*$^{f/+}$, and *K14-cre; Bmp2*$^{f/+}$*;Bmp4*$^{f/f}$ mice exhibited normal tooth roots (**Supplementary Figure 1**). These results implicated that the ectoderm-derived Bmp2 and Bmp4 were not only required for the root development in a very low dosage, but also had a functional redundancy during root development.

During the morphogenesis of tooth root, HERS induced *Nfic* expression in root mesenchyme and then underwent degeneration (Lee et al., 2014). The delayed degeneration of HERS was usually associated with SRA (Huang et al., 2012). In the dcKO mice, the reduced cell death detected the persistent HERS, which was similar to the outcomes of the *Bmp2* or *Smad4* inactivation in root odontoblasts (Wang et al., 2012). The decreased cell death in the persistent dcKO HERS could be attributed to the ectodermal abrogation of *Bmp2* and *Bmp4*, thus, the epithelial *Bmp2* and *Bmp4* were suggested to promote the degeneration of HERS. However, it was hard to distinguish the ectoderm-derived or the mesenchyme-derived BMPs responsible for the delayed HRES degeneration because the BMP-Smad4 signaling was down-regulated in the HERS

and root mesenchyme. A previous study demonstrated that the epithelial Smad4 was essential for the normal morphogenesis of HERS, as well as the root formation (Huang et al., 2010). Interestingly, the p-Erk1/2 and p-Junk were also reduced in the dcKO HERS, suggesting that the Erk and/or Junk signaling in HERS might be involved in the HERS degeneration. However, whether the epithelial BMP-Erk and/or BMP-Junk signaling play an essential role in the molar root development still requires further investigation, especially the phenotype of the *K14-cre;Erk2*$^{f/f}$ HERS and molar root.

In the dcKO molar roots, abrogation of *Bmp2* and *Bmp4* in ectoderm-derived HERS resulted in the reduction of BMP-Smad4 signaling in root mesenchyme, indicating a disruption of epithelium-mesenchyme interactions during root development. Since the BMP-Smad4 signaling in HERS was reported to activate *Shh* expression, which activated the *Nfic* expression in root mesenchyme (Li et al., 2015), the remarkable decrease of Shh in dcKO HERS and root mesenchyme, as well as the reduced Gli1 staining in dcKO root mesenchyme, were coincided to the down-regulated BMP-Smad4 signaling in the dcKO HERS. Consistent with the decreased Shh-Gli1 signaling in root mesenchyme, the Nfic immunohisto-staining in the dcKO root mesenchyme was found to be down-regulated, which indicated that the HERS-derived Bmps also was required for the differentiation and maturation of root mesenchyme.

OSX was regarded as a key down-stream target of Nfic because a series of conditional *OSX* knock-out mice exhibited a similar root phenotype to *Nfic* deficient mouse (Zhang et al., 2015). *OSX* was essential to activate *Dmp1* and *Dspp*, two key matrix proteins for root dentin (Zhang et al., 2018). Although the elongation and polarization of the root odontoblasts in the dcKO molars displayed no alteration, the reduced OSX-positive odontoblasts suggested an impaired odontogenic differentiation. The weakened DSP staining and reduced *Dspp* transcription also indicated a suppressed odontogenic differentiation and maturation of the root odontoblasts (Zhang et al., 2018). Therefore, the SRA in the dcKO mice was implicated in the suppression on root odontogenic differentiation. *Dspp* transgene at least partially rescued the significantly decreased length and thickness of the dcKO molar root, explicating that epithelial *Bmp2* and *Bmp4* deficiency impacted the root dentin formation through the epithelial-mesenchymal interactions.

In summary, our study indicated that although the ectoderm-derived Bmp2 and Bmp4 were not as robust as the Bmp2 and Bmp4 derived from root mesenchyme, they were critical to maintaining the epithelial-mesenchyme interaction during tooth root development, which was required for the degeneration of HERS, as well as the differentiation and maturation of root odontoblasts.

DATA AVAILABILITY STATEMENT

The original contributions presented in the study are included in the article/**Supplementary Material**, further inquiries can be directed to the corresponding authors.

ETHICS STATEMENT

The animal study was reviewed and approved by the Ethics Committee at The Second Affiliated Hospital of Harbin Medical University. Written informed consent was obtained from the owners for the participation of their animals in this study.

AUTHOR CONTRIBUTIONS

XX and BZ contributed to the conception and design of the study. XL and SG wrote the initial draft of the manuscript. HM, DS, HC, LL, HJ, and YL performed the experimental work and data analysis. XW revised the manuscript. All authors have read and approved the final version of the manuscript.

FUNDING

Research reported in this publication was supported by the National Natural Science Foundation of China (No. 81600848) to XX, the Postdoctoral Science Foundation of Heilongjiang Province (No. LBH-Z19079) to XX, the Natural Science Foundation of Heilongjiang Province of China (No. LH2020H056) to XX, the National Natural Science Foundation of China (No. 81870736) to BZ, and the Natural Science Foundation of Heilongjiang Province of China (No. ZD2019H002) to XW.

ACKNOWLEDGMENTS

We thank Yuanbo Zhan for providing the technical support for genotyping. We also thank Shouli Guo and Xue Guan for mouse breeding in the Laboratory Animal Center at The Second Affiliated Hospital of Harbin Medical University.

SUPPLEMENTARY MATERIAL

The Supplementary Material for this article can be found online at: https://www.frontiersin.org/articles/10.3389/fphys.2021.660644/full#supplementary-material

Supplementary Figure 1 | The plain X-ray images of the tooth root. **(A)** The plain X-ray images of the mandbiles from the P3W WT, *K14-cre; Bmp2*$^{f/+}$*;Bmp4*$^{f/+}$, *K14-cre; Bmp2*$^{f/f}$*;Bmp4*$^{f/+}$, *K14-cre; Bmp2*$^{f/+}$*;Bmp4*$^{f/f}$, and *K14-cre; Bmp2*$^{f/f}$*;Bmp4*$^{f/f}$ (dcKO) mice. **(B)** The plain X-ray images of the first molars from the P3W WT, *K14-cre; Bmp2*$^{f/+}$*;Bmp4*$^{f/+}$, *K14-cre; Bmp2*$^{f/f}$*;Bmp4*$^{f/+}$, *K14-cre; Bmp2*$^{f/+}$*;Bmp4*$^{f/f}$, and *K14-cre; Bmp2*$^{f/f}$*;Bmp4*$^{f/f}$ (dcKO) mice.

Supplementary Figure 2 | The histology of the P10W dcKO 1st molar root. **(A)** The H&E staining of the 1st molar root of P10W WT mouse. **(B)** The H&E staining of the 1st molar root of P10W dcKO mouse. **(C)** The K14 staining in the 1st molar root of P10W WT mouse. **(D)** The K14 staining in the 1st molar root of P10W dcKO mouse. Arrows in panel **D** delineated the K14 positive cells.

REFERENCES

Balic, A. (2019). Concise review: cellular and molecular mechanisms regulation of tooth initiation. *Stem Cells* 37, 26–32. doi: 10.1002/stem.2917

Bosshardt, D. D., Stadlinger, B., and Terheyden, H. (2015). Cell-to-cell communication –periodontal regeneration. *Clin. Oral Implants Res.* 26, 229–239. doi: 10.1111/clr.12543

Chai, Y., and Maxson, R. E. (2006). Recent advances in craniofacial morphogenesis. *Dev. Dyn.* 235, 2353–2375. doi: 10.1002/dvdy.20833

Guo, F., Feng, J., Wang, F., Li, W., Gao, Q., Chen, Z., et al. (2015). Bmp2 deletion causes an amelogenesis imperfecta phenotype via regulating enamel gene expression. *J. Cell. Physiol.* 230, 1871–1882. doi: 10.1002/jcp.24915

Huang, X., Bringas, P. Jr., Slavkin, H. C., and Chai, Y. (2009). Fate of HERS during tooth root development. *Dev. Biol.* 334, 22–30. doi: 10.1016/j.ydbio.2009.06.034

Huang, X., Xu, X., Bringas, P. Jr., Hung, Y. P., and Chai, Y. (2010). Smad4-Shh-Nfic signaling cascade-mediated epithelial-mesenchymal interaction is crucial in regulating tooth root development. *J. Bone Miner. Res.* 25, 1167–1178. doi: 10.1359/jbmr.091103

Huang, X. F., and Chai, Y. (2012). Molecular regulatory mechanism of tooth root development. *Int. J. Oral Sci.* 4, 177–181. doi: 10.1038/ijos.2012.61

Jani, P. H., Gibson, M. P., Liu, C., Zhang, H., Wang, X., Lu, Y., et al. (2016). Transgenic expression of Dspp partially rescued the long bone defects of Dmp1-null mice. *Matrix Biol.* 52-54, 95–112. doi: 10.1016/j.matbio.2015.12.001

Kim, T. H., Bae, C. H., Lee, J. C., Ko, S. O., Yang, X., Jiang, R., et al. (2013). β-catenin is required in odontoblasts for tooth root formation. *J. Dent. Res.* 92, 215–221. doi: 10.1177/0022034512470137

Kim, T. H., Bae, C. H., Yang, S., Park, J. C., and Cho, E. S. (2015). Nfic regulates tooth root patterning and growth. *Anat. Cell Biol.* 48, 188–194.

Lee, D. S., Choung, H. W., Kim, H. J., Gronostajski, R. M., Yang, Y. I., Ryoo, H. M., et al. (2014). NFI-C regulates osteoblast differentiation via control of osterix expression. *Stem Cells* 32, 2467–2479. doi: 10.1002/stem.1733

Lee, D. S., Park, J. T., Kim, H. M., Ko, J. S., Son, H. H., Gronostajski, R. M., et al. (2009). Nuclear factor I-C is essential for odontogenic cell proliferation and odontoblast differentiation during tooth root development. *J. Biol. Chem.* 284, 17293–17303. doi: 10.1074/jbc.M109.009084

Li, J., Feng, J., Liu, Y., Ho, T. V., Grimes, W., Ho, H. A., et al. (2015). BMP-SHH signaling network controls epithelial stem cell fate via regulation of its niche in the developing tooth. *Dev. Cell* 33, 125–135. doi: 10.1016/j.devcel.2015.02.021

Liu, Y., Feng, J., Li, J., Zhao, H., Ho, T. V., and Chai, Y. (2015). An Nfic-hedgehog signaling cascade regulates tooth root development. *Development* 142, 3374–3382. doi: 10.1242/dev.127068

Luder, H. U. (2015). Malformations of the tooth root in humans. *Front. Physiol.* 6:307. doi: 10.3389/fphys.2015.00307

Ono, W., Sakagami, N., Nishimori, S., Ono, N., and Kronenberg, H. M. (2016). Parathyroid hormone receptor signalling in osterix-expressing mesenchymal progenitors is essential for tooth root formation. *Nat. Commun.* 7:11277. doi: 10.1038/ncomms11277

Park, J. C., Herr, Y., Kim, H. J., Gronostajski, R. M., and Cho, M. I. (2007). Nfic gene disruption inhibits differentiation of odontoblasts responsible for root formation and results in formation of short and abnormal roots in mice. *J. Periodontol.* 78, 1795–1802. doi: 10.1902/jop.2007.060363

Puranik, C. P., Hill, A., Henderson Jeffries, K., Harrell, S. N., Taylor, R. W., and Frazier-Bowers, S. A. (2015). Characterization of short root anomaly in a Mexican cohort–hereditary idiopathic root malformation. *Orthod. Craniofac. Res.* 18 Suppl 1, 62–70. doi: 10.1111/ocr.12073

Steele-Perkins, G., Butz, K. G., Lyons, G. E., Zeichner-David, M., Kim, H. J., Cho, M. I., et al. (2003). Essential role for NFI-C/CTF transcription-replication factor in tooth root development. *Mol. Cell Biol.* 23, 1075–1084. doi: 10.1128/mcb.23.3.1075-1084.2003

Ten Cate, A. R. (1996). The role of epithelium in the development, structure and function of the tissues of tooth support. *Oral Dis.* 2, 55–62. doi: 10.1111/j.1601-0825.1996.tb00204.x

Torres, C. B., Alves, J. B., Silva, G. A., Goes, V. S., Nakao, L. Y., and Goes, A. M. (2008). Role of BMP-4 during tooth development in a model with complete dentition. *Arch. Oral Biol.* 53, 2–8. doi: 10.1016/j.archoralbio.2007.07.005

Wang, Y., Li, L., Zheng, Y., Yuan, G., Yang, G., He, F., et al. (2012). BMP activity is required for tooth development from the lamina to bud stage. *J. Dent. Res.* 91, 690–695. doi: 10.1177/0022034512448660

Xie, X., Liu, C., Zhang, H., Jani, P. H., Lu, Y., Wang, X., et al. (2016). Abrogation of epithelial BMP2 and BMP4 causes amelogenesis imperfecta by reducing MMP20 and KLK4 expression. *Sci. Rep.* 6:25364. doi: 10.1038/srep25364

Xiong, J., Gronthos, S., and Bartold, P. M. (2013). Role of the epithelial cell rests of Malassez in the development, maintenance and regeneration of periodontal ligament tissues. *Periodontology 2000* 63, 217–233. doi: 10.1111/prd.12023

Yamashiro, T., Tummers, M., and Thesleff, I. (2003). Expression of bone morphogenetic proteins and Msx genes during root formation. *J. Dent. Res.* 82, 172–176. doi: 10.1177/154405910308200305

Zhang, H., Jiang, Y., Qin, C., Liu, Y., Ho, S. P., and Feng, J. Q. (2015). Essential role of osterix for tooth root but not crown dentin formation. *J. Bone Miner. Res.* 30, 742–746. doi: 10.1002/jbmr.2391

Zhang, H., Xie, X., Liu, P., Liang, T., Lu, Y., and Qin, C. (2018). Transgenic expression of dentin phosphoprotein (DPP) partially rescued the dentin defects of DSPP-null mice. *PLoS One* 13:e0195854. doi: 10.1371/journal.pone.0195854

Conflict of Interest: The authors declare that the research was conducted in the absence of any commercial or financial relationships that could be construed as a potential conflict of interest.

Publisher's Note: All claims expressed in this article are solely those of the authors and do not necessarily represent those of their affiliated organizations, or those of the publisher, the editors and the reviewers. Any product that may be evaluated in this article, or claim that may be made by its manufacturer, is not guaranteed or endorsed by the publisher.

frontiers in Physiology

ORIGINAL RESEARCH
published: 26 August 2021
doi: 10.3389/fphys.2021.703593

Novel Molecule Nell-1 Promotes the Angiogenic Differentiation of Dental Pulp Stem Cells

Mengyue Li[1†], Qiang Wang[2†], Qi Han[1], Jiameng Wu[1], Hongfan Zhu[1], Yixuan Fang[1], Xiuting Bi[1], Yue Chen[1], Chao Yao[2] and Xiaoying Wang[1]*

[1] Shandong Key Laboratory of Oral Tissue Regeneration, Shandong Engineering Laboratory for Dental Materials and Oral Tissue Regeneration, School and Hospital of Stomatology, Cheeloo College of Medicine, Shandong University, Jinan, China, [2] Jinan Stomatological Hospital, Jinan, China

Introduction: This work aimed to reveal the crucial role of Nell-1 in the angiogenic differentiation of human dental pulp stem cells (DPSCs) alone or co-cultured with human umbilical vein endothelial cell (HUVECs) *in vitro* and whether this molecule is involved in the pulp exposure model *in vivo*.

Methods: Immunofluorescence was conducted to ascertain the location of Nell-1 on DPSCs, HUVECs, and normal rat dental tissues. RT-PCR, Western blot, and ELISA were performed to observe the expression levels of angiogenic markers and determine the angiogenic differentiation of Nell-1 on DPSCs alone or co-cultured with HUVECs, as well as *in vitro* tube formation assay. Blood vessel number for all groups was observed and compared using immunohistochemistry by establishing a rat pulp exposure model.

Results: Nell-1 is highly expressed in the nucleus of DPSCs and HUVECs and is co-expressed with angiogenic markers in normal rat pulp tissues. Hence, Nell-1 can promote the angiogenic marker expression in DPSCs alone and co-cultured with other cells and can enhance angiogenesis *in vitro* as well as in the pulp exposure model.

Conclusion: Nell-1 may play a positive role in the angiogenic differentiation of DPSCs.

Keywords: human dental pulp cells, nel-like molecule-1, human umbilical vein endothelial cells, angiogenesis, pulp regeneration

OPEN ACCESS

Edited by:
Q. Adam Ye, Massachusetts General Hospital and Harvard Medical School, United States

Reviewed by:
Angelo Leone, University of Palermo, Italy
Thanaphum Osathanon, Chulalongkorn University, Thailand

***Correspondence:**
Xiaoying Wang
xiaoyingwang@sdu.edu.cn

[†] These authors have contributed equally to this work and share first authorship

Specialty section:
This article was submitted to Craniofacial Biology and Dental Research, a section of the journal Frontiers in Physiology

Received: *30 April 2021*
Accepted: *05 August 2021*
Published: *26 August 2021*

Citation:
Li M, Wang Q, Han Q, Wu J, Zhu H, Fang Y, Bi X, Chen Y, Yao C and Wang X (2021) Novel Molecule Nell-1 Promotes the Angiogenic Differentiation of Dental Pulp Stem Cells. Front. Physiol. 12:703593. doi: 10.3389/fphys.2021.703593

INTRODUCTION

Nel-like molecule-1 (Nell-1) is a novel signaling molecule, with a crucial positive regulatory role in chondrogenesis and osteogenesis (Li C. et al., 2019); however, its involvement in pulp angiogenesis, which is an important part of pulp regeneration, remains poorly studied. Vasculogenesis is the differentiation of endothelial cells to form blood vessels during embryonic development, while angiogenesis means new vessels sprouting from pre-existing vasculature (Chung and Ferrara, 2011), both of them are mediated by angiogenic growth factors (Rombouts et al., 2017). Among which, vascular endothelial growth factor (VEGF) is a strong regulator of physiological and pathological angiogenesis during embryogenesis and pathological angiogenesis associated with tumors (Ferrara et al., 2003) and alveolar bone process morphogenesis (An et al., 2017). VEGF receptor (VEGFR) has a potential part in mediating the biological effects of VEGF, leading to homodimerization and autophosphorylation when VEGF dimers bind to VEGFR-1 and

VEGFR-2 (Ferrara, 2002). Activating VEGFR-2 (Flk-1) could induce angiogenesis and increase vascular permeability, mitogenesis, and chemotaxis in endothelial cells.

Nell-1 encodes a secreted protein (Zhang et al., 2010) and was discovered by Ting et al. (1999), when they accidentally operated for the surgical correction of unilateral coronal synostosis. In our previous study, Nell-1 shows spatiotemporal expression patterns during murine tooth (Tang et al., 2013) and is mainly expressed in the odontoblasts, pulp fibroblasts, and endothelial cells of the blood vessels in human teeth (Tang et al., 2013; Liu et al., 2016). Fahmy-Garcia et al. (2018) confirmed that Nell-1 can enhance the migration of mesenchymal stem cells (MSCs) and the angiogenesis of HUVECs. DPSCs form a dentin/pulp-like complex (Gronthos et al., 2000) with neural-like cells (Stevens et al., 2008; Gonmanee et al., 2018; Li D. et al., 2019), endotheliocytes (d'Aquino et al., 2007), and vascular tissues (Karbanova et al., 2011) and have a predominant pro-angiogenic influence compared with dental follicle precursor cells (FSCs) (Hilkens et al., 2014). These data indicate that DPSCs are a promising population of stem cells that could achieve angiogenesis. The potential of Nell-1 to induce the angiogenetic differentiation of DPSCs is of great interest.

The survival rate of regenerating vascular dependent tissues could be increased when MSCs are co-transplanted with hematopoietic stem cells (Moioli et al., 2008). Endothelial cells (ECs) are a potential source of neovascularization during tissue regeneration (Moioli et al., 2008). Angiogenesis highly occurs between stem cells and endothelial cells through synergistic effect or direct cell contact (Aguirre et al., 2010; Allen et al., 2011; Rao et al., 2012; Kang et al., 2013). Several studies also confirmed that the co-culture of HUVECs with stem cells from the apical papilla (SCAPs) or DPSCs can enhance the angiogenic potential (Dissanayaka et al., 2012; Liu et al., 2018). Whether Nell-1 is directly involved in the angiogenetic differentiation of DPSCs co-cultured with HUVECs must be explored.

MATERIALS AND METHODS

Isolation, Culture, and Identification of DPSCs and Co-culture of DPSCs With HUVECs

Third molars were acquired after obtaining informed consent from each patient (15–25 years of age, male and female) who underwent routine extraction with no caries or periodontal diseases. The extracted teeth were washed with PBS and cut with fissure in sterile conditions. The acquired pulp tissues were digested with 3% I-type collagenase (Solarbio, Beijing, China), and the dental tissues were transported in 25 cm^2 cell culture flasks. HUVECs and its specific endothelial cell medium (ECM) were acquired from ScienCell company (San Diego, United States) (Leopold et al., 2019). Each cell type was used at passages 3–5 in all experiments.

Human DPSCs at passage 3 were collected. The cells were tested for MSC markers CD90, CD44 and CD105, and hematopoietic stem markers CD34 and CD45 by using flow cytometric (CytoFLEX, CA, United States) with PBS as the negative control. Osteogenic and adipogenic differentiation assays were performed on the DPSCs to detect their multi-lineage differentiation ability. The cells were stained and examined under an inverted microscope after 21 days. The experiments group was grown in osteogenic differentiation medium (α-MEM containing 10%FBS, 0.01 nmol/l dexamethasone, 10 mmol/l β-glycerophosphate, and 50 mg/mL ascorbic acid) (Sigma, St Louis, MO, United States) or adipogenic differentiation medium (Pythonbio, China), and the control group was treated similarly to the above cell culture.

DPSCs and HUVECs were mixed directly at a 1:1 number ratio with new mixed medium prepared by mixing the α-MEM (containing 10% FBS) with ECM at 1:1 ratio.

RNA Extraction and Quantitative Real-Time Polymerase Chain Reaction (qRT-PCR)

DPSCs alone and co-culture groups were cultured in six-well plates in α-MEM (containing 10% FBS) or mixed medium with 0 and 50 ng/mL Nell-1 (CHO-derived human Nell-1 protein, R&D Systems, 5487-NL-050, Minneapolis, MN, United States) for 1, 2, 3, 7, and 14 days. Total RNA was isolated using Trizol (Takara, Tokyo, Japan). Isolated RNA sample of 1.0 μg weight was reverse-transcribed into cDNA with cDNA synthesis kit (Takara, Tokyo, Japan). qRT-PCR was performed with TB Green (Takara, Tokyo, Japan) and LightCycler 480 system. Primer sequences are shown in **Table 1**.

Western Blot

The cells were planked similarly to PCR, lysed with RIPA buffer containing 1% PMSF (Solarbio, Beijing, China) for 30 min. Cellular proteins were isolated and quantified by a BCA kit (Solarbio, Beijing, China), separated on 10% polyacrylamide gels, and transferred onto the polyvinylidene difluoride membranes (Millipore, Billerica, United States). Following washing with TBST, the membranes were incubated with primary antibodies including Flk-1 antibody (1:1,000 dilution; Novus, NB200-208, United States) and GAPDH antibody (1:10,000 dilution; Proteintech, China) overnight at 4°C. Then, the membranes were incubated with secondary antibodies for 2 h at RT and then washed again. The results were analyzed by Image J software.

ELISA

Quantikine ELISA kit (Dakewe, Shenzhen, China) was used to measure VEGF expression, and the process was similar to that in RNA extraction. Cell supernatants were collected at 1, 2, 3, 7, and

TABLE 1 | Primer sequences used for real-time PCR.

Gene	Forward sequences	Reverse sequences
GAPDH	ATCACCATCTCCAGGAGCGA	CCTTCTCCATGGTGGTGAAGAC
VEGF	GAGCCTTGCCTTGCTGCTCTAC	CACCAGGGTCTCGATTGGATG
Flk-1	AGCCAGCTCTGGATTTGTGGA	CATGCCCTTAGCCACTTGGAA

14 days with 0 and 50 ng/mL Nell-1. ELISA was performed in accordance with manufacturer's instructions.

Cell Immunofluorescence for Nell-1

DPSCs and HUVECs were separately cultured in 24-well plates for 24 h. The cells were fixed with 4% paraformaldehyde and sealed with normal goat serum (Zhongshan, Beijing, China) at 37°C for 30 min, and then incubated with primary antibody for Nell-1 (1:100 dilution; Proteintech, China) at 4°C overnight. After being washed three times in PBS, the second antibodies (1:500 dilution; Zhongshan, Beijing, China) were incubated for 2 h. DAPI (Solarbio, Beijing, China) was used to stain the nucleus of pulp tissues. The cells were observed under a fluorescence microscope.

In vitro Tube Formation Assay

To investigate which minimum concentration of Nell-1 could promote formation of endothelial tubules and a blood vessel network when DPSCs were co-cultured with HUVECs, Matrigel angiogenesis assay was carried out. Co-culture groups (HUVECs: DPSCs, 1:1) were cultured in 24-well plates in mixed medium (containing 0.5%FBS) with 0, 50, 100, and 200 ng/mL Nell-1 at 6 h. Images were observed under an inverted phase-contrast microscope.

Tooth Sample Collection and Preparation

All animal experimental protocols were performed in accordance with the guidelines of the Institutional Review Board of School of Stomatology, Shandong University. Twelve Wistar rats were randomly categorized into three groups: (1) collagen group, pulp cavity was covered with collagen sponge (BIOT Biology, China) soaked with PBS; (2) Nell-1 group, pulp cavity was covered with collagen sponge soaked with 700 ng/mL Nell-1; and (3) normal teeth group, upper molars did not receive cavities or any other treatments. The occlusal surface of non-carious upper first molars was selected to establish the rat pulpitis model with a #35 K-file under anesthesia. Afterward, the cavities were sealed with glass ions (VOCO, Ionofil Molar, Germany) as the bottom material and with resin (3MESPE, Filtek Z350 XT, United States) for the collagen and Nell-1 groups. After 1 week, the rats were sacrificed. The experimental teeth were fixed in 4% paraformaldehyde for 24 h, demineralized with 10% ethylenediaminetetraacetic acid solution, and cut with a blade (5 um serial sections). The sections were processed for histological and immunohistochemical examinations.

Histology, Immunohistochemistry, and Immunofluorescence

Hematoxylin and eosin (HE, Solarbio, Beijing, China) staining was used to observe the morphology and structure of pulp tissues.

Immunohistochemical staining and immunofluorescence were performed to observe the blood vessel count and distribution of Nell-1, VEGF, and Flk-1. Immunohistochemical analysis was performed by using the primary antibodies CD34 (absin, Shanghai, China) and CD31 (Servicebio, Wuhan, China), and the tissues were counterstained with hematoxylin. Double immunostaining of either VEGF (1:100 dilution; Novus, NB100-664SS, United States) or FLK-1 (1:100 dilution; Novus, NB200-208, United States) with Nell-1 (1:100 dilution; Proteintech, 21783-1-AP, China) and then immunostaining for second antibodies (1:500 dilution; absin, China) was performed to observe the relationship among Nell-1, VEGF, Flk-1. DAPI was used to stain the nucleus. Each slice was observed by a microscope (BX51, Olympus, Japan).

Statistical Analyses

Student's *t*-test or one-way ANOVA was used to compare statistical significance between various treatments and respective controls by using GraphPad Prism software. All experiments were repeated three times from independent samples from different donors. Data were expressed as mean ± standard deviation. $P < 0.05$ was considered statistically significant.

RESULTS

Isolation and Characterization of DPSCs

The primary cells were successfully isolated from pulp tissues and displayed a long spindle shape with adherent growth (**Figure 1A**). Alizarin red and oil red O staining showed that DPSCs possess strong osteo/dentinogenic and adipogenic potential (**Figures 1B–E**). Flow cytometry results showed that DPSCs are positive for CD90, CD44, and CD105 but negative for CD34, CD45 (**Figures 1F–J**).

Nell-1 Promoted the Angiogenesis-Related Gene and Protein Expression in DPSCs

Angiogenic markers including VEGF and Flk-1 were detected by qRT-PCR. In DPSC group, 50 ng/mL Nell-1 remarkably promoted VEGF and Flk-1 expression compared with those in the control in days 3, 7, and 14 (apart from Flk-1 in day 14) (**Figures 2A,B**). The gene expression levels of VEGF in DPSC group increased in days 1 and 2 compared with those in the control group; however, no statistical significance was found.

Western blot analysis was performed to detect relative protein expression. In the experiment group, the angiogenesis-related protein expression was increased in days 3 and 7, but no significant difference was observed in days 1, 2, and 14 compared with those in the control group (**Figures 2C,D**).

Nell-1 Promoted the Angiogenesis-Related Gene and Protein Expression and the Formation of Vessel-Like Structures in the Co-culture Group

On the basis of the VEGF expression levels, 50 ng/mL Nell-1 significantly promoted the angiogenetic differentiation in the

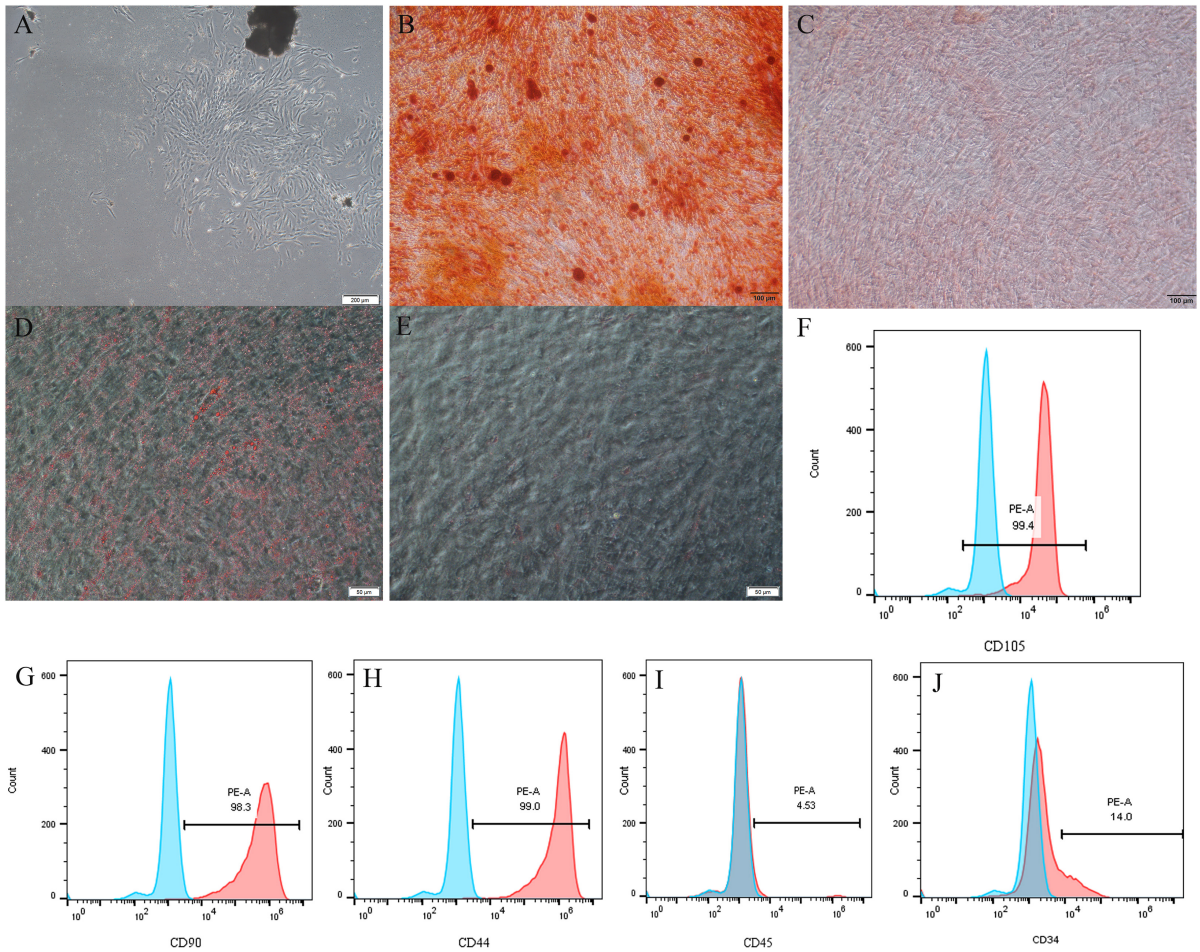

FIGURE 1 | Isolation and characterization of DPSCs. **(A)** Representative image to display primary DPSCs. **(B–E)** DPSCs underwent osteogenic/odontogenic and adipogenic differentiation and were stained after 21 days. Alizarin red staining indicated mineralized nodules in the osteogenic/odontogenic group **(B)** but negative for the control group **(C)**. Oil red O images indicated oil droplets in the adipogenic group **(D)** but negative for the control group **(E)**. DPSCs were positive for mesenchymal stem cells markers CD105 **(F)**, CD90 **(G)**, and CD44 **(H)**, but negative for hematopoietic stem cells markers CD45 **(I)** and CD34 **(J)**.

experiment group compared with that in the control in days 3 and 7, but no statistical significance was observed in days 1, 2, and 14 (**Figure 3A**). Flk-1 expression level was increased by 50 ng/mL Nell-1 treatment compared with that in the control in days 2 and 7 (**Figure 3B**). However, these levels decreased significantly in days 3 and 14.

Western blot analysis and ELISA were performed to investigate Flk-1 and VEGF protein expression, respectively. In the experiment group, the angiogenesis-related protein Flk-1 was increased in days 3, 7, and 14, but no significant difference was found in days 1 and 2 compared with that in the control group (**Figures 3C,D**). The concentration of VEGF protein in supernatants secreted by the co-culture group was increased by 50 ng/mL Nell-1 compared with that in the control group in days 3, 7, and 14 (**Figures 3E,F**).

Compared with control group, co-culture group seeded on Matrigel with 50 and 100 ng/mL Nell-1 formed more vessel-like structures, whereas no significant difference was observed in 200 ng/mL Nell-1 (**Figure 4**).

Nell-1 Distribution in DPSCs, HUVECs, and Normal Pulp Tissues

Cell immunofluorescence assay displayed that Nell-1 is mainly expressed in the nucleus of DPSCs and HUVECs (**Figures 5A–H**). HE staining and immunofluorescence were conducted to present the structure of normal pulp tissues and the distribution of Nell-1.

Double immunofluorescence of pulp tissue sections was used to observe the distribution of Nell-1, VEGF, and Flk-1 in the dental pulp (**Figures 5I–R**). High expression of Nell-1, VEGF, and Flk-1 was found in the odontoblasts, pulp fibroblasts, and endothelial cells of the blood vessels of the dental pulp. The merged picture showed that Nell-1 is co-expressed with VEGF and Flk-1.

Histology and Immunohistochemistry

At week 1, inflamed tissues around cavities were discovered by HE staining (**Figures 6A–C**). Immunohistochemical staining

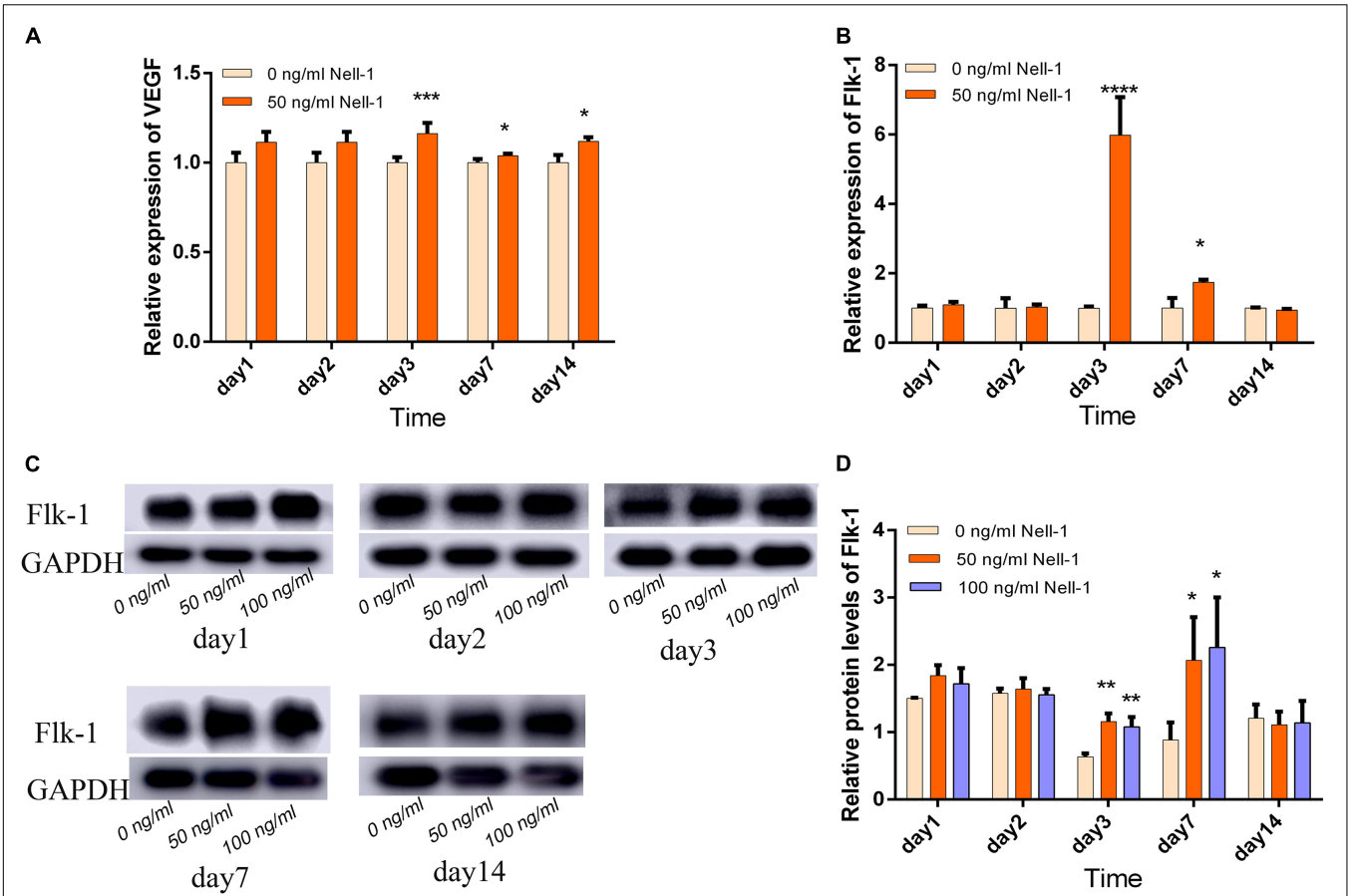

FIGURE 2 | Angiogenesis-related gene and protein expression in DPSCs. **(A)** VEGF gene expression was increased by 50 ng/mL Nell-1 treatment in days 3, 7, and 14. **(B)** Flk-1 gene expression was increased by 50 ng/mL Nell-1 treatment in days 3 and 7. **(C,D)** Flk-1 protein expression was increased by 50 and 100 ng/mL Nell-1 treatment in days 3 and 7. Data are shown as the mean ± SD. (*$p < 0.05$, **$p < 0.01$, ***$p < 0.001$, ****$p < 0.0001$).

of CD31 and CD34 revealed vascular lumens in pulp tissues. The collagen group had higher amount of inflammatory cell infiltration but lower numbers of blood vessels around cavities than the Nell-1 group (**Figures 6E,F,K,L**). Both groups had more inflammatory cell infiltration and fewer blood vessels than normal teeth group (**Figures 6D–L**). In addition, no significant difference in the area away from the cavities was found among the three groups (**Figures 6G–I**).

DISCUSSION

DPSCs are regarded as great stem cell sources in different generation fields because they could be easily isolated by a non-invasive method and without moral concern (Lee et al., 2019; Yamada et al., 2019). Direct co-culture of DPSCs and HUVECs was applied in this study according to the previous studies which has showed greater expression of angiogenic markers compared with DPSCs alone (Dissanayaka et al., 2012).

In this study, Nell-1 upregulated VEGF and Flk-1, which are responsible for proangiogenic properties. Flk-1 protein expression was downregulated in the co-culture group at day 3 when Nell-1 was added; however, the mechanisms are still unclear. Cell immunofluorescence staining revealed that Nell-1 is expressed in the nucleus of DPSCs and HUVECs and co-expressed with VEGF and Flk-1 in normal pulp tissues. This finding indicates that Nell-1 may have a synergistic or similar effect with VEGF and Flk-1 on promoting angiogenesis. The *in vitro* tube formation assay also confirmed Nell-1 effects on promoting angiogenesis.

The survival rate of inflamed pulp tissue is related to the surrounding angiogenesis (Saghiri et al., 2015). Immunohistochemical staining of CD31 and CD34 indicated that the number of blood vessels in the Nell-1 group is higher than that in the collagen group. This phenomenon can be explained as follows. *In vitro* experiment revealed that Nell-1 may promote angiogenesis by increasing the expression of VEGF and Flk-1 in DPSCs. Considering the co-expression of Nell-1 and angiogenetic markers, we speculate that Nell-1 may have a synergistic or similar effect to VEGF and Flk-1.

Pulp regeneration mainly includes blood vessels, nerves, and dentin. In an adult tooth, each large myelinated nerve fiber bundle surrounds a single arteriole in the root canals and pulp chambers (Steiniger et al., 2013). During early tooth formation,

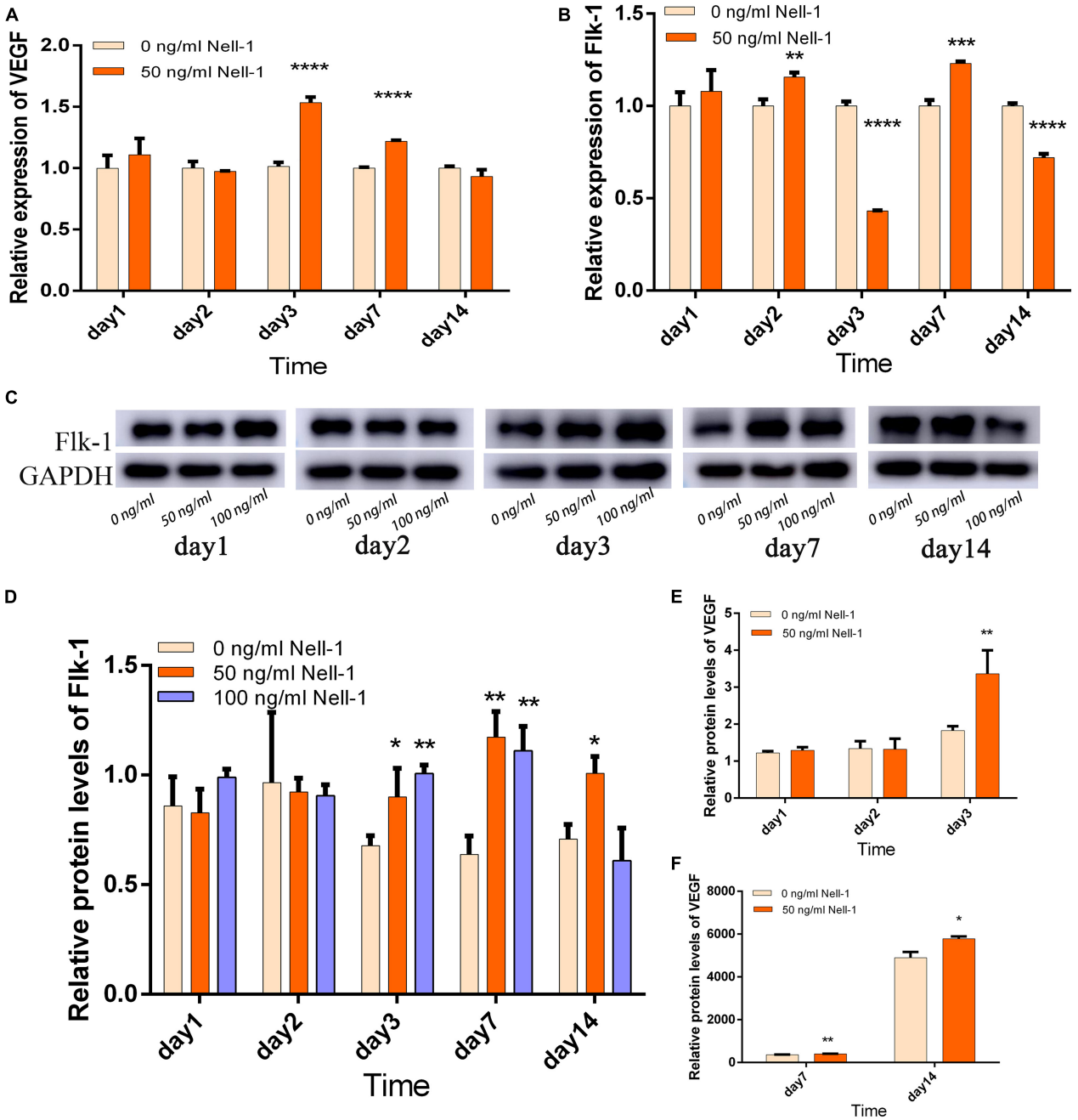

FIGURE 3 | Angiogenesis-related gene and protein expression in the co-culture group. **(A)** VEGF gene expression was improved by 50 ng/mL Nell-1 treatment in days 3 and 7. **(B)** Flk-1 gene expression was improved by 50 ng/mL Nell-1 treatment in days 2 and 7, but was decreased in day 3 and 14. **(C,D)** Flk-1 protein expression was increased by 50 and 100 ng/mL Nell-1 treatment in days 3, 7, and 14. **(E,F)** VEGF protein expression was increased by 50 ng/mL Nell-1 treatment in days 3, 7, and 14. Data are shown as the mean ± SD. (*$p < 0.05$, **$p < 0.01$, ***$p < 0.001$, ****$p < 0.0001$).

tooth innervation occurs through vasculogenesis (Shadad et al., 2019). In this study, we found that Nell-1 can enhance the expression of proteins and angiogenetic genes as early as day 2, which was almost the same rate as that of the odontoblastic and neural-like differentiation of DPSCs (Liu et al., 2016; Han et al., 2019). Subsequent experiments will be conducted to confirm the relevant mechanisms. Nell-1 application may be a promising strategy in dental pulp regeneration field since its contribution to dentin formation, neurogenesis and angiogenesis (Liu et al., 2016; Han et al., 2019).

Xuan et al. (2018) confirmed that human deciduous autologous tooth stem cells can regenerate the whole dental pulp and have a promising effect on pulp regeneration; however, the mechanisms are still unclear. The present study investigated

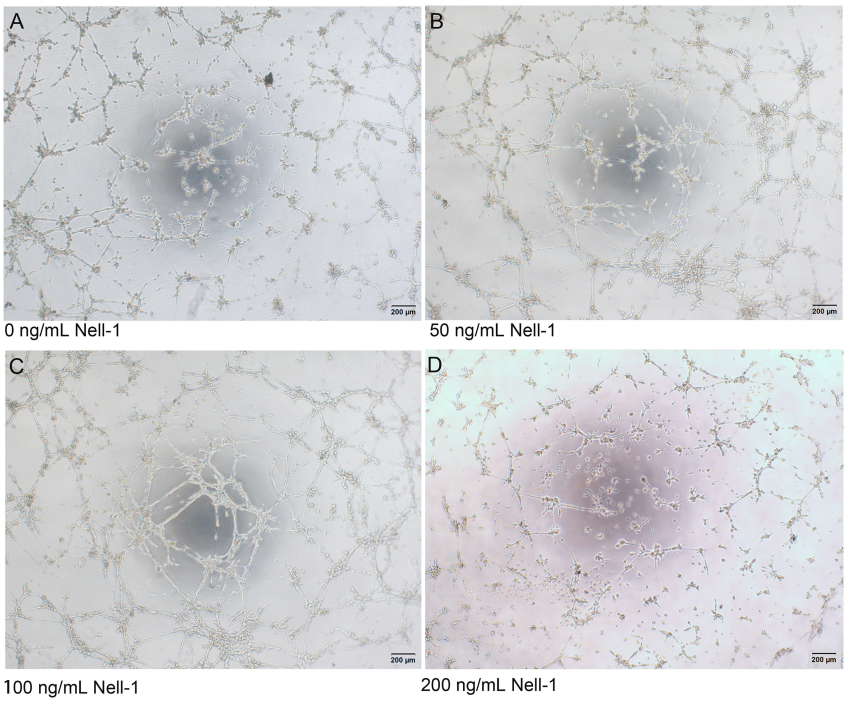

FIGURE 4 | *In vitro* tube formation assay. **(A–D)** Phase-contrast images (× 40) of mixed cells with 0, 50, 100, and 200 ng/mL Nell-1 at 6h after seeding on Matrigel. Compared with control group **(A)**, 50 and 100 ng/mL Nell-1 group **(B,C)** showed more number of branching points and tubular length while 200 ng/mL Nell-1 group **(D)** had no significant changes.

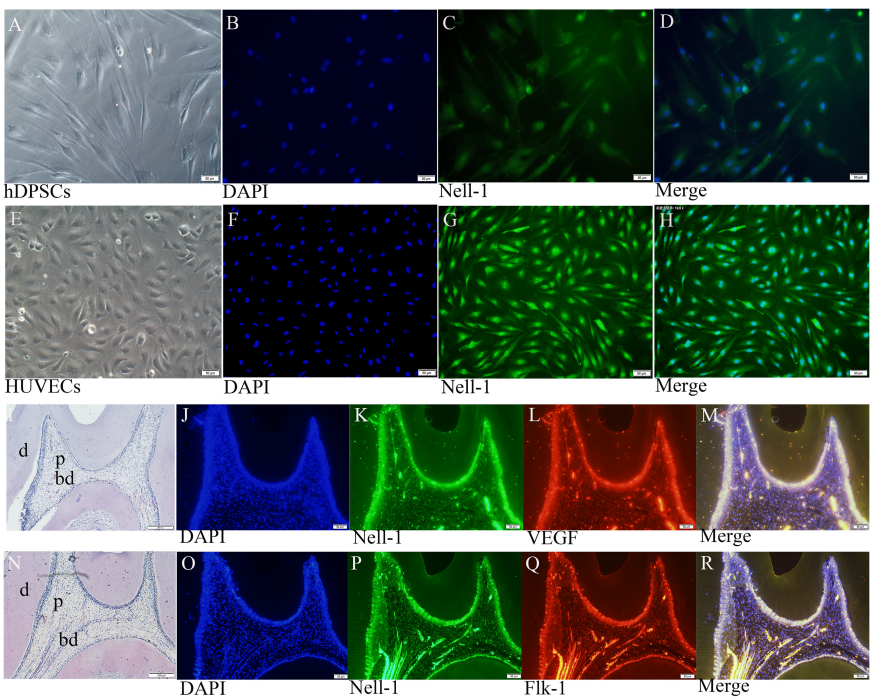

FIGURE 5 | Nell-1 distribution in DPSCs **(A–D)**, HUVECs **(E–H)**, and normal pulp tissues **(I–R)**. **(A,E)** Normal cell feature of DPSCs and HUVECs. **(B,F)** DAPI: nucleus stain. **(C,G)** green fluorescence can be observed in the nucleus of DPSCs and HUVECs. **(D,H)** Merged images. **(I,N)** HE staining displayed the morphology and structure of normal rat pulp tissues. **(K,L,P,Q)** Nell-1, VEGF and Flk-1 can be found in odontoblasts, pulp fibroblasts, and endothelial cells of the blood vessels. **(J,O)** DAPI: nucleus stain. **(M,R)** Merging Nell-1 with angiogenetic markers. d, dentin; p, dental pulp; bd, blood vessel.

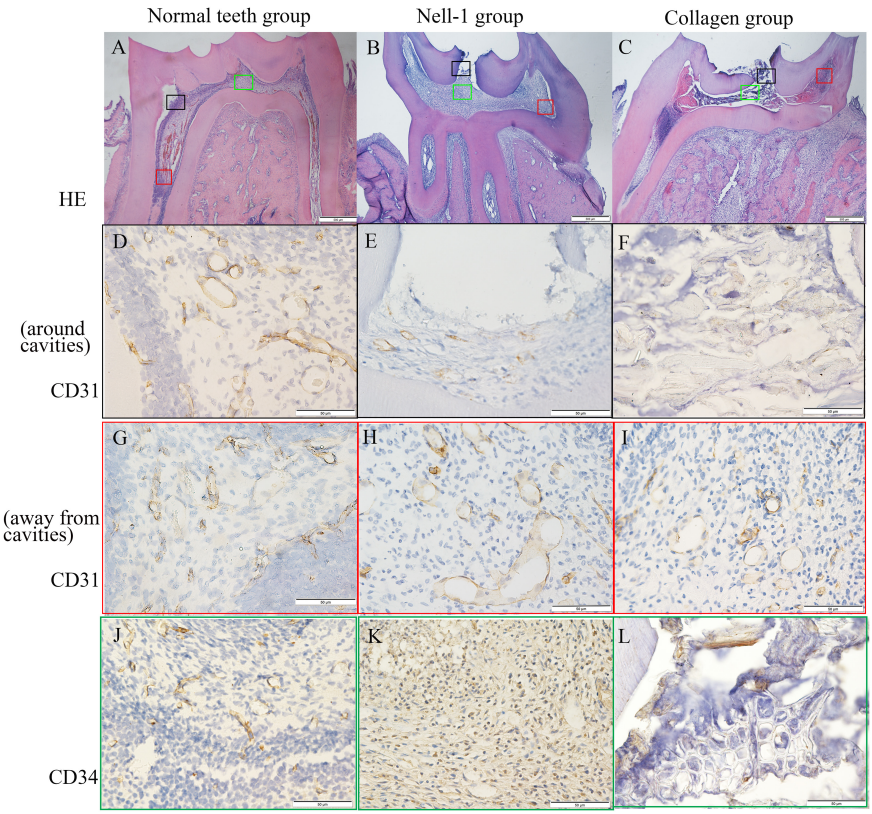

FIGURE 6 | Histology and immunohistochemistry staining. **(A)** Normal teeth group. **(B)** Nell-1 group. **(C)** Collagen group. HE staining showed the cavities, inflamed tissue, and normal structure of rat pulp tissues. The staining of CD31 **(D–I)** and CD34 **(J–L)** revealed the blood vessels in pulp tissues. Nell-1 induction group had higher number of blood vessels around cavities than the collagen group, and both of them had fewer blood vessels than negative control group **(D–F,J–L)**. There was no significant difference in the area away from the cavities between three groups **(G–I)**. d, dentin; p, dental pulp; bd, blood vessel.

the effect of Nell-1 on pulp angiogenesis and found that this molecule may promote the angiogenic differentiation of DPSCs, thus further confirming its role in pulp regeneration.

CONCLUSION

Nell-1 is highly expressed in the nucleus of DPSCs and HUVECs and co-expressed with angiogenetic markers in normal pulp tissues. This molecule could enhance the angiogenic differentiation of DPSCs *in vitro* and *in vivo* and thus may be a promising drug for the regeneration of the whole pulp.

DATA AVAILABILITY STATEMENT

The original contributions presented in the study are included in the article/supplementary material, further inquiries can be directed to the corresponding author/s.

ETHICS STATEMENT

The studies involving human participants were reviewed and approved by Institutional Review Board of School of Stomatology (No. R20180801). The patients/participants provided their written informed consent to participate in this study. The animal study was reviewed and approved by Institutional Review Board of School of Stomatology (No. D20180801).

AUTHOR CONTRIBUTIONS

XW and QW designed, supervised, and funded the study. ML performed the experiments and prepared the manuscript. QH, JW, and HZ performed the animal experiment. XB and YC performed the analysis. CY collected the clinical sample. All authors were actively involved with their work on this manuscript. All authors read and approved the final manuscript.

FUNDING

This work was supported by the Shandong Natural Science Foundation of China (Grant No. ZR2019MH014) and Science and Technology Development Project of Jinan City (Grant Nos. 201805047 and 201907089).

REFERENCES

Aguirre, A., Planell, J. A., and Engel, E. (2010). Dynamics of bone marrow-derived endothelial progenitor cell/mesenchymal stem cell interaction in co-culture and its implications in angiogenesis. *Biochem. Biophys. Res. Commun.* 400, 284–291. doi: 10.1016/j.bbrc.2010.08.073

Allen, P., Melero-Martin, J., and Bischoff, J. (2011). Type I collagen, fibrin and PuraMatrix matrices provide permissive environments for human endothelial and mesenchymal progenitor cells to form neovascular networks. *J. Tissue Eng. Regen. Med.* 5, e74–e86.

An, S. Y., Lee, Y. J., Neupane, S., Jun, J. H., Kim, J. Y., Lee, Y., et al. (2017). Effects of vascular formation during alveolar bone process morphogenesis in mice. *Histochem. Cell Biol.* 148, 435–443. doi: 10.1007/s00418-017-1584-2

Chung, A. S., and Ferrara, N. (2011). Developmental and pathological angiogenesis. *Annu. Rev. Cell Dev. Biol.* 27, 563–584. doi: 10.1146/annurev-cellbio-092910-154002

d'Aquino, R., Graziano, A., Sampaolesi, M., Laino, G., Pirozzi, G., De Rosa, A., et al. (2007). Human postnatal dental pulp cells co-differentiate into osteoblasts and endotheliocytes: a pivotal synergy leading to adult bone tissue formation. *Cell Death Differ.* 14, 1162–1171. doi: 10.1038/sj.cdd.4402121

Dissanayaka, W. L., Zhan, X., Zhang, C., Hargreaves, K. M., Jin, L., and Tong, E. H. (2012). Coculture of dental pulp stem cells with endothelial cells enhances osteo-/odontogenic and angiogenic potential in vitro. *J. Endod.* 38, 454–463. doi: 10.1016/j.joen.2011.12.024

Fahmy-Garcia, S., van Driel, M., Witte-Buoma, J., Walles, H., van Leeuwen, J. P. T. M., van Osch, G. J. V. M., et al. (2018). NELL-1, HMGB1, and CCN2 enhance migration and vasculogenesis, but not osteogenic differentiation compared to BMP2. *Tissue Eng. Part A* 24, 207–218. doi: 10.1089/ten.tea.2016.0537

Ferrara, N. (2002). Role of vascular endothelial growth factor in physiologic and pathologic angiogenesis: therapeutic implications. *Semin. Oncol.* 29(6 Suppl. 16), 10–14. doi: 10.1053/sonc.2002.37264

Ferrara, N., Gerber, H. P., and LeCouter, J. (2003). The biology of VEGF and its receptors. *Nat. Med.* 09, 669–676. doi: 10.1038/nm0603-669

Gonmanee, T., Thonabulsombat, C., Vongsavan, K., and Sritanaudomchai, H. (2018). Differentiation of stem cells from human deciduous and permanent teeth into spiral ganglion neuron-like cells. *Arch. Oral. Biol.* 88, 34–41. doi: 10.1016/j.archoralbio.2018.01.011

Gronthos, S., Mankani, M., Brahim, J., Robey, P. G., and Shi, S. (2000). Postnatal human dental pulp stem cells in vitro and in vivo. *PNAS* 97, 13625–13630.

Han, Q., Wang, Q., Wu, J., Li, M., Fang, Y., Zhu, H., et al. (2019). Nell-1 promotes the neural-like differentiation of dental pulp cells. *Biochem. Biophys. Res. Commun.* 513, 515–521. doi: 10.1016/j.bbrc.2019.04.028

Hilkens, P., Fanton, Y., Martens, W., Gervois, P., Struys, T., Politis, C., et al. (2014). Pro-angiogenic impact of dental stem cells in vitro and in vivo. *Stem Cell Res.* 12, 778–790. doi: 10.1016/j.scr.2014.03.008

Kang, Y., Kim, S., Fahrenholtz, M., Khademhosseini, A., and Yang, Y. (2013). Osteogenic and angiogenic potentials of monocultured and co-cultured human-bone-marrow-derived mesenchymal stem cells and human-umbilical-vein endothelial cells on three-dimensional porous beta-tricalcium phosphate scaffold. *Acta Biomater.* 9, 4906–4915. doi: 10.1016/j.actbio.2012.08.008

Karbanova, J., Soukup, T., Suchanek, J., Pytlík, R., Corbeil, D., and Mokrý, J. (2011). Characterization of dental pulp stem cells from impacted third molars cultured in low serum-containing medium. *Cells Tissues Organs* 193, 344–365. doi: 10.1159/000321160

Lee, Y. C., Chan, Y. H., Hsieh, S. C., Lew, W. Z., and Feng, S. W. (2019). Comparing the osteogenic potentials and bone regeneration capacities of bone marrow and dental pulp mesenchymal stem cells in a rabbit calvarial bone defect model. *Int. J. Mol. Sci.* 20:5015. doi: 10.3390/ijms20205015

Leopold, B., Strutz, J., Weiß, E., Gindlhuber, J., Birner-Gruenberger, R., Hackl, H., et al. (2019). Outgrowth, proliferation, viability, angiogenesis and phenotype of primary human endothelial cells in different purchasable endothelial culture media: feed wisely. *Histochem. Cell Biol.* 152, 377–390. doi: 10.1007/s00418-019-01815-2

Li, C., Zhang, X., Zheng, Z., Nguyen, A., Ting, K., and Soo, C. (2019). Nell-1 is a key functional modulator in osteochondrogenesis and beyond. *J. Dent. Res.* 98, 1458–1468. doi: 10.1177/0022034519882000

Li, D., Zou, X. Y., El-Ayachi, I., Romero, L. O., Yu, Z., Iglesias-Linares, A., et al. (2019). Human dental pulp stem cells and gingival mesenchymal stem cells display action potential capacity in vitro after neuronogenic differentiation. *Stem Cell Rev. Rep.* 15, 67–81. doi: 10.1007/s12015-018-9854-5

Liu, M., Wang, Q., Tang, R., Cao, R., and Wang, X. (2016). Nel-like molecule 1 contributes to the odontoblastic differentiation of human dental pulp cells. *J. Endod.* 42, 95–100. doi: 10.1016/j.joen.2015.08.024

Liu, M., Zhao, L., Hu, J., Wang, L., Li, N., Wu, D., et al. (2018). Endothelial cells and endothelin1 promote the odontogenic differentiation of dental pulp stem cells. *Mol. Med. Rep.* 18, 893–901.

Moioli, E. K., Clark, P. A., Chen, M., Dennis, J. E., Erickson, H. P., Gerson, S. L., et al. (2008). Synergistic actions of hematopoietic and mesenchymal stem/progenitor cells in vascularizing bioengineered tissues. *PLoS One* 3:e3922. doi: 10.1371/journal.pone.0003922

Rao, R. R., Peterson, A. W., Ceccarelli, J., Putnam, A. J., and Stegemann, J. P. (2012). Matrix composition regulates three-dimensional network formation by endothelial cells and mesenchymal stem cells in collagen/fibrin materials. *Angiogenesis* 15, 253–264. doi: 10.1007/s10456-012-9257-1

Rombouts, C., Giraud, T., Jeanneau, C., and About, I. (2017). Pulp vascularization during tooth development, regeneration, and therapy. *J. Dent. Res.* 96, 137–144. doi: 10.1177/0022034516671688

Saghiri, M. A., Asatourian, A., Sorenson, C. M., and Sheibani, N. (2015). Role of angiogenesis in endodontics: contributions of stem cells and proangiogenic and antiangiogenic factors to dental pulp regeneration. *J. Endod.* 41, 797–803. doi: 10.1016/j.joen.2014.12.019

Shadad, O., Chaulagain, R., Luukko, K., and Kettunen, P. (2019). Establishment of tooth blood supply and innervation is developmentally regulated and takes place through differential patterning processes. *J. Anat.* 234, 465–479. doi: 10.1111/joa.12950

Steiniger, B. S., Bubel, S., Bockler, W., Lampp, K., Seiler, A., Jablonski, B., et al. (2013). Immunostaining of pulpal nerve fibre bundle/arteriole associations in ground serial sections of whole human teeth embedded in technovit(R) 9100. *Cells Tissues Organs* 198, 57–65. doi: 10.1159/000351608

Stevens, A., Zuliani, T., Olejnik, C., LeRoy, H., Obriot, H., Kerr-Conte, J., et al. (2008). Human dental pulp stem cells differentiate into neural crest-derived melanocytes and have label-retaining and sphere-forming abilities. *Stem Cells Dev.* 17, 1175–1184. doi: 10.1089/scd.2008.0012

Tang, R., Wang, Q., Du, J., Yang, P., and Wang, X. (2013). Expression and localization of Nell-1 during murine molar development. *J. Mol. Histol.* 44, 175–181. doi: 10.1007/s10735-012-9472-5

Ting, K., Vastardis, H., Mulliken, J. B., Soo, C., Tieu, A., Do, H., et al. (1999). Human Nell-1 expressed in unilateral coronal synostosis. *J. Bone Miner. Res.* 14, 80–89. doi: 10.1359/jbmr.1999.14.1.80

Xuan, K., Li, B., Guo, H., Sun, W., Kou, X., He, X., et al. (2018). Deciduous autologous tooth stem cells regenerate dental pulp after implantation into injured teeth. *Sci. Transl. Med.* 10:eaaf3227. doi: 10.1126/scitranslmed.aaf3227

Yamada, Y., Nakamura-Yamada, S., Kusano, K., and Baba, S. (2019). Clinical potential and current progress of dental pulp stem cells for various systemic diseases in regenerative medicine: a concise review. *Int. J. Mol. Sci.* 20:1132. doi: 10.3390/ijms20051132

Zhang, X., Zara, J., Siu, R. K., Ting, K., and Soo, C. (2010). The role of Nell-1, a growth factor associated with craniosynostosis, in promoting bone regeneration. *J. Dent. Res.* 89, 865–878. doi: 10.1177/0022034510376401

Conflict of Interest: The authors declare that the research was conducted in the absence of any commercial or financial relationships that could be construed as a potential conflict of interest.

frontiers in Physiology

ORIGINAL RESEARCH
published: 24 September 2021
doi: 10.3389/fphys.2021.724098

Enamel Defects Associated With Dentin Sialophosphoprotein Mutation in Mice

Tian Liang[1†‡], Qian Xu[1‡], Hua Zhang[1], Suzhen Wang[1], Thomas G. H. Diekwisch[2], Chunlin Qin[1] and Yongbo Lu[1]*

[1]Department of Biomedical Sciences and Center for Craniofacial Research and Diagnosis, Texas A&M University College of Dentistry, Dallas, TX, United States, [2]Department of Periodontics and Center for Craniofacial Research and Diagnosis, Texas A&M University College of Dentistry, Dallas, TX, United States

OPEN ACCESS

Edited by:
Shuo Chen,
The University of Texas Health Science Center at San Antonio, United States

Reviewed by:
Angela Quispe-Salcedo, Niigata University, Japan
Janet Moradian-Oldak, University of Southern California, United States

***Correspondence:**
Yongbo Lu
ylu@tamu.edu

†Present address:
Tian Liang,
Department of Biologic and Materials Sciences, University of Michigan School of Dentistry, Ann Arbor, MI, United States

‡These authors have contributed equally to this work and share first authorship

Specialty section:
This article was submitted to Craniofacial Biology and Dental Research, a section of the journal Frontiers in Physiology

Received: 12 June 2021
Accepted: 31 August 2021
Published: 24 September 2021

Citation:
Liang T, Xu Q, Zhang H, Wang S, Diekwisch TGH, Qin C and Lu Y (2021) Enamel Defects Associated With Dentin Sialophosphoprotein Mutation in Mice. Front. Physiol. 12:724098. doi: 10.3389/fphys.2021.724098

Dentin sialophosphoprotein (DSPP) is an extracellular matrix protein that is highly expressed in odontoblasts, but only transiently expressed in presecretory ameloblasts during tooth development. We previously generated a knockin mouse model expressing a mouse equivalent (DSPP, p.P19L) of human mutant DSPP (p.P17L; referred to as "*Dspp*$^{P19L/+}$"), and reported that *Dspp*$^{P19L/+}$ and *Dspp*$^{P19L/P19L}$ mice manifested a dentin phenotype resembling human dentinogenesis imperfecta (DGI). In this study, we analyzed pathogenic effects of mutant P19L-DSPP on enamel development in *Dspp*$^{P19L/+}$ and *Dspp*$^{P19L/P19L}$ mice. Micro-Computed Tomography (μCT) analyses of 7-week-old mouse mandibular incisors showed that *Dspp*$^{P19L/P19L}$ mice had significantly decreased enamel volume and/or enamel density at different stages of amelogenesis examined. Acid-etched scanning electron microscopy (SEM) analyses of mouse incisors demonstrated that, at the mid-late maturation stage of amelogenesis, the enamel of wild-type mice already had apparent decussating pattern of enamel rods, whereas only minute particulates were found in *Dspp*$^{P19L/+}$ mice, and no discernible structures in *Dspp*$^{P19L/P19L}$ mouse enamel. However, by the time that incisor enamel was about to erupt into oral cavity, distinct decussating enamel rods were evident in *Dspp*$^{P19L/+}$ mice, but only poorly-defined enamel rods were revealed in *Dspp*$^{P19L/P19L}$ mice. Moreover, μCT analyses of the mandibular first molars showed that *Dspp*$^{P19L/+}$ and *Dspp*$^{P19L/P19L}$ mice had a significant reduction in enamel volume and enamel density at the ages of 2, 3, and 24 weeks after birth. Backscattered and acid-etched SEM analyses revealed that while 3-week-old *Dspp*$^{P19L/+}$ mice had similar pattern of enamel rods in the mandibular first molars as age-matched wild-type mice, no distinct enamel rods were observed in *Dspp*$^{P19L/P19L}$ mice. Yet neither *Dspp*$^{P19L/+}$ nor *Dspp*$^{P19L/P19L}$ mice showed well-defined enamel rods in the mandibular first molars by the age of 24 weeks, as judged by backscattered and acid-etched SEM. *In situ* hybridization showed that *DSPP* mRNA level was markedly reduced in the presecretory ameloblasts, but immunohistochemistry revealed that DSP/DSPP immunostaining signals were much stronger within the presecretory ameloblasts in *Dspp* mutant mice than in wild-type mice. These results suggest that mutant P19L-DSPP protein caused developmental enamel

defects in mice, which may be associated with intracellular retention of mutant DSPP in the presecretory ameloblasts.

Keywords: tooth development, enamel, amelogenesis, ameloblasts, cell differentiation, mineralization, dentin sialophosphoprotein

INTRODUCTION

Tooth development involves a series of sequential interactions that occur between dental epithelium and underlying mesenchyme (Thesleff, 2003; Balic and Thesleff, 2015). The dental epithelium differentiates into ameloblasts, which form enamel. Enamel formation occurs in three major stages, including presecretory, secretory, and maturation stages (Warshawsky and Smith, 1974; Hu et al., 2007; Moradian-Oldak, 2012; Balic and Thesleff, 2015). During the presecretory stage, the dental epithelium differentiates into presecretory ameloblasts. As the presecretory ameloblasts differentiate into secretory ameloblasts, they acquire a special apical structure known as "Tomes' process." The secretory ameloblasts with Tomes' processes produce and secrete a specific set of proteins to form organic enamel matrix, which is then partially replaced by minerals during the secretory stage. The full thickness of enamel is achieved at the end of the secretory stage, and the organic matrix is completely removed and replaced by minerals during the maturation stage. The underlying mesenchyme differentiates into odontoblasts, which form dentin located directly underneath enamel in the crown of a tooth (Balic and Thesleff, 2015).

Mutations in the genes encoding enamel matrix proteins as well as other proteins involved in enamel formation result in a group of inherited enamel defects, known as "Amelogenesis Imperfecta (AI; Smith et al., 2017)." Based on the phenotypic defects of enamel, AI may be classified into hypoplastic and hypomineralized forms (Hu et al., 2007; Smith et al., 2017). Hypoplastic AI is characterized by the formation of a thin but mineralized layer of enamel that results from an insufficient apposition of enamel during the secretory stage of amelogenesis. In contrast, hypomineralized AI is distinguished by the formation of a full thickness but soft layer of enamel caused by a failure in enamel maturation. Hypomineralized AI can be further subclassified into hypomaturation and hypocalcified forms (Hu et al., 2007; Smith et al., 2017). Hypomaturation AI is due to an incomplete removal of the organic enamel matrix proteins that separate adjacent enamel crystals, whereas hypocalcified AI is caused by an insufficient deposition of minerals, particularly calcium ions.

Dentin sialophosphoprotein (DSPP) is a non-collagenous extracellular matrix protein and is a member of the SIBLING (Small integrin-binding ligand N-linked glycoprotein) family (Fisher et al., 2001; Fisher and Fedarko, 2003). It is highly expressed in odontoblasts, but transiently expressed in differentiating ameloblasts, as its transcripts are only observed in presecretory ameloblasts and early secretory ameloblasts during tooth development (D'Souza et al., 1997; Ritchie et al., 1997; Begue-Kirn et al., 1998; MacDougall et al., 1998; Bleicher et al., 1999). DSPP is synthesized as a single large protein, which is subsequently processed into an amino-terminal fragment called dentin sialoprotein (DSP) and a carboxyl-terminal fragment known as dentin phosphoprotein (DPP; MacDougall et al., 1997; Sun et al., 2010; von Marschall and Fisher, 2010; Zhu et al., 2012). DSP is a proteoglycan containing two glycosaminoglycan chains (Ritchie et al., 1994; Zhu et al., 2010; Yamakoshi et al., 2011), whereas DPP is a highly phosphorylated and very acidic protein (Butler et al., 1983; George et al., 1996; Ritchie and Wang, 1996). In addition, a third cleaved fragment, named "dentin glycoprotein (DGP)," is identified in porcine and is derived from the middle region of DSPP (Yamakoshi et al., 2005).

Mutations in the *DSPP* gene in humans affect tooth development, resulting in an inheritable autosomal dominant dental disorder. Consistent with its high level of expression in odontoblasts, the primary dental defect associated with DSPP mutations in humans is the formation of various types of abnormal dentin (Kim and Simmer, 2007). Based on the phenotypic differences, the dental defects caused by DSPP mutations may be classified into dentinogenesis imperfecta (DGI) Type II (OMIM #125490), characterized by pulp chamber obliteration, DGI Type III (OMIM #125500), featured by pulp chamber enlargement and thinner dentin, and dentin dysplasia (DD) Type II (OMIM #125420), which manifests relatively mild dental defects (Shields et al., 1973; MacDougall et al., 2006; Kim and Simmer, 2007). Similarly, *Dspp* ablation in mice causes a defective dentin mineralization, resulting in a tooth phenotype similar to that observed in human DGI type III patients (Sreenath et al., 2003). In addition to dentin, enamel formation may be affected by DSPP mutations in DGI patients (Lee et al., 2011; Wang et al., 2011; Bloch-Zupan et al., 2016; Taleb et al., 2018). However, very limited studies have been done to understand how mutant DSPP proteins interfere with amelogenesis to date.

We previously generated a mouse model (referred to as "*Dspp*$^{P19L/+}$" mice), that expressed a mutant DSPP, in which the proline residue at position 19 was replaced by a leucine residue (p.P19L; Liang et al., 2019). The proline residue at position 19 in mouse DSPP is the second amino acid residue from the signal peptide cleavage site, and it corresponds to the proline residue P17 in human DSPP. Our findings demonstrated that *Dspp*$^{P19L/+}$ and *Dspp*$^{P19L/P19L}$ mice manifested a DGI Type III-like phenotype at younger age, and acquired a DGI Type II-like defect as they grew older, which is similar to the dental phenotype of human patients carrying the corresponding p.P17L mutation (Li et al., 2012; Lee et al., 2013; Porntaveetus et al., 2019). In this study, we reported the ultrastructural changes in enamel as well as the molecular changes in differentiating ameloblasts in *Dspp*$^{P19L/+}$ and *Dspp*$^{P19L/P19L}$ mice. We showed that the *Dspp* mutant mice had reduced

enamel formation, delayed enamel maturation, and ultrastructural enamel defects; and we demonstrated that such enamel defects may be associated with an accumulation of mutant DSPP protein within the presecretory ameloblasts.

MATERIALS AND METHODS

Generation of *Dspp*$^{P19L/+}$ and *Dspp*$^{P19L/P19L}$ Mice

Generation and genotyping of *Dspp*$^{P19L/+}$ and *Dspp*$^{P19L/P19L}$ mice was described in our previous report (Liang et al., 2019). All mice were maintained on a C57BL/6 genetic background on a 12 h light/dark cycle with free access to water and standard pelleted food. Both male and female mice were used for analyses of the enamel phenotypes, as there was no phenotypic difference between sexes for each genotype. All animal procedures were approved by the Institutional Animal Care and Use Committee of Texas A&M University College of Dentistry (Dallas, TX, United States).

Plain X-Ray Radiography and Micro-Computed Tomography

The left mandibles from 2-, 3-, 7-, and 24-week-old *Dspp*$^{+/+}$, *Dspp*$^{P19L/+}$, and *Dspp*$^{P19L/P19L}$ mice were dissected and processed for plain x-ray radiography and/or μCT analyses, as previously described (Bouxsein et al., 2010; Liang et al., 2019). Seven-week-old mouse mandibles were first evaluated using a plain X-ray radiography system (Faxitron MX-20DC 12; Tucson, AZ, United States) to obtain an overall morphological assessment of the mandibular incisors; they were then scanned with a Scanco μCT35 imaging system (Scanco Medical, Brüttisellen, Switzerland) at three regions that contain the mandibular incisor enamel segment 1 (ES1), ES2, and ES3, respectively (**Figure 1A**). ES1 is a 1-mm-long incisor enamel segment located immediately distal to the distal aspect of the third molar crown, representing the late secretory stage amelogenesis; ES2 is a 1-mm-long incisor enamel segment located right underneath the proximal root of first molar, representing the mid-late maturation stage amelogenesis; ES3 is a 1-mm-long incisor enamel segment that is located below the labial alveolar crest, that is about to erupt into oral cavity, and that has undergone extensive maturation (enamel mineral density reaches its peak). For the morphometric analyses of ES1, ES2, and ES3, the enamel layer was manually delineated to separate enamel from the subjacent dentin; and a threshold of 120 was then chosen to exclude any soft tissues/ameloblasts. The left mandibles from 2-, 3-, and 24-week-old *Dspp*$^{+/+}$, *Dspp*$^{P19L/+}$, and *Dspp*$^{P19L/P19L}$ mice were scanned for mandibular first molars. For three-dimensional (3D) construction and morphometric analyses of mandibular first molars, the whole teeth were outlined, and an appropriate threshold was determined for each age (a threshold of 515 for 2-week-old mice, 563 for 3-week-old mice, and 600 for 24-week-old mice), based on the visual comparisons to include enamel but not adjacent tissues. All morphometric parameters were evaluated using the μCT built-in software (Bouxsein et al., 2010). Data obtained from 3 to 5 independent mice for each group were used for quantitative analysis.

Resin-Casted Backscattered and Acid-Etched Scanning Electron Microscopy

The 3-, 7-, and 24-week-old left mandible samples were processed for resin-casted backscattered and acid-etched SEM analysis, as described previously (Gibson et al., 2013; Zhang et al., 2018; Liang et al., 2019). Briefly, the mandible samples were dehydrated in gradient ethanol (from 70 to 100%) and xylene before embedded in methyl methacrylate (MMA). For resin-casted backscattered SEM analysis of the molars, the buccal-lingual sections crossing the middle of the proximal root of mandibular first molars were chosen. The cut surface was polished and dehydrated, followed by gold coating. Scanning was performed in backscattered electronic shadow (BES) mode in a JEOL JSM-6010 LA SEM (JEOL, Japan). Following resin-casted backscattered SEM analysis, the molar sections were further processed for acid-etched SEM analysis. The coating particles were removed, and sample surface was re-polished and etched with 10% phosphoric acid for 7–14 s, followed by immersing in 5% sodium hypochlorite for 20 min twice. The samples were gold-coated and scanned in secondary electron image (SEI) mode in the same SEM. For acid-etched SEM analysis of 7-week-old mandibular incisors, the mandibles were cross sectioned to obtain sections at the levels of ES2 and ES3, which were subsequently processed for acid-etched SEM analysis as the molar sections. Two independent mice were analyzed for molars or incisors for each genotype of 3-, 7-, and 24-week-old mice.

Sample Processing and Histological Analysis

The right mandibles from 1-week-old *Dspp*$^{+/+}$, *Dspp*$^{P19L/+}$, and *Dspp*$^{P19L/P19L}$ mice were harvested and fixed in freshly prepared 4% paraformaldehyde in diethyl pyrocarbonate (DEPC)-treated 0.1 M phosphate-buffered saline (pH 7.4) at 4°C overnight and then decalcified in 15% ethylenediaminetetraacetate (EDTA) solution (pH 7.4) at 4°C for 3 days. The decalcified samples were dehydrated, and embedded in paraffin following standard histological procedures. The tissue blocks were cut into serial sagittal sections at a thickness of 5 μm, which were used for Hematoxylin and Eosin (H&E) staining, and other histological analyses, as previously described (Zhang et al., 2018; Liang et al., 2019).

In situ Hybridization

In situ hybridization (ISH) was performed to detect DSPP transcripts, as previously described (Meng et al., 2015; Liang et al., 2019). Briefly, RNA probes for mouse DSPP were labeled with digoxigenin (DIG) by using an RNA Labeling Kit (Roche, Indianapolis, IN, United States), according to the manufacturer's instruction. The DIG-labeled RNA probes were used to hybridize with the DSPP transcripts in the mandibular first molars. After hybridization, the hybridized DIG-labeled RNA probes were

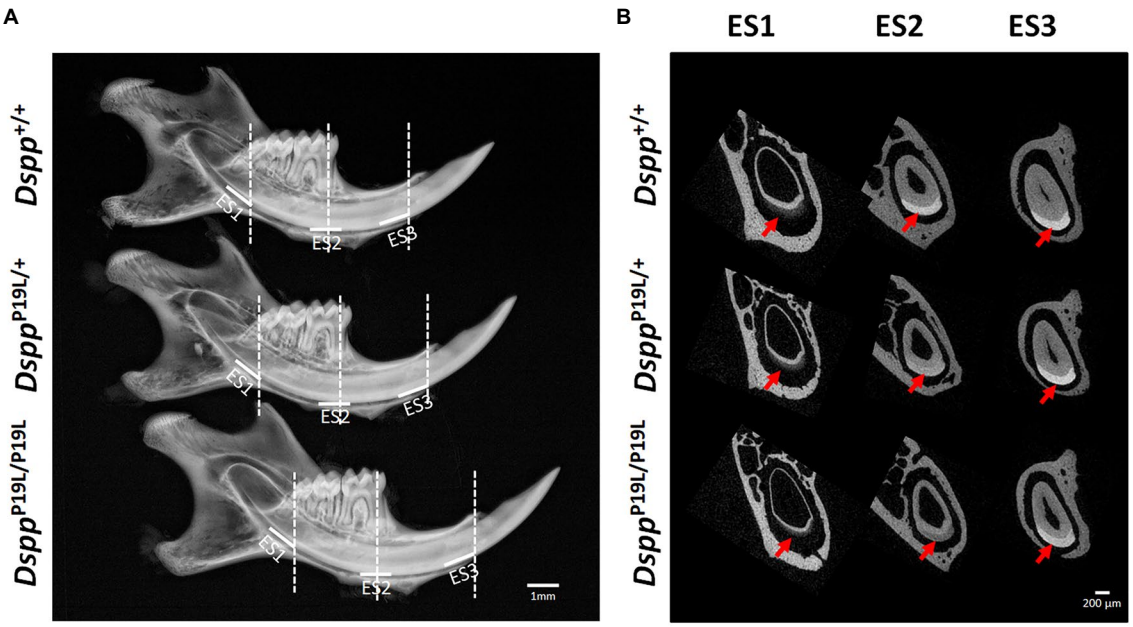

FIGURE 1 | Gross overview of the tooth phenotype of *Dspp*$^{P19L/+}$ and *Dspp*$^{P19L/P19L}$ mice. **(A)** Representative plain x-ray radiographic images of the mandibles of 7-week-old wild-type *Dspp*$^{+/+}$, heterozygous *Dspp*$^{P19L/+}$ and homozygous *Dspp*$^{P19L/P19L}$ mice. The white horizontal lines denote the enamel segments, ES1, ES2, and ES3, that were quantified by μCT analyses. ES1 corresponds to the late secretory stage amelogenesis; ES2 corresponds to mid-late maturation stage amelogenesis; and ES3 is the enamel segment that has undergone extensive maturation and is about to erupt. The dashed vertical white lines in **(A)** mark the locations of reconstructed trans-axial μCT images shown in **(B)**. Red arrows indicate the mandibular incisor enamel in the trans-axial images. Scale bars: 1 mm in A; 200 μm in B.

detected by an enzyme-linked immunoassay with an alkaline phosphatase-conjugated anti-DIG antibody (1:2000; Roche), and an NBT/BCIP (nitro blue tetrazolium/5-bromo-4-chloro-3-indolyl-phosphate) substrate (Roche, Mannheim, Germany). The sections were counterstained with nuclear fast red (Sigma, Saint Louis, MO, United States). At least three individual samples were analyzed.

Immunohistochemistry

Immunohistochemistry (IHC) was carried out to assess DSP/DSPP, amelogenin (AMEL), and ameloblastin (AMBN) proteins, as previously described (Meng et al., 2015; Li et al., 2019; Liang et al., 2019). Briefly, sections were incubated with a rabbit anti-DSP polyclonal antibody (recognizing both DSP and full-length DSPP), a mouse monoclonal antibody raised against the full-length human AMEL (Santa Cruz Biotechnology; 1:500), or a rabbit polyclonal antibody generated against the C-terminus of mouse AMBN (Santa Cruz Biotechnology; 1:800), followed by incubating in a biotinylated anti-rabbit IgG or anti-mouse IgG secondary antibody (1:200, Vector Laboratories, Burlingame, CA, United States). The immunostaining signals were visualized using the DAB (3,3′-diaminobenzidine) kit (Vector Laboratories), according to the manufacturer's instructions. The sections were counterstained with methyl green (Sigma). At least three individual samples were analyzed. The same concentrations of nonimmune rabbit IgG or mouse IgG were used to replace the polyclonal or monoclonal antibodies as negative controls.

Statistical Analysis

One-way ANOVA was conducted to compare the differences among three groups. If significant differences were found by One-way ANOVA, Bonferroni method was used as *post hoc*. The quantified results were represented as mean ± SD. $p < 0.05$ was considered statistically significant.

RESULTS

Delayed Incisor Enamel Maturation in *Dspp*$^{P19L/+}$ and *Dspp*$^{P19L/P19L}$ Mice

Rodent incisors continuously grow and erupt, so that different stages of amelogenesis can be evaluated in the same incisor (Robinson et al., 1977; Smith and Nanci, 1989; Smith et al., 2011; Schmitz et al., 2014). We first examined the mandibular incisor phenotype of 7-week-old *Dspp*$^{P19L/+}$ and *Dspp*$^{P19L/P19L}$ mice. Plain x-ray radiography demonstrated that *Dspp*$^{P19L/+}$ and *Dspp*$^{P19L/P19L}$ mice had no apparent difference in the overall appearance of the mandibular incisors, compared to the age-matched *Dspp*$^{+/+}$ control mice (**Figure 1A**). The trans-axial μCT images demonstrated that *Dspp*$^{P19L/+}$ and *Dspp*$^{P19L/P19L}$ mice had reduced radiopacity in enamel, compared to *Dspp*$^{+/+}$ mice at the late secretory stage (ES1) and at the mid-late maturation stage (ES2; **Figure 1B**). Such reduced radiopacity was more prominent at the mid-late maturation stage and was also more severe in *Dspp*$^{P19L/P19L}$ mice (**Figure 1B**). However, for the enamel segment (ES3), which was immediately before eruption, *Dspp*$^{P19L/+}$ and

Dspp$^{P19L/P19L}$ mice achieved a radiopacity that was very close to that of *Dspp*$^{+/+}$ mice (**Figure 1B**). Quantitative μCT analyses showed that *Dspp*$^{P19L/P19L}$ mice had a significant reduction in enamel volume at all three stages of amelogenesis examined, whereas *Dspp*$^{P19L/+}$ mice only displayed reduced enamel volume at the level of ES2, compared to *Dspp*$^{+/+}$ control mice (**Table 1**). In addition, both *Dspp*$^{P19L/+}$ and *Dspp*$^{P19L/P19L}$ mice had significantly reduced enamel density at the level of ES2, compared to *Dspp*$^{+/+}$ mice (**Table 1**). We also analyzed the ultrastructural changes in the mandibular incisor enamel. Acid-etched scanning electron microscopy (SEM) analyses demonstrated that, at the mid-late maturation stage of amelogenesis, the wild-type mice already had apparent decussating pattern of enamel rods, whereas only minute particulates were found in *Dspp*$^{P19L/+}$ mice, and no discernible structures in *Dspp*$^{P19L/P19L}$ mice (**Figure 2A**). However, by the stage that the incisor enamel is about to erupt into the oral cavity, distinct decussating enamel rods were evident in *Dspp*$^{P19L/+}$ mice, but only poorly-defined enamel rods were revealed in *Dspp*$^{P19L/P19L}$ mice (**Figure 2B**). Taken together, these results demonstrated that *Dspp*$^{P19L/+}$ and *Dspp*$^{P19L/P19L}$ mice showed reduced incisor enamel formation, and delayed enamel maturation.

Reduced Molar Enamel Formation and Accelerated Molar Enamel Attrition in *Dspp*$^{P19L/+}$ and *Dspp*$^{P19L/P19L}$ Mice

Next, we analyzed the mandibular first molars (M1) of *Dspp*$^{P19L/+}$ and *Dspp*$^{P19L/P19L}$ mice at postnatal 2 weeks (M1 at the beginning of eruption phase before it is exposed to oral cavity; Komiyama et al., 2013), 3 weeks (M1 at the beginning of post-eruptive phase when it reaches the occlusal plane; Komiyama et al., 2013), and 24 weeks (when M1 has undergone substantial attrition). In contrast to incisors, rodent molars have limited growth as no more enamel will be formed once enamel formation is complete. Reconstructed 3D μCT images showed that the enamel was poorly formed in *Dspp*$^{P19L/+}$ and *Dspp*$^{P19L/P19L}$ mice, particularly in *Dspp*$^{P19L/P19L}$ mice, at the age of 2 weeks before the teeth were exposed to oral cavity (**Figure 3A**). Moreover, *Dspp*$^{P19L/P19L}$ mice showed a more severe loss of enamel with age after tooth eruption, compared with age-matched *Dspp*$^{+/+}$ and *Dspp*$^{P19L/+}$ mice (**Figures 3B,C**). Quantitative μCT analyses confirmed that *Dspp*$^{P19L/+}$ and *Dspp*$^{P19L/P19L}$ mice had a significant reduction in both enamel volume and enamel density of the mandibular first molars at the age of 2 weeks, compared to *Dspp*$^{+/+}$ mice (**Table 2**). The enamel volumes and densities of *Dspp*$^{P19L/+}$ and *Dspp*$^{P19L/P19L}$ mouse molars remained significantly lower than those of age-matched *Dspp*$^{+/+}$ mice when the teeth reached occlusion at the age of 3 weeks (**Table 2**). Even though all three groups of mice showed reduced molar enamel volumes with age due to attrition, *Dspp*$^{P19L/+}$ and *Dspp*$^{P19L/P19L}$ mouse molars apparently showed a more severe loss of enamel volume (with a loss of 15.74 and 33.48% total enamel volume, respectively) from the age of 3 to 24 weeks, compared to the *Dspp*$^{+/+}$ mice (with a loss of 7.48% total enamel volume; **Table 2**). In contrast to enamel volume, the molar enamel densities increased with age among all three groups of mice; however, the enamel densities of *Dspp*$^{P19L/+}$ and *Dspp*$^{P19L/P19L}$ mouse molars remained significantly lower, compared to that of *Dspp*$^{+/+}$ mice at the age 24 weeks (**Table 2**). These data suggest that the molar enamel was less formed and hypomineralized in *Dspp*$^{P19L/+}$ and *Dspp*$^{P19L/P19L}$ mice and was subject to rapid attrition with age after teeth reach occlusion.

Ultrastructural Changes in Molar Enamel in *Dspp*$^{P19L/+}$ and *Dspp*$^{P19L/P19L}$ Mice

We then examined the ultrastructural changes in the molar enamel by backscattered and acid-etched SEM analyses, as previously described (Liang et al., 2019). Backscattered SEM analysis demonstrated that 3-week-old *Dspp*$^{+/+}$ mice showed a decussating pattern of enamel rods in the inner enamel, a parallel pattern in the outer enamel and were rod-free in the superficial enamel (**Figure 4A**). Three-week-old *Dspp*$^{P19L/+}$ mice showed a similar organization of enamel rods as age-matched *Dspp*$^{+/+}$ mice, but there was a complete lack of clearly defined enamel rods in 3-week-old *Dspp*$^{P19L/P19L}$ mice (**Figure 4A**). By 24 weeks, the decussating pattern enamel rods remained in *Dspp*$^{+/+}$ mice (**Figure 4B**). However, the enamel rod boundaries became blurred in *Dspp*$^{P19L/+}$ mice, whereas only poorly-defined enamel rods were observed in *Dspp*$^{P19L/P19L}$ mice (**Figure 4B**). Acid-etched SEM analyses revealed that *Dspp*$^{P19L/+}$ mice showed an acid-etching pattern in enamel that was similar to that of the wild-type mice, at the age of 3 weeks (**Figure 5A**). At the age of 24 weeks, *Dspp*$^{+/+}$ mice presented an acid-etching pattern, with the cross-sectioned enamel rods preferentially removed by acid (**Figure 5B**). Although *Dspp*$^{P19L/+}$ mice displayed a similar pattern, the cross-sectioned enamel rods were not as well-defined as the wild-type mice (**Figure 5B**). There were no recognizable enamel rods in *Dspp*$^{P19L/P19L}$ mice at both ages

TABLE 1 | Micro-Computed Tomography analysis of 7-week-old mouse mandibular incisor enamel.

		ES1	ES2	ES3
Enamel volume (mm^3)	*Dspp*$^{+/+}$	0.0656 ± 0.0150	0.0821 ± 0.0029	0.0844 ± 0.0034
	Dspp$^{P19L/+}$	0.0473 ± 0.0052	0.0748 ± 0.0045[a]	0.0807 ± 0.0060
	Dspp$^{P19L/P19L}$	0.0297 ± 0.0073[a,b]	0.0647 ± 0.0073[a]	0.0737 ± 0.0015[a]
Enamel density (mg/cm^3 HA)	*Dspp*$^{+/+}$	309.84 ± 41.09	1621.64 ± 39.04	1792.34 ± 27.20
	Dspp$^{P19L/+}$	300.53 ± 33.98	1308.87 ± 192.25[a]	1731.77 ± 67.96
	Dspp$^{P19L/P19L}$	251.09 ± 32.32	1006.10 ± 388.08[a]	1558.77 ± 189.55

n = 3–4; ES, enamel segment; values are mean ± SD.

[a]*Statistically different from Dspp*$^{+/+}$ *($p < 0.05$).*

[b]*Statistically different from Dspp*$^{P19L/+}$ *($p < 0.05$).*

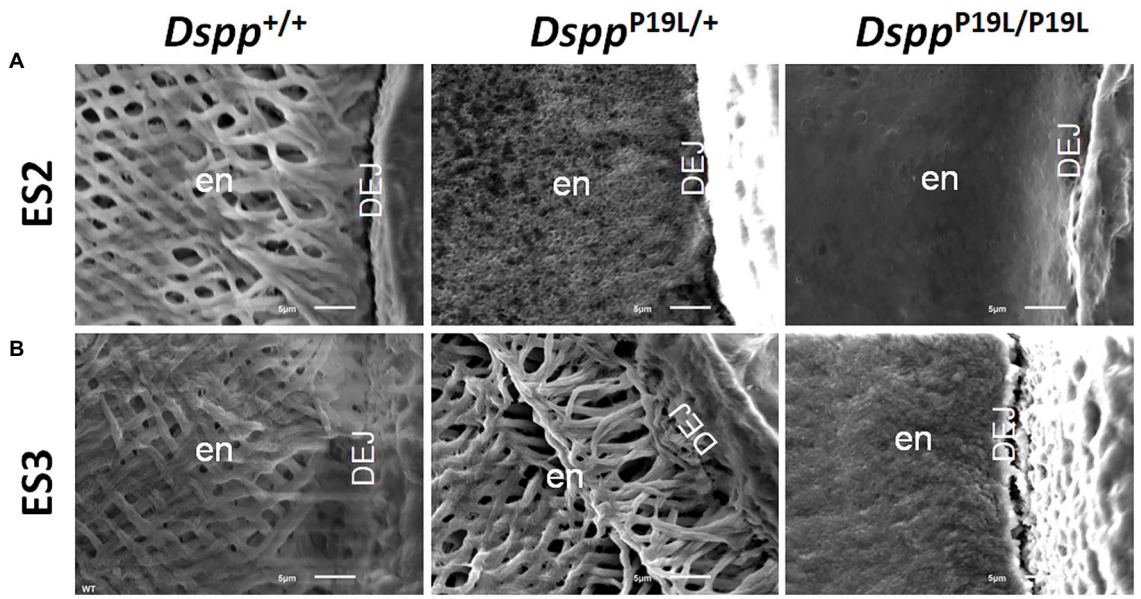

FIGURE 2 | Acid-etched scanning electron microscopy (SEM) analyses of the mandibular incisors. Shown are the acid-etched SEM images of the mandibular incisors of 7-week-old wild-type *Dspp*$^{+/+}$, heterozygous *Dspp*$^{P19L/+}$ and homozygous *Dspp*$^{P19L/P19L}$ mice. All images are the cross sections obtained at the levels of ES2 **(A)** and ES3 **(B)**. Note that the enamel from *Dspp*$^{+/+}$ mice showed decussating pattern of enamel rods at both ES2 and ES3 levels. In *Dspp*$^{P19L/+}$ mouse incisors, even though only minute particulates were observed at the level of ES2, distinct decussating enamel rods were present at the level of ES3. In the *Dspp*$^{P19L/P19L}$ mouse incisors, there was a complete absence of any discernible structures at the level of ES2, and only poorly-defined enamel rods were found at the level of ES3. en, enamel and DEJ, dentinoenamel junction. Scale bars: 5 μm.

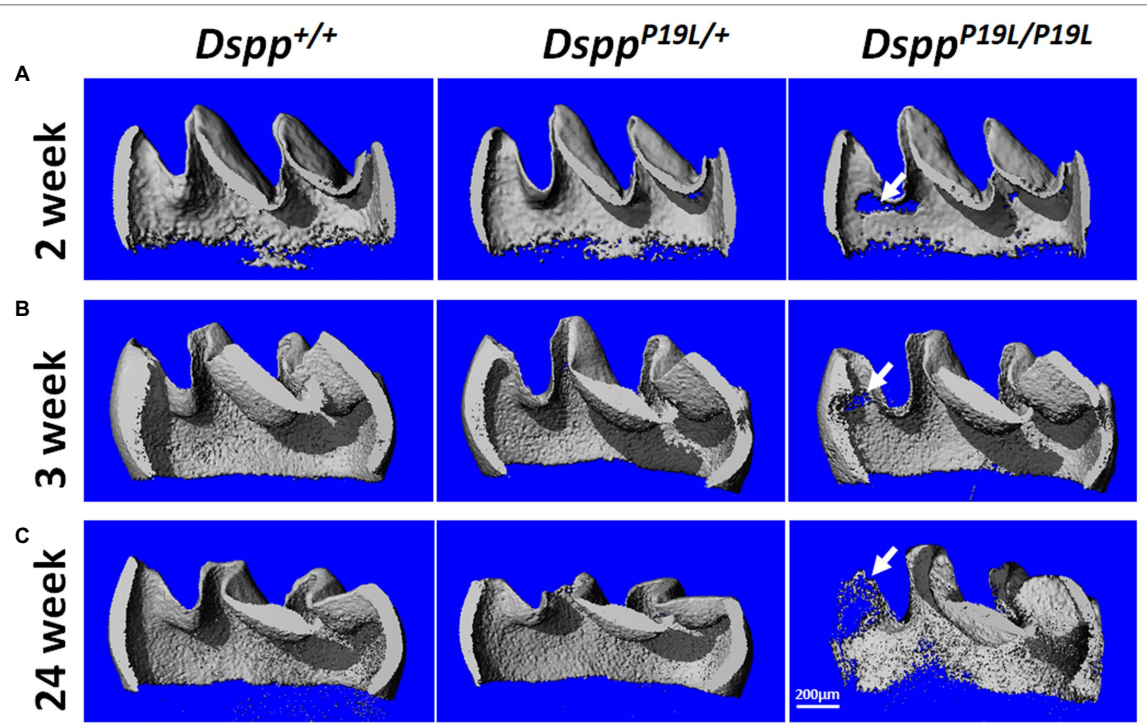

FIGURE 3 | Micro-Computed Tomography (μCT) analyses of the mandibular first molars. Shown are the representative 3D reconstructed μCT images (sagittal sections) of enamel of the mandibular first molars of 2-week-old **(A)**, 3-week-old **(B)**, and 24-week-old **(C)** wild-type *Dspp*$^{+/+}$, heterozygous *Dspp*$^{P19L/+}$, and homozygous *Dspp*$^{P19L/P19L}$ mice. The enamel was poorly formed in *Dspp*$^{P19L/+}$ and *Dspp*$^{P19L/P19L}$ mice, particularly in *Dspp*$^{P19L/P19L}$ mice (arrows), at the age of 2 weeks. There was also a severe loss of enamel in the *Dspp*$^{P19L/P19L}$ mice (arrows) with age, in comparison to age-matched *Dspp*$^{+/+}$ and *Dspp*$^{P19L/+}$ mice. Scale bar: 200 μm.

TABLE 2 | Micro-Computed Tomography analysis of mandibular first molar enamel.

		2 Weeks	3 Weeks	24 Weeks
Enamel volume (mm^3)	*Dspp*$^{+/+}$	0.1643 ± 0.0068	0.1617 ± 0.0130	0.1496 ± 0.0092
	Dspp$^{P19L/+}$	0.1384 ± 0.0109[a]	0.1245 ± 0.0225[a]	0.1049 ± 0.0140[a]
	Dspp$^{P19L/P19L}$	0.0987 ± 0.0007[a,b]	0.1129 ± 0.0147[a]	0.0751 ± 0.0187[a]
Enamel density (mg/cm^3 HA)	*Dspp*$^{+/+}$	1709.6854 ± 18.2788	1779.91 ± 31.70	1899.49 ± 34.74
	Dspp$^{P19L/+}$	1644.3523 ± 25.0770[a]	1723.43 ± 39.34[a]	1833.88 ± 17.12[a]
	Dspp$^{P19L/P19L}$	1582.3119 ± 30.2098[a,b]	1729.06 ± 30.36[a]	1819.08 ± 12.19[a]

n = 3–5; values are mean ± SD.
[a]*Statistically different from Dspp*$^{+/+}$ *($p < 0.05$).*
[b]*Statistically different from Dspp*$^{P19L/+}$ *($p < 0.05$).*

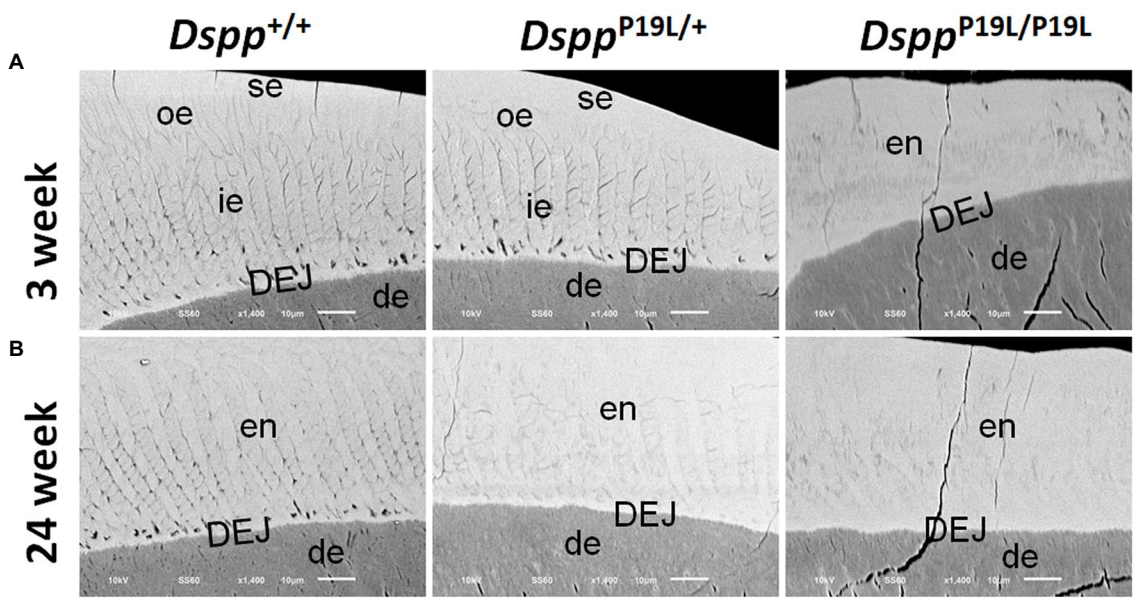

FIGURE 4 | Backscattered SEM analyses of the mandibular first molars. Shown are the backscattered SEM images of the mandibular first molars of 3- **(A)** and 24- **(B)** week-old wild-type *Dspp*$^{+/+}$, heterozygous *Dspp*$^{P19L/+}$ and homozygous *Dspp*$^{P19L/P19L}$ mice. All images are the longitudinal sections and buccal sides of the mandibular first molars. Three-week-old *Dspp*$^{+/+}$ mice showed a decussating pattern of enamel rods in the inner enamel (ie), a parallel pattern in the outer enamel (ore), and were rod-free in the superficial enamel (se). Three-week-old *Dspp*$^{P19L/+}$ mice showed a similar arrangement of enamel rods as the age-matched wild-type mice, but there were no discernable enamel rods in 3-week-old *Dspp*$^{P19L/P19L}$ mice. By 24 weeks, the decussating enamel rods remain in *Dspp*$^{+/+}$ mice. However, the enamel rod boundaries became blurred in *Dspp*$^{P19L/+}$ mice, whereas only poorly-defined enamel rods were observed in *Dspp*$^{P19L/P19L}$ mice. ie, inner enamel; oe, outer enamel; en, enamel; se, superficial enamel; de, dentin; and DEJ, dentinoenamel junction. Scale bars: 10 μm.

(**Figures 5A**,**B**). In addition, the dentinoenamel junction (DEJ) appeared to be altered in *Dspp*$^{P19L/P19L}$ mice, compared to age-matched *Dspp*$^{P19L/+}$ and *Dspp*$^{P19L/+}$ mice (**Figures 5A**,**B**). Taken together, these findings support that the molar enamel was poorly formed in *Dspp*$^{P19L/+}$ and *Dspp*$^{P19L/P19L}$ mice, particularly in *Dspp*$^{P19L/P19L}$ mice.

An Accumulation of DSPP Protein Within the Presecretory Ameloblasts in *Dspp*$^{P19L/+}$ and *Dspp*$^{P19L/P19L}$ Mice

To determine the molecular changes that occurred in the differentiating ameloblasts, we examined the expression of the *Dspp* gene at both mRNA and protein levels in the mandibular first molars (pre-eruptive phase) of 7-day-old *Dspp*$^{P19L/+}$ and *Dspp*$^{P19L/P19L}$ mice. Histologic analyses showed that the secretory ameloblasts in *Dspp*$^{P19L/+}$ and *Dspp*$^{P19L/P19L}$ mice appeared to be similar in morphology to those in the *Dspp*$^{+/+}$ mice (**Figure 6A**). *In situ* hybridization demonstrated that a low level of *DSPP* mRNAs was observed in the presecretory ameloblasts in *Dspp*$^{+/+}$ mice (**Figure 6B**). Unlike the strong and sustained *Dspp* expression in the opposing odontoblasts, the *Dspp* expression abruptly diminished as the presecretory ameloblasts differentiated into secretory ameloblasts (**Figure 6B**). Compared to *Dspp*$^{+/+}$ mice, there was a moderate decrease in *DSPP* mRNA signal in both presecretory ameloblasts and odontoblasts in *Dspp*$^{P19L/+}$ mice and a great decrease in *Dspp*$^{P19L/P19L}$ mice (**Figure 6B**). In contrast to the changes in *DSPP* mRNA, immunohistochemical signals for DSP/DSPP protein were weakly detected in the presecretory ameloblasts and odontoblasts in *Dspp*$^{+/+}$ mice (**Figure 6C**). There was a moderate increase in the DSP/DSPP signals in both presecretory ameloblasts and odontoblasts in *Dspp*$^{P19L/+}$ mice, and a strong increase in

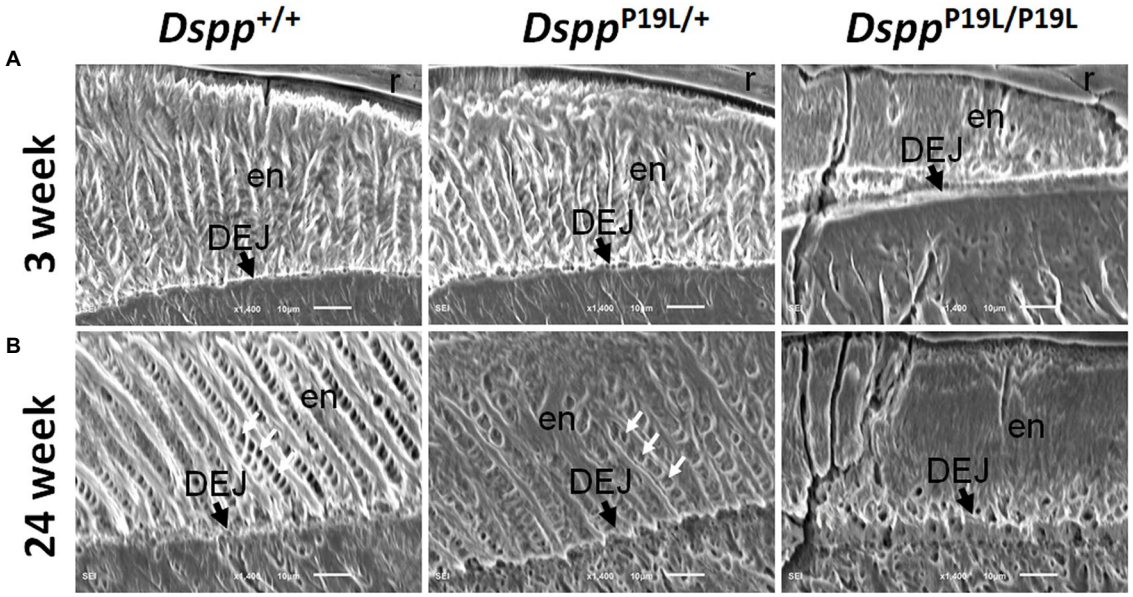

FIGURE 5 | Acid-etched SEM analyses of the mandibular first molars. Shown are the acid-etched SEM images of the mandibular first molars of 3- **(A)** and 24- **(B)** week-old wild-type *Dspp*$^{+/+}$, heterozygous *Dspp*$^{P19L/+}$ and homozygous *Dspp*$^{P19L/P19L}$ mice. All images are the longitudinal sections and buccal sides of the mandibular first molars. At the age of 3 weeks, *Dspp*$^{P19L/+}$ mice showed a similar acid-etching pattern in enamel (en) as the wild-type mice. At the age of 24 weeks, *Dspp*$^{+/+}$ mice presented an acid-etching pattern, with the cross-sectioned enamel rods (pointed by white arrows) preferentially removed by acid; although *Dspp*$^{P19L/+}$ mice displayed a similar pattern, the cross-sectioned enamel rods (pointed by white arrows) were not as well-defined as the wild-type mice. There were no recognizable enamel rods in *Dspp*$^{P19L/P19L}$ mice at both ages. The dentinoenamel junction (DEJ) appeared to be different in *Dspp*$^{P19L/P19L}$ mice, compared to age-matched *Dspp*$^{+/+}$ and *Dspp*$^{P19L/+}$ mice. en, enamel; DEJ, dentinoenamel junction; and r, resin. Scale bars: 10 μm.

Dspp$^{P19L/P19L}$ mice (**Figure 6C**). Nevertheless, immunohisto chemistry showed that there was no obvious difference in the level and distribution of two secretory stage ameloblast markers, AMEL and AMBN, in the enamel matrices among all three groups of mice (**Figures 7A**,**B**). These results suggest that the defective enamel may be associated with an accumulation of the mutant P19L-DSPP protein within the presecretory ameloblasts in *Dspp*$^{P19L/+}$ and *Dspp*$^{P19L/P19L}$ mice.

DISCUSSION

The enamel defects are less-well studied in human DGI patients associated with DSPP mutations because of rapid enamel attrition in human patients and lack of an appropriate animal model. We previously generated a mouse model that expresses P19L-DSPP – a mouse equivalent of human mutant P17L-DSPP, and reported the dentin/pulp phenotypes of *Dspp*$^{P19L/+}$ and *Dspp*$^{P19L/P19L}$ mice. In this study, we presented the ultrastructural enamel defects of these mice as well as the molecular changes in the differentiating ameloblasts and demonstrated that the enamel defects may be associated with an accumulation of the mutant P19L-DSPP protein within the presecretory ameloblasts.

The teeth often undergo rapid and severe attrition in DGI patients associated with DSPP mutations. It is generally believed that enamel readily chips off from the underlying defective dentin and/or abnormal DEJ after tooth eruption, thereby exposing the softer and malformed dentin to rapid attrition (Wright and Gantt, 1985; Kim et al., 2004; MacDougall et al., 2006; Hart and Hart, 2007; Kida et al., 2009; Min et al., 2014; Porntaveetus et al., 2018). However, it has also become evident that in some cases, the enamel itself may have intrinsic developmental defects (Lee et al., 2011; Wang et al., 2011; Bloch-Zupan et al., 2016; Taleb et al., 2018), which may be a direct contributing factor to rapid tooth wear observed in DGI patients. Consistently, we previously reported that both *Dspp*$^{P19L/+}$ and *Dspp*$^{P19L/P19L}$ mice showed significantly reduced thickness of dental pulp chamber roof dentin and reduced dentin mineral densities (Liang et al., 2019), suggesting that the defective dentin may contribute to the accelerated tooth attrition as it cannot provide adequate support to the overlying enamel. In this study, we further demonstrated that *Dspp*$^{P19L/+}$ and *Dspp*$^{P19L/P19L}$ mice displayed delayed enamel maturation and reduced enamel mineral densities, corroborating the intrinsic defects in the enamel. Similar to human DGI patients, the malformed enamel experienced accelerated attrition after the teeth erupted in *Dspp*$^{P19L/+}$ and *Dspp*$^{P19L/P19L}$ mice. These human and animal genetic studies strongly demonstrate that DSPP mutations can cause both enamel and dentin defects, which may together contribute to the severe tooth attrition seen in DGI patients. However, it is of note that some DSPP mutations may have no or negligible effects on enamel formation (McKnight et al., 2008; Nieminen et al., 2011; Verdelis et al., 2016; Yang et al., 2016; Park et al., 2020).

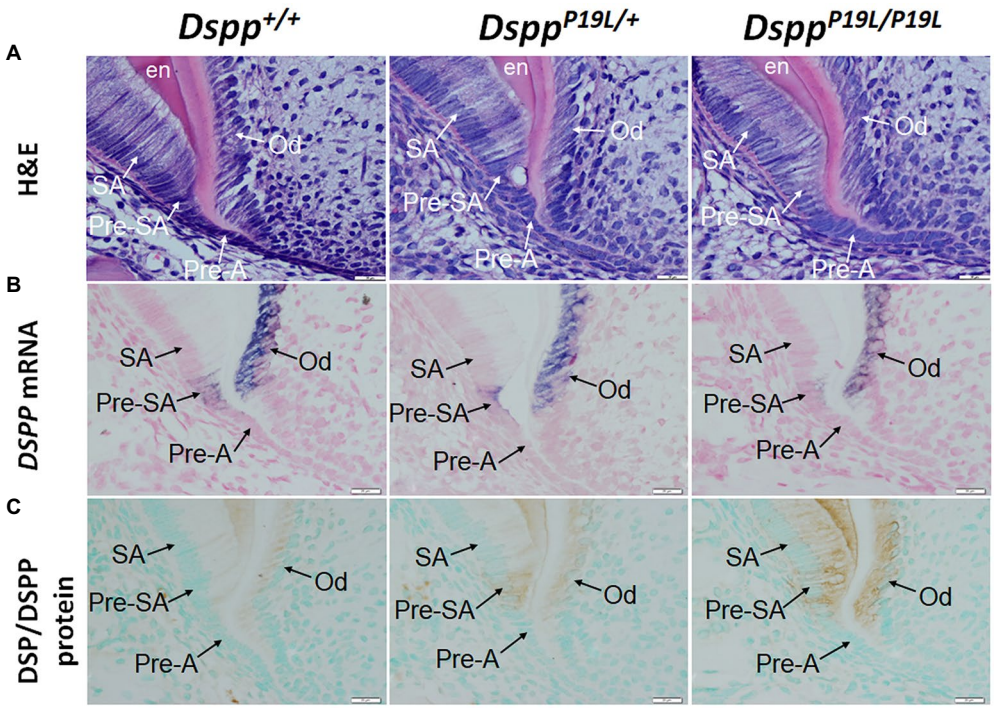

FIGURE 6 | Intracellular accumulation of dentin sialophosphoprotein (DSPP) protein in presecretory ameloblasts. All images are the sagittal section and distal cervical region of the mandibular first molars of 1-week-old wild-type *Dspp*$^{+/+}$, heterozygous *Dspp*$^{P19L/+}$ and homozygous *Dspp*$^{P19L/P19L}$ mice. **(A)** H&E staining. **(B)** *In situ* hybridization analysis of *DSPP* mRNA (signal in purple). *Dspp*$^{P19L/+}$ mice had a moderate decrease, whereas homozygous *Dspp*$^{P19L/P19L}$ mice showed a marked decrease in *DSPP* mRNA level in both odontoblasts and presecretory ameloblasts, compared to the wild-type mice. **(C)** Immunohistochemical staining of DSP/DSPP protein (signal in brown). The immunohistochemical staining signals for DSP/DSPP protein were weakly detected in the presecretory ameloblasts and odontoblasts in the wild-type mice. There was a moderate increase in the DSP/DSPP signals in both presecretory ameloblasts and odontoblasts in *Dspp*$^{P19L/+}$ mice, and a strong increase in *Dspp*$^{P19L/P19L}$ mice. SA, secretory ameloblasts; Pre-SA, presecretory ameloblast, Pre-A, preameloblasts; OD, odontoblasts; and en, enamel. Scale bars: 20 μm in A–I.

During tooth development, *Dspp* is transiently expressed by the presecretory ameloblasts (D'Souza et al., 1997; Ritchie et al., 1997; Begue-Kirn et al., 1998; MacDougall et al., 1998; Bleicher et al., 1999). Thereby, it has been speculated that the enamel defects may be due to ameloblast pathology caused by mutant DSPP proteins (Lee et al., 2011; Wang et al., 2011). Indeed, we found that even though the level of DSPP mRNA was markedly reduced in the presecretory ameloblasts, and the mutant P19L-DSPP protein was accumulated within the cells in both *Dspp*$^{P19L/+}$ and *Dspp*$^{P19L/P19L}$ mice. We have previously reported that the mutant P19L-DSPP protein was accumulated in the endoplasmic reticulum when it was transiently expressed in *in vitro* cultured odontoblast-like cells (Liang et al., 2019). Therefore, it is most likely that the mutant P19L-DSPP protein was also retained in the ER within the presecretory ameloblasts. DSPP is highly acidic as it contains a large number of aspartate and glutamate residues (Prasad et al., 2010). If the full-length DSPP was accumulated in the ER, the highly acidic DSPP could incur pathogenic ER stress. It has been shown that ER stress and its associated unfolded protein response (UPR) is involved in AI caused by mutations in the genes that encode enamel matrix proteins (Brookes et al., 2014, 2017a,b; Hetz et al., 2020). Therefore, it is reasonable to postulate that the enamel defects observed in *Dspp*$^{P19L/+}$ and *Dspp*$^{P19L/P19L}$ mice may be associated with ER stress and its activated UPR caused by mutant P19L-DSPP protein.

It is important to note that even though the mutant *Dspp*^{P19L} allele, like the wild-type *Dspp* allele, was only transiently expressed in the presecretory ameloblasts, it caused an irreversible damage on ameloblast differentiation and function. First, we demonstrated that the function of the secretory-stage ameloblasts was affected as evidenced by reduced enamel formation, even though the levels of AMEL and AMBN in the enamel matrices appeared to be normal in *Dspp*$^{P19L/+}$ and *Dspp*$^{P19L/P19L}$ mice. Secondly, the function of the maturation-stage ameloblasts was also compromised as reflected by delayed enamel maturation in *Dspp*$^{P19L/+}$ and *Dspp*$^{P19L/P19L}$ mice. These findings further emphasize the notion that the presecretory ameloblasts are very sensitive to their intracellular and extracellular disturbances so that any pathological conditions may affect their function and continual differentiation and cause developmental enamel defects (Lee et al., 2011; Wang et al., 2011). Further studies are needed to determine how the mutant P19L-DSPP protein exerted its negative effect on the presecretory ameloblasts, and their subsequent differentiation into secretory stage ameloblasts and maturation stage ameloblasts.

Dspp$^{P19L/+}$ and *Dspp*$^{P19L/P19L}$ mice manifested an enamel phenotype that is quite different from *Dspp*-null mice. It

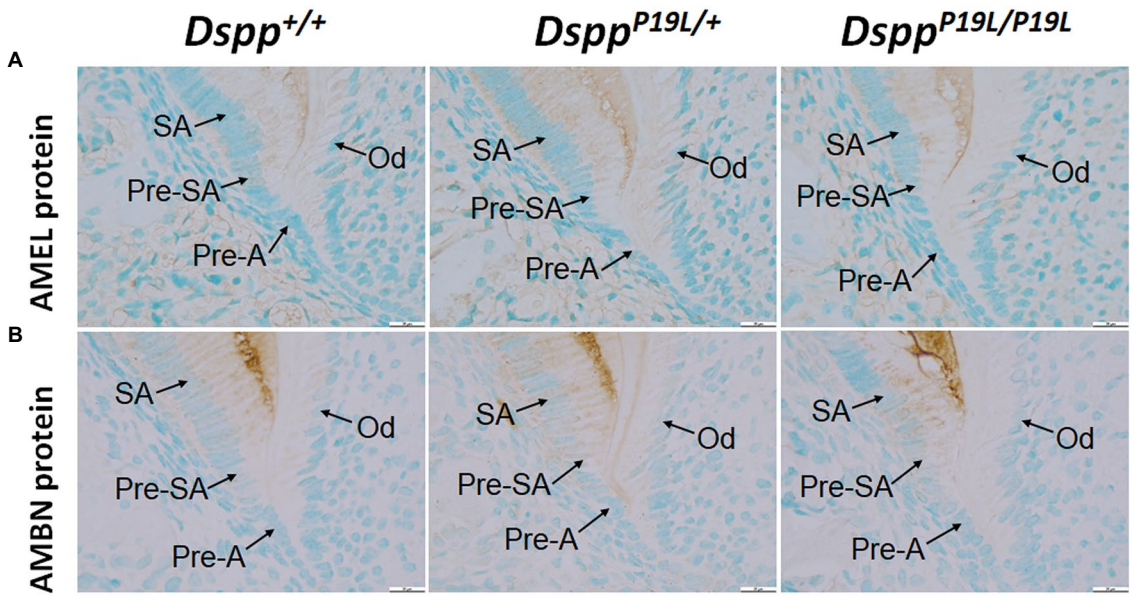

FIGURE 7 | Immunohistochemical staining of amelogenin (AMEL) and ameloblastin (AMBN). All images are the sagittal section and distal cervical region of the mandibular first molars of 1-week-old wild-type *Dspp*$^{+/+}$, heterozygous *Dspp*$^{P19L/+}$ and homozygous *Dspp*$^{P19L/P19L}$ mice. **(A)** Immunohistochemical staining of AMEL (signal in brown). **(B)** Immunohistochemical staining of AMBN (signal in brown). All three groups of mice showed a similar distribution and intensity of AMEL and AMBN immunostaining signals in the enamel matrices. SA, secretory ameloblasts; Pre-SA, presecretory ameloblast, Pre-A, preameloblasts; and OD, odontoblasts. Scale bars: 20 μm in A–F.

has been reported that even though *Dspp*-null mice had earlier onset of enamel matrix deposition in mandibular incisors, they did not exhibit any major phenotypic abnormalities in mature enamel with regards to enamel structural organization, mineral density, or hardness (Verdelis et al., 2016). Nevertheless, *Dspp*-null mice did show a defect in DEJ, which might be due to either the loss of DSPP function in the formation of this dentin and enamel interface or the earlier onset of enamel deposition (Verdelis et al., 2016). In contrast, *Dspp*$^{P19L/+}$ and *Dspp*$^{P19L/P19L}$ mice not only displayed an abnormal DEJ as evidenced by acid-etched SEM analysis, they also had reduced enamel formation as well as intrinsic structural defects in enamel. Moreover, unlike *Dspp* heterozygous mice who did not show any apparent dental phonotype (Sreenath et al., 2003; Suzuki et al., 2009; Verdelis et al., 2016), our current and previous studies showed that the *Dspp*$^{P19L/+}$ mice developed a similar, though less severe, tooth phenotype as *Dspp*$^{P19L/P19L}$ mice (Liang et al., 2019). The phenotypic difference between the *Dspp* mutant mice and *Dspp*-null mice support that the enamel phenotypes of *Dspp*$^{P19L/+}$ and *Dspp*$^{P19L/P19L}$ mice were not simply caused by a loss of DSPP function in the presecretory ameloblasts.

Moreover, previous studies have shown that ectopic overexpression of DSP in secretory ameloblasts in mice resulted in an increase in enamel hardness, whereas similar overexpression of DPP weakened enamel and made it more prone to wear (Paine et al., 2005; White et al., 2007). Yet, it is very unlikely that the enamel phenotypes of *Dspp*$^{P19L/+}$ and *Dspp*$^{P19L/P19L}$ mice were caused by ectopic overexpression of DSP or DPP. First, we have demonstrated that the mutant *Dspp*^{P19L} allele, like the wild-type *Dspp* allele, was only transiently expressed in the presecretory ameloblasts. Secondly, our previous studies have demonstrated that although the secretion of P19L-DSPP was impaired, Western-blotting analysis of the total proteins extracted from the dental pulps and dentin matrices of first molars of *Dspp*$^{P19L/P19L}$ mice as well as the proteins from the conditioned media harvested from cells transfected with the mutant P19L-DSPP-expressing construct revealed that the mutant P19L-DSP/DSPP proteins showed a similar migrating pattern as the normal DSP/DSPP proteins, suggesting that the secreted mutant and normal DSPP proteins were subject to similar posttranslational modifications and proteolytic processing (Liang et al., 2019). Therefore, it is reasonable to exclude the possibility that the enamel phenotypes of the *Dspp* mutant mice were caused by a gain of DSP or DPP function in the presecretory/secretory ameloblasts.

In summary, we have demonstrated that DSPP mutations could affect enamel formation and cause severe intrinsic enamel defects. Future studies are warranted to determine the molecular pathogenesis underlying the enamel defects associated with the mutant P19L-DSPP protein.

DATA AVAILABILITY STATEMENT

The original contributions presented in this study are included in the article/supplementary material; further inquiries can be directed to the corresponding author.

ETHICS STATEMENT

The animal study was reviewed and approved by the Institutional Animal Care and Use Committee of Texas A&M University College of Dentistry.

AUTHOR CONTRIBUTIONS

TL and QX contributed to design, data acquisition, analysis and interpretation, drafted, and critically revised the manuscript. HZ and SW contributed to data acquisition, analysis, interpretation, drafted, and critically revised the manuscript. TD and CQ contributed to interpretation, drafted, and critically revised the manuscript. YL contributed to conception, design, interpretation, drafted, and critically revised the manuscript. All authors approved the final version of the submitted manuscript and agree to be accountable for all aspects of the work.

FUNDING

This work was supported by National Institute of Dental & Craniofacial Research (NIDCR) grant DE027345.

REFERENCES

Balic, A., and Thesleff, I. (2015). Tissue interactions regulating tooth development and renewal. *Curr. Top. Dev. Biol.* 115, 157–186. doi: 10.1016/bs.ctdb.2015.07.006

Begue-Kirn, C., Krebsbach, P. H., Bartlett, J. D., and Butler, W. T. (1998). Dentin sialoprotein, dentin phosphoprotein, enamelysin and ameloblastin: tooth-specific molecules that are distinctively expressed during murine dental differentiation. *Eur. J. Oral Sci.* 106, 963–970. doi: 10.1046/j.0909-8836.1998.eos106510.x

Bleicher, F., Couble, M. L., Farges, J. C., Couble, P., and Magloire, H. (1999). Sequential expression of matrix protein genes in developing rat teeth. *Matrix Biol.* 18, 133–143. doi: 10.1016/S0945-053X(99)00007-4

Bloch-Zupan, A., Huckert, M., Stoetzel, C., Meyer, J., Geoffroy, V., Razafindrakoto, R. W., et al. (2016). Detection of a novel DSPP mutation by NGS in a population isolate in Madagascar. *Front. Physiol.* 7:70. doi: 10.3389/fphys.2016.00304

Bouxsein, M. L., Boyd, S. K., Christiansen, B. A., Guldberg, R. E., Jepsen, K. J., and Muller, R. (2010). Guidelines for assessment of bone microstructure in rodents using micro-computed tomography. *J. Bone Miner. Res.* 25, 1468–1486. doi: 10.1002/jbmr.141

Brookes, S. J., Barron, M. J., Boot-Handford, R., Kirkham, J., and Dixon, M. J. (2014). Endoplasmic reticulum stress in amelogenesis imperfecta and phenotypic rescue using 4-phenylbutyrate. *Hum. Mol. Genet.* 23, 2468–2480. doi: 10.1093/hmg/ddt642

Brookes, S. J., Barron, M. J., Dixon, M. J., and Kirkham, J. (2017a). The unfolded protein response in amelogenesis and enamel pathologies. *Front. Physiol.* 8:653. doi: 10.3389/fphys.2017.00653

Brookes, S. J., Barron, M. J., Smith, C. E. L., Poulter, J. A., Mighell, A. J., Inglehearn, C. F., et al. (2017b). Amelogenesis imperfecta caused by N-terminal enamelin point mutations in mice and men is driven by endoplasmic reticulum stress. *Hum. Mol. Genet.* 26, 1863–1876. doi: 10.1093/hmg/ddx090

Butler, W. T., Bhown, M., Dimuzio, M. T., Cothran, W. C., and Linde, A. (1983). Multiple forms of rat dentin phosphoproteins. *Arch. Biochem. Biophys.* 225, 178–186. doi: 10.1016/0003-9861(83)90021-8

D'Souza, R. N., Cavender, A., Sunavala, G., Alvarez, J., Ohshima, T., Kulkarni, A. B., et al. (1997). Gene expression patterns of murine dentin matrix protein 1 (Dmp1) and dentin sialophosphoprotein (DSPP) suggest distinct developmental functions in vivo. *J. Bone Miner. Res.* 12, 2040–2049. doi: 10.1359/jbmr.1997.12.12.2040

Fisher, L. W., and Fedarko, N. S. (2003). Six genes expressed in bones and teeth encode the current members of the SIBLING family of proteins. *Connect. Tissue Res.* 44(Suppl. 1), 33–40. doi: 10.1080/03008200390152061

Fisher, L. W., Torchia, D. A., Fohr, B., Young, M. F., and Fedarko, N. S. (2001). Flexible structures of SIBLING proteins, bone sialoprotein, and osteopontin. *Biochem. Biophys. Res. Commun.* 280, 460–465. doi: 10.1006/bbrc.2000.4146

George, A., Bannon, L., Sabsay, B., Dillon, J. W., Malone, J., Veis, A., et al. (1996). The carboxyl-terminal domain of phosphophoryn contains unique extended triplet amino acid repeat sequences forming ordered carboxyl-phosphate interaction ridges that may be essential in the biomineralization process. *J. Biol. Chem.* 271, 32869–32873. doi: 10.1074/jbc.271.51.32869

Gibson, M. P., Zhu, Q., Wang, S., Liu, Q., Liu, Y., Wang, X., et al. (2013). The rescue of dentin matrix protein 1 (DMP1)-deficient tooth defects by the transgenic expression of dentin sialophosphoprotein (DSPP) indicates that DSPP is a downstream effector molecule of DMP1 in dentinogenesis. *J. Biol. Chem.* 288, 7204–7214. doi: 10.1074/jbc.M112.445775

Hart, P. S., and Hart, T. C. (2007). Disorders of human dentin. *Cells Tissues Organs* 186, 70–77. doi: 10.1159/000102682

Hetz, C., Zhang, K., and Kaufman, R. J. (2020). Mechanisms, regulation and functions of the unfolded protein response. *Nat. Rev. Mol. Cell Biol.* 21, 421–438. doi: 10.1038/s41580-020-0250-z

Hu, J. C., Chun, Y. H., Al Hazzazzi, T., and Simmer, J. P. (2007). Enamel formation and amelogenesis imperfecta. *Cells Tissues Organs* 186, 78–85. doi: 10.1159/000102683

Kida, M., Tsutsumi, T., Shindoh, M., Ikeda, H., and Ariga, T. (2009). De novo mutation in the DSPP gene associated with dentinogenesis imperfecta type II in a Japanese family. *Eur. J. Oral Sci.* 117, 691–694. doi: 10.1111/j.1600-0722.2009.00683.x

Kim, J. W., Nam, S. H., Jang, K. T., Lee, S. H., Kim, C. C., Hahn, S. H., et al. (2004). A novel splice acceptor mutation in the DSPP gene causing dentinogenesis imperfecta type II. *Hum. Genet.* 115, 248–254. doi: 10.1007/s00439-004-1143-5

Kim, J. W., and Simmer, J. P. (2007). Hereditary dentin defects. *J. Dent. Res.* 86, 392–399. doi: 10.1177/154405910708600502

Komiyama, Y., Ohba, S., Shimohata, N., Nakajima, K., Hojo, H., Yano, F., et al. (2013). Tenomodulin expression in the periodontal ligament enhances cellular adhesion. *PLoS One* 8:e60203. doi: 10.1371/journal.pone.0060203

Lee, S. K., Lee, K. E., Hwang, Y. H., Kida, M., Tsutsumi, T., Ariga, T., et al. (2011). Identification of the DSPP mutation in a new kindred and phenotype-genotype correlation. *Oral Dis.* 17, 314–319. doi: 10.1111/j.1601-0825.2010.01760.x

Lee, S. K., Lee, K. E., Song, S. J., Hyun, H. K., Lee, S. H., and Kim, J. W. (2013). A DSPP mutation causing dentinogenesis imperfecta and characterization of the mutational effect. *Biomed. Res. Int.* 2013:948181. doi: 10.1155/2013/948181

Li, D., Du, X., Zhang, R., Shen, B., Huang, Y., Valenzuela, R. K., et al. (2012). Mutation identification of the DSPP in a Chinese family with DGI-II and an up-to-date bioinformatic analysis. *Genomics* 99, 220–226. doi: 10.1016/j.ygeno.2012.01.006

Li, L., Saiyin, W., Zhang, H., Wang, S., Xu, Q., Qin, C., et al. (2019). FAM20A is essential for amelogenesis, but is dispensable for dentinogenesis. *J. Mol. Histol.* 50, 581–591. doi: 10.1007/s10735-019-09851-x

Liang, T., Zhang, H., Xu, Q., Wang, S., Qin, C., and Lu, Y. (2019). Mutant dentin sialophosphoprotein causes dentinogenesis imperfecta. *J. Dent. Res.* 98, 912–919. doi: 10.1177/0022034519854029

MacDougall, M., Dong, J., and Acevedo, A. C. (2006). Molecular basis of human dentin diseases. *Am. J. Med. Genet. A* 140, 2536–2546. doi: 10.1002/ajmg.a.31359

MacDougall, M., Nydegger, J., Gu, T. T., Simmons, D., Luan, X., Cavender, A., et al. (1998). Developmental regulation of dentin sialophosphoprotein during ameloblast differentiation: a potential enamel matrix nucleator. *Connect. Tissue Res.* 39, 25–37. doi: 10.3109/03008209809023909

MacDougall, M., Simmons, D., Luan, X., Nydegger, J., Feng, J., and Gu, T. T. (1997). Dentin phosphoprotein and dentin sialoprotein are cleavage products expressed from a single transcript coded by a gene on human chromosome 4. Dentin phosphoprotein DNA sequence determination. *J. Biol. Chem.* 272, 835–842. doi: 10.1074/jbc.272.2.835

McKnight, D. A., Simmer, J. P., Hart, P. S., Hart, T. C., and Fisher, L. W. (2008). Overlapping DSPP mutations cause dentin dysplasia and dentinogenesis imperfecta. *J. Dent. Res.* 87, 1108–1111. doi: 10.1177/154405910808701217

Meng, T., Huang, Y., Wang, S., Zhang, H., Dechow, P. C., Wang, X., et al. (2015). Twist1 is essential for tooth morphogenesis and odontoblast differentiation. *J. Biol. Chem.* 290, 29593–29602. doi: 10.1074/jbc.M115.680546

Min, B., Song, J. S., Lee, J. H., Choi, B. J., Kim, K. M., and Kim, S. O. (2014). Multiple teeth fractures in dentinogenesis imperfecta: a case report. *J. Clin. Pediatr. Dent.* 38, 362–365. doi: 10.17796/jcpd.38.4.q523456j733642r2

Moradian-Oldak, J. (2012). Protein-mediated enamel mineralization. *Front. Biosci.* 17, 1996–2023. doi: 10.2741/4034

Nieminen, P., Papagiannoulis-Lascarides, L., Waltimo-Siren, J., Ollila, P., Karjalainen, S., Arte, S., et al. (2011). Frameshift mutations in dentin phosphoprotein and dependence of dentin disease phenotype on mutation location. *J. Bone Miner. Res.* 26, 873–880. doi: 10.1002/jbmr.276

Paine, M. L., Luo, W., Wang, H. J., Bringas, P. Jr., Ngan, A. Y., Miklus, V. G., et al. (2005). Dentin sialoprotein and dentin phosphoprotein overexpression during amelogenesis. *J. Biol. Chem.* 280, 31991–31998. doi: 10.1074/jbc.M502991200

Park, H., Hyun, H. K., Woo, K. M., and Kim, J. W. (2020). Physicochemical properties of dentinogenesis imperfecta with a known DSPP mutation. *Arch. Oral Biol.* 117:104815. doi: 10.1016/j.archoralbio.2020.104815

Porntaveetus, T., Nowwarote, N., Osathanon, T., Theerapanon, T., Pavasant, P., Boonprakong, L., et al. (2019). Compromised alveolar bone cells in a patient with dentinogenesis imperfecta caused by DSPP mutation. *Clin. Oral Investig.* 23, 303–313. doi: 10.1007/s00784-018-2437-7

Porntaveetus, T., Osathanon, T., Nowwarote, N., Pavasant, P., Srichomthong, C., Suphapeetiporn, K., et al. (2018). Dental properties, ultrastructure, and pulp cells associated with a novel DSPP mutation. *Oral Dis.* 24, 619–627. doi: 10.1111/odi.12801

Prasad, M., Butler, W. T., and Qin, C. (2010). Dentin sialophosphoprotein in biomineralization. *Connect. Tissue Res.* 51, 404–417. doi: 10.3109/03008200903329789

Ritchie, H. H., Berry, J. E., Somerman, M. J., Hanks, C. T., Bronckers, A. L., Hotton, D., et al. (1997). Dentin sialoprotein (DSP) transcripts: developmentally-sustained expression in odontoblasts and transient expression in pre-ameloblasts. *Eur. J. Oral Sci.* 105, 405–413. doi: 10.1111/j.1600-0722.1997.tb02137.x

Ritchie, H. H., Hou, H., Veis, A., and Butler, W. T. (1994). Cloning and sequence determination of rat dentin sialoprotein, a novel dentin protein. *J. Biol. Chem.* 269, 3698–3702. doi: 10.1016/S0021-9258(17)41916-8

Ritchie, H. H., and Wang, L. H. (1996). Sequence determination of an extremely acidic rat dentin phosphoprotein. *J. Biol. Chem.* 271, 21695–21698. doi: 10.1074/jbc.271.36.21695

Robinson, C., Lowe, N. R., and Weatherell, J. A. (1977). Changes in amino-acid composition of developing rat incisor enamel. *Calcif. Tissue Res.* 23, 19–31. doi: 10.1007/BF02012762

Schmitz, J. E., Teepe, J. D., Hu, Y., Smith, C. E., Fajardo, R. J., and Chun, Y. H. (2014). Estimating mineral changes in enamel formation by ashing/BSE and microCT. *J. Dent. Res.* 93, 256–262. doi: 10.1177/0022034513520548

Shields, E. D., Bixler, D., and El-Kafrawy, A. M. (1973). A proposed classification for heritable human dentine defects with a description of a new entity. *Arch. Oral Biol.* 18, 543–553. doi: 10.1016/0003-9969(73)90075-7

Smith, C. E., Hu, Y., Richardson, A. S., Bartlett, J. D., Hu, J. C., and Simmer, J. P. (2011). Relationships between protein and mineral during enamel development in normal and genetically altered mice. *Eur. J. Oral Sci.* 119(Suppl 1), 125–135. doi: 10.1111/j.1600-0722.2011.00871.x

Smith, C. E., and Nanci, A. (1989). A method for sampling the stages of amelogenesis on mandibular rat incisors using the molars as a reference for dissection. *Anat. Rec.* 225, 257–266. doi: 10.1002/ar.1092250312

Smith, C. E. L., Poulter, J. A., Antanaviciute, A., Kirkham, J., Brookes, S. J., Inglehearn, C. F., et al. (2017). Amelogenesis imperfecta; genes, proteins, and pathways. *Front. Physiol.* 8:435. doi: 10.3389/fphys.2017.00435

Sreenath, T., Thyagarajan, T., Hall, B., Longenecker, G., D'Souza, R., Hong, S., et al. (2003). Dentin sialophosphoprotein knockout mouse teeth display widened predentin zone and develop defective dentin mineralization similar to human dentinogenesis imperfecta type III. *J. Biol. Chem.* 278, 24874–24880. doi: 10.1074/jbc.M303908200

Sun, Y., Lu, Y., Chen, S., Prasad, M., Wang, X., Zhu, Q., et al. (2010). Key proteolytic cleavage site and full-length form of DSPP. *J. Dent. Res.* 89, 498–503. doi: 10.1177/0022034510363109

Suzuki, S., Sreenath, T., Haruyama, N., Honeycutt, C., Terse, A., Cho, A., et al. (2009). Dentin sialoprotein and dentin phosphoprotein have distinct roles in dentin mineralization. *Matrix Biol.* 28, 221–229. doi: 10.1016/j.matbio.2009.03.006

Taleb, K., Lauridsen, E., Daugaard-Jensen, J., Nieminen, P., and Kreiborg, S. (2018). Dentinogenesis imperfecta type II- genotype and phenotype analyses in three Danish families. *Mol. Genet. Genomic Med.* 6, 339–349. doi: 10.1002/mgg3.375

Thesleff, I. (2003). Epithelial-mesenchymal signalling regulating tooth morphogenesis. *J. Cell Sci.* 116, 1647–1648. doi: 10.1242/jcs.00410

Verdelis, K., Szabo-Rogers, H. L., Xu, Y., Chong, R., Kang, R., Cusack, B. J., et al. (2016). Accelerated enamel mineralization in Dspp mutant mice. *Matrix Biol.* 52-54, 246–259. doi: 10.1016/j.matbio.2016.01.003

von Marschall, Z., and Fisher, L. W. (2010). Dentin sialophosphoprotein (DSPP) is cleaved into its two natural dentin matrix products by three isoforms of bone morphogenetic protein-1 (BMP1). *Matrix Biol.* 29, 295–303. doi: 10.1016/j.matbio.2010.01.002

Wang, S. K., Chan, H. C., Rajderkar, S., Milkovich, R. N., Uston, K. A., Kim, J. W., et al. (2011). Enamel malformations associated with a defined dentin sialophosphoprotein mutation in two families. *Eur. J. Oral Sci.* 119 (Suppl. 1), 158–167. doi: 10.1111/j.1600-0722.2011.00874.x

Warshawsky, H., and Smith, C. E. (1974). Morphological classification of rat incisor ameloblasts. *Anat. Rec.* 179, 423–446. doi: 10.1002/ar.1091790403

White, S. N., Paine, M. L., Ngan, A. Y., Miklus, V. G., Luo, W., Wang, H., et al. (2007). Ectopic expression of dentin sialoprotein during amelogenesis hardens bulk enamel. *J. Biol. Chem.* 282, 5340–5345. doi: 10.1074/jbc.M604814200

Wright, J. T., and Gantt, D. G. (1985). The ultrastructure of the dental tissues in dentinogenesis imperfecta in man. *Arch. Oral Biol.* 30, 201–206. doi: 10.1016/0003-9969(85)90116-5

Yamakoshi, Y., Hu, J. C., Fukae, M., Zhang, H., and Simmer, J. P. (2005). Dentin glycoprotein: the protein in the middle of the dentin sialophosphoprotein chimera. *J. Biol. Chem.* 280, 17472–17479. doi: 10.1074/jbc.M413220200

Yamakoshi, Y., Nagano, T., Hu, J. C., Yamakoshi, F., and Simmer, J. P. (2011). Porcine dentin sialoprotein glycosylation and glycosaminoglycan attachments. *BMC Biochem.* 12:6. doi: 10.1186/1471-2091-12-6

Yang, J., Kawasaki, K., Lee, M., Reid, B. M., Nunez, S. M., Choi, M., et al. (2016). The dentin phosphoprotein repeat region and inherited defects of dentin. *Mol. Genet. Genomic Med.* 4, 28–38. doi: 10.1002/mgg3.176

Zhang, H., Xie, X., Liu, P., Liang, T., Lu, Y., and Qin, C. (2018). Transgenic expression of dentin phosphoprotein (DPP) partially rescued the dentin defects of DSPP-null mice. *PLoS One* 13:e0195854. doi: 10.1371/journal.pone.0209862

Zhu, Q., Gibson, M. P., Liu, Q., Liu, Y., Lu, Y., Wang, X., et al. (2012). Proteolytic processing of dentin sialophosphoprotein (DSPP) is essential to dentinogenesis. *J. Biol. Chem.* 287, 30426–30435. doi: 10.1074/jbc.M112.388587

Zhu, Q., Sun, Y., Prasad, M., Wang, X., Yamoah, A. K., Li, Y., et al. (2010). Glycosaminoglycan chain of dentin sialoprotein proteoglycan. *J. Dent. Res.* 89, 808–812. doi: 10.1177/0022034510366902

Conflict of Interest: The authors declare that the research was conducted in the absence of any commercial or financial relationships that could be construed as a potential conflict of interest.

Publisher's Note: All claims expressed in this article are solely those of the authors and do not necessarily represent those of their affiliated organizations, or those of the publisher, the editors and the reviewers. Any product that may be evaluated in this article, or claim that may be made by its manufacturer, is not guaranteed or endorsed by the publisher.

frontiers in Physiology

ORIGINAL RESEARCH
published: 24 September 2021
doi: 10.3389/fphys.2021.748574

Connexin 43-Mediated Gap Junction Communication Regulates Ameloblast Differentiation *via* ERK1/2 Phosphorylation

*Aya Yamada[1†], Keigo Yoshizaki[2†], Masaki Ishikawa[3], Kan Saito[1], Yuta Chiba[4], Emiko Fukumoto[1], Ryoko Hino[1], Seira Hoshikawa[1], Mitsuki Chiba[1], Takashi Nakamura[5], Tsutomu Iwamoto[6] and Satoshi Fukumoto[1,4]**

[1]Division of Pediatric Dentistry, Department of Oral Health and Development Sciences, Tohoku University Graduate School of Dentistry, Sendai, Japan, [2]Section of Orthodontics and Dentofacial Orthopedics, Division of Oral Health, Growth and Development, Faculty of Dental Science, Kyushu University, Fukuoka, Japan, [3]The Department of Pathology and Laboratory Medicine, Perelman School of Medicine at the University of Pennsylvania, Philadelphia, PA, United States, [4]Section of Oral Medicine for Children, Division of Oral Health, Growth and Development, Faculty of Dental Science, Kyushu University, Fukuoka, Japan, [5]Division of Molecular Pharmacology and Cell Biophysics, Department of Oral Biology, Tohoku University Graduate School of Dentistry, Sendai, Japan, [6]Division of Oral Health Science, Department of Pediatric Dentistry/Special Needs Dentistry, Graduate School of Medical and Dental Science, Tokyo Medical and Dental University, Tokyo, Japan

OPEN ACCESS

Edited by:
Q. Adam Ye, Massachusetts General Hospital and Harvard Medical School, United States

Reviewed by:
Xiaoying Wang, Shandong University, China
Yiping Chen, Tulane University, United States

***Correspondence:**
Satoshi Fukumoto
fukumoto@dent.tohoku.ac.jp

[†]These authors have contributed equally to this work and share first authorship

Specialty section:
This article was submitted to Craniofacial Biology and Dental Research, a section of the journal Frontiers in Physiology

Received: *28 July 2021*
Accepted: *25 August 2021*
Published: *24 September 2021*

Citation:
Yamada A, Yoshizaki K, Ishikawa M, Saito K, Chiba Y, Fukumoto E, Hino R, Hoshikawa S, Chiba M, Nakamura T, Iwamoto T and Fukumoto S (2021) Connexin 43-Mediated Gap Junction Communication Regulates Ameloblast Differentiation via ERK1/2 Phosphorylation. Front. Physiol. 12:748574. doi: 10.3389/fphys.2021.748574

Connexin 43 (Cx43) is an integral membrane protein that forms gap junction channels. These channels mediate intercellular transport and intracellular signaling to regulate organogenesis. The human disease oculodentodigital dysplasia (ODDD) is caused by mutations in Cx43 and is characterized by skeletal, ocular, and dental abnormalities including amelogenesis imperfecta. To clarify the role of Cx43 in amelogenesis, we examined the expression and function of Cx43 in tooth development. Single-cell RNA-seq analysis and immunostaining showed that *Cx43* is highly expressed in pre-secretory ameloblasts, differentiated ameloblasts, and odontoblasts. Further, we investigated the pathogenic mechanisms of ODDD by analyzing *Cx43*-null mice. These mice developed abnormal teeth with multiple dental epithelium layers. The expression of enamel matrix proteins such as ameloblastin (Ambn), which is critical for enamel formation, was significantly reduced in *Cx43*-null mice. TGF-β1 induces *Ambn* transcription in dental epithelial cells. The induction of Ambn expression by TGF-β1 depends on the density of the cultured cells. Cell culture at low densities reduces cell–cell contact and reduces the effect of TGF-β1 on Ambn induction. When cell density was high, Ambn expression by TGF-β1 was enhanced. This induction was inhibited by the gap junction inhibitors, oleamide, and 18α-grycyrrhizic acid and was also inhibited in cells expressing Cx43 mutations (R76S and R202H). TGF-β1-mediated phosphorylation and nuclear translocation of ERK1/2, but not Smad2/3, were suppressed by gap junction inhibitors. Cx43 gap junction activity is required for TGF-β1-mediated Runx2 phosphorylation through ERK1/2, which forms complexes with Smad2/3. In addition to its gap junction activity, Cx43 may also function as a Ca^{2+} channel that regulates slow Ca^{2+} influx and ERK1/2 phosphorylation. TGF-β1 transiently increases intracellular calcium levels, and the increase in intracellular calcium

over a short period was not related to the expression level of Cx43. However, long-term intracellular calcium elevation was enhanced in cells overexpressing Cx43. Our results suggest that Cx43 regulates intercellular communication through gap junction activity by modulating TGF-β1-mediated ERK signaling and enamel formation.

Keywords: connexin, gap junction, ameloblast, tooth development, dental epithelium

INTRODUCTION

Cell–cell interactions through gap junctions are important for cell differentiation and the maintenance of cellular functions. Gap junction proteins form hexameric complexes that allow the intercellular transport of small molecules, including Ca^{2+}, IP3, and cAMP (Harris, 2007; Nielsen et al., 2012). The *Gja1* gene, which encodes a typical gap junction protein, connexin 43 (Cx43), has been identified as a tumor suppressor gene (Loewenstein and Kanno, 1966, 1967; Aasen et al., 2016). This gene is important for the electrical conduction system of the heart, which may synchronize concurrent functions in cells (Verheule and Kaese, 2013; Kurtenbach et al., 2014; Macquart et al., 2018). Cx43 is also involved in the human disease oculodentodigital dysplasia (ODDD; Paznekas et al., 2003, 2009; Laird, 2014), a disorder characterized by congenital missing teeth, microdontia, enamel hypoplasia, syndactyly, osteodysplasia, and craniofacial deformities (Judisch et al., 1979; Paznekas et al., 2003). Since the epithelial–mesenchymal interaction in tooth development is similar to interactions in the apical ectodermal ridge region during limb development, disorders presenting with simultaneous malformations of the teeth and fingers are frequently observed in human genetic diseases.

Regarding the role of Cx43 in tooth development, immunostaining for Cx43 has been reported in tooth germ layers, particularly in the inner enamel epithelium and ameloblasts (Al-Ansari et al., 2018; Nakamura et al., 2020). However, an analysis of teeth in Cx43 gene-deficient mice has not been sufficiently performed because the mice die during the fetal period due to heart and lung malformations (Reaume et al., 1995; Huang et al., 1998; Nagata et al., 2009). In *Gja1Jrt/+* mice with mutations in the *Cx43* gene, the effect of *Cx43* gene abnormalities on tooth formation was reported. Since these mice are viable, unlike *Cx43* gene-deficient mice, it was possible to analyze tooth formation after eruption. In this mouse, enamel hypoplasia and abnormalities in the arrangement of ameloblasts were observed (Flenniken et al., 2005; Toth et al., 2010). Furthermore, in mice in which the *Cx43* gene was ablated selectively in DMP1-expressing cells, a decrease in enamel formation and reduced mineral density were observed. This evidence suggests that Cx43 may be involved in the regulation of mineral transport in mature ameloblasts. However, these mice were analyzed mainly using histological examination, which does not fully clarify the underlying molecular function. Thus, the role of Cx43 in ameloblasts and its effects on tooth development are still unknown.

We identified tooth-specific molecules and analyzed their functions to clarify the differentiation mechanism of ameloblasts. Ameloblasts express the enamel matrix, which is a cell-specific extracellular matrix. Enamel is formed through the decomposition and absorption of the substrates. AMBN-deficient mice exhibit severe enamel hypoplasia and the formation of odontogenic tumors (Fukumoto et al., 2004). In addition, various transcription factors are involved in AMBN expression. Among them, Sp6/Epfn is strongly expressed in the inner enamel epithelium and ameloblasts. Sp6/epiprofin-deficient mice have an increased number of tooth germs, and teeth are formed without enamel (Nakamura et al., 2008, 2017). Sox21 is also involved in the regulation of *Ambn* expression and in the fate determination of invaginated epithelial cells. In Sox21-deficient mice, hair develops from the dental epithelium and epithelial–mesenchymal transition occurs in some tooth cells (Saito et al., 2020). Furthermore, Panx3, which is a gap junction strongly expressed in teeth, is expressed in odontoblast progenitor cells, is involved in dentin formation, and plays an important role in bone formation (Iwamoto et al., 2010, 2017; Ishikawa et al., 2011). Panx3 induces Cx43 expression and plays an important role in gap junction formation and osteoblast differentiation in bone (Ishikawa et al., 2016). Specifically, Panx3 and Cx43 regulate bone formation through their coordinated and continuous spatiotemporal expression. While Cx43 is expressed in ameloblasts, Panx3 is not, suggesting that hard tissue formation in ameloblasts may be regulated by a mechanism different from that of bone.

The aim of this study was to clarify the function of Cx43 in tooth development and to elucidate the common system involved in ectodermal organogenesis.

MATERIALS AND METHODS

Reagents

Anti-Cx43 and Runx2 antibodies were obtained from Santa Cruz Biotechnology. Anti-ERK1/2, phospho-ERK1/2, Smad2/3, phospho-Smad2/3(465/467), SAPK, phospho-SAPK, p38, phospho-p38, and HPRP-conjugated anti-rabbit IgG were obtained from Cell Signaling Technology. Anti-phospho-serine antibodies were purchased from Sigma-Aldrich. The anti-AMBN antibody has been previously described (Fukumoto et al., 2004). Alexa-488 or 594 conjugated anti-rabbit IgG was purchased from Molecular Probes. 18α-glycyrrhetinic acid (18α-GA), oleamide, adenophostin-A, and 2-APB were obtained from Sigma-Aldrich. PD98059 was obtained from Cell Signaling Technology. Fura-2AM was obtained from Invitrogen. TGF-β1, BMP2, and BMP4 were obtained from R&D Systems. Briefly, the pEF6/Cx43 vector was constructed by cloning the coding sequence of mouse

Cx43 cDNA into the pEF6/V5-His TOPO vector (Invitrogen). Cx43 expression vectors carrying R76S or R202H mutations were prepared using a Quick Change Site-Directed Mutagenesis Kit (Stratagene). siRNA for Cx43 was purchased from Invitrogen.

Single-Cell Preparation, Library Construction, and Sequencing

To prepare single-cell RNA sequencing (scRNA-seq) samples, we dissected the incisors from littermates of Krt14-RFP mice, as previously described (Chiba et al., 2020; Wang et al., 2020). Single cells were captured and a single-cell library was constructed using a 10x Chromium Single-Cell 3' Reagent Kit (10x Genomics, San Francisco, CA, USA). Then, libraries were sequenced on a NextSeq 500 sequencer (Illumina, San Francisco, CA, USA). The experiments were independently performed twice. Data processing was performed using the 10x Genomics workflow (Zheng et al., 2017). Demultiplexing, barcode assignment, and unique molecular identifier (UMI) quantification was performed using the Cell Ranger Single-Cell Software Suite (10x Genomics). The datasets generated for this study can be found in the NCBI GEO: GSE146855.

Semiquntitive and Real-Time PCR

Total RNA was isolated using TRIzol reagent (Invitrogen). Then, total RNA (2 μg) was reverse-transcribed into cDNA in 20 μl 1× first-strand buffer containing 0.5 μg oligo(dT) primers, 500 μM dNTP, and 200 units of SuperScript III (Invitrogen). PCR was performed in 25 μl 1× first PCR buffer containing 2 μl reverse transcription products, 1 unit of Ex TaqDNA polymerase (Takara, Japan), 200 μM dNTP, and 0.4 μM of the primer pair. The specific forward and reverse primers used for PCR were as follows: *Cx43*; 5'-GAGTCAGCTTGGGGTGATGAACAG-3' and 5'-AGCAGGAAGGCCACCTCGAAGACAGAC-3'; *Ambn*; 5'-GCGTTTCCAAGAGCCCTGATAAC-3' and 5'-AAGAAGCAGTGTCACATTTCCTGG-3'; *Enam*; 5'-GTGAGGAAAAATACTCCATATTCTGG-3' and 5'-GTTGAAGCGATCCCTAAGCCTGAAGCAG-3'; *Amel*; 5'-ATTCCACCCCAGTCTCATCAG-3' and 5'-CCACTTCGGTTCTCTCATTTTCTG-3'; *Bmp2*, 5'-GGGACCCGCTGTCTTCTAGT-3' and 5'-TCAACTCAAATTCGCTGAGGAC-3'; *Bmp4*, 5'-ACTGCCGCAGCTTCTCTGAG-3' and 5'-TTCTCCAGATGTTCTTCGTG-3'; *Hprt*; 5'-GCGTCGTGATTAGCGATGATGA-3' and 5'-GTCAAGGGCATATCCAACAACA-3'; *Runx2*; 5'-GAGGCCGCCGCACGACAACCG-3' and 5'-CTCCGGCCCACAAATCTCAGA-3'. The PCR products were separated on 1.5% agarose gels. Real-time PCR amplification was performed using primers with SYBR Green PCR master mix and a TaqMan 7700 Sequencer (Applied Biosystems). PCR was performed for 40 cycles of 95°C for 1 min, 60°C for 1 min, and 72°C for 1 min.

Preparation of Tissue Samples and Immunostaining

All animal experiments were approved by the ethics committee of Kyushu University Animal Experiment Center, and all procedures were performed in accordance with the relevant guidelines and regulations. The ICR mice (SLC) and Cx43-null mutants (Jackson Labs) used for experiments were previously described (Nagata et al., 2009; Ishikawa et al., 2016; Yamada et al., 2016). The tooth germ was dissected at postnatal day 3 (P3), and brain, lung, heart, liver, kidney, testis, and skin were obtained from 8-week-old ICR mice. Incisor presecretory (PS), secretory (S), early maturation (EM), and late maturation (LM) samples were dissected from the lower incisors of 8-week-old ICR mice. Molar samples were collected from embryonic day 13.5 (E13.5) to P7 ICR mice and newborn *Cx43*$^{-/-}$ mice. The dental epithelium and dental mesenchyme of E17.5 and P1 molars were treated with 0.1% collagenase, 0.05% trypsin, and 0.5 mM EDTA and separated under a microscope. For histological analysis, P0 mouse heads were dissected and fixed with 4% paraformaldehyde in phosphate-buffered saline overnight at 4°C. Tissues were embedded in OCT compound (Sakura Finetechnical Co.) cut at 8 μm thickness with a cryostat (2,800 Frigocut, Leica, Inc.) for frozen sectioning. Additional fixed tissue samples were cleared with xylene, dehydrated with a graded ethanol series, embedded in Paraplast paraffin (Oxford Laboratories), and sectioned at 10 μm with a microtome (RM2155, Leica, Inc.). For morphological analysis of the molars and incisors, sections were stained with Harris hematoxylin (Sigma) and eosin Y (Sigma). Immunohistochemistry was performed on sections, which were blocked in 1% bovine serum albumin/phosphate-buffered saline for 1 h and incubated with primary antibody. Primary antibodies were detected using AlexaFluor 488- or 594-conjugated secondary antibodies (Molecular Probes). Nuclei were stained with Vectashield-DAPI hard set (Vector). Tissue and cell samples for immunohistochemistry were examined using a fluorescence microscope (Biozero-8,000; Keyence, Japan).

Cell Culture and Transfection

Dental epithelial cell cultures were derived from molars dissected from newborn mice. The molars were treated with 0.1% collagenase, 0.05% trypsin, and 0.5 mM EDTA for 10 min to separate the dental epithelium from the mesenchyme. The separated dental epithelium was treated with 0.1% collagenase, 0.05% trypsin, and 0.5 mM EDTA for 15 min. The cells were dispersed into culture wells by repeated withdrawal and release using a pipette. Dental epithelial cells were then selected after 7 days of culture in keratinocyte-serum-free medium (Invitrogen) supplemented with epidermal growth factor and bovine pituitary extract, which removed contaminating mesenchymal cells. Cells were then detached with 0.05% EDTA, washed with DME containing 0.1% bovine serum albumin, resuspended to a concentration of 1.0×10^5/ml, and used for cell adhesion assays. SF2 cells from rat dental epithelium were maintained in Dulbecco's modified Eagle's medium/F-12 medium supplemented with 10% fetal bovine serum (Arakaki et al., 2012). All cells were cultured with 1% penicillin and streptomycin (Invitrogen) at 37°C in a humidified atmosphere containing 5% CO_2. SF2 cells were transiently transfected with Cx43, Cx43-R76S, or Cx43-R202H expression plasmids or Cx43 siRNA using Lipofectamine 2000 and Oligofectamine (Invitrogen), respectively.

Western Blotting

Cells were washed twice with 1 mM ice-cold sodium orthovanadate (Sigma), lysed with Nonidet P-40 buffer supplemented with protease inhibitors at 4°C for 10 min, and centrifuged. Then, the supernatants were transferred to a fresh tube. After boiling for 10 min, the proteins were separated by 12% SDS-PAGE and analyzed by Western blotting. Blots were probed using anti-ERK1/2, phospho-ERK1/2, Smad2/3, phospho-Smad2/3(465/467), SAPK, phospho-SAPK, p38, phospgo-p38, phospho-serine, and Runx2 with horseradish peroxidase-linked anti-rabbit secondary antibody (Cell Signaling). Proteins were detected with ECL Western blotting detection reagents (Amersham Biosciences) and exposed to X-ray film or imaged using a LAS-4000 system (Fuji Film, Japan). For immunoprecipitation assays, cells were seeded in 10-cm dishes at a density of 1×10^6/dish and cultured for 1 week and then harvested for protein extraction. Immunoprecipitation was carried out using a Dynabeads Protein G kit (Life Technologies). Anti-Runx2 antibodies were fused to protein G magnetic beads and incubated with the samples for 1 h at 4°C. The complex was eluted and denatured with NuPAGE LDS sample buffer (Life Technologies) supplemented with 1% 2-mercaptoethanol. The samples were analyzed using Western blotting.

Intracellular Calcium Measurement

SF2 cells were grown in a 96-well plate for 3 days and then incubated with 5 μM Fura-2 AM (Invitrogen) prepared in HBSS for 45 min at 37°C in 5% CO_2. After 3 days, the SF2 cells were transiently transfected with either Cx43 or control siRNA. The Ca^{2+} transients were recorded as the 340/380 nm ratio (R) of the resulting 510-nm emission using a plate reader (Mithras LB 940; Berthold Technologies). For stimulation, TGF-β1 was automatically injected into cells using the Mithras 940 instrument. For inhibition experiments, cells were incubated for 30 min before analysis with wither 100 μM 2-APB (to block IP3R) or 18α-Gly (to block gap junctions). After 3 days of transfection, the intracellular calcium ($[Ca^{2+}]_i$) was measured. The $[Ca^{2+}]_i$ levels were calculated as described previously (Grynkiewicz et al., 1985; Ishikawa et al., 2011) using the equation $[Ca^{2+}]_i = K_d (R - R_{min})/(R_{max} - R)(F^{380}{}_{max}/F^{380}{}_{min})$, where R_{min} is the ratio at zero Ca^{2+}, R_{max} is the ratio when Fura-2 is completely saturated with Ca^{2+}, $F^{380}{}_{min}$ is the fluorescence at 380 nm for zero Ca^{2+}, and $F^{380}{}_{max}$ is the fluorescence at saturating Ca^{2+} and $K_d = 224$ nM.

Data Analysis

Statistical differences between two groups of data were analyzed using Student's *t*-test. One-way ANOVA was used to analyze multiple groups. Differences were considered statistically significant at $p < 0.05$.

RESULTS

Expression of *Cx43* in Tooth Germ

scRNA-seq was performed using dissociated cells from Krt14-RFP mouse incisors to obtain single-cell gene expression profiles as described previously (**Figure 1A**; Chiba et al., 2020). In the incisors, well-distinguished cell types were observed: inner enamel epithelium (iee), pre-ameloblasts (pam), ameloblasts (am), outer enamel epithelium (oee), stratum intermedium (st), stellate reticulum (sr) as dental epithelial cells, odontoblasts (od), dental pulp cells (dp), dental follicles (df), and periodontal ligament cells (dl) as dental mesenchymal cells. *Gja1* (Cx43), *Gjb2*, and *Panx1* were expressed in the dental epithelium. *Cx43*, *Gjb2*, and *Panx3* were expressed in the dental mesenchyme (**Figure 1B**).

To confirm the expression of *Cx43* in the tooth germ, we performed real-time PCR. *Cx43* was highly expressed in the tooth germ compared to expression in other tissues (**Figure 2A**). In the incisors, *Cx43* expression increased as differentiation progressed, and was located in the ameloblast and odontoblast layers during the secretory stage (**Figures 2B,C**). In molars, the enamel epithelium differentiates into ameloblasts around birth, when it begins to secrete the enamel matrix. *Cx43* expression intensified in the dental epithelium and mesenchyme after birth (**Figures 2B,D**). Further, Cx43 protein localized at the cell–cell interface of cultured dental epithelial cells and formed gap junctions (**Figure 2E**). These observations suggest that Cx43 may regulate the differentiation of ameloblasts and odontoblasts during tooth development.

Disorganization of Ameloblasts and Decreased Ameloblastin Expression in *Cx43* Null Mice

Cx43-null mice ($Cx43^{-/-}$) showed cyanosis and died after birth due to malformations of the heart and lungs (Reaume et al., 1995; Huang et al., 1998; Nagata et al., 2009). No significant changes were noted in tooth size or shape in $Cx43^{-/-}$ mice (**Figure 3A**), but the inner enamel epithelium (iee) lost its polarity and formed multiple layers (**Figure 3A**). The number of inner enamel epithelial cells and odontoblasts (od) increased, but neither stratum intermedium (st) nor stellate reticulum (si) cells were observed (**Figure 3B**). The expression of BMP-2 and -4, which are involved in ameloblast differentiation, was unchanged in the teeth of $Cx43^{-/-}$ mice (**Figure 3C**). Enamel matrix proteins such as Ambn and Enam decreased significantly in $Cx43^{-/-}$ teeth (**Figure 3C**). Further, immunostaining showed that Ambn protein expression was decreased in the $Cx43^{-/-}$ tooth germ (**Figure 3D**). These mice died shortly after birth, so it was not possible to verify whether amelogenesis occurs in the absence of Cx43. In the case of postnatal lethality, it is also possible to observe enamel formation by transplantation of tooth germs under the renal capsule. However, enamel hypoplasia was observed in mice with a partial genetic abnormality of Cx43. The ameloblast disorganization and the decreased expression of the enamel matrix we observed are consistent with previous reports.

TGF-β1-Induced Meloblastin Expression Is Regulated by Gap Junctional Communication

We investigated the role of Cx43 in dental epithelial cell proliferation and differentiation by examining the expression of

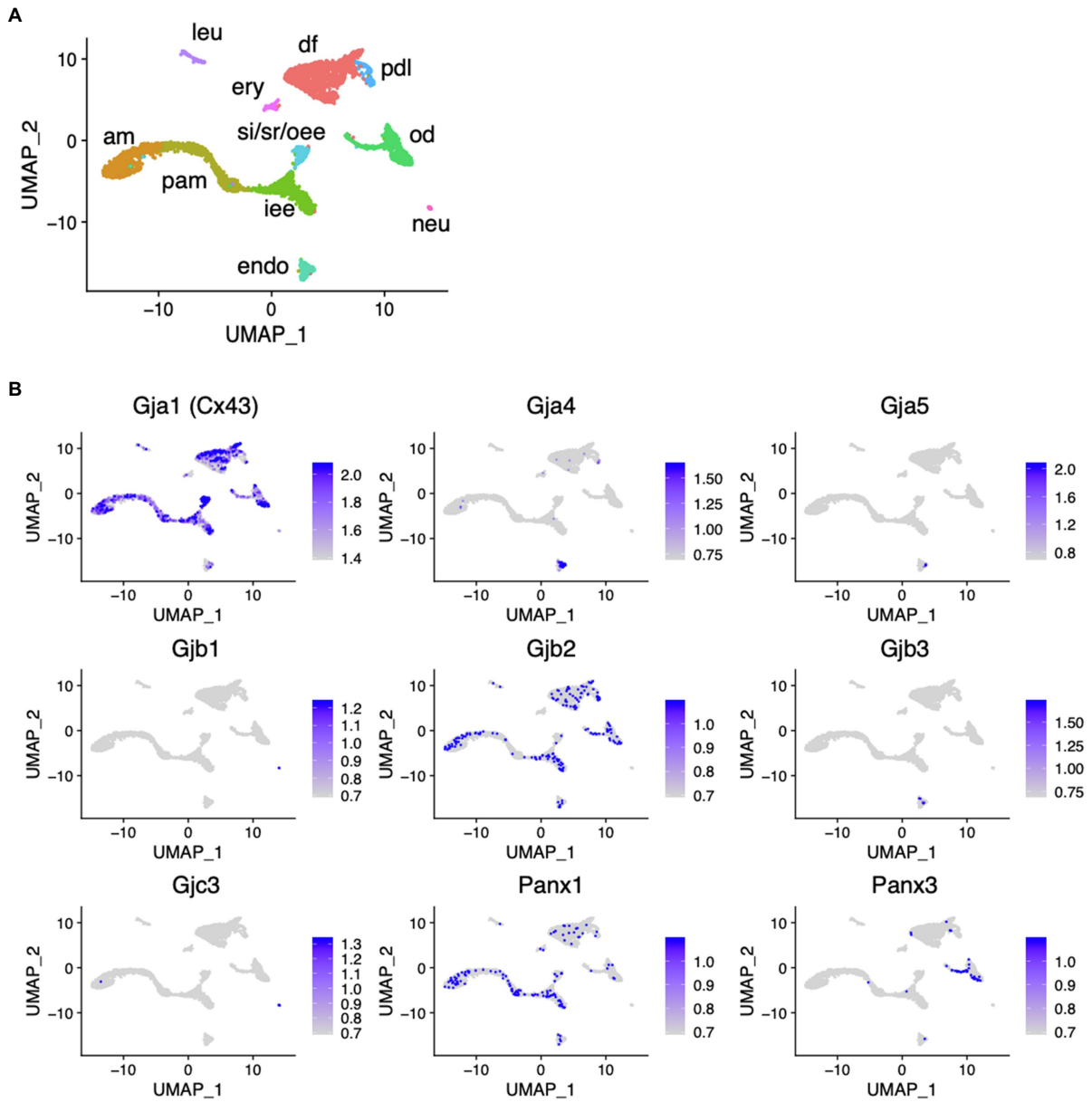

FIGURE 1 | Expression pattern of connexin family members during tooth development. **(A)** Differential expression of analysis of cell-type marker genes using uniform manifold approximation and projection (UMAP) visualization of single-cell RNA-seq libraries from postnatal (P) day P7 Krt14-RFP mice incisors (Chiba et al., 2020). am, ameloblast; Pam, pre-ameloblast; iee, inner enamel epithelium; si/sr/oee, stratum intermedium, stellate reticulum, and outer enamel epithelium; od, odontblast; df, dental follicle; pdl, periodontal ligament; leu, leukocyte; ery, erythrocyte; neu, neural cell; encoendothelium. **(B)** Differential gene expression analysis of connexin family members detected in single-cell RNA-seq libraries from P7 Krt14-RFP mice incisors.

Ambn in dental epithelial cells cultured at different cell densities (**Figure 4A**). Cx43 expression increased as the number of cells in contact increased (**Figure 4B**), but Ambn was not induced until a certain number of cells were in contact (**Figure 4C**). Ambn expression at a higher cell density was almost completely inhibited in the presence of the gap junction inhibitors (18α-GA) and oleamide (**Figure 4C**). However, Cx43 expression was not inhibited by gap junction inhibitors (**Figure 4D**). These results suggest that Cx43 gap junction activity is involved in the regulation of Ambn expression during amelogenesis.

TGF-β1 induced the expression of Ambn, which is involved in amelogenesis (**Figure 4E**). Additionally, TGF-β1 induced ERK1/2 phosphorylation and inhibited the proliferation of dental epithelial cells in BrdU incorporation assays (data not shown). In mammary gland epithelial cells, Cx43 expression is induced by TGF-β1 *via* the p38 and PI3 kinase/Akt pathways (Tacheau et al., 2008). However, Cx43 expression in dental epithelial cells was not affected by TGF-β1 (**Figure 4D**), with or without gap junction inhibitors, whereas gap junction inhibitors significantly reduced TGF-β1-induced Ambn

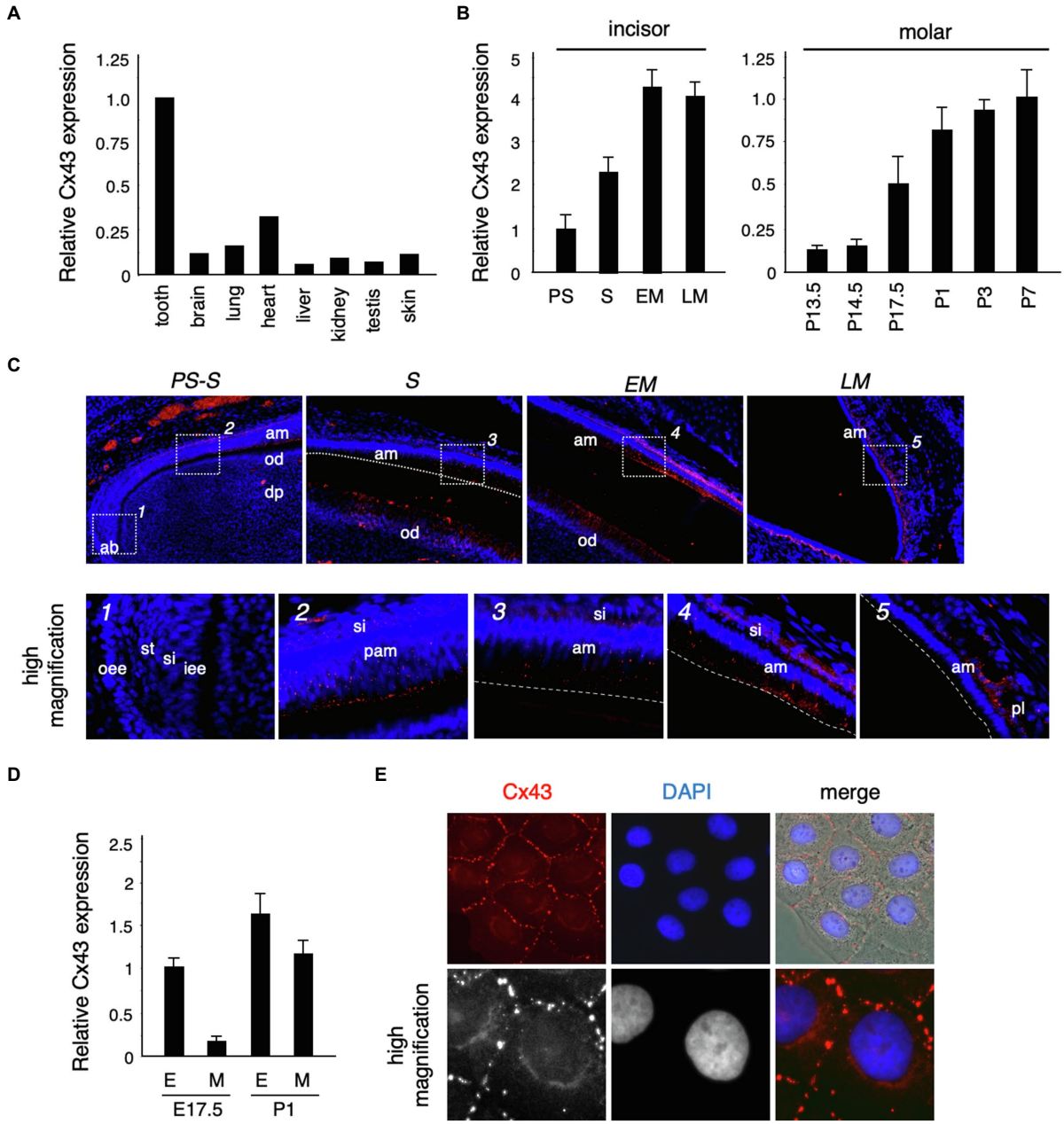

FIGURE 2 | Connexin 43 (*Cx43*) expression in tooth germ development. **(A)** Expression of *Cx43* mRNA in various tissues. **(B)** Expression of *Cx43* mRNA by ameloblasts in the presecretory (PS), secretory (S), early maturation (EM), and late maturation (LM) stages of incisor development. Expression of *Cx43* mRNA from embryonic day 13.5 (E13.5) to postnatal day 7 (P7) in tooth germs from whole molars. **(C)** Localization of Cx43 in developing upper incisors. A high-magnification image of the area indicated by a dotted line is shown in the lower panel. **(D)** Expression of Cx43 mRNA in separated epithelial (E) and mesenchymal (M) tooth germs. **(E)** Localization of Cx43 in cultured SF2 cells. Cx43 (red), DAPI (blue), and the merged image. High-magnification images are shown in the lower panel. ab, apical bud; am, ameloblast; od, odontoblast; dp, dental pulp; oee, outer enamel epithelium; st, stellate reticulum; si, stratum intermedium; iee, inner enamel epithelium; pam, pre-ameloblast; and pl, papillary layer.

expression (**Figure 4E**). Furthermore, we examined the expression of Ambn induced by TGF-β1 in cultured dental epithelial cells from *Cx43*$^{-/-}$ mice. In *Cx43*$^{-/-}$-derived cells, TGF-β1-induced expression of Ambn was suppressed, similar to gap junction inhibitors (**Figure 4E**). These findings suggest that the presence of gap junctions is important for TGF-β1-mediated Ambn expression. We also tested whether Cx43 activity was required for Ambn expression by transfecting dental epithelial cells with an expression vector for Cx43 carrying R76S or R202H mutations, as identified in patients with ODDD. In these cells, gap junction activity was reduced, as shown by dye transfer analysis (**Figure 4F**), and

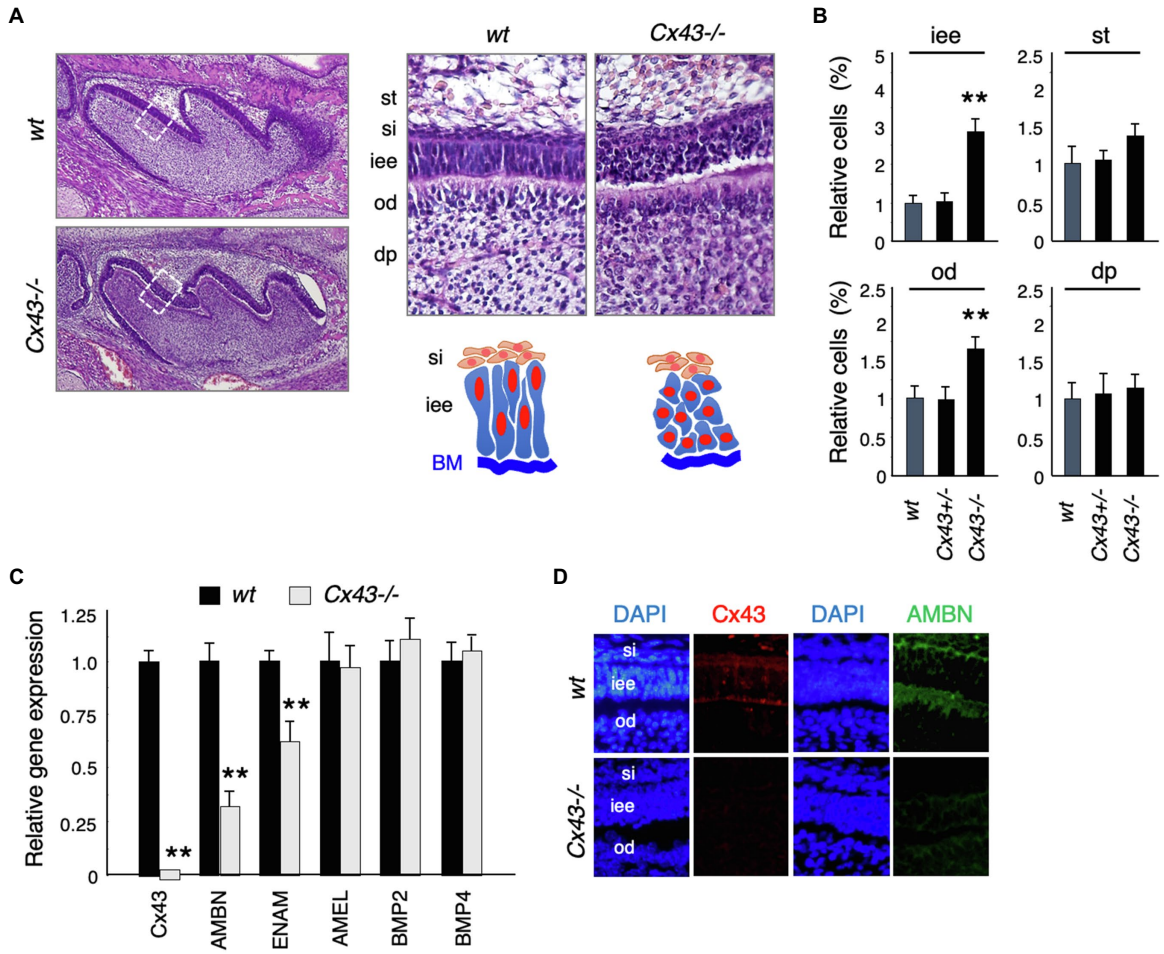

FIGURE 3 | Tooth phenotypes in *Cx43*-deficient mice. **(A)** Hematoxylin staining of upper first molars in *wt* and *Cx43*$^{-/-}$ mice, and high-magnification images and scheme of dental epithelial cells in newborn *wt* and *Cx43*$^{-/-}$ mice. st, stellate reticulum; si, stratum intermedium; iee, inner enamel epithelium; od, odontoblast; dp, dental papilla. **(B)** Relative numbers of each cell types in *wt*, *Cx43*$^{+/-}$, and *Cx43*$^{-/-}$ mice. *n*–5, $^{**}p < 0.01$. **(C)** Expression of *Cx43*, enamel matrix proteins, and BMPs in first molar tooth germs in P3 *WT* and *Cx43*$^{-/-}$ mice. *Ambn*, ameloblastin; *Enam*, enamelin; *Amel*, amelogenin. *n*–4, $^{**}p < 0.01$. **(D)** Localization of Cx43 (red) and Ambn (green) in *wt* and *Cx43*$^{-/-}$ molars.

TGF-β1-induced Ambn expression was suppressed. The inhibitory effect on Ambn expression was less profound than that observed using gap junction inhibitors (**Figure 4F**), which is likely due to the presence of endogenous Cx43. An almost complete lack of Ambn induction by TGF-β1 was observed in a primary culture of *Cx43*$^{-/-}$ dental epithelial cells (**Figure 4E**). These results suggest that Cx43 gap junction activity is essential for TGF-β1-mediated expression of Ambn and dental epithelial differentiation.

ERK Phosphorylation and Nuclear Translocation Are Decreased by Gap Junction Inhibitors

We investigated the mechanism of Cx43 in TGF-β1-induced Ambn expression by analyzing TGF-β1 signaling pathways using gap junction inhibitors and Cx43 mutants. TGF-β1-induced phosphorylation of Smad2/3 was not affected by gap junction inhibitors (**Figure 5A**), and Smad4 levels remained unchanged (**Figure 5A**). In non-Smad TGF-β1 pathways, the phosphorylation of ERK1/2, but not SAPK/JNK and p38, was almost completely blocked by gap junction inhibitors (**Figure 5A**). In dental epithelial cells overexpressing the non-functional R76S- or R202H-Cx43 mutants, TGF-β1-stimulated ERK1/2 phosphorylation was reduced compared with that in wild-type Cx43-overexpressing cells (**Figure 5B**). Phosphorylated Smad2/3 forms a complex with Smad4 and translocates into the nucleus after TGF-β1 stimulation (Schmierer and Hill, 2007). In SF2 cells, this translocation was not affected by the gap junction inhibitor, oleamide (**Figure 5C**). TGF-β1 stimulation resulted in the translocation of most of the ERK1/2 into the nucleus. However, oleamide inhibited the nuclear translocation of ERK1/2 (**Figure 5C**). These results indicate that blocking gap junction activity inhibits the phosphorylation and nuclear translocation of ERK1/2. A similar regulation of ERK1/2 phosphorylation was observed following BMP2 and BMP4 stimulation

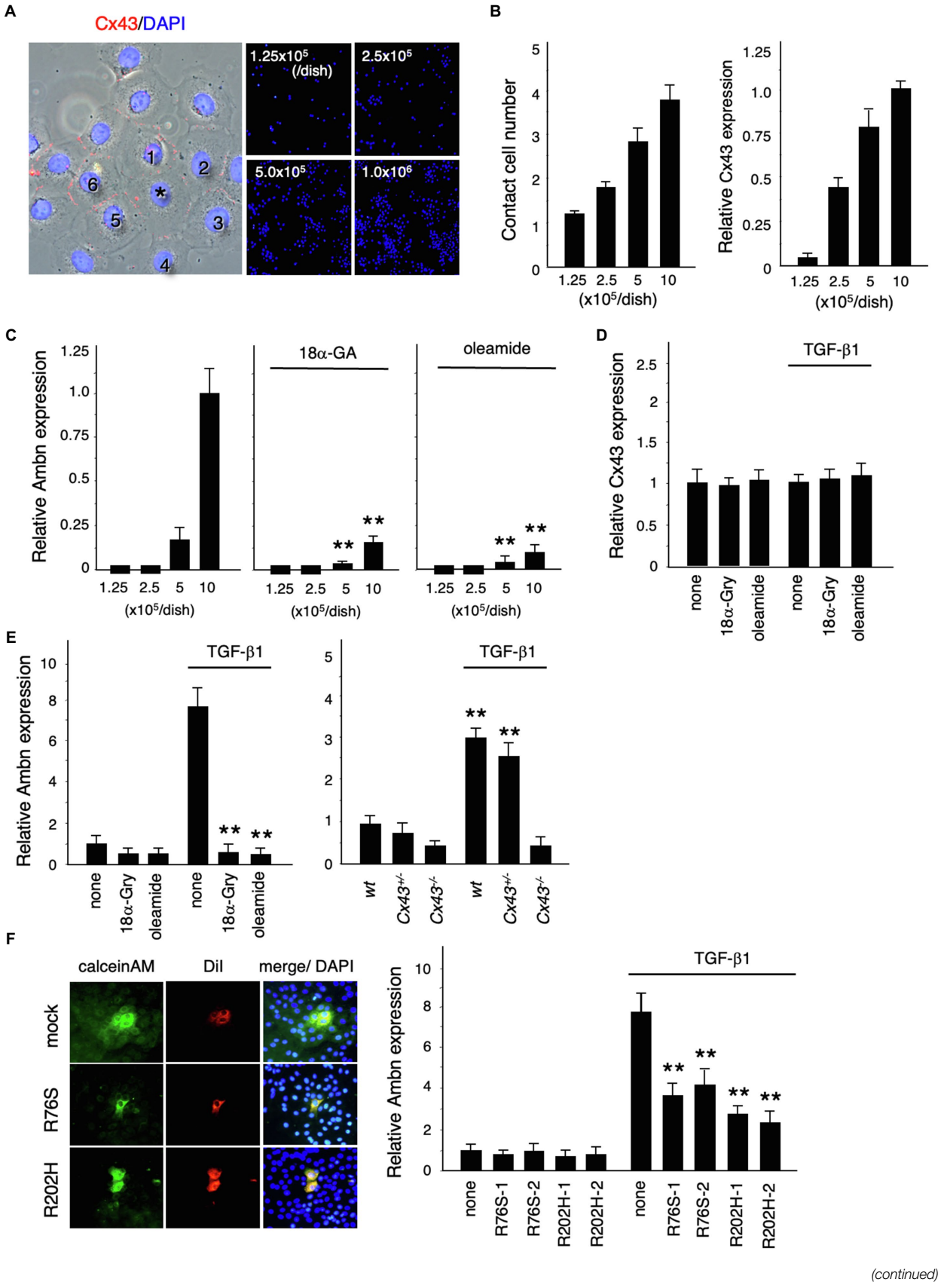
A
Cx43/DAPI
1.25x10⁵ (/dish)
2.5x10⁵
5.0x10⁵
1.0x10⁶
B
Contact cell number
(x10⁵/dish)
Relative Cx43 expression
C
Relative Ambn expression
18α-GA
oleamide
D
Relative Cx43 expression
TGF-β1
none
18α-Gry
oleamide
E
Relative Ambn expression
TGF-β1
wt
Cx43+/-
Cx43-/-
F
calceinAM
DiI
merge/ DAPI
mock
R76S
R202H
Relative Ambn expression
TGF-β1
none
R76S-1
R76S-2
R202H-1
R202H-2

(continued)

FIGURE 4 | Regulation of Ambn expression in dental epithelial cells by gap junction communication. **(A)** Immunostaining of Cx43 (red) and nuclear staining with DAPI (blue) in cultured dental epithelial cells. The cell marked with an asterisk contacts six cells *via* gap junctions. **(B)** The average number of contact cells at each cell density is shown in the left panel. Expression of *Cx43* in cultured dental epithelial cells at each cell density is shown in the right panel. **(C)** Expression of Ambn at each cell density with or without the gap junction inhibitors 18α-Glycyrrhetinic acid (18α-GA) and oleamide. **(D)** Effect of gap junction inhibitors on *Cx43* after 48 h of TGF-β1 stimulation (1 ng/ml). **(E)** Effect of the gap junction inhibitors 18α-Gly and oleamide on Ambn expression (left panel) or on *Cx43*$^{-/-}$ cells (right panel). **(F)** Gap junction activity was measured by transfecting dental epithelial cells with a Cx43 expression vector carrying R76S or R202H mutations. CalceinAM and DiI were injected into the center of cell. Ambn expression in cells stably transfected with Cx43 expression vectors harboring R76S or R202H mutations, which are found in human oculodentodigital dysplasia (ODDD) patients, after stimulation with TGF-β1 is shown in the right panel. $^{**}p < 0.01$.

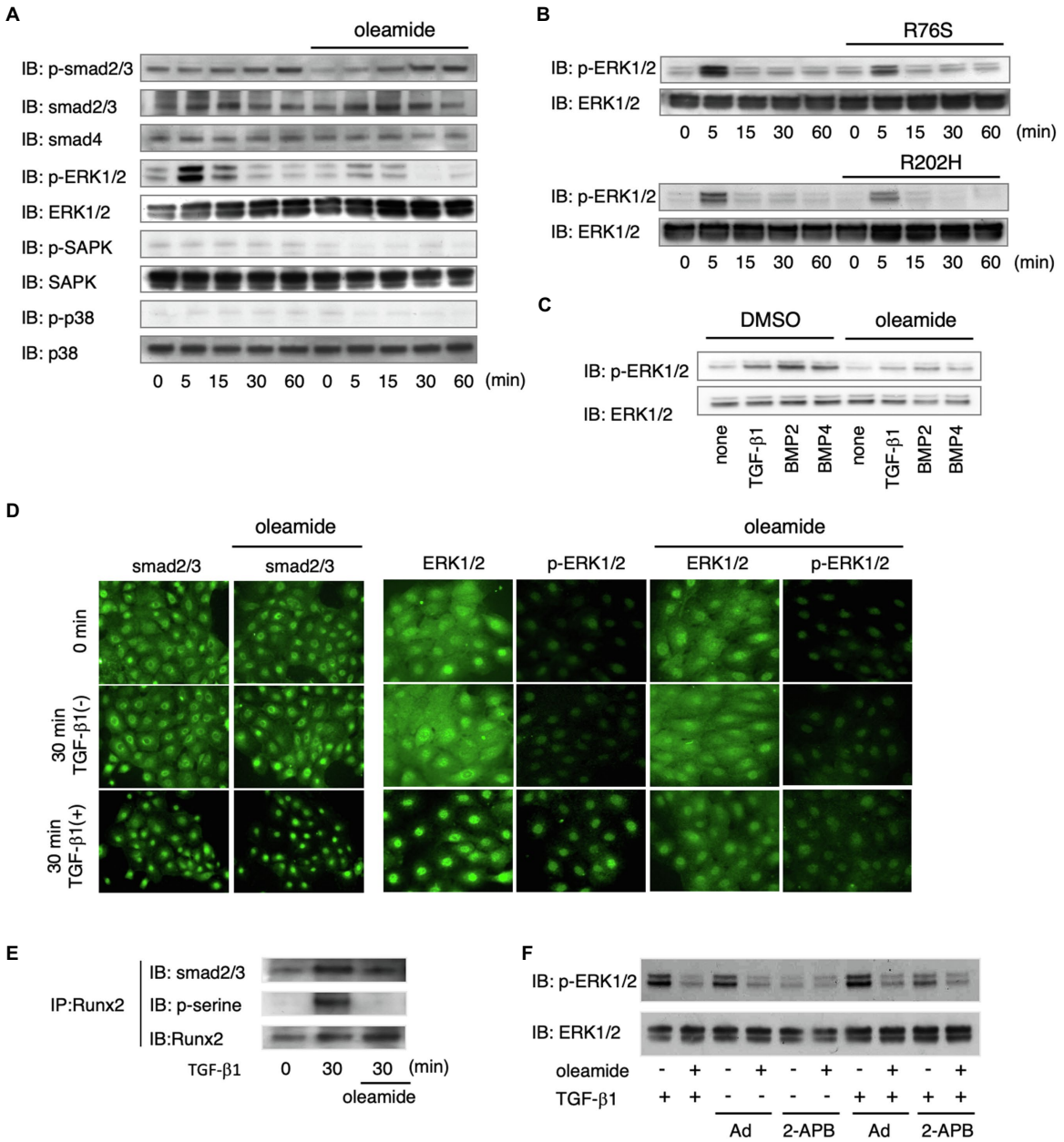

FIGURE 5 | ERK1/2 phosphorylation is regulated by Cx43-mediated gap junction communication. **(A)** Phosphorylation of Smad2/3, ERK1/2, and p38 after stimulation by TGF-β1 with or without oleamide. $n = 5$. **(B)** Phosphorylation of ERK1/2 after stimulation by TGF-β1 after transfection with expression vectors for Cx43 mutants (R76S or R202H). $n = 5$. **(C)** Phosphorylation of ERK1/2 after stimulation by TGF-β1, BMP2, and BMP4 with or without oleamide. $n = 5$. **(D)** Localization of Smad2/3 after stimulation by TGF-β1 with or without oleamide. $n = 5$. Localization of ERK1/2 and phospho-ERK1/2 after stimulation by TGF-β1 with or without oleamide. $n = 5$. **(E)** Immunoprecipitation of Runx2 in TGF-β1-stimulated dental epithelial cells. TGF-β1 induced Runx2 phosphorylation and caused the association of Runx2 with Smad2/3. Phosphorylation of serine residues of Runx2 and binding with Smad2/3 were inhibited by oleamide. $n = 5$. **(F)** Phosphorylation of ERK1/2 in the presence of the IP3R agonist, adenophostin-A (Ad), or the IP3R antagonist, 2-APB, with or without TGF-β1 or oleamide.

(**Figure 5B**). Furthermore, this phenomenon was observed in dental epithelial cells and in primary cultures of calvarial osteoblasts and osteoblastic MC3T3-E1 cells (data not shown).

The translocation of phosphorylated ERK1/2 participates in the phosphorylation of Runx2, a transcription factor essential for osteogenesis, and consequently regulates the transcription of osteocalcin (Ge et al., 2007). ERK1/2 is also involved in interactions between cells and the extracellular matrix, hormones, and growth factor signals, and increases its own activity (Keshet and Seger, 2010; Guo et al., 2020). Therefore, we investigated the role of ERK1/2 in Runx2 phosphorylation during TGF-β1-mediated differentiation of dental epithelial cells. Runx2 was phosphorylated by TGF-β1, and this phosphorylation was blocked by oleamide (**Figure 5E**). These results suggest that Runx2 phosphorylation occurs through the TGF-β1-Cx43-ERK1/2 pathway. Immunoprecipitation analysis revealed that Smad2/3 was associated with Runx2 when stimulated by TGF-β1 in a manner similar to Smad1/Runx2 interactions during BMP-2 stimulation (Selvamurugan et al., 2004). However, the association of Smad2/3 with Runx2 was significantly reduced in the presence of oleamide, most likely due to reduced Runx2 phosphorylation (**Figure 5D**). Cx43 is required for growth factor-stimulated ERK1/2 phosphorylation. However, the mechanism by which Cx43 gap junction activity regulates ERK1/2 phosphorylation is not yet clear. Gap junction channels allow the transfer of IP3 and Ca^{2+} between cells. IP3 binds to its receptors (IP3Rs) in the endoplasmic reticulum (ER) membrane and promotes Ca^{2+} release from the ER (Mikoshiba, 2007), thereby increasing intracellular Ca^{2+}. Ca^{2+} efflux from the ER *via* the IP3R Ca^{2+} channel is essential for the conversion of Ras-GDP to its GTP form, which is upstream of ERK1/2 (Pérez-Sala and Rebollo, 1999). We explored the involvement of the IP3/IP3R channel in the regulation of ERK1/2 phosphorylation through gap junctions by examining the effects of an IP3R agonist and antagonist on ERK1/2 phosphorylation. When dental epithelial cells were treated with the IP3R agonist adenophostin-A (Ad), which stimulates the release of Ca^{2+} from the ER, ERK1/2 phosphorylation was induced by TGF-β1 stimulation (**Figure 5F**). In contrast, treatment with the IP3R antagonist 2-APB inhibited ERK1/2 phosphorylation induced by TGF-β1 (**Figure 5F**). The phosphorylation of ERK1/2 induced by adenophostin-A was blocked by oleamide (**Figure 5F**). These results suggest that IP3R is involved in TGF-β1-induced ERK1/2 phosphorylation.

Late-Phase Intracellular Calcium Level Regulated by Cx43

Since intracellular calcium levels may be involved in ERK phosphorylation, we investigated whether intracellular Ca^{2+} dynamics are regulated by Cx43. We examined the role of Cx43 in maintaining intracellular Ca^{2+} levels by comparing the $[Ca^{2+}]_i$ levels after TGF-β1 stimulation in Cx43-overexpressing and control dental epithelial cells. The $[Ca^{2+}]_i$ level was increased by TGF-β1 stimulation and reduced by 2-APB (**Figure 6A**). No differences were observed in ER Ca^{2+} channel activity between Cx43-overexpressing and control cells within 120 s (**Figure 6A**, left). However, the $[Ca^{2+}]_i$ level after 180 s gradually increased in Cx43 expressing cells, with or without 2-APB, compared to control cells (**Figure 6A** right). Treatment with Cx43 siRNA and the gap junction inhibitor 2-APB inhibited the late phase $[Ca^{2+}]_i$ increase (**Figure 6B**). A similar phenomenon was observed using 18α-GA (**Figure 6C**), indicating that this late phase increase may be due to gap junctions, but not the ER channel. These results suggest that Cx43 may allow slow Ca^{2+} influx *via* gap junctions, but is not involved in the early phase $[Ca^{2+}]_i$ increase from the ER channel. Additionally, these results suggest that Cx43 regulates ERK1/2 phosphorylation (**Figure 7**).

In this study, we showed that Cx43 expression is induced in the dental epithelium when the cells are in contact with each other. Our results suggest that Cx43 gap junctions are critical for the maintenance of polarity and differentiation of dental epithelial cells. Cx43 gap junctions are also required for TGF-β1- and BMP-induced expression of enamel matrix proteins, especially Ambn. This gene induction is mediated by ERK1/2 activation *via* Cx43 gap junction activity (**Figure 7**). These findings provide mechanistic insights into the development of dental epithelial cells and the pathogenesis of genetic disorders.

DISCUSSION

The phenotype similar to ODDD patients has not been adequately analyzed because Cx43-deficient mice are embryonic lethal (Reaume et al., 1995; Huang et al., 1998; Nagata et al., 2009). A mouse model of ODDD carrying a missense mutation in the *Cx43* gene (*Gja1Jrt/+* mice) was isolated from an N-ethyl-N-nitrosourea mutagenesis screen (Flenniken et al., 2005). Unlike Cx43-deficient mice, this mutation is non-lethal, which allowed histological analysis of Cx43 in teeth. However, the molecular function of Cx43 in tooth development has not been sufficiently analyzed, although Cx43 dysfunction causes severe enamel hypoplasia and maxillofacial bone deformity. In our study, analysis using *Cx43*$^{-/-}$ mice revealed decreased expression of Ambn during tooth development, revealing that this molecule is regulated by Cx43-mediated signaling. Enamel hypoplasia in ODDD patients and in Cx43 mutant mice likely arises, at least in part, due to reduced Ambn expression. The phenotype of the multilayer formation was similar to that found in the teeth of mice with Ambn deficiency (Fukumoto et al., 2004). Ambn is an enamel matrix protein secreted specifically by ameloblasts that functions as a cell adhesion molecule. *Ambn*$^{-/-}$ mice display abnormal dental epithelium proliferation and multiple cell layers, and also develop severe enamel dysplasia and odontogenic tumors (Fukumoto et al., 2004). Furthermore, in *Ambn*$^{-/-}$ mice, ameloblast polarization is inhibited during the secretory stage and cell proliferation of the inner enamel epithelium is increased. In fact, even in *Cx43*$^{-/-}$ mice, ameloblast polarity was lost (**Figure 3A**). Further, the number of cells in the inner enamel epithelium, but not in the stratum intermedium, was increased (**Figure 3B**). Thus, the abnormal tooth phenotypes observed in *Cx43*$^{-/-}$ mice were partly due to the reduced expression of enamel matrix proteins such as Ambn.

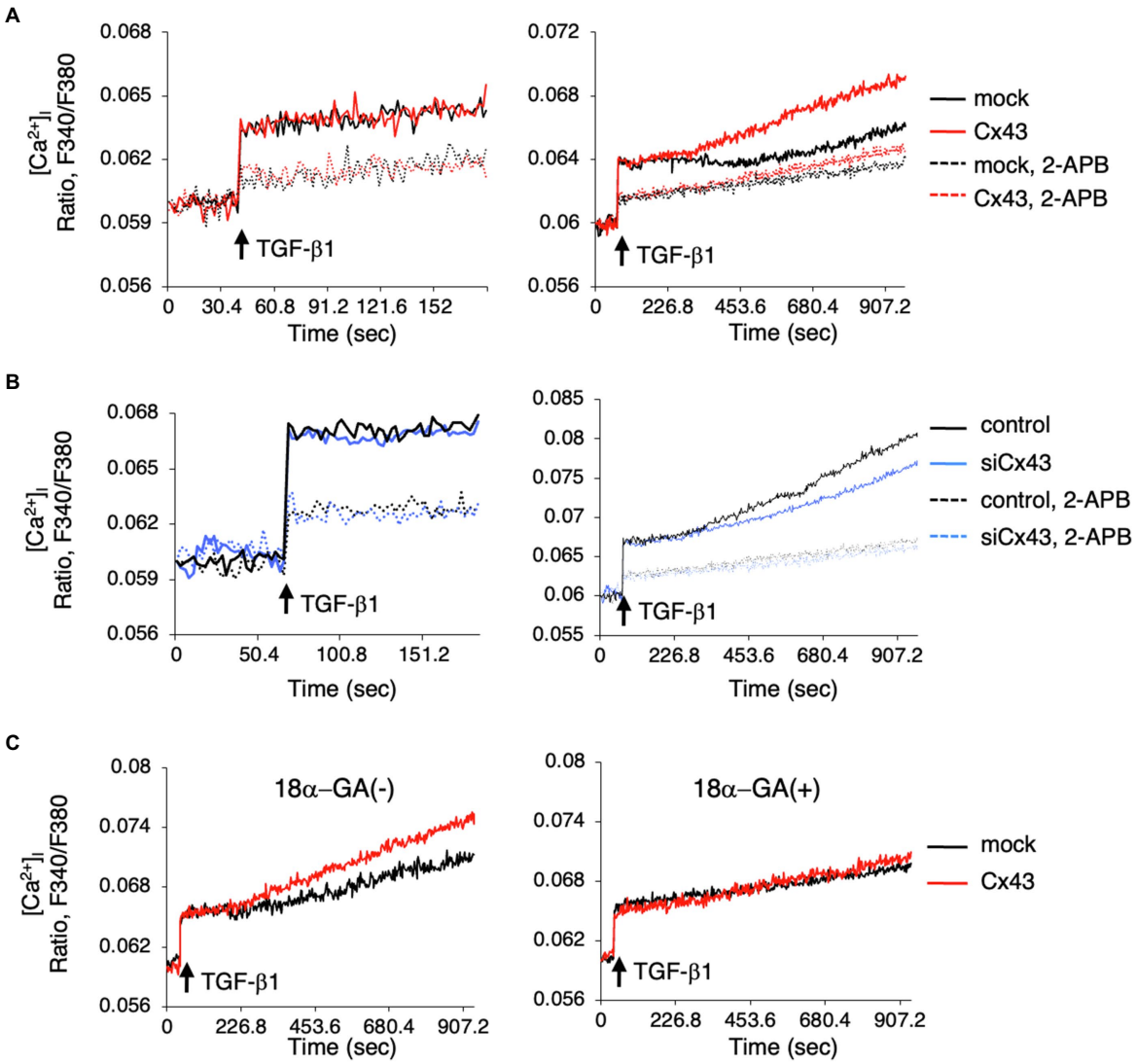

FIGURE 6 | Intracellular Ca^{2+} release is induced by Cx43-containing gap junctions localized in the cell membrane. **(A)** Cells were incubated with Fura2 (10 μM) with or without 2-APB (100 μM). TGF-β1 induced $[Ca^{2+}]_i$ levels were not changed in Cx43-transfected cells compared to control cells over a short period. However, $[Ca^{2+}]_i$ levels were increased in Cx43-overexpressing cells after 180 s compared with non-transfected cells. **(B)** $[Ca^{2+}]_i$ level after stimulation by TGF-β1 in Cx43 siRNA transfected cells with or without 2-APB for a short period (left panel) or a long time (right panel). **(C)** $[Ca^{2+}]_i$ levels after stimulation by TGF-β1 in Cx43-transfected cells with or without 18α-GA for a long period.

In dental epithelial cells, TGF-β1 and BMPs induce Ambn expression. TGF-β1 and BMP bind to their receptors and phosphorylate the downstream signaling molecules Smad and ERK1/2 (Guo and Wang, 2009; Luo, 2017). BMPs are important molecules for bone formation and are involved in the activation and induction of bone-specific transcription factors such as Runx2 (Komori et al., 1997; Chen et al., 2012). A Runx2 binding region is present in the promoter region of the *Ambn* gene (Dhamija and Krebsbach, 2001; Camilleri and McDonald, 2006; Kim et al., 2018), suggesting that TGF-β1 and BMP signaling are important for the expression of Ambn *via* Runx2. In fact, phosphorylation by ERK1/2 is required for the activation of Runx2, and phosphorylated Runx2 binds to Smad molecules to activate gene transcription (Lai and Cheng, 2002; Franceschi and Xiao, 2003; Chen et al., 2012). Both TGF-β1-overexpressing and -deficient mice have severe enamel hypoplasia (Haruyama et al., 2006; Song et al., 2018). These results indicate that the expression of TGF-β1 and its signaling pathway are important for enamel formation during tooth development. However, it is unclear how TGF-β1 and BMP signals are controlled by Cx43.

In osteoblastic ROS 17/2.8 cells, overexpressing the active forms of MEK, Raf, or Ras enhances the transcription of the osteocalcin gene through the connexin response element, whereas MEK and PI3K inhibitors repress transcription (Stains and Civitelli, 2005). In addition, this gene activation requires phosphorylation of the transcription factor Sp1 by ERK1/2. These results suggest that gap junctions, especially Cx43, may selectively regulate ERK1/2 phosphorylation induced by

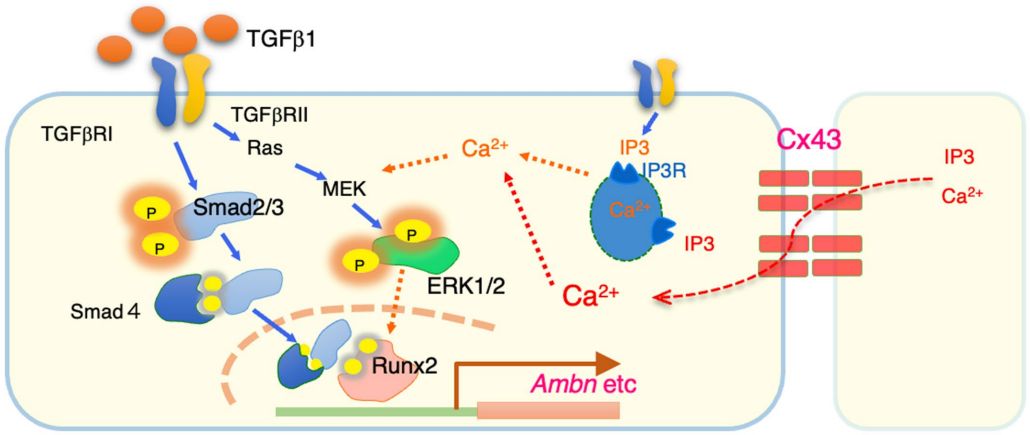

FIGURE 7 | A summary of intracellular signals regulated by Cx43. Cx43 exists between cells and allows to permeate calcium ions from neighboring cells. The resulting increase in intracellular calsium promotes phosphorylation of ERK1/2 by TGF-b1. Phosphorylated ERK1/2 is thought to bind to the Smad complex in the nucleus and regulate the transcription such as Ambn.

TGF-β1 in dental epithelial cells. Since Sp1 is expressed in almost all tissues, it is unlikely that it has a specific action during tooth development. Sp3 and Sp6/epiprofin are Sp family transcription factors that are involved in tooth development. The transcriptional activity of Ambn was induced by TGF-β, but not in the presence of oleamide (**Figure 4C**). TGF-β1-induced Ambn promoter activity was further enhanced by Sp6/epiprofin overexpression in dental epithelial cells. This facilitation was almost completely blocked by oleamide (data not shown), suggesting that the induction of Ambn expression by Sp6/epiprofin may require Sp6/epiprofin and a synergistic interaction with active Runx2. Alternatively, although Sp1 is phosphorylated by ERK1/2 and regulates osteocalcin transcription (Stains and Civitelli, 2005), Sp1 involvement has yet to be reported in tooth development. Enamel hypoplasia and decreased Ambn levels are observed in Sp3-deficient mice, similar to observations in Sp6/epiprofin-deficient mice (Bouwman et al., 2000; Nakamura et al., 2008). Since Sp3 expression was not affected by TGF-β1 stimulation or by gap junction inhibitors (data not shown), Sp3 may be ubiquitously expressed. Similar to Sp6/epiprofin, Sp3 may directly or indirectly regulate Ambn expression through ERK1/2, though this remains to be investigated.

The phosphorylation of ERK1/2 by Cx43 is important for Runx2-mediated transcriptional regulation of Ambn. However, it is unclear how Cx43 regulates ERK phosphorylation. Cx43 is required for growth factor-stimulated ERK1/2 phosphorylation; however, the mechanism by which Cx43 gap junction activity regulates ERK1/2 phosphorylation is not yet clear. Gap junction channels allow for the transfer of IP3 and Ca^{2+} between cells. The binding of IP3 to its receptors in the ER membrane promotes Ca^{2+} release from the ER (Mikoshiba, 2007), thereby increasing intracellular Ca^{2+}. Further, Ca^{2+} efflux from the ER *via* the IP3R Ca^{2+} channel is essential for the conversion of Ras-GDP to its -GTP form, an upstream molecule of ERK1/2 (Pérez-Sala and Rebollo, 1999). We explored the involvement of the IP3/IP3R channel in the regulation of ERK1/2 phosphorylation through gap junctions by examining the effects of an IP3R agonist and antagonist on ERK1/2 phosphorylation. When dental epithelial cells were treated with the IP3R agonist, adenophostin-A, which stimulates the release of Ca^{2+} from the ER, ERK1/2 phosphorylation was induced without TGF-β1 stimulation. In contrast, treatment with the IP3R antagonist 2-APB inhibited TGF-β1-induced ERK1/2 phosphorylation (**Figure 5F**). These results suggest that IP3R is involved in ERK1/2 phosphorylation induced by TGF-β1.

An increase in intracellular calcium levels induced by Ca^{2+} ionophores reduces the permeability of Cx43 gap junctions (Lurtz and Louis, 2007). Decreased permeability through gap junctions is prevented by calmodulin inhibitors, but it is not affected by inhibitors of calmodulin-dependent protein kinase II or protein kinase C (Lurtz and Louis, 2007), which indicates that the interaction between intracellular Ca^{2+} and calmodulin plays an important role in Cx43 gating. Pretreatment with ionomycin prior to TGF-β1 stimulation suppressed ERK1/2 phosphorylation (data not shown). This may be because the Cx43 gates were closed by ionomycin. In any case, IP3R in the ER membrane is involved in ERK1/2 phosphorylation, and Cx43 may be involved in this process. When dental epithelial cells are stimulated with TGF-β1, the intracellular calcium concentration rapidly increases. This increase in intracellular calcium is triggered by IP3 binding to receptors on the ER membrane, which subsequently triggers calcium release from the ER. Calcium release from the ER was unchanged with or without Cx43 overexpression. Previously, we reported that gap junction proteins such as Panx3 may regulate calcium release from the ER (Ishikawa et al., 2011). Gap junctional proteins, but not Cx43 may regulates calcium release from ER membrane. However, a subsequent slow increase in intracellular calcium levels was observed in Cx43-overexpressing cells (**Figure 6A**). This enhanced intracellular calcium level was suppressed by the gap junction inhibitor 18α-GA (**Figure 6C**), and was also observed in cells in which siCx43 suppressed CX43

expression (**Figure 6B**). In contrast, intracellular calcium levels regulated by Cx43 were not inhibited by 2-APB, which inhibits calcium release from the ER. This result revealed that Cx43 regulates intracellular calcium levels *via* gap junctions rather than by calcium release from the ER. In fact, stimulation with TGF-β1 when cells are sparsely cultured does not adequately phosphorylate ERK1/2. Therefore, we believe that calcium influx through gap junctions may be important for ERK1/2 phosphorylation. Further, these results show that Cx43 may regulate ERK1/2 phosphorylation *via* intracellular calcium levels.

DATA AVAILABILITY STATEMENT

The original contributions presented in the study are publicly available. This data can be found here: https://www.ncbi.nlm.nih.gov/geo/GSE146855.

ETHICS STATEMENT

The animal study was reviewed and approved by ethics committee of Kyushu University Animal Experiment Center.

AUTHOR CONTRIBUTIONS

AY and KY carried out experimental work, data analysis, interpretation, and writing of the manuscript. MI, KS, YC, RH, EF, SH, MC, TN, and TI contributed to experimental work. AY, KY, and SF carried out data interpretation and manuscript revision. AY and SF contributed to concept and design of research. All authors contributed to the article and approved the submitted version.

FUNDING

This study was supported by a Grant-in-Aid from the Japan Society for the Promotion of Science (JSPS) KAKENHI (JP24390460 to AY, JP17H01606 and JP20K20612 to SF, and JP18H03012 to KY).

ACKNOWLEDGMENTS

We thank Yoshihiko Yamada (NIH/NIDCR) for consulting on this research. We thank Editage (www.editage.com) for English language editing.

REFERENCES

Aasen, T., Mesnil, M., Naus, C. C., Lampe, P. D., and Laird, D. W. (2016). Gap junctions and cancer: communicating for 50 years. *Nat. Rev. Cancer* 16, 775–788. doi: 10.1038/nrc.2016.105

Al-Ansari, S., Jalali, R., Plotkin, L. I., Bronckers, A., Denbesten, P., Zhang, Y., et al. (2018). The importance of connexin 43 in enamel development and mineralization. *Front. Physiol.* 9:750. doi: 10.3389/fphys.2018.00750

Arakaki, M., Ishikawa, M., Nakamura, T., Iwamoto, T., Yamada, A., Fukumoto, E., et al. (2012). Role of epithelial-stem cell interactions during dental cell differentiation. *J. Biol. Chem.* 287, 10590–10601. doi: 10.1074/jbc.M111.285874

Bouwman, P., Göllner, H., Elsässer, H. P., Eckhoff, G., Karis, A., Grosveld, F., et al. (2000). Transcription factor Sp3 is essential for post-natal survival and late tooth development. *EMBO J.* 19, 655–661. doi: 10.1093/emboj/19.4.655

Camilleri, S., and Mcdonald, F. (2006). Runx2 and dental development. *Eur. J. Oral Sci.* 114, 361–373. doi: 10.1111/j.1600-0722.2006.00399.x

Chen, G., Deng, C., and Li, Y. P. (2012). TGF-β and BMP signaling in osteoblast differentiation and bone formation. *Int. J. Biol. Sci.* 8, 272–288. doi: 10.7150/ijbs.2929

Chiba, Y., Saito, K., Martin, D., Boger, E. T., Rhodes, C., Yoshizaki, K., et al. (2020). Single-cell RNA-sequencing from mouse incisor reveals dental epithelial cell-type specific genes. *Front. Cell Dev. Biol.* 8:841. doi: 10.3389/fcell.2020.00841

Dhamija, S., and Krebsbach, P. H. (2001). Role of Cbfa1 in ameloblastin gene transcription. *J. Biol. Chem.* 276, 35159–35164. doi: 10.1074/jbc.M010719200

Flenniken, A. M., Osborne, L. R., Anderson, N., Ciliberti, N., Fleming, C., Gittens, J. E., et al. (2005). A Gja1 missense mutation in a mouse model of oculodentodigital dysplasia. *Development* 132, 4375–4386. doi: 10.1242/dev.02011

Franceschi, R. T., and Xiao, G. (2003). Regulation of the osteoblast-specific transcription factor, Runx2: responsiveness to multiple signal transduction pathways. *J. Cell. Biochem.* 88, 446–454. doi: 10.1002/jcb.10369

Fukumoto, S., Kiba, T., Hall, B., Iehara, N., Nakamura, T., Longenecker, G., et al. (2004). Ameloblastin is a cell adhesion molecule required for maintaining the differentiation state of ameloblasts. *J. Cell Biol.* 167, 973–983. doi: 10.1083/jcb.200409077

Ge, C., Xiao, G., Jiang, D., and Franceschi, R. T. (2007). Critical role of the extracellular signal-regulated kinase-MAPK pathway in osteoblast differentiation and skeletal development. *J. Cell Biol.* 176, 709–718. doi: 10.1083/jcb.200610046

Grynkiewicz, G., Poenie, M., and Tsien, R. Y. (1985). A new generation of Ca2+ indicators with greatly improved fluorescence properties. *J. Biol. Chem.* 260, 3440–3450. doi: 10.1016/S0021-9258(19)83641-4

Guo, Y. J., Pan, W. W., Liu, S. B., Shen, Z. F., Xu, Y., and Hu, L. L. (2020). ERK/MAPK signalling pathway and tumorigenesis. *Exp. Ther. Med.* 19, 1997–2007. doi: 10.3892/etm.2020.8454

Guo, X., and Wang, X. F. (2009). Signaling cross-talk between TGF-beta/BMP and other pathways. *Cell Res.* 19, 71–88. doi: 10.1038/cr.2008.302

Harris, A. L. (2007). Connexin channel permeability to cytoplasmic molecules. *Prog. Biophys. Mol. Biol.* 94, 120–143. doi: 10.1016/j.pbiomolbio.2007.03.011

Haruyama, N., Thyagarajan, T., Skobe, Z., Wright, J. T., Septier, D., Sreenath, T. L., et al. (2006). Overexpression of transforming growth factor-beta1 in teeth results in detachment of ameloblasts and enamel defects. *Eur. J. Oral Sci.* 114(Suppl. 1), 30–34. doi: 10.1111/j.1600-0722.2006.00276.x

Huang, G. Y., Wessels, A., Smith, B. R., Linask, K. K., Ewart, J. L., and Lo, C. W. (1998). Alteration in connexin 43 gap junction gene dosage impairs conotruncal heart development. *Dev. Biol.* 198, 32–44. doi: 10.1006/dbio.1998.8891

Ishikawa, M., Iwamoto, T., Nakamura, T., Doyle, A., Fukumoto, S., and Yamada, Y. (2011). Pannexin 3 functions as an ER Ca(2+) channel, hemichannel, and gap junction to promote osteoblast differentiation. *J. Cell Biol.* 193, 1257–1274. doi: 10.1083/jcb.201101050

Ishikawa, M., Williams, G. L., Ikeuchi, T., Sakai, K., Fukumoto, S., and Yamada, Y. (2016). Pannexin 3 and connexin 43 modulate skeletal development through their distinct functions and expression patterns. *J. Cell Sci.* 129, 1018–1030. doi: 10.1242/jcs.176883

Iwamoto, T., Nakamura, T., Doyle, A., Ishikawa, M., De Vega, S., Fukumoto, S., et al. (2010). Pannexin 3 regulates intracellular ATP/cAMP levels and promotes chondrocyte differentiation. *J. Biol. Chem.* 285, 18948–18958. doi: 10.1074/jbc.M110.127027

Iwamoto, T., Nakamura, T., Ishikawa, M., Yoshizaki, K., Sugimoto, A., Ida-Yonemochi, H., et al. (2017). Pannexin 3 regulates proliferation and differentiation of odontoblasts via its hemichannel activities. *PLoS One* 12:e0177557. doi: 10.1371/journal.pone.0177557

Judisch, G. F., Martin-Casals, A., Hanson, J. W., and Olin, W. H. (1979). Oculodentodigital dysplasia: four new reports and a literature review. *Arch. Ophthalmol.* 97, 878–884. doi: 10.1001/archopht.1979.01020010436007

Keshet, Y., and Seger, R. (2010). The MAP kinase signaling cascades: a system of hundreds of components regulates a diverse array of physiological functions. *Methods Mol. Biol.* 661, 3–38. doi: 10.1007/978-1-60761-795-2_1

Kim, Y., Hur, S. W., Jeong, B. C., Oh, S. H., Hwang, Y. C., Kim, S. H., et al. (2018). The Fam50a positively regulates ameloblast differentiation via interacting with Runx2. *J. Cell. Physiol.* 233, 1512–1522. doi: 10.1002/jcp.26038

Komori, T., Yagi, H., Nomura, S., Yamaguchi, A., Sasaki, K., Deguchi, K., et al. (1997). Targeted disruption of Cbfa1 results in a complete lack of bone formation owing to maturational arrest of osteoblasts. *Cell* 89, 755–764. doi: 10.1016/S0092-8674(00)80258-5

Kurtenbach, S., Kurtenbach, S., and Zoidl, G. (2014). Gap junction modulation and its implications for heart function. *Front. Physiol.* 5:82. doi: 10.3389/fphys.2014.00082

Lai, C. F., and Cheng, S. L. (2002). Signal transductions induced by bone morphogenetic protein-2 and transforming growth factor-beta in normal human osteoblastic cells. *J. Biol. Chem.* 277, 15514–15522. doi: 10.1074/jbc.M200794200

Laird, D. W. (2014). Syndromic and non-syndromic disease-linked Cx43 mutations. *FEBS Lett.* 588, 1339–1348. doi: 10.1016/j.febslet.2013.12.022

Loewenstein, W. R., and Kanno, Y. (1966). Intercellular communication and the control of tissue growth: lack of communication between cancer cells. *Nature* 209, 1248–1249. doi: 10.1038/2091248a0

Loewenstein, W. R., and Kanno, Y. (1967). Intercellular communication and tissue growth. I. Cancerous growth. *J. Cell Biol.* 33, 225–234. doi: 10.1083/jcb.33.2.225

Luo, K. (2017). Signaling cross talk between TGF-β/Smad and other signaling pathways. *Cold Spring Harb. Perspect. Biol.* 9:a022137. doi: 10.1101/cshperspect.a022137

Lurtz, M. M., and Louis, C. F. (2007). Intracellular calcium regulation of connexin43. *Am. J. Phys. Cell Physiol.* 293, C1806–C1813. doi: 10.1152/ajpcell.00630.2006

Macquart, C., Jüttner, R., Morales Rodriguez, B., Le Dour, C., Lefebvre, F., Chatzifrangkeskou, M., et al. (2018). Microtubule cytoskeleton regulates Connexin 43 localization and cardiac conduction in cardiomyopathy caused by mutation in A-type lamins gene. *Hum. Mol. Genet.* 28, 4043–4052. doi: 10.1093/hmg/ddy227

Mikoshiba, K. (2007). IP3 receptor/Ca2+ channel: from discovery to new signaling concepts. *J. Neurochem.* 102, 1426–1446. doi: 10.1111/j.1471-4159.2007.04825.x

Nagata, K., Masumoto, K., Esumi, G., Teshiba, R., Yoshizaki, K., Fukumoto, S., et al. (2009). Connexin43 plays an important role in lung development. *J. Pediatr. Surg.* 44, 2296–2301. doi: 10.1016/j.jpedsurg.2009.07.070

Nakamura, T., De Vega, S., Fukumoto, S., Jimenez, L., Unda, F., and Yamada, Y. (2008). Transcription factor epiprofin is essential for tooth morphogenesis by regulating epithelial cell fate and tooth number. *J. Biol. Chem.* 283, 4825–4833. doi: 10.1074/jbc.M708388200

Nakamura, T., Iwamoto, T., Nakamura, H. M., Shindo, Y., Saito, K., Yamada, A., et al. (2020). Regulation of miR-1-mediated connexin 43 expression and cell proliferation in dental epithelial cells. *Front. Cell Dev. Biol.* 8:156. doi: 10.3389/fcell.2020.00156

Nakamura, T., Jimenez-Rojo, L., Koyama, E., Pacifici, M., De Vega, S., Iwamoto, M., et al. (2017). Epiprofin regulates enamel formation and tooth morphogenesis by controlling epithelial-mesenchymal interactions during tooth development. *J. Bone Miner. Res.* 32, 601–610. doi: 10.1002/jbmr.3024

Nielsen, M. S., Axelsen, L. N., Sorgen, P. L., Verma, V., Delmar, M., and Holstein-Rathlou, N. H. (2012). Gap junctions. *Compr. Physiol.* 2, 1981–2035. doi: 10.1002/cphy.c110051

Paznekas, W. A., Boyadjiev, S. A., Shapiro, R. E., Daniels, O., Wollnik, B., Keegan, C. E., et al. (2003). Connexin 43 (GJA1) mutations cause the pleiotropic phenotype of oculodentodigital dysplasia. *Am. J. Hum. Genet.* 72, 408–418. doi: 10.1086/346090

Paznekas, W. A., Karczeski, B., Vermeer, S., Lowry, R. B., Delatycki, M., Laurence, F., et al. (2009). GJA1 mutations, variants, and connexin 43 dysfunction as it relates to the oculodentodigital dysplasia phenotype. *Hum. Mutat.* 30, 724–733. doi: 10.1002/humu.20958

Pérez-Sala, D., and Rebollo, A. (1999). Novel aspects of Ras proteins biology: regulation and implications. *Cell Death Differ.* 6, 722–728. doi: 10.1038/sj.cdd.4400557

Reaume, A. G., De Sousa, P. A., Kulkarni, S., Langille, B. L., Zhu, D., Davies, T. C., et al. (1995). Cardiac malformation in neonatal mice lacking connexin43. *Science* 267, 1831–1834. doi: 10.1126/science.7892609

Saito, K., Michon, F., Yamada, A., Inuzuka, H., Yamaguchi, S., Fukumoto, E., et al. (2020). Sox21 regulates Anapc10 expression and determines the fate of ectodermal organ. *iScience* 23:101329. doi: 10.1016/j.isci.2020.101329

Schmierer, B., and Hill, C. S. (2007). TGFbeta-SMAD signal transduction: molecular specificity and functional flexibility. *Nat. Rev. Mol. Cell Biol.* 8, 970–982. doi: 10.1038/nrm2297

Selvamurugan, N., Kwok, S., Alliston, T., Reiss, M., and Partridge, N. C. (2004). Transforming growth factor-beta 1 regulation of collagenase-3 expression in osteoblastic cells by cross-talk between the Smad and MAPK signaling pathways and their components, Smad2 and Runx2. *J. Biol. Chem.* 279, 19327–19334. doi: 10.1074/jbc.M314048200

Song, W., Wang, Y., Chu, Q., Qi, C., Gao, Y., Gao, Y., et al. (2018). Loss of transforming growth factor-β1 in epithelium cells affects enamel formation in mice. *Arch. Oral Biol.* 96, 146–154. doi: 10.1016/j.archoralbio.2018.09.003

Stains, J. P., and Civitelli, R. (2005). Gap junctions regulate extracellular signal-regulated kinase signaling to affect gene transcription. *Mol. Biol. Cell* 16, 64–72.

Tacheau, C., Fontaine, J., Loy, J., Mauviel, A., and Verrecchia, F. (2008). TGF-beta induces connexin43 gene expression in normal murine mammary gland epithelial cells via activation of p38 and PI3K/AKT signaling pathways. *J. Cell. Physiol.* 217, 759–768. doi: 10.1002/jcp.21551

Toth, K., Shao, Q., Lorentz, R., and Laird, D. W. (2010). Decreased levels of Cx43 gap junctions result in ameloblast dysregulation and enamel hypoplasia in Gja1Jrt/+ mice. *J. Cell. Physiol.* 223, 601–609. doi: 10.1002/jcp.22046

Verheule, S., and Kaese, S. (2013). Connexin diversity in the heart: insights from transgenic mouse models. *Front. Pharmacol.* 4:81. doi: 10.3389/fphar.2013.00081

Wang, X., Chiba, Y., Jia, L., Yoshizaki, K., Saito, K., Yamada, A., et al. (2020). Expression patterns of claudin family members during tooth development and the role of claudin-10 (Cldn10) in cytodifferentiation of stratum intermedium. *Front. Cell Dev. Biol.* 8:595593. doi: 10.3389/fcell.2020.620603

Yamada, A., Futagi, M., Fukumoto, E., Saito, K., Yoshizaki, K., Ishikawa, M., et al. (2016). Connexin 43 is necessary for salivary gland branching morphogenesis and FGF10-induced ERK1/2 phosphorylation. *J. Biol. Chem.* 291, 904–912. doi: 10.1074/jbc.M115.674663

Zheng, G. X., Terry, J. M., Belgrader, P., Ryvkin, P., Bent, Z. W., Wilson, R., et al. (2017). Massively parallel digital transcriptional profiling of single cells. *Nat. Commun.* 8:14049. doi: 10.1038/ncomms14049

Conflict of Interest: The authors declare that the research was conducted in the absence of any commercial or financial relationships that could be construed as a potential conflict of interest.

Publisher's Note: All claims expressed in this article are solely those of the authors and do not necessarily represent those of their affiliated organizations, or those of the publisher, the editors and the reviewers. Any product that may be evaluated in this article, or claim that may be made by its manufacturer, is not guaranteed or endorsed by the publisher.

frontiers in Physiology

ORIGINAL RESEARCH
published: 06 October 2021
doi: 10.3389/fphys.2021.723210

Cells at the Edge: The Dentin–Bone Interface in Zebrafish Teeth

*Joana T. Rosa[1,2], Paul Eckhard Witten[1] and Ann Huysseune[1]**

[1]*Research Group Evolutionary Developmental Biology, Biology Department, Ghent University, Ghent, Belgium,* [2]*Comparative, Adaptive and Functional Skeletal Biology (BIOSKEL), Centre of Marine Sciences (CCMAR), University of Algarve, Campus Gambelas, Faro, Portugal*

OPEN ACCESS

Edited by:
Huan Liu,
Wuhan University, China

Reviewed by:
Aaron R. H. LeBlanc,
King's College London, United Kingdom
Joy Richman,
University of British Columbia, Canada
Kazuhiko Kawasaki,
The Pennsylvania State University (PSU), United States

***Correspondence:**
Ann Huysseune
ann.huysseune@ugent.be

Specialty section:
This article was submitted to Craniofacial Biology and Dental Research, a section of the journal Frontiers in Physiology

Received: *10 June 2021*
Accepted: *08 September 2021*
Published: *06 October 2021*

Citation:
Rosa JT, Witten PE and Huysseune A (2021) Cells at the Edge: The Dentin–Bone Interface in Zebrafish Teeth. Front. Physiol. 12:723210. doi: 10.3389/fphys.2021.723210

Bone-producing osteoblasts and dentin-producing odontoblasts are closely related cell types, a result from their shared evolutionary history in the ancient dermal skeleton. In mammals, the two cell types can be distinguished based on histological characters and the cells' position in the pulp cavity or in the tripartite periodontal complex. Different from mammals, teleost fish feature a broad diversity in tooth attachment modes, ranging from fibrous attachment to firm ankylosis to the underlying bone. The connection between dentin and jaw bone is often mediated by a collar of mineralized tissue, a part of the dental unit that has been termed "bone of attachment". Its nature (bone, dentin, or an intermediate tissue type) is still debated. Likewise, there is a debate about the nature of the cells secreting this tissue: osteoblasts, odontoblasts, or yet another (intermediate) type of scleroblast. Here, we use expression of the P/Q rich secretory calcium-binding phosphoprotein 5 (*scpp5*) to characterize the cells lining the so-called bone of attachment in the zebrafish dentition. *scpp5* is expressed in late cytodifferentiation stage odontoblasts but not in the cells depositing the "bone of attachment". nor in *bona fide* osteoblasts lining the supporting pharyngeal jaw bone. Together with the presence of the osteoblast marker Zns-5, and the absence of covering epithelium, this links the cells depositing the "bone of attachment" to osteoblasts rather than to odontoblasts. The presence of dentinal tubule-like cell extensions and the near absence of osteocytes, nevertheless distinguishes the "bone of attachment" from true bone. These results suggest that the "bone of attachment" in zebrafish has characters intermediate between bone and dentin, and, as a tissue, is better termed "dentinous bone". In other teleosts, the tissue may adopt different properties. The data furthermore support the view that these two tissues are part of a continuum of mineralized tissues. Expression of *scpp5* can be a valuable tool to investigate how differentiation pathways diverge between osteoblasts and odontoblasts in teleost models and help resolving the evolutionary history of tooth attachment structures in actinopterygians.

Keywords: odontoblast, osteoblast, dentin, bone, tooth attachment, zebrafish, dermal skeleton, *scpp*

INTRODUCTION

Bone and dentin were concomitantly present in the earliest elements of the dermal skeleton (Ørvig, 1951; Sire and Kawasaki, 2012; Keating et al., 2018). The first mineralized skeleton appeared in jawless vertebrates of the Ordovician, the pteraspidomorphs ("heterostracomorphs", Donoghue and Sansom, 2002; Keating et al., 2018). Their body armor consisted of scales, ornamented with tubercles or ridges composed of a superficial layer of dentin, acellular bone, and, in some taxa, enameloid (Donoghue and Sansom, 2002). As a result of their shared evolutionary history, bone and dentin have many important characters in common (see e.g., Ørvig, 1951, 1967, and many references therein). Not surprisingly, the cells that secrete these matrices, osteoblasts and odontoblasts, are closely related cell types. This was already recognized by Klaatsch (1890, cited in Ørvig, 1951), who designated the term "scleroblast" for any cell participating in hard tissue formation.

In the mammalian jaw complex, osteoblasts and odontoblasts can usually easily be distinguished, as bone and dentin are well delimited anatomically and distinctive histologically. Mammalian teeth form discrete units with an internal cavity paved by odontoblasts. The root dentin that these cells produce is covered outward by cementum and delimited from the alveolar bone by the periodontal ligament. Within this tripartite periodontal complex, the tissues are kept well apart and are maintained through tightly balanced interactions (Fleischmannova et al., 2010). Different from mammals where tissue identification is commonly unambiguous, non-mammalian amniotes with ankylosed teeth possess an attachment tissue whose identification has raised considerable debate. It may either be related to cementum or to alveolar bone, but nevertheless appears to be clearly distinguishable from dentin (Bertin et al., 2018).

The large group of teleost fish (about 30,000 species), on the other hand, features a broad diversity of tooth attachment modes, ranging from fibrous attachment of the dentin base to the underlying bone, to firm ankylosis (Gaengler, 2000). The part of the tooth that is not covered by the hypermineralized cap of enameloid is sometimes called a root (e.g., Bemis et al., 2005). However, the term "root" for teleost (or even actinopterygian) teeth is not widely accepted. Many teleosts have teeth anchored on top of the bone, either during the entire lifetime of the animal, or at least in the first tooth generations (Trapani, 2001; Sire et al., 2002). This type of attachment, or ankylosis, begins when the base of the elongating tooth germ approaches the jaw bone. Outgrowths of the tooth and the adjacent bone then form a composite tissue in which bone and dentin are in intimate contact (Berkovitz and Shellis, 2016). This is distinguished from gomphosis, or anchoring in an alveolus. Furthermore, unlike "rooted" teeth, teleost teeth are broadest in their basal area, generally with a wide open pulp cavity (Peyer, 1968). Therefore, the proximal part of teleost teeth is commonly labeled as "basal portion" or "base" (Peyer, 1968), or remains an unnamed part of the "shaft" (Berkovitz and Shellis, 2016). Here, we will adopt the term "base". Fink (1981) distinguished four types of attachment in actinopterygians, with the participation of a histologically distinct structure, which he referred to as "attachment bone" (here referred to as "bone of attachment", a term originally coined by Tomes, 1875, 1882). In his type 1 mode (**Figure 1A**), the mature tooth is completely ankylosed to the bone – that is, mineralization is continuous between the tooth base and the "bone of attachment", a situation considered to be the primitive actinopterygian condition (Fink, 1981). For example, in zebrafish (a cyprinid, and a common developmental and genetic model species), the entire connection between the dentin base and the supporting, dentigerous, bone is mineralized (**Figures 1B**,**C**; Huysseune et al., 1998; Van der heyden et al., 2000). In contrast, many teleosts possess a small area of unmineralized collagen persisting as a ligament between the dentin base and the cylinder of hard tissue ("bone of attachment"; type 2 attachment in Fink's classification, **Figure 1A**; Huysseune, 1983). In highly evolved teleosts with intramedullary tooth development, e.g., cichlids, this cylinder is deeply inserted into the jaw bone, and fused to the surrounding dentigerous bone *via* spongy bone (**Figure 1A**). Shellis (1982) and Berkovitz and Shellis (2016) reserve the term "bone of attachment" exclusively for type 1 attachment of Fink (1981). They call the cylinder of hard tissue, ligamentously connected to the dentin (Fink's type 2 attachment), "pedicel", and reserve the term "bone of attachment" for the bone tissue interconnecting pedicels or attaching pedicels to the jaw bone (Shellis, 1982; Berkovitz and Shellis, 2016; **Figure 1A**). The two other types described by Fink (1981) represent more specialized types of anchorage. Still other types of attachment exist (e.g., Soule, 1969; Bemis et al., 2005).

The nature of the tissue, attaching the tooth to the supporting bone in teleosts, whether the "attachment bone" of Fink (1981) or the "pedicel" of Shellis (1982) and Berkovitz and Shellis (2016), has been a matter of considerable discussion. In some species, it has been described as dentin (even if covered by osteoblasts on the outside). In such a case, the term "bone of attachment" would be inappropriate to describe this tissue (e.g., in sea bream species, Hughes et al., 1994). In other species, it has been claimed to have a bony nature, its development being initiated by the dentigerous bone (Clemen et al., 1997), justifying the term "bone of attachment", or "attachment bone". Perhaps the wide variety of dentins encountered in actinopterygians (Ørvig, 1967) may at least partly explain the structural diversity of the "bone of attachment". Irrespective of the nature of the tissue, and whether partly or entirely mineralized, it presents as a cylinder (or collar) in the prolongation of the dentin base. Likewise, the layer of cells that secretes the dentin appears to extend from the pulp cavity along the inside of the "bone of attachment" down to the supporting bone (described for, e.g., zebrafish, Huysseune et al., 1998; sparids, Hughes et al., 1994; *Lophius*, Kerebel et al., 1979). As a result, it is unclear whether the cells that line the "bone of attachment" on its inside are odontoblasts, osteoblasts, or yet another (intermediate) type of hard tissue forming cell ("scleroblast", Klaatsch, 1890, cited in Ørvig, 1951). Often, it is the assumed nature of the attachment tissue that is used to qualify the cells that produce this matrix as odontoblasts, or osteoblasts.

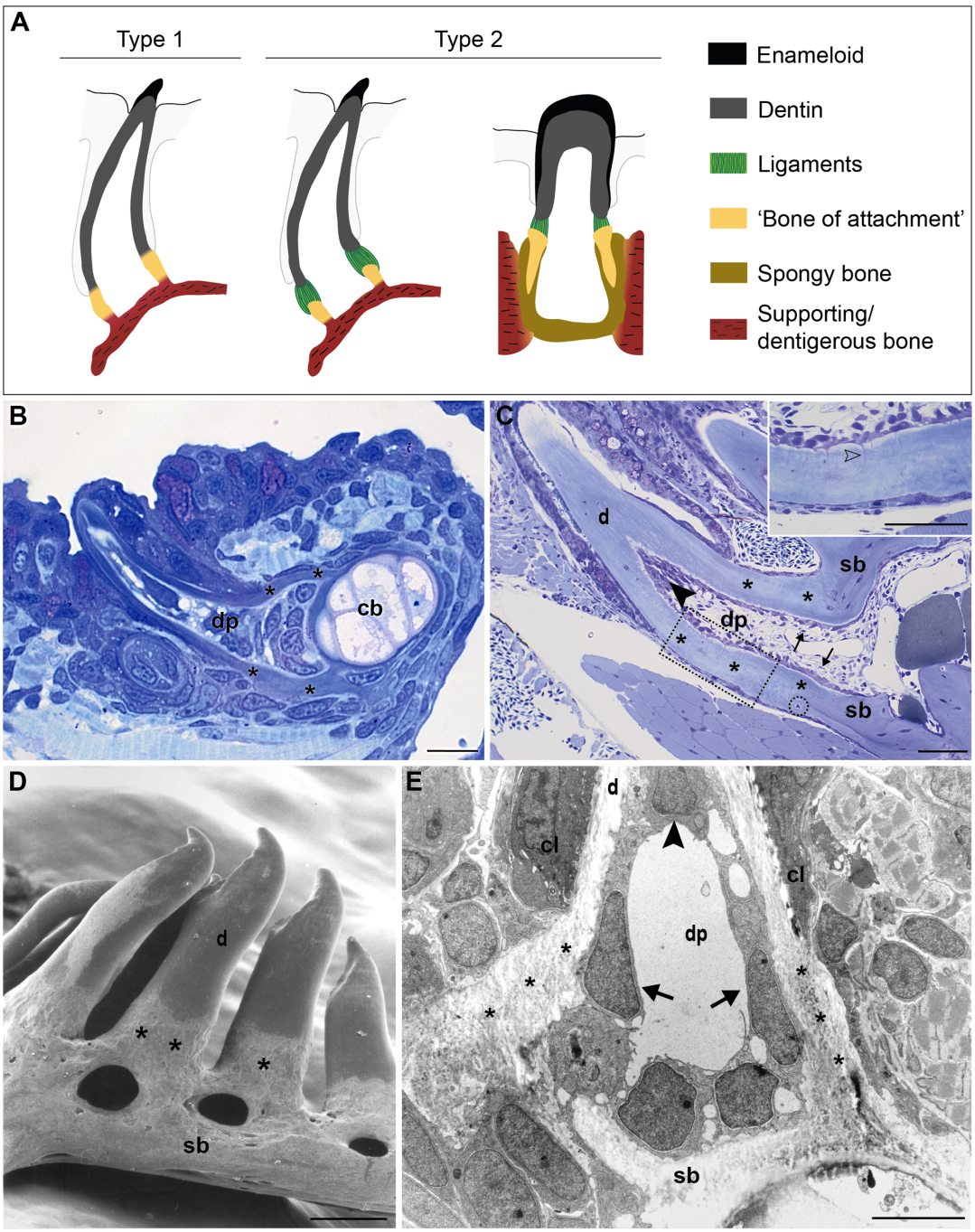

FIGURE 1 | Tooth attachment in actinopterygians. **(A)** Schematic representation of type 1 and type 2 tooth attachment modes according to Fink (1981). In type 1 (e.g., zebrafish), a cylindrical collar of tissue, hitherto called "bone of attachment" ("attachment bone" in the terminology of Fink, 1981), firmly ankyloses the tooth to the supporting bone, resulting in continuous mineralization between the tooth base and the supporting (dentigerous) bone. In type 2, the cylindrical collar of "bone of attachment" is connected to the tooth by a ligament. The collar is positioned either on top, or inserted into the supporting bone. Note that in the latter case, Berkovitz and Shellis (2016) label the "bone of attachment" as "pedicel", reserving the term "bone of attachment" for the tissue serving to attach the pedicels. Note that the term "bone of attachment" is used between quotation marks, pending a more appropriate term based on the findings in this study. **(B)** and **(C)** Toluidine blue-stained semi-thin sections of a zebrafish initiator tooth at 6 dph **(B)** and an adult tooth **(C)**, both attached, as in type 1 attachment. Note multiple osteocytes in the adult supporting bone, a single one in the "bone of attachment" (encircled). Inset: enlargement of "bone of attachment" (dotted rectangle) with cell prolongations (open arrowhead). **(D)** Scanning electron micrograph of attached adult zebrafish teeth. **(E)** Overview transmission electron microscopy (TEM) picture of the base of a zebrafish first-generation tooth at the level of the cervical loop. The dentin, "bone of attachment" and supporting bone form a continuous mineralized tissue, covered along the pulpal side with scleroblasts that appear to be involved in the deposition of more than one matrix. cb, ceratobranchial cartilage; cl, cervical loop; d, dentin; dp, dental pulp; sb, supporting bone; asterisks, "bone of attachment"; arrows, scleroblasts forming "bone of attachment"; black arrowheads, odontoblasts. Scale bar **(B)** = 10 µm, **(C)** = 50 µm, **(D)** = 100 µm, and **(E)** = 5 µm.

Given the close evolutionary, chemical and structural relationship of bone and dentin, it is not surprising that very few genes are expressed exclusively in just one of both cell types – osteoblasts or odontoblasts – rendering an unambiguous characterization of the attachment tissue difficult. Differentiation of epithelial cells into enamel/enameloid-producing cells, on the one hand, and mesenchymal cells into dentin-producing cells, on the other hand, relies on common genetic toolkits, namely genes encoding secreted signaling factors and their receptors, and transcription factors. Differences in their spatiotemporal pattern or strength of expression may alter the outcome. In contrast, extracellular matrix (ECM) proteins are more specific to mineralizing tissues and can thus be much more informative as to the structure of a particular tissue, hence the cell type that produces it (Kawasaki and Weiss, 2006). In 2009, Kawasaki (2009) reported the repertoire of secretory calcium binding phosphoproteins (SCPPs) in zebrafish and frogs and their expression in dental and skeletal tissues. The family of secretory calcium-binding phosphoproteins includes SCPPs involved in bone and dentin formation (the so-called acidic SCPPs or SIBLING proteins), as well as proteins involved in enamel formation, milk caseins and some salivary proteins (the so-called Pro/Gln (P/Q)-rich SCPPs; Kawasaki, 2009, 2011). Differential expression of SCPP genes in bone and dentin has been reported (see Kawasaki, 2009, 2011; Sire and Kawasaki, 2012 for an overview). Yet, only expression of *scpp5* was reported by Kawasaki (2009) to allow distinction between odontoblasts and osteoblasts in zebrafish. Thus, *scpp5* may be a good starting point to elucidate the nature of the "bone of attachment" in the zebrafish dentition.

In this paper, we examine the dentin-bone interface in the pharyngeal teeth and jaws of the zebrafish (the only tooth-bearing jaws in this species). We first highlight the resemblance between the different matrices, that is, dentin, supporting bone, and the collar of attachment tissue that has been termed "bone of attachment" in previous papers (Huysseune et al., 1998; Van der heyden et al., 2000). We next study the expression of *scpp5* in the different developmental stages of the initiator tooth (called tooth $4V^1$, Van der heyden and Huysseune, 2000; Gibert et al., 2019), other first-generation teeth, as well as adult teeth. Including both first-generation and adult teeth in the study is important because of substantial structural differences between the tooth generations. Indeed, first-generation teeth may well be more easily accessible for experimentation and (whole mount) gene expression studies, but they are extremely small, have an enamel organ and dental papilla containing a few cells only, and a pulp devoid of nerves and blood vessels. Unlike in their adult counterparts, their dentin is atubular, and supporting bone structures are still thin and virtually anosteocytic (Huysseune et al., 1998; Huysseune, 2000; Sire et al., 2002). The aims are (1) to reveal exactly where and in which stages of tooth development *scpp5* is expressed, both in early life stages and in the adult, and (2) to elucidate if the scleroblasts depositing the "bone of attachment" have an odontoblast or osteoblast character. These data are complemented by immunocytochemical data on the distribution of Zns-5, a cell surface antigen that has been used as an osteoblast-specific marker (Johnson and Weston, 1995). Together with structural data, the temporal and spatial distribution of *scpp5* and Zns-5 inform us on the nature of the cells producing the attachment tissue, and whether labeling it as "bone of attachment" is justified. This study contributes to the understanding of the character and the evolutionary history of tooth attachment in actinopterygians.

MATERIALS AND METHODS

Zebrafish Maintenance and Breeding

Adult zebrafish (AB wild-type strain) were maintained and spawned according to Westerfield (2000). Embryos and early postembryonic stages were raised in egg water at 28.5°C and staged according to Kimmel et al. (1995). Early postembryonic stages from 72 h post-fertilization (hpf) to 6 d post-fertilization (dpf), as well as 4-month-old adults were sacrificed by an overdose of 1% ethyl 3-aminobenzoate methanesulfonate (MS-222; E10521-10G, Sigma Aldrich) and further processed.

Sample Processing for *in situ* Hybridization and Immunohistochemistry

Early postembryonic stages were fixed for 4 h at 4°C in 4% paraformaldehyde [PFA; pH 7.4 in 1x phosphate-buffered saline in DEPC-H_2O (PBS)], washed 3 × 5 min with 1xPBS, dehydrated through a PBS/methanol gradient and stored in 100% methanol at 4°C. Prior to *in situ* hybridization, samples were rehydrated through an ascending methanol/PBS series. Pharyngeal jaws were dissected from adult zebrafish, fixed for 24 h at 4°C in 4% PFA, rinsed in 1xPBS for 1 h, and decalcified with 10% EDTA in Tris buffer-DEPC (100 mmol, pH 7.2) at 4°C for 3 weeks. Following dehydration, specimens were preserved at 4°C in 100% methanol until embedding. For paraffin inclusions, samples were first passed through an ascending methanol/xylene series, embedded in paraffin and then cross-sectioned (Microm HM360, Prosan). Sections (5 µm thick) were collected on TESPA (3-aminopropyltriethoxysilane, Sigma-Aldrich) coated slides, dried for 4 h at 37°C and kept at 4°C until further processed. For agar inclusions, samples were soaked in 5% sucrose in 1x PBS overnight and subsequently embedded in 1.5% agar/5% sucrose in 1x PBS. After solidifying, the blocks were transferred to 30% sucrose in PBS and kept at 4°C overnight. Blocks were then cross-sectioned on a cryotome (11 µm thick; Shandon cryotome FSE), the sections collected on TESPA-coated slides, allowed to dry, and stored at −20°C until use.

For *in situ* hybridization, sense and antisense RNA probes were generated from 1 µg of linearized pCR2.1-TOPO plasmid containing *scpp5* complete cDNA (EU642611) using T7 or SP6 polymerases, and then labeled with digoxigenin-dUTP (DIG RNA labeling kit, Roche Diagnostics, Mannheim, Germany). Riboprobes were treated with RNase-free DNase, recovered by ethanol precipitation and their integrity assessed through agarose gel electrophoresis. Whole mount *in situ* hybridization (used for early stages) was performed following the protocol described

in Verstraeten et al. (2012). These specimens were then dehydrated in an ascending series of PBS/ethanol, embedded in epon and serially sectioned at 2 µm. *In situ* hybridization on paraffin sections was performed using a protocol previously described by Rosa et al. (2016).

Immunohistochemistry on cryosections was performed using a monoclonal mouse anti-Zns-5 primary antibody (1:100, AB_10013796, ZIRC) and an Alexa Fluor® 594 (goat anti-mouse IgG, 1:200, Abcam) as secondary antibody. Negative controls were performed by omitting the primary antibody from the reaction mixture. Briefly, sections were thawed for 30 min at room temperature, washed 3 × 20 min in 1x PBS, permeabilized with acetone for 7 min at −20°C and washed 2 × 15 min in pre-blocking solution (0.5x PBS with 1% BSA, 1% DMSO and 0.5% Triton). Sections were then blocked for 1 h 30 min in blocking solution (pre-blocking solution with 1.5% goat serum) and incubated overnight at 4°C with the primary antibody diluted in blocking solution. The day after, sections were washed 8 × 10 min with pre-blocking solution and incubated with secondary antibody overnight at 4°C. Finally, sections were washed with PBT (1x PBS with 0.3% Triton) and mounted with DAKO mounting medium (Agilent, Ref. S3023).

Histology, Scanning and Transmission Electron Microscopy

Specimens for scanning electron microscopy (SEM) were prepared from cleared and stained adult jaws [maceration: 1–2% KOH; staining: 0.1% alizarin red S (Sigma) in 0.5% KOH]. After dehydration through a graded series of ethanol, specimens were dried (critical point drying, Balzers, CPD 020) and gold-coated (Balzers, SCD 040). Specimens were observed under a Jeol JSM-840 scanning electron microscope, operating at 15 kV. For high resolution histology and transmission electron microscopy (TEM), samples were fixed in a mixture of 1.5% PFA and 1.5% glutaraldehyde as previously described (Huysseune and Sire, 1992), embedded in epon, serially sectioned at 1 µm, and stained with toluidine blue. Ultrathin sections were prepared on an ultratome (Reichert Ultracut E), contrasted with uranyl acetate and lead citrate, and observed in a Philips 201 transmission electron microscope operating at 80 kV. Tissues and cellular structures in sections of adult specimens were identified through Heidenhain's Azan-staining following the protocol described in Romeis (1989). Sections were observed on a Zeiss Axio Imager Z1[1]. Photomicrographs were taken with an MRC camera and processed using ZEN software (Zeiss; see foot note 1). Computer-generated images were processed for color balance, contrast, and brightness only, and applied to all parts of the figures equally.

Ethical Statement

Animal care and sacrifice complied with European Directive 2010/63/EU of 22 September, 2010. The experimental protocols involved euthanasia only (no animal experiments); all animal procedures used in this study were approved by Flemish authorities (laboratory permit number LA1400452).

Data Availability

All sections used for this study are kept in the slide collection of the Research Group "Evolutionary Developmental Biology" at the Biology Department of Ghent University and are available for inspection upon request.

RESULTS

Dentin, "Bone of Attachment", and Supporting Bone

In zebrafish, a collar of mineralized tissue, hitherto called "bone of attachment", ankyloses the mature tooth to the supporting, dentigerous bone of the fifth ceratobranchial (type 1 attachment, **Figure 1A**), both in first-generation teeth (**Figure 1B**) as well as in later tooth generations and adult teeth (**Figure 1C**). Note that the term "bone of attachment" will be used here between quotation marks, pending the identification of the cells producing this tissue. The prospective site of formation of the "bone of attachment" becomes visible once the dentin cone has obtained its full length. A collagenous matrix is then deposited in the prolongation of the tooth base, from the level of the cervical loop down to the surface of the supporting bone (Huysseune et al., 1998; Van der heyden et al., 2000). Mineralization appears to occur instantaneously and fast throughout the "bone of attachment". Once mineralized, the "bone of attachment" forms a continuous structure, connecting the base of the dentin to the dentigerous bone, and is almost indistinguishable from either of these matrices (**Figures 1B**,**C**). A scanning electron micrograph of attached adult teeth (**Figure 1D**) confirms the continuous connection between the dentin, the "bone of attachment" and the underlying supporting bone of the fifth ceratobranchial. However, the "bone of attachment" distinguishes itself by its pitted surface from the smooth surface of the dentin. In this character, the "bone of attachment" resembles the dentigerous bone matrix rather than the dentin, as can also be appreciated from a low magnification TEM micrograph (**Figure 1E**). At an ultrastructural level, dentin and "bone of attachment" can be distinguished based on the organization of the collagenous matrix, which coincides with the position of the cervical loop tip (**Figure 1E**, and see Huysseune et al., 1998; Van der heyden et al., 2000 for more details). In the dentin, the collagen fibrils are homogeneously distributed and preferentially oriented along the long axis of the tooth. In contrast, the "bone of attachment", as well as the dentigerous bone, presents a woven-fibred matrix in which patches of electron-dense ground substance can be observed (**Figure 1E**). Yet, while the dentigerous bone contains osteocytes, at least when it has reached a sufficient thickness, the "bone of attachment" is virtually free of osteocytes, except for an occasional cell close to where the "bone of attachment" joins the dentigerous bone (**Figure 1C**). Most remarkably, however, the cells that line the three matrices inside the dental pulp do not appear

[1]www.zeiss.com

to respect strict demarcations. In large (adult) teeth, the cells lining the dentin and the "bone of attachment" form an uninterrupted layer and the cells facing the "bone of attachment" present small prolongations not unlike dentinal tubules (**Figure 1C**, inset). These tubules, likely one per cell, extend perpendicular for some distance through the dentin and are unbranched. Their length decreases in a proximal direction. In first-generation teeth, tubules are absent, both in the dentin and the "bone of attachment". Interestingly, a single cell can be found to be positioned adjacent to both dentin and "bone of attachment" (**Figure 1E**). Below, another cell, with different shape, adjoins both the "bone of attachment" and the dentigerous bone. Clearly, neither position nor morphology of these cells allows to establish their identity, let alone infer their role in the formation of dentin or the "bone of attachment". Similar difficulties for establishing boundaries at the tooth base have been encountered in medaka (Larionova et al., 2021).

scpp5 Expression in First-Generation Teeth and Adult Teeth

To learn whether the cells depositing the "bone of attachment" are odontoblasts, osteoblasts, or yet another (intermediate) type of hard tissue forming cell, we have turned to *scpp5* as a specific marker of odontoblasts (Kawasaki, 2009). Zebrafish teeth go through five successive developmental stages: initiation, morphogenesis, early and late cytodifferentiation, and attachment (Huysseune et al., 1998; Van der heyden et al., 2000; Borday-Birraux et al., 2006). *scpp5* transcripts are first detected at the late cytodifferentiation (LC) stage of the initiator tooth ($4V^1$), around 72 hpf, in both ameloblasts and odontoblasts (**Figure 2A**). However, once $4V^1$ is attached, between 80 and 96 hpf, the expression of *scpp5* is no longer detected in any of the cells of the dental unit, neither in the structures adjoining the tooth (**Figure 2B**). This profile of expression is also observed for the first-generation teeth adjacent to $4V^1$ (i.e., $3V^1$ and $5V^1$). A strong and specific signal from the *scpp5* riboprobe is observed in ameloblasts and odontoblasts at the LC stage of $3V^1$ and $5V^1$ (**Figures 2B–D**), but no signal is detected at early cytodifferentiation (EC; **Figure 2A**) or attachment (data not shown) stages, nor in any other cell types. Between 96 and 120 hpf the second generation of teeth starts to develop. Again, *scpp5* transcripts are only detectable at LC stages and restricted to ameloblasts and odontoblasts (**Figures 2D**,**E**). In adult teeth, the expression of *scpp5* has a slightly different temporal pattern. Already during the stage of morphogenesis, both ameloblasts and odontoblasts express *scpp5*, an expression that is maintained during EC (**Figure 2F**) and LC (**Figure 2G**). When the teeth start to attach (**Figure 2H**), odontoblasts maintain *scpp5* expression but the expression by the ameloblasts is downregulated and it is only detectable at the tip of the cervical loop. Once the tooth is fully attached, ameloblasts completely cease to express the gene and its expression becomes restricted to the odontoblasts (**Figures 2I**,**J**). Most importantly, at no moment is expression of *scpp5* detected in osteoblasts adjacent to the dentigerous bone or in cells lining the "bone of attachment". Instead, there is a well-defined separation between *scpp5*-expressing odontoblasts in the pulp cavity, down to where the cervical loop marks the boundary of the dentin, and the adjacent cells, that line the "bone of attachment" internally, and that do not express the gene.

Zns-5 Expression in Adult Teeth

Irrespective of their differentiation status, osteoblasts in zebrafish can be specifically labeled by immunohistochemistry for the cell surface antigen Zns-5 (Johnson and Weston, 1995; Knopf et al., 2011). To elucidate if the cells that line the "bone of attachment", and that do not express *scpp5*, have an osteogenic character, Zns-5 immunostaining was applied to adult zebrafish teeth of different developmental stages (**Figure 3**). The osteoblasts lining the supporting, dentigerous bone are specifically and strongly labeled both in areas where bone resorption already occurred and near to newly formed dentigerous bone (**Figures 3C**,**C′**). Importantly, the cells lining the "bone of attachment", both on its internal and external surface, are also labeled by Zns-5 (**Figures 3C**,**C′**). These cells form an uninterrupted layer that connects with the labeled osteoblasts lining the supporting bone. Importantly, Zns-5 positive cells were never found distal to the level of the cervical loop. Instead, a clear boundary exists between the cells lining the "bone of attachment", that are positive for Zns-5, and the adjoining odontoblasts, that face the dentin and are not labeled by the Zns-5 antibody. Interestingly, and despite the previously reported specificity of Zns-5 for osteogenic cells, Zns-5 was also found to label ameloblasts at I and M, EC, and LC tooth developmental stages (**Figures 3A,A′,B,B′**).

DISCUSSION

Our results clearly show that in the zebrafish pharyngeal jaw complex, odontoblasts are *scpp5* positive and Zns-5 negative, but cells lining the "bone of attachment", like the osteoblasts, are *scpp5* negative and Zns-5 positive. However, unlike bone, the "bone of attachment" is predominantly anosteocytic, and the matrix contains small cell prolongations not unlike dentinal tubules, making it resemble dentin. These results suggest that the "bone of attachment" in zebrafish has characters that make an unambiguous assignment to either dentin or bone very difficult. We suggest the term "dentinous bone" to reflect the ambiguous nature of the tissue. The term "pedicel" may then replace "bone of attachment" when referring to the anatomical entity that it represents. In this way, we follow the terminology for type 2 as employed by Berkovitz and Shellis (2016), but propose to use the term "pedicel" instead of "bone of attachment" also for the attachment structure in type 1, based on assumptions of homology (unpublished results). The term "pedicel" does not imply a qualification of tissue type. It is dentinous bone in zebrafish, but may well qualify as dentin in other teleosts (e.g., in sea bream species, Hughes et al., 1994).

Various studies on actinopterygian teeth have shown that the deposition of tooth matrix continues uninterruptedly from the base of the dentin cone toward the supporting bone (e.g., Kerr, 1960; Huysseune et al., 1998; Van der heyden et al., 2000; Huysseune and Witten, 2008). Thus, one could have

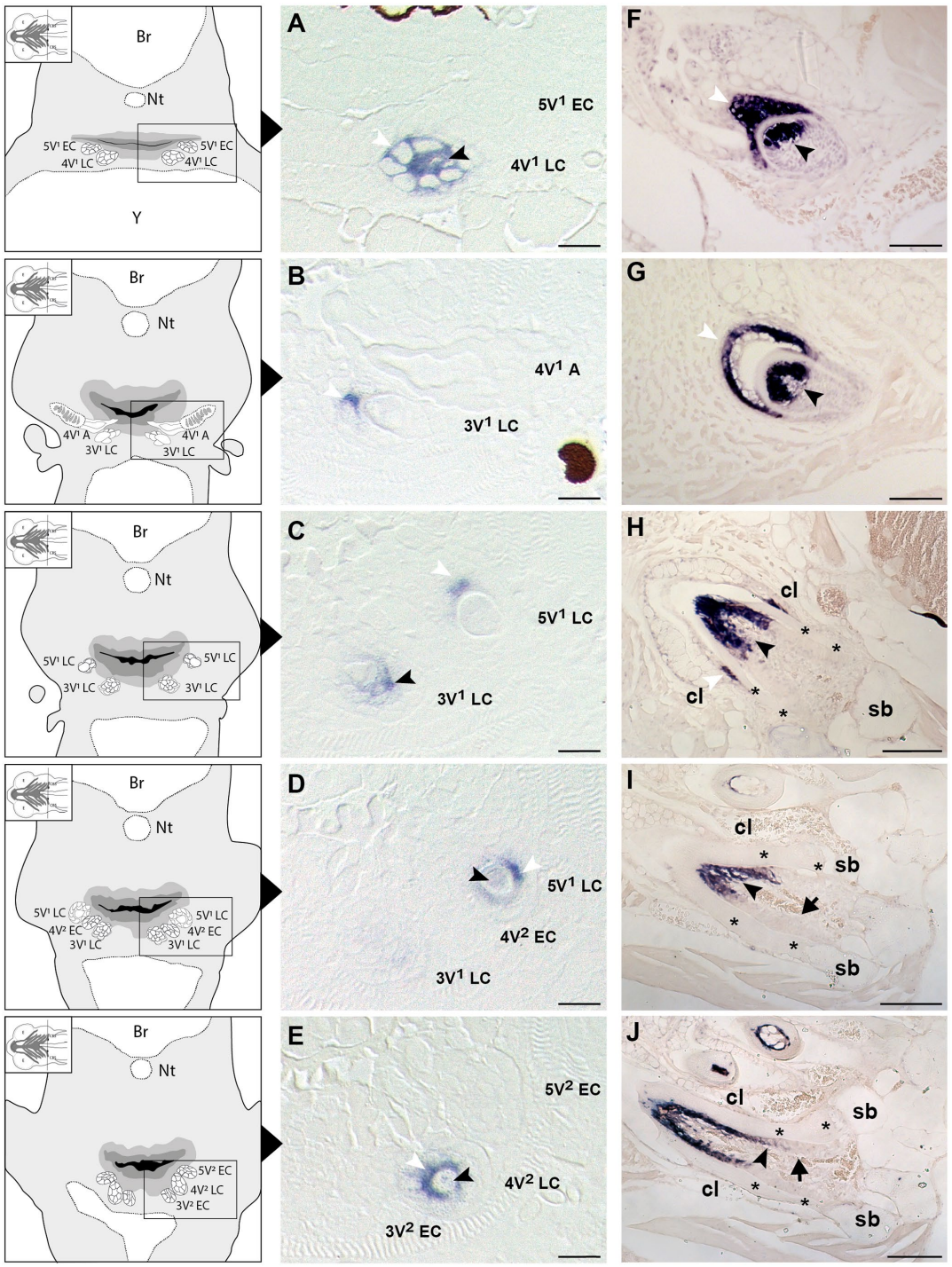

FIGURE 2 | Expression of secretory calcium-binding phosphoprotein 5 (*scpp5*) during zebrafish tooth development. Transverse sections of zebrafish postembryonic stages (72–120 hpf – **A–E**) and adults **(F–J)** in the region of the pharyngeal jaws, with explanatory schemes for postembryonic stages. At 72 hpf **(A)** the initiator tooth ($4V^1$) at LC stage expresses *scpp5* in both ameloblasts and odontoblasts, whereas no expression is detected for the first-generation teeth $3V^1$ and $5V^1$, still at EC stage. Between 80 **(B)** and 96 hpf **(C)** tooth $4V^1$, now attached, shows no expression of *scpp5*, while $3V^1$ and $5V^1$ at LC stages start to express *scpp5* in both ameloblasts and odontoblasts. Between 96 **(D)** and 120 hpf **(E)** the second-generation teeth ($4V^2$, $3V^2$, and $5V^2$) fail to express *scpp5* during EC but upregulate expression in both ameloblasts and odontoblasts at LC. During the development of adult teeth, the expression of *scpp5* is detected in both ameloblasts and odontoblasts at EC **(F)**, LC **(G)** and when the tooth starts to attach to bone **(H)**. Expression is restricted to odontoblasts when the tooth is completely attached [**(I)** and **(J)**]. Tooth developmental stages: A, phase of attachment; EC, early cytodifferentiation; LC, late cytodifferentiation. Br, brain; cl, cervical loop; Nt, notochord; sb, supporting bone; Y, yolk; asterisks, "bone of attachment"; arrows, cells forming "bone of attachment"; white arrowheads, ameloblasts; black arrowheads, odontoblasts. Scale bar **(A-E)** = 10 μm, **(F–G)** = 50 μm, **(H–J)** = 100 μm.

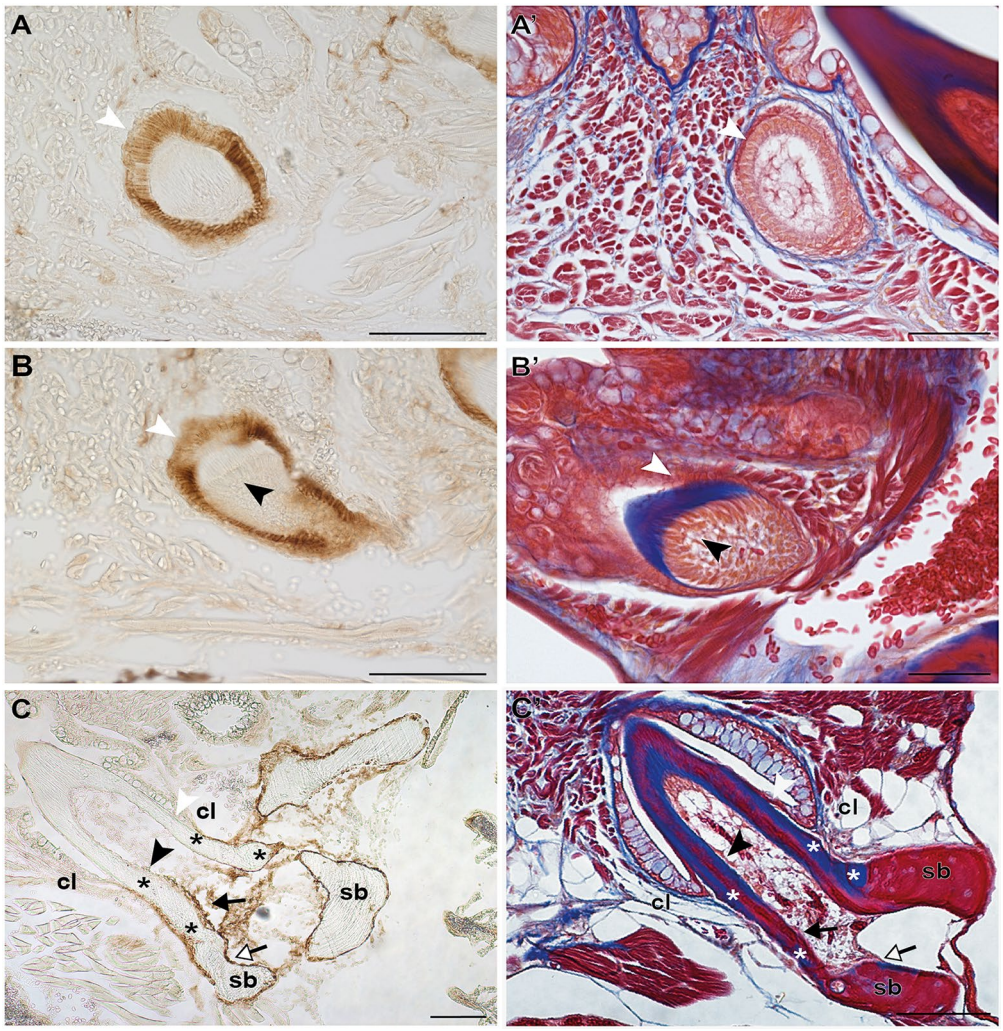

FIGURE 3 | Zns-5 immunodetection during adult zebrafish tooth development. Transverse sections of adult zebrafish in the region of the pharyngeal jaws, used for Zns-5 immunohistochemistry **(A–C)** or stained with azan **(A'–C')**. During EC **(A,A')** and LC **(B,B')**, Zns-5 is localized in ameloblasts, with no signal detected in odontoblasts. When teeth are attached **(C,C')** ameloblasts cease to stain for Zns-5 and the antigen is only detected in the cells lining the "bone of attachment" and the osteoblasts lining the supporting bone. Note osteocytes in the supporting bone, but their absence in the "bone of attachment" **(C')**. cl, cervical loop; sb, supporting bone; asterisks, "bone of attachment"; black arrowheads, odontoblasts; black arrows, cells forming "bone of attachment"; white arrowheads, ameloblasts; white arrows, osteoblasts. Scale bar **(A–D, C,'D')** = 100 μm, **(A',B')** = 50 μm.

raised the question, at the onset of the study, whether the dentin cone does not simply extend toward the bone surface, and subsequently fuses to the bone, making the cylinder of attachment tissue simply part of the dental unit. For example, the description of tooth attachment in salmon (and for that matter in other basal actinopterygians) by Moy-Thomas (1934) specifies that there is no intermediate structure and that teeth are attached to the bone directly or to upgrowths more or less continuous with the bones. The cylinder of attachment tissue has indeed been assigned to the dental unit by various authors. Huysseune (1983) considered the collar of "bone of attachment" in a cichlid (a highly evolved teleost) as part of the dental unit. Likewise, Smith and Hall (1993) included the "bone of attachment" within the fundamental odontogenetic unit. Butler (1995) also considered "bone of attachment" to be derived from the mesenchyme of the dental papilla. However, being part of the dental unit does not automatically mean that the cylinder of attachment tissue is also dentin. In fact, the question whether there is truly a separate entity that merits a study, must be answered positively.

The data presented here, along with literature reports, provide several arguments in favor of the idea that a structure that is *not* true dentin connects the tooth to the supporting bone (summarized in **Figure 4**). First, the cervical loop delimits the extent of the epithelium and thus the direct interactions that can take place with odontoblasts *via* the basal lamina. One can argue that dentin is only produced where mesenchymal cells are covered by epithelium (Sire and Huysseune, 2003). That dentin development – in contrast to bone tissue – requires the proximity of an epithelium was also recognized by Ørvig

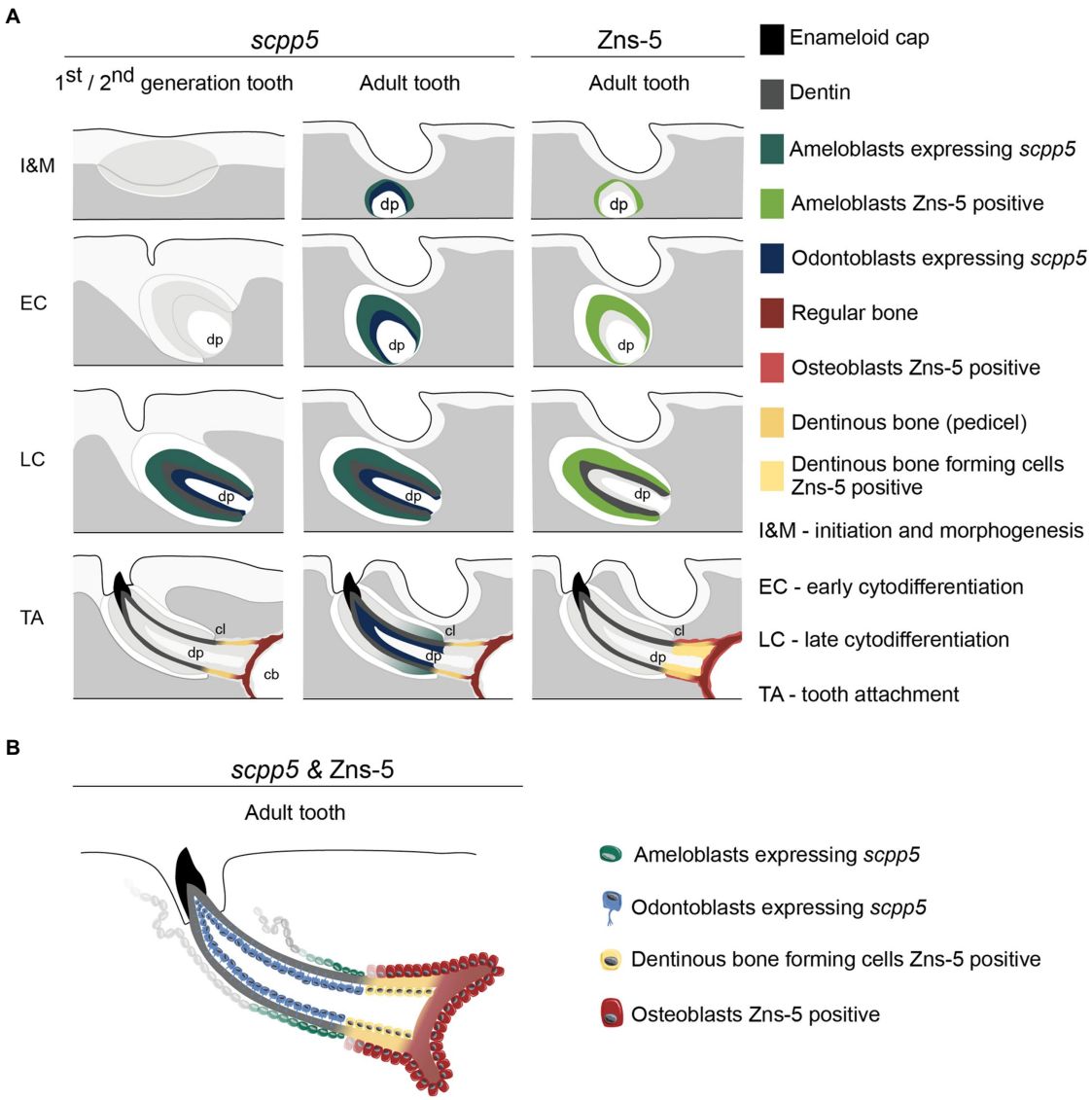

FIGURE 4 | Interpretative scheme showing localization of *scpp5* transcripts and Zns-5 detection during zebrafish tooth development. Panel **(A)** shows a representation of *scpp5* expression during first and second generation and adult tooth formation, from the stage of initiation and morphogenesis to tooth attachment, and of Zns-5 detection in adult teeth, at the same developmental stages. Panel **(B)** shows the comparison between the expression of *scpp5* and the localization of Zns-5, the former being exclusively expressed by ameloblasts and odontoblasts and the latter by cells forming the pedicel and by osteoblasts. In both panels, the adult tooth is depicted in a similar way as the first/second-generation teeth, although the tooth is larger, with thicker walls, and is attached to bone with all cartilage having been resorbed in this area. cb, ceratobranchial cartilage; cl, cervical loop; and dp, dental pulp.

(1967) and more recently by Sire and Huysseune (2003) and Sire and Kawasaki (2012). Both Osborn (1984) and Berkovitz and Shellis (2016) accepted the significance of the epithelium but reached a somewhat different conclusion. Osborn (1984), referring to description of tooth attachment of Shellis (1982) in the ballan wrasse, *Labrus bergylta*, recognized that odontoblasts differentiate under the influence of the epithelium (termed Hertwig's root sheath, HRS, both by Shellis, 1982, and Osborn, 1984), but at the same time argued that the cylinder of root dentin is continued beyond HRS by cells differentiated from the base of the dental papilla. He called this tissue "attachment dentine", and distinguished this from the bone-like tissue ("bone of attachment"), surrounding the base and produced by cells derived from soft tissue surrounding the developing tooth. Berkovitz and Shellis (2016) highlighted the ongoing discussion about the role (and potential retraction) of the epithelial sheath in the development of the attachment structures. They concluded that, whatever the role of the epithelial sheath, the pedicel is a joint product of the internal odontoblasts and the osteoblasts which cover the outer surface. Similar discussions have been ongoing regarding the role of Hertwig's root sheath and the origin and nature of cementoblasts depositing acellular or

cellular cementum during root formation in mammals (e.g., Bosshardt, 2005; Yamamoto et al., 2016).

Second, we now provide evidence that the cells that deposit the pedicel differ in their expression profile from *bona fide* odontoblasts. To start, we show that *scpp5* is exclusively expressed in developing teeth, confirming the observations of Kawasaki (2009) that the gene is specific for odontogenic, but not osteogenic cells. Likewise, based on RNA-seq data collected from the cichlid *Astatoreochromis alluaudi*, Karagic et al. (2020) found that *scpp5* is upregulated on tooth-bearing in contrast to nontoothed gill arches. Kawasaki (2009) showed the gene to be expressed both in the inner dental epithelium (IDE)/ameloblasts and odontoblasts but did not report anything on the pedicel. Here, we confirm the expression of *scpp5* in the ameloblasts and odontoblasts (at least in late cytodifferentiation stage). At no time did we observe any transcripts in the osteoblasts lining the dentigerous bone, or, for that matter, any other bone in the cranial and postcranial skeleton (data not shown). Most importantly, like true osteoblasts, the cells lining the pedicel do not express the gene. In this sense, these scleroblasts resemble osteoblasts. Moreover, there is a clearcut boundary between the proximalmost odontoblast, that expresses *scpp5*, and the distalmost scleroblast, that does not express the gene. Together with the presence of the osteoblast-specific marker Zns-5 in these scleroblasts, and its absence in odontoblasts, this strongly indicates that the cells lining the pedicel resemble osteoblasts rather than odontoblasts. A more detailed characterization of these cells would benefit from expression studies of other markers, such as *runx2*, a strong transcriptional activator for osteoblast-specific genes, and *sp7*, a transcription factor directly regulated by *runx2* (Komori, 2019). Both have been characterized as markers for zebrafish osteoblasts (e.g., Li et al., 2009; DeLaurier et al., 2010). Of relevance, *runx2* is expressed also in zebrafish odontoblasts (Kague et al., 2012, 2018) and *sp7* in zebrafish odontoblasts, osteoblasts and cells lining the "bone of attachment" (Kague et al., 2018). The studies of Kague et al. (2012, 2018) nevertheless rely on promotor-driven transgene expression; papers detailing endogenous *runx2* or *sp7* expression in odontoblasts of zebrafish (or any other teleost species) are currently lacking. However, various studies have shown that there is a close correspondence between endogenous expression of *sp7* (*via in situ* hybridization or antibody staining) and promotor-driven transgene expression (Renn and Winkler, 2009; DeLaurier et al., 2010; de Vrieze et al., 2015; Ando et al., 2017). A similar matching between endogenous and transgene expression has been observed for *runx2b* (Knopf et al., 2011). It is not excluded that a detailed analysis of endogenous *runx2* or *sp7* expression might reveal more specific expression patterns, restricted to certain mesenchymal cell types in the teeth. However, *sp7* is also expressed in zebrafish chondrocytes (Hammond and Schulte-Merker, 2009), as are the zebrafish *runx2* orthologs (Flores et al., 2006). The emerging picture of a chondrocyte-to-osteoblast lineage continuum (Beresford, 1981; Roach et al., 1995; Yang et al., 2014), along with the bone-dentin-enamel(oid)-continuum (Kawasaki and Weiss, 2008; Kawasaki, 2009), and the insight that bone- and dentin-forming cells are part of a unique cell population (Sire and Kawasaki, 2012), makes it unlikely that cells intermediate between odontoblasts and osteoblasts will differentially express these transcription factors. Fine scale studies required to uncover possible subtle differences are furthermore rendered difficult by the small cell size and number of odontoblasts in teleost fish, in some cases down to as little as one odontoblast (Larionova et al., 2021).

Unlike the supporting bone, on the other hand, the pedicel is largely devoid of osteocytes. If, as argued above, the pedicel is deposited by cells that resemble osteoblasts, suggesting the matrix deposited could be more bone-like, then there is a need to explain the lack of osteocytes. First, the absence of osteocytes in bone, even in a cellular-boned fish, is not unusual (Moss, 1961). In early life stages, when the bone is still very thin, cellular bone is often acellular (Huysseune, 2000). Thus, the absence of osteocytes may not be a character of sufficient weight to reject a bone-like character. Second, the outside of the pedicel is covered by mesenchymal cells that are to be considered as genuine osteoblasts. That these osteoblasts do not become entrapped in the pedicel either may well depend on their gene expression profile, compared to the osteoblasts lining the supporting bone and that become entrapped as osteocytes (Franz-Odendaal et al., 2006). Recent insights also point to the role of the highly dynamic nature of collagen assembly and maturation in the entrapment of osteocytes (Shiflett et al., 2019). According to this scenario, possible subtle differences in the organization of the collagen in the pedicel versus the supporting bone may trigger differences in entrapment of osteocytes.

The small cell prolongations, not unlike dentinal tubules, extending into the pedicel, represent another feature that questions the rather osteoblastic nature of the cells depositing the pedicel. However, not even this character can be unambiguously attributed to odontoblasts. Such cell prolongations, issuing from cells that remain at the surface of the matrix deposited, are reminiscent of the canaliculi of Williamson, described in the bone of extant holosteans (e.g., *Amia*, *Lepisosteus*; Sire and Meunier, 1994). Their nature has been heavily debated – whether of osteoblastic or odontoblastic origin – but arguments prevail to consider them to have an osteoblastic origin (Sire and Meunier, 1994).

What can these results teach us about osteoblast/odontoblast dichotomy and differentiation pathways? Ørvig (1951) described how, in the case of osteodentin (as in *Esox*), osteoblast-like cells that send short branching processes into the matrix modify directly into odontoblasts with a long peripherically directed odontoblast process. Thus, Ørvig (1951, 1967) considered that, in the teeth of some actinopterygian fishes, osteoblasts may turn into odontoblasts, but argued that, conversely, odontoblasts never transform into osteoblasts. He regarded odontoblasts as a special kind of osteoblasts. It is indeed remarkable how similar both cells are functionally (An, 2018). Even today, very often no distinction is made between both cell types and reference is simply made to "osteo/odontogenic differentiation" (e.g., Lin et al., 2019). Ariffin et al. (2017) nevertheless list a number of differences between odontoblasts and osteoblasts. However, this is a largely mammalian-centered view with limited

relevance to the current study. Sire and Kawasaki (2012) argue that bone and dentin are the expression of two developmental pathways from a unique cell population with common origin. These different pathways are dictated by the environment in which the cells reside: distance from a signaling center in the overlying epithelium, and presence of a vascular (pulp) cavity. Likewise, Hall and Witten (2007, 2019) view bone and dentin as a continuum with typical bone and typical orthodentin at both sides of the spectrum. Our expression data support these views: cells covered by epithelium (odontoblasts) are *scpp5*-positive and Zns-5 negative, while the cells that lie beyond the cervical loop and deposit the pedicel are *scpp5*-negative and Zns-5 positive, like osteoblasts.

The *scpp5* gene is also expressed in ameloblasts. This may not be too remarkable. Indeed, P/Q-rich SCPPs (to which SCPP5 belongs) are primarily deposited by dental epithelial cells (ameloblasts) and are employed to form the tooth surface (Kawasaki and Weiss, 2008). This is different from acidic SCPPs, which are principally secreted from mesenchymally derived osteoblasts, osteocytes, and/or odontoblasts and which are used for bone and dentin. Thus, it is rather surprising that *scpp5* is expressed in odontoblasts. In fact, based on the lack of expression of *scpp5* in odontoblasts of the gar, *Lepisosteus oculatus*, Kawasaki et al. (2021) suggest that *scpp5* expression is a derived character in teleost odontoblasts. On the other hand, enameloid is built on a collagenous matrix, and both ameloblasts and odontoblasts express collagen type 1 (as demonstrated for Atlantic salmon, Huysseune et al., 2008). Kawasaki (2009) already considered the shared expression of *COL1*, *SPARC*, *SCPP5*, and *SCPP1* in odontoblasts and IDE cells as an indication of the use of common ECM proteins in dentin and enameloid. Likewise, Kawasaki and Weiss (2008) supported the idea that the teleost IDE cell has a gene expression profile intermediate between an odontoblast and a (tetrapod) ameloblast and that enameloid and dentin are closely related "in mode of mineralization, tissue origin and constitutive proteins". The same line of thoughts can be followed for Zns-5. Whether its expression in the ameloblasts is transient or constitutional, and what its function is, needs however to be further explored.

In conclusion, the cells that, in zebrafish, deposit the dentinous bone of the pedicel have a molecular signature that approaches them to osteoblasts. Yet, the tissue they deposit does not truly qualify either as bone, or as dentin. Rather, the inference that the dentinous bone has characters that link it both to dentin (part of the tooth-forming developmental cascade, presence of cell prolongations), as well as to bone (lack of epithelial cover, expression profile of the scleroblasts, occasional presence of osteocytes) is in line with the conclusion of Kawasaki et al. (2009) that "there are only graded differences among bone, dentin, enameloid, and enamel, and these four tissues constitute an evolutionary continuum". This view was also expressed by Kerebel et al. (1979), Hall and Witten (2007), and Sire and Kawasaki (2012), among others. Sire and Kawasaki (2012) furthermore suggested that osteoblasts and odontoblasts differentiated from a same cell population in the earliest vertebrates. Comparative developmental studies of dermal skeletal elements in extant species support this view (Sire and Huysseune, 2003). The latter authors considered the vicinity of the epithelium as a decisive factor in which developmental pathway is chosen. The dentinous bone discussed here may well be in support of this view, given that the expression profile of the scleroblasts changes at the very point where the epithelium is not present anymore. On the other hand, dentinous bone is just one of the possible tissue types that make up the pedicel in teleosts. Clearly, the evolutionary history of the attachment tissue as an entity requires further studies. Given that *scpp5* has also been found in the gar, *L. oculatus*, a basal actinopterygian (Kawasaki et al., 2017), as well as in highly evolved teleosts, such as fugu (*Takifugu rubripes*; Kawasaki and Weiss, 2006; where it is also expressed in IDE and odontoblasts), the use of this gene opens interesting perspectives for tracing the evolutionary history of attachment tissues in actinopterygians. Finally, it can also serve in studies of miniaturized teeth, such as found in the teleost medaka (*Oryzias latipes*), where a scleroblast of elusive identity complements the single odontoblast present (Larionova et al., 2021).

DATA AVAILABLITY STATEMENT

The original contributions presented in the study are included in the article, further inquiries can be directed to the corresponding author.

ETHICS STATEMENT

Ethical review and approval was not required for the animal study because the experimental protocols involved euthanasia only (no animal experiments); in such a case no approval of the ethical committee is required. All animal procedures used in this study were approved by Flemish authorities (laboratory permit number LA1400452).

AUTHOR CONTRIBUTIONS

AH designed the research. JTR carried out the research. JTR, PEW, and AH analyzed the results and corrected and finalized the manuscript. JTR and AH drafted the manuscript. All authors contributed to the article and approved the submitted version.

FUNDING

JTR and AH acknowledge a grant of the Ghent University Research Fund (n° BOF24J2015001401).

ACKNOWLEDGMENTS

M. Soenens is acknowledged for expert technical assistance.

REFERENCES

An, S. (2018). The emerging role of extracellular Ca^{2+} in osteo/odontogenic differentiation and the involvement of intracellular Ca^{2+} signaling: from osteoblastic cells to dental pulp cells and odontoblasts. *J. Cell. Physiol.* 234, 2169–2193. doi: 10.1002/jcp.27068

Ando, K., Shibata, E., Hans, S., Brand, M., and Kawakami, A. (2017). Osteoblast production by reserved progenitor cells in zebrafish bone regeneration and maintenance. *Dev. Cell* 43, 643–650. doi: 10.1016/j.devcel.2017.10.015

Ariffin, S. H. Z., Manogaran, T., Abidin, I. Z. Z., Wahab, R. M. A., and Senafi, S. (2017). A perspective on stem cells as biological systems that produce differentiated osteoblasts and odontoblasts. *Curr. Stem Cell Res. Ther.* 12, 247–259. doi: 10.2174/1574888X11666161026145149

Bemis, W. E., Giuliano, A., and McGuire, B. (2005). Structure, attachment, replacement and growth of teeth in bluefish, *Pomatomus saltatrix* (Linnaeus, 1766), a teleost with deeply socketed teeth. *Zoology* 108, 317–327. doi: 10.1016/j.zool.2005.09.004

Beresford, W. A. (1981). *Chondroid Bone, Secondary Cartilage and Metaplasia*. Baltimore and Munich: Urban & Schwarzenberg.

Berkovitz, B., and Shellis, P. (2016). *The Teeth of Non-Mammalian Vertebrates*. Amsterdam and Boston: Academic Press.

Bertin, T. J. C., Thivichon-Prince, B., LeBlanc, A. R. H., Caldwell, M. W., and Viriot, L. (2018). Current perspectives on tooth implantation, attachment, and replacement in Amniota. *Front. Physiol.* 9:1630. doi: 10.3389/fphys.2018.01630

Borday-Birraux, V., Van der heyden, C., Debiais-Thibaud, M., Verreijdt, L., Stock, D. W., Huysseune, A., et al. (2006). Expression of dlx genes in zebrafish tooth development: evolutionary implications. *Evol. Dev.* 8, 130–141. doi: 10.1111/j.1525-142X.2006.00084.x

Bosshardt, D. D. (2005). Are cementoblasts a subpopulation of osteoblasts or a unique phenotype? *J. Dent. Res.* 84, 390–406. doi: 10.1177/154405910508400501

Butler, P. M. (1995). Ontogenetic aspects of dental evolution. *Int. J. Dev. Biol.* 39, 25–34

Clemen, G., Wanninger, A.-C., and Greven, H. (1997). The development of the dentigerous bones and teeth in the hemiramphid fish *Dermogenys pusillus* (Atheriniformes, Teleostei). *Ann. Anat.* 179, 165–174. doi: 10.1016/S0940-9602(97)80099-4

de Vrieze, E., Zethof, J., Schulte-Merker, S., Flik, G., and Metz, J. R. (2015). Identification of novel osteogenic compounds by an ex-vivo sp7:luciferase zebrafish scale assay. *Bone* 74, 106–113. doi: 10.1016/j.bone.2015.01.006

DeLaurier, A., Eames, B. F., Blanco-Sanchez, B. F., Peng, G., He, X., Swartz, M. E., et al. (2010). Zebrafish sp7:EGFP: a transgenic for studying otic vesicle formation, skeletogenesis, and bone regeneration. *genesis* 48, 505–511. doi: 10.1002/dvg.20639

Donoghue, P. C. J., and Sansom, I. J. (2002). Origin and early evolution of vertebrate skeletonization. *Microsc. Res. Tech.* 59, 352–372. doi: 10.1002/jemt.10217

Fink, W. L. (1981). Ontogeny and phylogeny of tooth attachment modes in actinopterygian fishes. *J. Morphol.* 167, 167–184. doi: 10.1002/jmor.1051670203

Fleischmannova, J., Matalova, E., Sharpe, P. T., Misek, I., and Radlanski, R. J. (2010). Formation of the tooth-bone interface. *J. Dent. Res.* 89, 108–115. doi: 10.1177/0022034509355440

Flores, M. V., Lam, E. Y. N., Crosier, P., and Crosier, K. (2006). A hierarchy of Runx transcription factors modulate the onset of chondrogenesis in craniofacial endochondral bones in zebrafish. *Dev. Dyn.* 235, 3166–3176. doi: 10.1002/dvdy.20957

Franz-Odendaal, T. A., Hall, B. K., and Witten, P. E. (2006). Buried alive: how osteoblasts become osteocytes. *Dev. Dyn.* 235, 176–190. doi: 10.1002/dvdy.20603

Gaengler, P. (2000). "Chapter 12. Evolution of tooth attachment in lower vertebrates to tetrapods," in *Development, Function and Evolution of Teeth*. eds. M. F. Teaford, M. M. Smith and M. W. J. Ferguson (Cambridge: Cambridge University Press), 173–185.

Gibert, Y., Samarut, E., Ellis, M. K., Jackman, W. R., and Laudet, V. (2019). The first formed tooth serves as a signalling centre to induce the formation of the dental row in zebrafish. *Proc. R. Soc. B* 286:20190401. doi: 10.1098/rspb.2019.0401

Hall, B. K., and Witten, P. E. (2007). "Plasticity of and transitions between skeletal tissues in vertebrate evolution and development," in *Major Transitions in Vertebrate Evolution*. eds. J. S. Anderson and H. D. Sues (Bloomington, IN: Indiana University Press), 13–56.

Hall, B. K., and Witten, P. E. (2019). "Plasticity and variation of skeletal cells and tissues and the evolutionary development of actinopterygian fishes," in *Evolution and Development of Fishes*. eds. Z. Johanson, C. Underwood and M. Richter (Cambridge: Cambridge University Press), 126–143.

Hammond, C. L., and Schulte-Merker, S. (2009). Two populations of endochondral osteoblasts with differential sensitivity to hedgehog signalling. *Development* 136, 3991–4000. doi: 10.1242/dev.042150

Hughes, D. R., Bassett, J. R., and Moffat, L. A. (1994). Structure and origin of the tooth pedicel (the so-called bone of attachment) and dental-ridge bone in the mandibles of the sea breams *Acanthopagrus australis*, *Pagrus auratus* and *Rhabdosargus sarba* (Sparidae, Perciformes, Teleostei). *Anat. Embryol.* 189, 51–69. doi: 10.1007/BF00193129

Huysseune, A. (1983). Observations on tooth development and implantation in the upper pharyngeal jaws in *Astatotilapia elegans* (Trewavas, 1933; Teleostei: Cichlidae). *J. Morphol.* 175, 217–234. doi: 10.1002/jmor.1051750302

Huysseune, A. (2000). "Skeletal system," in *The Laboratory Fish*. ed. G. Ostrander (London: Academic Press), 307–317.

Huysseune, A., and Sire, J.-Y. (1992). Development of cartilage and bone tissues of the anterior part of the mandible in cichlid fish: a light and TEM study. *Anat. Rec.* 233, 357–375. doi: 10.1002/ar.1092330304

Huysseune, A., Takle, H., Soenens, M., Taerwe, K., and Witten, P. E. (2008). Unique and shared gene expression patterns in Atlantic salmon (*Salmo salar*) tooth development. *Dev. Genes Evol.* 218, 427–437. doi: 10.1007/s00427-008-0237-9

Huysseune, A., Van der heyden, C., and Sire, J.-Y. (1998). Early development of the zebrafish (*Danio rerio*) pharyngeal dentition (Teleostei, Cyprinidae). *Anat. Embryol.* 198, 289–305. doi: 10.1007/s004290050185

Huysseune, A., and Witten, P. E. (2008). An evolutionary view on tooth development and replacement in wild Atlantic salmon (*Salmo salar* L.). *Evol. Dev.* 10, 6–14. doi: 10.1111/j.1525-142X.2007.00209.x

Johnson, S. L., and Weston, J. A. (1995). Temperature-sensitive mutations that cause stage-specific defects in zebrafish fin regeneration. *Genetics* 141, 1583–1595. doi: 10.1093/genetics/141.4.1583

Kague, E., Gallagher, M., Burke, S., Parsons, M., Franz-Odendaal, T., and Fisher, S. (2012). Skeletogenic fate of zebrafish cranial and trunk neural crest. *PLoS One* 7:e47394. doi: 10.1371/journal.pone.0047394

Kague, E., Witten, P. E., Soenens, M., Campos, C. L., Lubiana, T., Fisher, S., et al. (2018). Zebrafish sp7 mutants show tooth cycling independent of attachment, eruption and poor differentiation of teeth. *Dev. Biol.* 435, 176–184. doi: 10.1016/j.ydbio.2018.01.021

Karagic, N., Schneider, R. F., Meyer, A., and Hulsey, C. D. (2020). A genomic cluster containing novel and conserved genes is associated with cichlid fish dental developmental convergence. *Mol. Biol. Evol.* 37, 3165–3174. doi: 10.1093/molbev/msaa153

Kawasaki, K. (2009). The SCPP gene repertoire in bony vertebrates and graded differences in mineralized tissues. *Dev. Genes Evol.* 219, 147–157. doi: 10.1007/s00427-009-0276-x

Kawasaki, K. (2011). The SCPP gene family and the complexity of hard tissues in vertebrates. *Cells Tissues Organs* 194, 108–112. doi: 10.1159/000324225

Kawasaki, K., Buchanan, A. V., and Weiss, K. M. (2009). Biomineralization in humans: making the hard choices in life. *Annu. Rev. Genet.* 43, 119–142. doi: 10.1146/annurev-genet-102108-134242

Kawasaki, K., Keating, J. N., Nakatomi, M., Welten, M., Mikami, M., Sasagawa, I., et al. (2021). Coevolution of enamel, ganoin, enameloid, and their matrix SCPP genes in osteichthyans. *iScience* 24:102023. doi: 10.1016/j.isci.2020.102023

Kawasaki, K., Mikami, M., Nakatomi, M., Braasch, I., Batzel, P., Postlethwait, J. H., et al. (2017). SCPP genes and their relatives in gar: rapid expansion of mineralization genes in osteichthyans. *J. Exp. Zool. B Mol. Dev. Evol.* 328, 645–665. doi: 10.1002/jez.b.22755

Kawasaki, K., and Weiss, K. M. (2006). Evolutionary genetics of vertebrate tissue mineralization: the origin and evolution of the secretory calcium-binding phosphoprotein family. *J. Exp. Zool. B Mol. Dev. Evol.* 306, 295–316. doi: 10.1002/jez.b.21088

Kawasaki, K., and Weiss, K. M. (2008). SCPP gene evolution and the dental mineralization continuum. *J. Dent. Res.* 87, 520–531. doi: 10.1177/154405910808700608

Keating, J. N., Marquart, C. L., Marone, F., and Donoghue, P. C. J. (2018). The nature of aspidin and the evolutionary origin of bone. *Nat. Ecol. Evol.* 2, 1501–1506. doi: 10.1038/s41559-018-0624-1

Kerebel, L.-M., Le Cabellec, M.-T., and Geistdoerfer, P. (1979). The attachment of teeth in *Lophius*. *Can. J. Zool.* 57, 711–718. doi: 10.1139/z79-089

Kerr, T. (1960). Development and structure of some actinopterygian and urodele teeth. *Proc. Zool. Soc. London* 133, 401–422. doi: 10.1111/j.1469-7998.1960.tb05570.x

Kimmel, C. B., Ballard, W. W., Kimmel, S. R., Ullmann, B., and Schilling, T. F. (1995). Stages of embryonic development of the zebrafish. *Dev. Dyn.* 203, 253–310. doi: 10.1002/aja.1002030302

Knopf, F., Hammond, C., Chekuru, A., Kurth, T., Hans, S., Weber, C., et al. (2011). Bone regenerates via dedifferentiation of osteoblasts in the zebrafish fin. *Dev. Cell* 20, 713–724. doi: 10.1016/j.devcel.2011.04.014

Komori, T. (2019). Regulation of proliferation, differentiation and functions of osteoblasts by Runx2. *Int. J. Mol. Sci.* 20:1694. doi: 10.3390/ijms20071694

Larionova, D., Lesot, H., and Huysseune, A. (2021). Miniaturization: how many cells are needed to build a tooth? *Dev. Dyn.* 250, 1021–1035. doi: 10.1002/dvdy.300

Li, N., Felber, K., Elks, P., Croucher, P., and Roeh, H. H. (2009). Tracking gene expression during zebrafish osteoblast differentiation. *Dev. Dyn.* 238, 459–466. doi: 10.1002/dvdy.21838

Lin, W. Z., Gao, L., Jiang, W. X., Niu, C. G., Yuan, K. Y., Hu, X. C., et al. (2019). The role of osteomodulin on osteo/odontogenic differentiation in human dental pulp stem cells. *BMC Oral Health* 19:22. doi: 10.1186/s12903-018-0680-6

Moss, M. L. (1961). Studies of the acellular bone of teleost fish. I. Morphological and systematic variations. *Acta Anat.* 46, 343–362.

Moy-Thomas, J. A. (1934). On the teeth of the larval *Belone vulgaris*, and the attachment of teeth in fishes. *Quart. J. Micr. Sci.* 76, 481–498.

Ørvig, T. (1951). Histologic studies of placoderms and fossil elasmobranchs. 1. The endoskeleton, with remarks on the hard tissues of lower vertebrates in general. *Ark. Zool.* 2, 321–454.

Ørvig, T. (1967). "Phylogeny of tooth tissues: evolution of some calcified tissues in early vertebrates," in *Structural and Chemical Organization of Teeth*. ed. A. E. W. Miles, Vol 1 (London: Academic Press), 45–110.

Osborn, J. W. (1984). From reptile to mammal: evolutionary considerations of the dentition with emphasis on tooth attachment. *Symp. Zool. Soc. Lond.* 52, 549–574.

Peyer, B. (1968). *Comparative Odontology*. Chicago and London: The University of Chicago Press.

Renn, J., and Winkler, C. (2009). *Osterix*-mcherry transgenic medaka for in vivo imaging of bone formation. *Dev. Dyn.* 238, 241–248. doi: 10.1002/dvdy.21836

Roach, H. I., Erenpreisa, J., and Aigner, T. (1995). Osteogenic differentiation of hypertrophic chondrocytes involves asymmetric cell division and apoptosis. *J. Cell Biol.* 131, 483–493. doi: 10.1083/jcb.131.2.483

Romeis, B. (1989). Mikroskopische Technik, 17. Auflage. München – Wien – Baltimore: Urban und Schwarzenberg.

Rosa, J., Tiago, D. M., Marques, C. L., Vijayakumar, P., Fonseca, L., Cancela, M. L., et al. (2016). Central role of betaine-homocysteine S-methyltransferase 3 in chondral ossification and evidence for sub-functionalization in neoteleost fish. *Biochim. Biophys. Acta* 1860, 1373–1387. doi: 10.1016/j.bbagen.2016.03.034

Shellis, R. P. (1982). "Chapter 1. Comparative anatomy of tooth attachment," in *The Periodontal Ligament in Health and Disease*. eds. B. K. B. Berkovitz, B. J. Moxham and H. N. Newman (Oxford, New York: Pergamon Press), 3–24.

Shiflett, L. A., Tiede-Lewis, L. M., Xie, Y., Lu, Y., Ray, E. C., and Dallas, S. L. (2019). Collagen dynamics during the process of osteocyte embedding and mineralization. *Front. Cell Dev. Biol.* 7:178. doi: 10.3389/fcell.2019.00178

Sire, J.-Y., Davit-Beal, T., Delgado, S., Van der heyden, C., and Huysseune, A. (2002). First-generation teeth in nonmammalian lineages: evidence for a conserved ancestral character? *Microsc. Res. Tech.* 59, 408–434. doi: 10.1002/jemt.10220

Sire, J.-Y., and Huysseune, A. (2003). Formation of dermal skeletal and dental tissues in fish: a comparative and evolutionary approach. *Biol. Rev.* 78, 219–249. doi: 10.1017/S1464793102006073

Sire, J.-Y., and Kawasaki, K. (2012). "Origin and evolution of bone and dentin and of acidic secretory calcium-binding phosphoproteins," in *Phosphorylated Extracellular Matrix Proteins of Bone and Dentin*. ed. M. Goldberg, Vol. 2 (Sharjah, U.A.E.: Bentham Science Publishers, Bentham eBook), 3–60.

Sire, J.-Y., and Meunier, F. J. (1994). The canaliculi of Williamson in holostean bone (Osteichthyes, Actinopterygii): a structural and ultrastructural study. *Acta Zool.* 75, 235–247. doi: 10.1111/j.1463-6395.1994.tb01211.x

Smith, M. M., and Hall, B. K. (1993). "A developmental model for evolution of the vertebrate exoskeleton and teeth. The role of cranial and trunk neural crest," in *Evolutionary Biology*. eds. M. K. Hecht, R. J. MacIntyre and M. T. Clegg, Vol. 27 (New York: Plenum Press), 387–448.

Soule, J. D. (1969). Tooth attachment by means of a periodontium in the triggerfish (Balistidae). *J. Morphol.* 127, 1–6. doi: 10.1002/jmor.1051270102

Tomes, C. S. (1875). Studies upon the attachment of teeth. *Trans. Odontol. Soc.* Great Britain 7, 41–58.

Tomes, C. S. (1882). *A Manual of Dental Anatomy: Human and Comparative*. Philadelphia: Presley Blakiston.

Trapani, J. (2001). Position of developing replacement teeth in teleosts. *Copeia* 2001, 35–51. doi: 10.1643/0045-8511(2001)001[0035:PODRTI]2.0.CO;2

Van der heyden, C., and Huysseune, A. (2000). Dynamics of tooth formation and replacement in the zebrafish (*Danio rerio*) (Teleostei, Cyprinidae). *Dev. Dyn.* 219, 486–496. doi: 10.1002/1097-0177(2000)9999:9999<::AID-DVDY1069>3.0.CO;2-Z

Van der heyden, C., Huysseune, A., and Sire, J.-Y. (2000). Development and fine structure of pharyngeal replacement teeth in juvenile zebrafish (*Danio rerio*) (Teleostei, Cyprinidae). *Cell Tissue Res.* 302, 205–219. doi: 10.1007/s004410000180

Verstraeten, B., Sanders, E., and Huysseune, A. (2012). Whole mount immunohistochemistry and in situ hybridization of larval and adult zebrafish dental tissues. *Methods Mol. Biol.* 887, 179–191. doi: 10.1007/978-1-61779-860-3_16

Westerfield, M. (2000). *The Zebrafish Book: A Guide for the Laboratory Use of Zebrafish Danio (Brachydanio rerio)*. Oregon: University of Oregon Press.

Yamamoto, T., Hasegawa, T., Yamamoto, T., Hongo, H., and Amizuka, N. (2016). Histology of human cementum: its structure, function, and development. *Jpn. Dent. Sci. Rev.* 52, 63–74. doi: 10.1016/j.jdsr.2016.04.002

Yang, L., Tsang, K. Y., Tang, H. C., Chan, D., and Cheah, K. S. E. (2014). Hypertrophic chondrocytes can become osteoblasts and osteocytes in endochondral bone formation. *Proc. Natl. Acad. Sci. U. S. A.* 111, 12097–12102. doi: 10.1073/pnas.1302703111

Conflict of Interest: The authors declare that the research was conducted in the absence of any commercial or financial relationships that could be construed as a potential conflict of interest.

frontiers in Physiology

ORIGINAL RESEARCH
published: 22 November 2021
doi: 10.3389/fphys.2021.767136

Mechanosensitive Piezo1 in Periodontal Ligament Cells Promotes Alveolar Bone Remodeling During Orthodontic Tooth Movement

Yukun Jiang[1], Yuzhe Guan[1], Yuanchen Lan[1], Shuo Chen[1], Tiancheng Li[1], Shujuan Zou[1], Zhiai Hu[1] and Qingsong Ye[2,3]*

[1] State Key Laboratory of Oral Diseases, National Clinical Research Center for Oral Diseases, West China Hospital of Stomatology, Sichuan University, Chengdu, China, [2] Center of Regenerative Medicine, Renmin Hospital of Wuhan University, Wuhan, China, [3] Center of Regenerative Medicine, Massachusetts General Hospital, Harvard Medical School, Boston, MA, United States

OPEN ACCESS

Edited by:
Guohua Yuan,
Wuhan University, China

Reviewed by:
Liu Man,
Shenzhen Polytechnic, China
Xunwei Wu,
Shandong University, China

***Correspondence:**
Zhiai Hu
huzhiai121027@gmail.com

Specialty section:
This article was submitted to Craniofacial Biology and Dental Research, a section of the journal Frontiers in Physiology

Received: *30 August 2021*
Accepted: *29 September 2021*
Published: *22 November 2021*

Citation:
Jiang Y, Guan Y, Lan Y, Chen S, Li T, Zou S, Hu Z and Ye Q (2021) Mechanosensitive Piezo1 in Periodontal Ligament Cells Promotes Alveolar Bone Remodeling During Orthodontic Tooth Movement. Front. Physiol. 12:767136. doi: 10.3389/fphys.2021.767136

Orthodontic tooth movement (OTM) is a process depending on the remodeling of periodontal tissues surrounding the roots. Orthodontic forces trigger the conversion of mechanical stimuli into intercellular chemical signals within periodontal ligament (PDL) cells, activating alveolar bone remodeling, and thereby, initiating OTM. Recently, the mechanosensitive ion channel Piezo1 has been found to play pivotal roles in the different types of human cells by transforming external physical stimuli into intercellular chemical signals. However, the function of Piezo1 during the mechanotransduction process of PDL cells has rarely been reported. Herein, we established a rat OTM model to study the potential role of Piezo1 during the mechanotransduction process of PDL cells and investigate its effects on the tension side of alveolar bone remodeling. A total of 60 male Sprague-Dawley rats were randomly assigned into three groups: the OTM + inhibitor (INH) group, the OTM group, and the control (CON) group. Nickel-titanium orthodontic springs were applied to trigger tooth movement. Mice were sacrificed on days 0, 3, 7, and 14 after orthodontic movement for the radiographic, histological, immunohistochemical, and molecular biological analyses. Our results revealed that the Piezo1 channel was activated by orthodontic force and mainly expressed in the PDL cells during the whole tooth movement period. The activation of the Piezo1 channel was essential for maintaining the rate of orthodontic tooth movement and facilitation of new alveolar bone formation on the tension side. Reduced osteogenesis-associated transcription factors such as Runt-related transcription factor 2 (RUNX2), Osterix (OSX), and receptor activator of nuclear factor-kappa B ligand (RANKL)/osteoprotegerin (OPG) ratio were examined when the function of Piezo1 was inhibited. In summary, Piezo1 plays a critical role in mediating both the osteogenesis and osteoclastic activities on the tension side during OTM.

Keywords: Piezo1, bone remodeling, orthodontic tooth movement, alveolar bone, mechanotransduction

INTRODUCTION

Induced by mechanical loading, orthodontic tooth movement (OTM) is a process depending on the remodeling of periodontal tissues (mainly alveolar bone, periodontal ligament, and cementum) surrounding the roots (Kumar et al., 2015). During tooth movement, alveolar bone remodeling is triggered by biologic responses of periodontal ligament (PDL), with bone formation taking place on the tension side and resorption occurring on the compression side (Vansant et al., 2018). The association between the mechanical stimuli and periodontal ligament has been demonstrated by lots of previous studies from the viewpoints of both cellular biology and signaling molecules.

Periodontal ligament cells play crucial roles in maintaining periodontal homeostasis and regulating periodontal tissue remodeling. PDL cells have multiple functions locally including forming and maintaining periodontal ligaments, mediating alveolar bone and cementum repair, and periodontal tissue regeneration (Liu et al., 2018; Maeda, 2020). According to recent studies, PDL cells can sense mechanical stress, transform mechanical stimuli into biochemical signals, and eventually regulate alveolar bone remodeling by secreting multiple factors (Yang et al., 2018). For example, tissue plasminogen activator (tPA) and plasminogen activator inhibitor-1 (PAI-1), matrix metalloproteinases (MMPs) and their inhibitors, and cytokines including prostaglandin 2 (PGE2) and interleukin-6 (IL-6) are secreted under mechanical stimuli to regulate periodontal tissues remodeling (Römer et al., 2013; Schara et al., 2013; Wu et al., 2015), whereas receptor activator of nuclear factor-kappa B ligand (RANKL), RANK, and osteoprotegerin (OPG) system are reported to be involved in the regulation of osteoclast differentiation by PDL cells (Grant et al., 2013; Feng et al., 2018). However, during OTM, the specific mechanism by which PDL cells perceive the mechanical stimulus, transfer it into biological signals, and ultimately contribute to alveolar bone remodeling remains unclear.

Recently, the ion channels on the surface of PDL cells involved in mechanotransduction pathways have been proposed as a promising new research direction to this problem (Sachs, 2015; Jin S.S. et al., 2020). The Piezo family of non-selective cationic channels was first identified as pore-forming subunits of excitatory mechanosensitive ion channels permeable to Na^+, K^+, and Ca^{2+} in 2010 (Coste et al., 2010). The mammalian Piezo channel is a three-bladed, propeller-shaped trimeric complex containing over 2,500 amino acids, which includes two subtypes, Piezo1 and Piezo2 (Wang and Xiao, 2018). Piezo1 is predominantly expressed in non-sensory tissues exposed to mechanical force, while Piezo2 is primarily expressed in sensory tissues (Wu et al., 2017). The Piezo1 channel has been implicated in bone remodeling by growing literature. Several *in vivo* studies have provided evidence that Piezo1 removed from mice osteoblastic cells caused bone loss and spontaneous fractures with increased bone resorption, suggesting the possible role of Piezo1 in regulating mechanical load-dependent bone formation and remodeling (Li et al., 2019; Wang et al., 2020b; Zhou et al., 2020). Piezo1 is also expressed in mesenchymal stem cells (MSCs) as a factor for cell fate determination of MSCs under hydrostatic pressure, which also implies the relevance of Piezo1 and bone formation (Sugimoto et al., 2017).

Piezo1 also exists on the membrane of primary PDL cells (Jin et al., 2015). *In vitro* studies have confirmed that the Piezo1 ion channel can transmit mechanical signals and regulate both the osteogenic differentiation and osteoclastogenesis of PDL cells *via* various signaling including extracellular regulated protein kinases (ERK), nuclear factor-kappa B (NF-κB), and Notch1 signaling pathways (Jin et al., 2015; Shen et al., 2020; Wang et al., 2020a). These results suggest the possible mechanotransduction role of Piezo1 in the process of OTM. Till now, the functional relevance of Piezo1 and alveolar bone remodeling on the tension side remains unclear.

This study investigated the hypothesis that Piezo1 might function as a critical mechanotransducer that mediates mechanotransduction process of PDL cells, consequently determining alveolar bone remodeling. Firstly, the expression patterns of the Piezo1 channel during OTM were explored in a rat model on the tension side. Then, the mechanotransduction role of the Piezo1 channel in alveolar bone remodeling was verified via local periodontal inhibition of Piezo1 channel activity.

MATERIALS AND METHODS

Establishment of Animal Models

The Research Ethics Committee approved all the animal experiments of the State Key Laboratory of Oral Diseases in Chengdu, China (WCHSIRB-D-2017-181). A total of 72 male Sprague-Dawley rats aged 8 weeks (weighing 200 ± 10 g) were obtained from the Experimental Animal Center of the Sichuan University. Then, the animals were randomly divided into three groups of 24 animals each: the OTM + inhibitor (INH) group, the OTM group, and the control (CON) group. The rats in the OTM and OTM + INH groups received orthodontic appliances and the CON group did not receive the appliance. The OTM animal model was established as described previously (Li et al., 2013). A nickel-titanium coil spring (3M Unitek, Monrovia, CA, United States) was fixed between the maxillary left first molar and the incisors to generate a force of 40 g. The appliances were activated immediately upon insertion and the fit was checked daily. No reactivation was performed during the experimental period. The animals in the OTM + INH group received a subcutaneous injection of Piezo1 inhibitor Grammostola spatulata mechanotoxin 4 (GsMTx4) (Abcam, San Francisco, CA, United States) at a dosage of 20 μl with a concentration of 10 μM every other day, whereas the OTM and CON groups received only the vehicle. A total of six rats of each group were killed immediately on day 0 (the day before orthodontic force application) to serve as negative controls and on days 3, 7, and 14 after tooth movement. Alveolar bone blocks included the left first molar, which was harvested for further analysis.

Micro-CT Analysis

The samples were fixed in 4% paraformaldehyde solution for 24 h and scanned by using a high-resolution Micro-CT50 system (Scanco Medical, Wangen-Brüttisellen, Switzerland). Scanning of

the specimens was carried out at 70 kV and 114 mA with an integration time of 500 ms and a voxel resolution of 10 μm. The amount of OTM was measured by the spacing between the cementum–enamel junction (CEJ) levels of the first and second left molars. In this study, a 200 μm × 200 μm × 600 μm cube of trabecular bone distal to the middle part of the distal buccal root of the maxillary left first molar was selected as the region of interest for analysis. The distance between the cube and the root was 100 μm. Then, parameters including the bone volume/total volume (BV/TV) ratio, trabecular spacing (Tb.Sp), trabecular number (Tb.N), and trabecular thickness (Tb.Th) were calculated at days 3, 7, and 14 after the OTM.

Histological Staining

After micro-CT scanning, the left half of the maxilla of each animal was decalcified in 14% ethylenediaminetetraacetic acid (EDTA) (pH 7.4) for a month. Then, all the specimens were dehydrated in a series of alcohol baths and embedded in paraffin. Next, the samples, including the maxillary molars, were excised into 5 μm thick frontal sections in the sagittal direction. H&E staining (G1120; Solarbio, Beijing, China), tartrate-resistant acid phosphatase (TRAP) staining (Sigma-Aldrich, St. Louis, MO, United States), and Masson's trichrome staining (G1340; Solarbio, Beijing, China) were performed for the histological analyses. Multinucleated cells adjacent to the tension side of the periodontal area were counted as TRAP-positive osteoclasts. Two independent investigators counted the number of TRAP-positive cells. Masson's trichrome staining was used to identify the collagen fiber arrangement on the tension side.

Immunofluorescence Staining

Tissue sections were heated at 95°C for 30 min for antigen retrieval, washed with phosphate-buffered saline (PBS) for 5 min, and blocked in 10% goat serum for 30 min at 37°C. Then, the samples were incubated with rabbit anti-Piezo1 (Abcam, Cambridge, MA, United States, 1:200) overnight at 4°C. On the following day, slides were incubated with the Alexa Fluor 488 goat anti-rabbit (ZF-0511, 1:200, Zhongshan Bio-Tech, Beijing, China) for 1 h at 37°C and counterstained with 4',6-diamidino-2-phenylindole (DAPI) (Sigma, St. Louis, MO, United States) for 15 min. After washing with PBS, stained sections were observed by using fluorescent microscopy (DMI 6000; Leica, Wetzlar, Germany). Quantitative analyses of the images were done by the Image-Pro Plus 6.0 Software (Media Cybernetics, Bethesda, MD, United States).

Immunohistochemical Staining

Immunohistochemical staining was performed as described previously (Li et al., 2021). Sections were incubated with primary antibodies diluted in blocking solution with different optimized dilution rates: OPG (dilution 1:100; R1608-4), Runt-related transcription factor 2 (RUNX2) (dilution 1:100; ET1612-47), Osterix (OSX) (dilution 1:400; ER1914-47), collagen type 1 (COL1) (dilution 1:100; ET1609-68), and alkaline phosphatase (ALP) (dilution 1:100; ET1601-21) from Huabio (Hangzhou, China); RANKL (dilution 1:200, ab169966) from Abcam (Shanghai, China). After rinsing, the slides were incubated with goat anti-rabbit immunoglobulin G (IgG) secondary antibody horseradish peroxidase (HRP) conjugated (SP-9001, Zhongshan Bio-Tech, Beijing, China) for 30 min at 37°C. The immune reaction was visualized by using a 3,3′-diaminobenzidine (DAB) Kit (ZLI-9017, Zhongshan Bio-Tech, Beijing, China) according to the instructions of the manufacturers. Slides were counterstained with H&E and viewed by using a light microscope (Nikon Eclipse 80i microscope, Tokyo, Japan). The means of integrated optical density (IOD) of IHC staining was analyzed by the Image-Pro Plus 6.0 Software (Media Cybernetics, Bethesda, MD, United States).

Western Blotting

Total proteins from all three groups were extracted from fresh tissue on day 3 and day 7 by using the Minute^{TM} Total Protein Extraction Kit for Bone Tissue (Invent Biotechnologies Incorporation, Eden Prairie, MN, United States) according to the instructions of the manufacturer. 50 μg of proteins from each sample were loaded on sodium dodecyl sulfate (SDS)–polyacrylamide gel electrophoresis (PAGE) and electrotransferred to polyvinylidene difluoride (PVDF) membranes (Invitrogen, Carlsbad, CA, United States). The membranes were blocked with 5% bovine serum albumin (BSA) and incubated with primary antibodies overnight. The following antibodies were used in this study to examine the protein levels: RANKL (dilution 1:1000, ab239607) from the Abcam (Shanghai, China); OPG (dilution 1:1000; R1608-4), RUNX2 (dilution 1:1000; ET1612-47), OSX (dilution 1:1000; ER1914-47), COL1 (dilution 1:1000; ET1609-68), and ALP (dilution 1:1000; ET1601-21) from the Huabio (Hangzhou, China). On the next day, blots were incubated with horseradish peroxidase conjugated with anti-rabbit IgG secondary antibodies (dilution 1:500; Thermo Pierce, Rockford, IL, United States) and detected by using an enhanced chemiluminescence substrate kit (Applygen, Beijing, China). The intensity of each band was quantified by using the Image-Pro Plus 6.0 Software (Media Cybernetics, Bethesda, MD, United States) and normalized to glyceraldehyde-3-phosphate dehydrogenase (GAPDH) values.

Statistical Analysis

The GraphPad Prism Software version 7 (GraphPad, San Diego, CA, United States) was used for statistical analysis. Data were expressed as the mean ± SD from at least three independent experiments. The statistical difference among the three groups was analyzed by the one-way ANOVA analysis followed by the Student-Newman-Keuls (SNK) methods of analysis of variance. $p < 0.05$ was considered statistically significant.

RESULTS

Piezo1 Channel Was Activated by Orthodontic Force on the Tension Side During Orthodontic Tooth Movement

To test our hypothesis that the Piezo1 channel is a crucial mechanosensor required for alveolar bone remodeling, the expression patterns of Piezo1 within the periodontal area on the tension side were first examined by IF staining. Our results

showed that Piezo1 was mainly expressed in the PDL, while it is rarely found in the alveolar bone. Specifically, the Piezo1 expressed faintly in the PDL of the CON group, while activated by orthodontic force application in the OTM group during the entire experimental period (**Figure 1**). Semi-quantitative analysis revealed that the expression of Piezo1 in the OTM group started to increase on day 3, reached its peak after 7 days of tooth movement, and only declined on day 14 compared to the CON group. When Piezo1 channel inhibitor GsMTx4 was applied, no significant change of the expression of Piezo1 was found in the OTM + INH group. These findings indicated that the expression of Piezo1 was activated by orthodontic force in the PDL during OTM.

Inhibition of Piezo1 Channel Hinders Orthodontic Tooth Movement and Decreases Bone Mass

To confirm the effect of the Piezo1 channel on OTM, the Piezo1 inhibitor GsMTx4 was adopted in this study to inactivate the Piezo1 channel. Under normal circumstances, the distance between the first and second molars was increased over time with a relatively rapid increment on the late-stage (day 7 to day 14). When the Piezo1 channel was inactivated by GsMTx4, the distance of tooth movement was significantly decreased from day 7 to day 14 (**Figures 2A,B**). These results suggested that the proper function of the Piezo1 channel was necessary for achieving the usual distance and rate of OTM.

Next, to evaluate the alveolar bone mass and microarchitectural changes of alveolar bone in the tension area of all the three groups, the parameters of BV/TV, Tb.N, Tb.Sp, and Tb.Th were examined through micro-CT analysis. As shown in **Figure 2C**, all the parameters showed stable expression levels in the CON group with no statistical difference throughout the experiment. When all the three groups were compared together, we found that BV/TV and Tb.Th in the tension area of the OTM group were significantly higher than that in the OTM + INH group and CON group on day 14 of OTM. No significant difference in values for Tb.N and trabecular spacing (Th.Sp) was found among the three groups. The above results showed that alveolar bone mass was decreased by inhibiting the Piezo1 channel during OTM.

Histological Changes of Periodontal Tissues During Orthodontic Tooth Movement

Histological changes of PDL cells were examined by using the H&E and Masson's trichrome staining. On day 0, periodontal fibers showed a meshwork arrangement and each PDL fiber showed a wavy configuration in the PDL in all three groups. After 3 days of orthodontic movement, periodontal ligament space gradually increased in the OTM and OTM + INH groups. In both the OTM and OTM + INH groups, the typical wavy arrangement of the periodontal fibers was lost and the periodontal fibers were stretched between the bone and the root. On day 7, periodontal ligament fibers appeared to be relaxed in the OTM group compared to day 3, while fully stretched in the OTM + INH group. On day 14, fiber arrangement in the OTM groups recovered to the wavy configuration before OTM, while slightly stretched in the OTM + INH group. At this time, periodontal ligament fibers on the tension side were arranged again in all three groups (**Figures 3A,B**).

Piezo1 Channel Is Critical for Enhanced Expression of Osteogenesis-Related Factors on the Tension Side During Orthodontic Tooth Movement

Immunohistochemical expression of osteogenesis-related factors was examined to evaluate the further correlation between Piezo1 and osteogenesis (**Figures 4A–D**). After applying orthodontic force, the expression of RUNX2, OSX, ALP, and COL1 in the

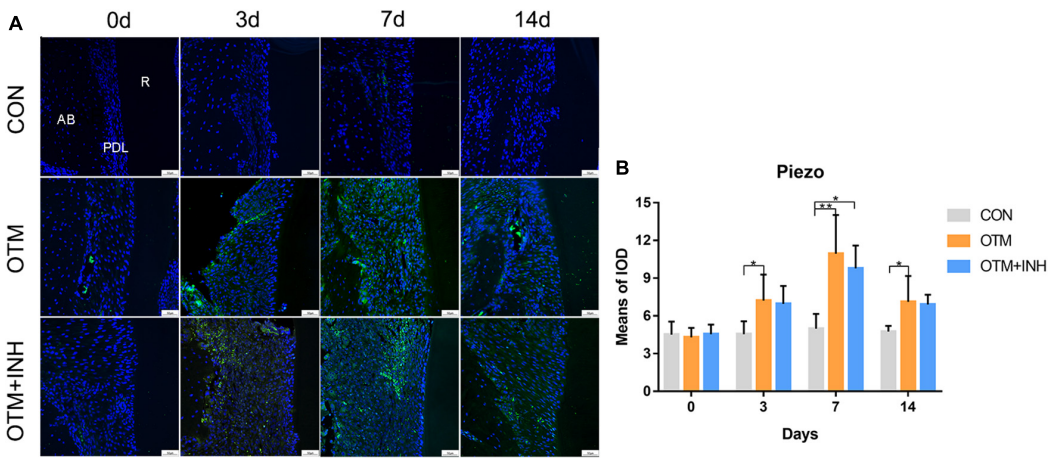

FIGURE 1 | The expression of Piezo1 was activated by orthodontic force on the tension side of distobuccal roots. **(A)** Immunofluorescence staining showed that Piezo1 was mainly expressed in the PDL of the OTM and OTM + INH groups after orthodontic force application. **(B)** The means of the fluorescent intensity of Piezo1. The expression of Piezo1 in the OTM group was significantly greater than that in the CON group from day 3 to day 14. Data are presented as the mean ± SD. $^{*}p < 0.05$. $^{**}p < 0.01$. Scale bar = 50 μm. INH, inhibitor; OTM: orthodontic tooth movement; AB, alveolar bone; PDL, periodontal ligament; R, root.

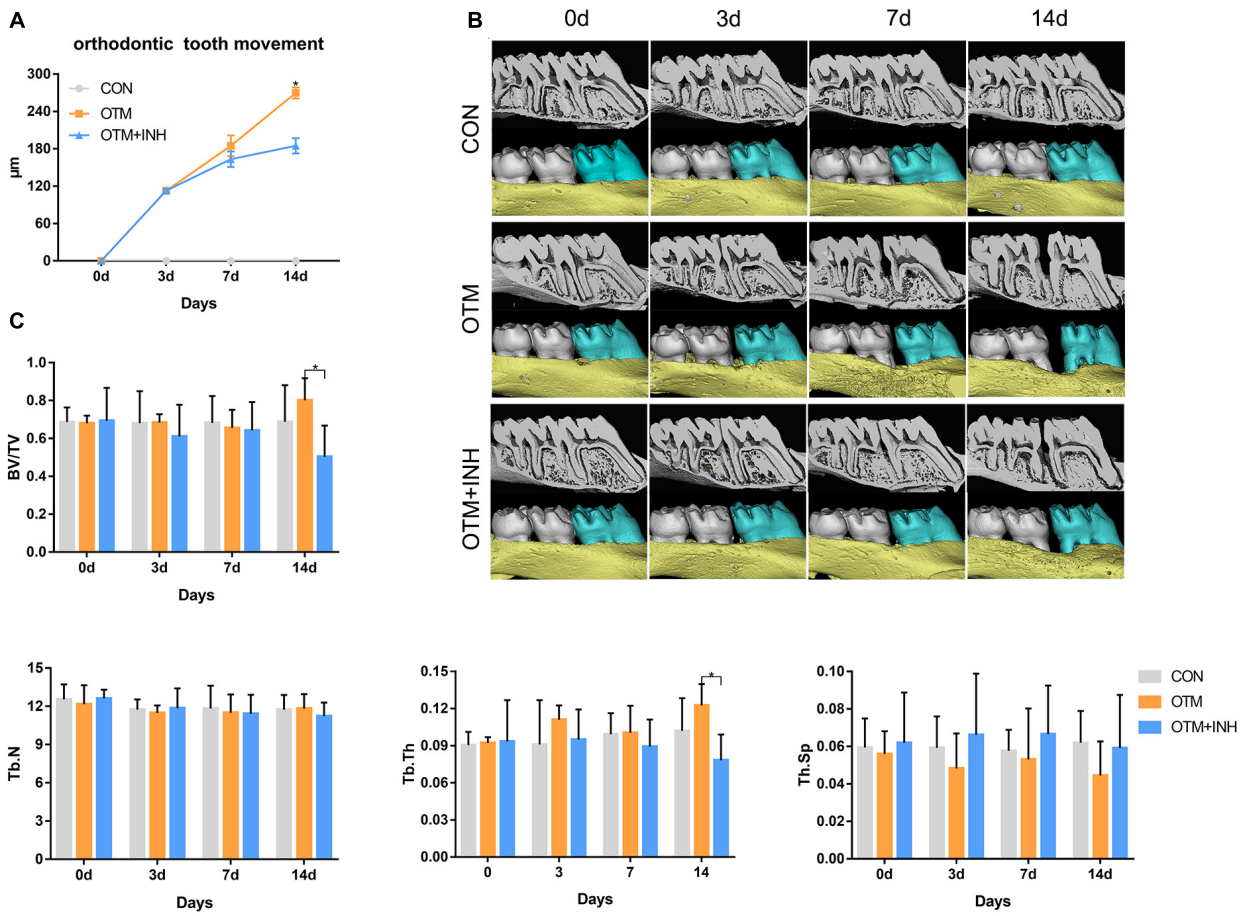

FIGURE 2 | Inhibition of Piezo1 hindered the distance of OTM and decreased bone mass. **(A)** Micro-CT and three-dimensional (3D) reconstruction images showed the distance of OTM. **(B)** The distance of OTM from day 0 to day 14. The distance was increased by orthodontic force overtime in the OTM group while declined by GsMTx4 in the OTM + INH group. *$p < 0.05$, the OTM vs. OTM + INH groups. **(C)** Parameters including bone volume/total volume (BV/TV), trabecular number (Tb.N), trabecular thickness (Tb.Th), and trabecular spacing (Tb.Sp) were examined from day 0 to day 14. BV/TV and Tb.Th of the OTM group were significantly greater than that of the OTM + INH and control (CON) groups on day 14 of OTM. *$p < 0.05$. Data are presented as the mean ± SD.

OTM group was all significantly increased on days 3, 7, and 14 compared with the CON group. All the factors reached peak expression in the OTM group on day 7 (with over 2-fold greater OD values for RUNX2 and OSX and 3-fold greater OD values for ALP and COL1) compared with those in the CON group. When Piezo1 was inhibited by GsMTx4, the expression of these osteogenesis-related factors was all decreased in the OTM + INH group. The expression of RUNX2 and ALP of the OTM + INH group was significantly lower than the OTM group on day 7. For OSX, its expression in the OTM + INH group was significantly lower than the OTM group on day 3 and day 7. For COL1, the OTM + INH group was significantly lower than the OTM group on day 7 and day 14 (**Figures 4E–H**). Consistent with IHC staining, Western Blot (WB) results showed that protein levels of osteogenesis factors on day 7 were all reduced by GsMTx4 in the OTM + INH group, which indicated that the Piezo1 channel was critical for the expression of osteogenesis-related factors on the tension side during OTM (**Figure 4I**).

Inhibition of Piezo1 Channel Suppressed Osteoclastic Activities on the Tension Side During Orthodontic Tooth Movement

The osteoclastic activities were also investigated on the tension side during OTM. TRAP staining was performed to observe the proportion of TRAP-positive cells among the three groups. On day 3, a remarkable increase in the number of osteoclasts was observed in the OTM group which is significantly higher than the OTM + INH and CON groups ($p < 0.05$). On days 7 and 14, only a few TRAP-positive cells were observed and no significant difference was found among the three groups (**Figures 5A,D**). Then, the expression of RANKL and OPG was evaluated. The immunoreactivity of RANKL was mainly observed in the osteoblasts and osteoclast-like cells on the surface of alveolar bone with strongly positive staining in the cytoplasm and weakly positive staining in the extracellular matrix of the periodontal ligament area. The expression level of RANKL in the

OTM group was significantly higher than the OTM + INH and CON groups on day 3 and declined after that. No significant change was found among all the three groups on days 7 and 14 (**Figures 5B,E**). The immunoreactivity of OPG was mainly observed in some osteoblasts with strongly positive staining in the cytoplasm and weakly positive staining in the extracellular matrix of the periodontal ligament. In this study, the expression of OPG in the OTM group was gradually increased from day 3, peaked on day 7, and decreased slightly after that. With respect to the CON group, the OPG expression in the OTM group was significantly higher on day 3. On day 7, the OPG expression in the OTM group was significantly higher than in the OTM + INH and CON groups (**Figures 5C,F**). The RANKL/OPG increased rapidly in the OTM group and was significantly greater than OTM + INH and CON groups on day 3 (**Figure 5G**). On days 7 and 14, no significant change was found in the ratio of RANKL/OPG among all three groups. On day 3, the WB results of RANKL/OPG were consistent with the IHC staining (**Figure 5H**).

DISCUSSION

Alveolar bone and PDL undertake a mechanical loading-induced remodeling process during OTM. However, it remains unclear how the alveolar bone and PDL sense mechanical force. Piezo1, a non-selective cationic channel, responds to various forms of mechanical stimulation including poking, stretching, shear stress, substrate deflection, and mediates Ca^{2+} influx upon opening to initiate downstream Ca^{2+} signaling (Sun et al., 2019). Recently, the engagement of Piezo1 in bone remodeling has been reported by an increasing number of studies (Li et al., 2019; Sun et al., 2019). To reveal the possible mechanotransduction role of Piezo1 in the process of OTM, this study focused on characterizing the expression and function of the mechanically activated Piezo1 channel of PDL cells on alveolar bone remodeling.

In this study, the localization of IF results showed that Piezo1 was mainly expressed on PDL cells and located in the plasma membrane and nucleus. The expression of Piezo1 in the OTM group was upgraded during the application of orthodontic force. Similar results recently reported that mechanical stress is associated with increased Piezo1 activation in PDL cells (Jin et al., 2015; Shen et al., 2020; Wang et al., 2020a). Therefore, we speculated that the Piezo1 channel is a crucial mechanosensor through which the PDL senses and translates the orthodontic force into a biological response, which further influences the alveolar bone remodeling.

To verify our assumption concerning the regulation effect of the Piezo1 channel, we administered the Piezo1 inhibitor GsMTx4 to orthodontically loaded rats as the OTM + INH group. No significant change in the expression of Piezo1 was found in the OTM + INH group when GsMTx4 was applied. This observation can be explained as follows. As a Piezo1-specific inhibitor, GsMTx4 acts by perturbing the interface between the Piezo1 channel and the lipid bilayer, which selectively blocks the gating of this cation-selective channel (Gnanasambandam et al., 2017; Suchyna, 2017). In other words, the GsMTx4 blocks

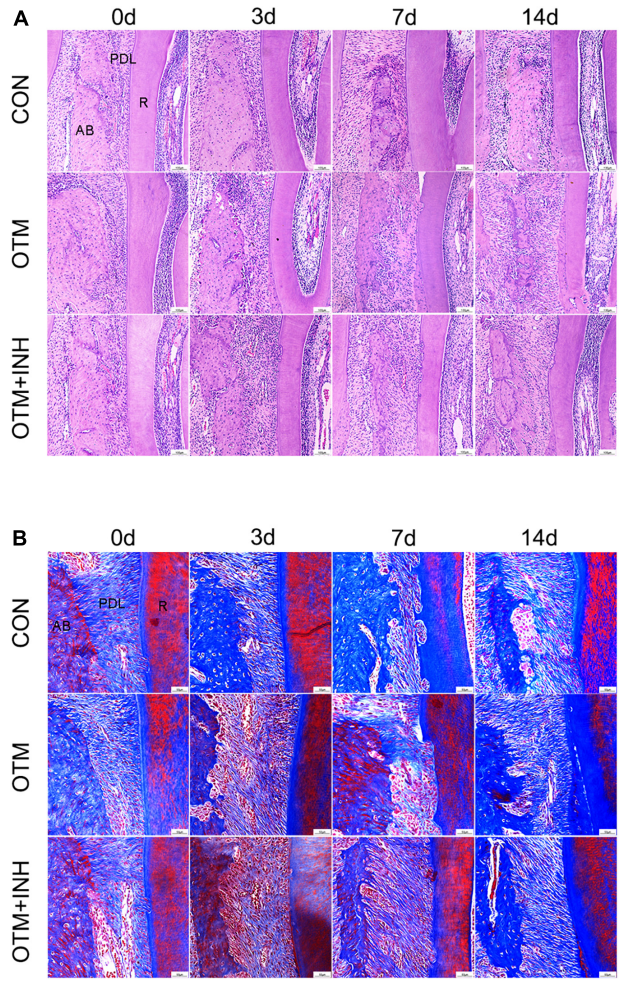

FIGURE 3 | Histological changes of PDL on the tension side of the distobuccal roots. HE staining **(A)** and Masson's trichrome staining **(B)** of PDL. Periodontal fibers were stretched by applying orthodontic force in the OTM group, while remodeling was delayed by the inhibitor of Piezo1 in the OTM + INH group. Scale bar for **(A)** = 100 μm. Scale bar for **(B)** = 50 μm. AB, alveolar bone; R, root.

the function of the Piezo1 channel without interfering with its expression and our result was consistent with its mechanism of action. In fact, GsMTx4 significantly reduced OTM in both the distance and rate and delayed the fiber remodeling. Micro-CT revealed that BV/TV and Tb.Th in the OTM + INH group tension area was significantly lower than in the OTM group, especially on day 14 of OTM. Taken together, this part of the experiment revealed that the inhibition of the Piezo1 channel by GsMTx4 local injection hinders OTM and new bone formation on the tension side.

Meanwhile, it is interesting to note that although the Piezo1 channel was greatly inhibited by GsMTx4, the OTM was not completely ceased in the OTM + INH group. Generally speaking, various mechanosensors, including ion channels, function synergistically during OTM (Guo et al., 2019; Du et al., 2020; Jin P. et al., 2020). We speculated that the

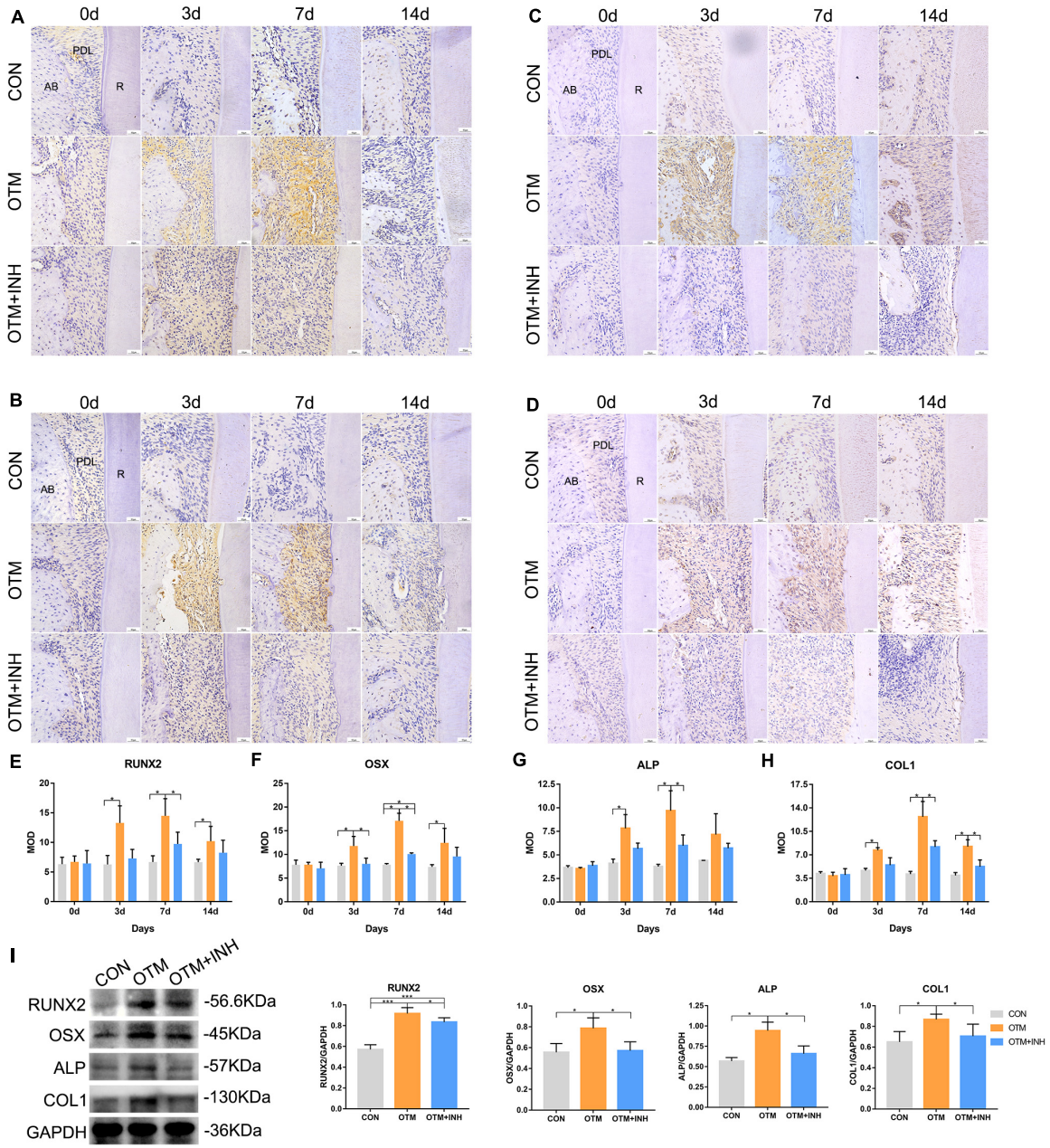

FIGURE 4 | Inhibition of Piezo1 channel suppressed expression of osteogenesis-related factors during OTM on the tension side. Immunohistochemical staining of RUNX2 **(A)**, OSX **(B)**, ALP **(C)**, and COL1 **(D)** of PDL on the tension side of the distobuccal roots and the means of the integrated optical density (IOD) of RUNX2 **(E)**, OSX **(F)**, ALP **(G)**, and COL1 **(H)**. The expression of RUNX2, OSX, ALP, and COL1 in the OTM group increased significantly on days 3, 7, and 14 compared with that of the CON group, while it was significantly reduced by GsMTx4 on day 3 and day 7 for OSX, day 7 for RUNX2 and ALP, and day 7 and day 14 for COL1. **(I)** Western blot analyses were carried out to detect the protein levels of RUNX2, OSX, ALP, and COL1 on day 7 of OTM. GsMTx4 significantly reduced the protein expression of RUNX2, OSX, ALP, and COL1 on day 7 in the OTM + INH group. Data are presented as the mean ± SD. $^{*}p < 0.05$, $^{***}p < 0.001$. Scale bar = 50 μm. RUNX2, Runt-related transcription factor 2; OSX, Osterix; ALP, alkaline phosphatase; COL1, collagen type 1; AB, alveolar bone; R, root.

biological communication between other mechanosensors and their corresponding downstream molecules might be responsible for the OTM in the OTM + INH group.

Since alveolar bone remodeling during OTM is a constant balanced coupling reaction by bone-resorbing osteoclasts and bone-forming osteoblasts working together, we further investigated the regulatory effects of Piezo1 on the downstream osteoblastic- and osteoclastic-related biomarkers. Zhou et al. (2020) reported mechanosensitive channels Piezo1 as critical force sensors required for bone development and osteoblast differentiation. In mesenchymal or osteoblast progenitor cells, loss of Piezo1 inhibited osteoblast differentiation and

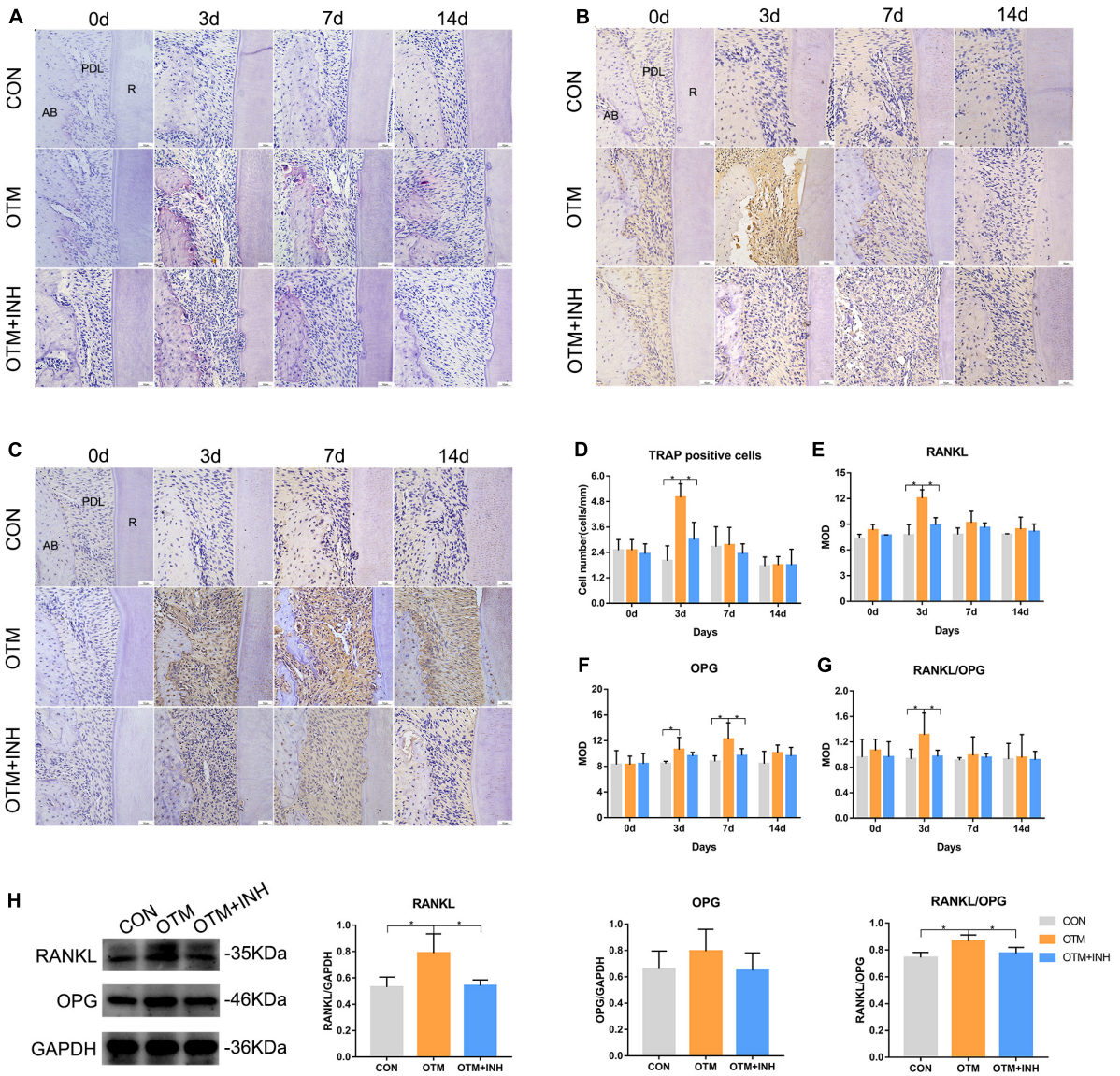

FIGURE 5 | Inhibition of Piezo1 suppressed osteoclastic activities on the tension side. TRAP staining **(A)** and quantification of TRAP-positive cells **(D)**. TRAP-positive osteoclasts were detected near the tension side of the roots. On day 3, the number of osteoclasts in the OTM group was significantly greater than that of the CON and the OTM + INH groups. Scale bar = 50 μm. Immunohistochemical staining of RANKL **(B)** and OPG **(C)** of PDL on the tension side of the distobuccal roots. The means of the integrated optical density (IOD) of RANKL **(E)**, OPG **(F)**, and RANKL/OPG ratio **(G)** were shown. On day 3, the RANKL/OPG ratio of the OTM group was significantly greater than that of the CON and OTM + INH groups. Western blot analyses **(H)** were carried out to detect the protein levels of RANKL and OPG on day 3 of OTM. The protein expression of the RANKL/OPG ratio increased significantly in the OTM group and was reduced by GsMTx4 in the OTM + INH group. Data are presented as the mean ± SD. *$p < 0.05$. Scale bar = 50 μm. TRAP, tartrate-resistant acid phosphatase; RANKL, receptor activator of nuclear factor-kappa B ligand; OPG, osteoprotegerin; AB, alveolar bone; R: root.

increased bone resorption, leading to multiple spontaneous bone fractures in newborn mice (Zhou et al., 2020). As described in the results, this study found that inhibition of the Piezo1 channel inhibited osteogenic activity (Li et al., 2019). ALP is commonly considered an early bone marker and COL1, a major component of the new bone matrix, is considered a midmarker (Saleh et al., 2018). Together with critical osteogenesis-associated transcription factors RUNX2 and OSX, they were adopted in this study to investigate the osteogenic activities on the tension side. IHC staining showed that RUNX2, OSX, ALP, and COL1 expression levels increased with time, which indicated active osteogenesis on the tension side of alveolar bone under mechanical force. When the Piezo1 channel was blocked by inhibitor GsMTx4, the expression of RUNX2, OSX, ALP, and COL1 were all significantly decreased. Western blot analysis was also adopted in this study to determine the protein levels of these osteogenesis-related factors on the tension side of alveolar bone.

As expected, western blot results showed a significant decrease in the protein expression level of RUNX2, OSX, ALP, and COL1 in the OTM + INH group compared with the OTM group. Previous studies showed that conditional deletion of Piezo1 in the osteoblasts and osteocytes notably reduced bone mass and strength in mice (Li et al., 2019; Zhou et al., 2020). Conversely, administration of a Piezo1 agonist to adult mice increased bone mass, mimicking the effects of mechanical loading. Our results were consistent with these previous studies. Taken together, these results suggested Piezo1 channel was essential for the regulation of the normal osteogenesis process of alveolar bone remodeling on the tension side.

The number of TRAP-positive cells and the ratio of RANKL/OPG were adopted in this study to reflect the osteoclastic activities during OTM. In this study, the number of TRAP-positive cells increased on day 3 in the OTM group and was significantly higher than the other two groups. The expression levels of RANKL and OPG were determined by both IHC staining and Western blot to reflect the role of the Piezo1 channel in the osteoclastic activities. Both methods showed consistent results that RANKL/OPG was more significant in the OTM group than the other two groups. It was demonstrated that Piezo1 might have a vital transduction role in osteoclastogenesis. Piezo1, in osteoblastic cells, in response to mechanical loads, controls the yes-associated protein (YAP)-dependent expression of type II and IX collagens, which regulate osteoclast differentiation (Wang et al., 2020b). Moreover, Jin et al. (2015) found that Piezo1 inhibitor GsMTx4 repressed osteoclastogenesis in the mechanical stress pretreated PDLCs-RAW264.7 coculture system *in vitro*. Our findings were consistent with these previous studies.

Taken together, our investigation demonstrated that the Piezo1 channel played a critical role in mediating both the osteogenesis and osteoclastic activities, and thus, promoting bone remodeling during OTM. By inducing the expression of critical osteogenesis-associated transcription factors such as RUNX2 and OSX, the Piezo1 channel facilitated new alveolar bone formation on the tension side. The activated expression level of the Piezo1 channel may be essential for maintaining the regular rate of OTM and may contribute to the stability of bone remodeling in the late phase of tooth movement. The specific molecular mechanisms behind the Piezo1 pathway on alveolar bone remodeling are worthy of being further elucidated.

CONCLUSION

In summary, this study first reveals the expression patterns of the Piezo1 channel on the tension side during OTM. The Piezo1 channel plays a vital role in bone remodeling on the tension side, promoting osteogenesis and osteoclastic activities. Via essential mechanotransduction approaches, the activation of the Piezo1 channel is essential for maintaining the OTM and alveolar bone homeostasis. The conclusion of this study may provide a theoretical basis for therapeutic applications of local regulation of the Piezo1 channel, which represents an intriguing target for inducing stable and controlled accelerated alveolar bone remodeling during tooth movement.

DATA AVAILABILITY STATEMENT

The raw data supporting the conclusions of this article will be made available by the authors, without undue reservation.

ETHICS STATEMENT

The animal study was reviewed and approved by the Research Ethics Committee of State Key Laboratory of Oral Diseases in Chengdu.

AUTHOR CONTRIBUTIONS

YJ, SZ, and ZH designed the experiments. YJ, YG, YL, and TL performed the *in vivo* experiments. YJ, YG, and SC collected and analyzed the *in vivo* experiments. YJ, TL, QY, and ZH analyzed and confirmed all the data and prepared the manuscript. SZ, QY, and ZH made final approval of the manuscript. All authors reviewed the manuscript.

FUNDING

This study was financially supported by the National Natural Science Foundation of China (No. 82071150 to SZ and No. 82001108 to ZH) and the China Postdoctoral Science Foundation (No. 2020M683331 to ZH).

ACKNOWLEDGMENTS

This study was technically supported by the State Key Laboratory of Oral Diseases and National Clinical Research Center for Oral Diseases and West China Hospital of Stomatology, Sichuan University.

REFERENCES

Coste, B., Mathur, J., Schmidt, M., Earley, T. J., Ranade, S., Petrus, M. J., et al. (2010). Piezo1 and Piezo2 are essential components of distinct mechanically activated cation channels. *Science* 330, 55–60. doi: 10.1126/science.1193270

Du, G., Li, L., Zhang, X., Liu, J., Hao, J., Zhu, J., et al. (2020). Roles of TRPV4 and piezo channels in stretch-evoked Ca(2+) response in chondrocytes. *Exp. Biol. Med. (Maywood)* 245, 180–189. doi: 10.1177/1535370219892601

Feng, Q., Zheng, S., and Zheng, J. (2018). The emerging role of microRNAs in bone remodeling and its therapeutic implications for osteoporosis. *Biosci. Rep.* 38:BSR20180453. doi: 10.1042/bsr20180453

Gnanasambandam, R., Ghatak, C., Yasmann, A., Nishizawa, K., Sachs, F., Ladokhin, A. S., et al. (2017). GsMTx4: mechanism of inhibiting mechanosensitive ion channels. *Biophys. J.* 112, 31–45. doi: 10.1016/j.bpj.2016.11.013

Grant, M., Wilson, J., Rock, P., and Chapple, I. (2013). Induction of cytokines, MMP9, TIMPs, RANKL and OPG during orthodontic tooth movement. *Eur. J. Orthod.* 35, 644–651. doi: 10.1093/ejo/cjs057

Guo, R., Zhou, Y., Long, H., Shan, D., Wen, J., Hu, H., et al. (2019). Transient receptor potential Vanilloid 1-based gene therapy alleviates orthodontic pain in rats. *Int. J. Oral. Sci.* 11:11. doi: 10.1038/s41368-019-0044-3

Jin, P., Jan, L. Y., and Jan, Y. N. (2020). Mechanosensitive ion channels: structural features relevant to mechanotransduction mechanisms. *Annu. Rev. Neurosci.* 43, 207–229. doi: 10.1146/annurev-neuro-070918-050509

Jin, S. S., He, D. Q., Wang, Y., Zhang, T., Yu, H. J., Li, Z. X., et al. (2020). Mechanical force modulates periodontal ligament stem cell characteristics during bone remodelling via TRPV4. *Cell Prolif.* 53:e12912. doi: 10.1111/cpr.12912

Jin, Y., Li, J., Wang, Y., Ye, R., Feng, X., Jing, Z., et al. (2015). Functional role of mechanosensitive ion channel Piezo1 in human PDL cells. *Angle Orthod.* 85, 87–94. doi: 10.2319/123113-955.1

Kumar, A. A., Saravanan, K., Kohila, K., and Kumar, S. S. (2015). Biomarkers in orthodontic tooth movement. *J. Pharm. Bioallied Sci.* 7, S325–S330. doi: 10.4103/0975-7406.163437

Li, F., Li, G., Hu, H., Liu, R., Chen, J., and Zou, S. (2013). Effect of parathyroid hormone on experimental tooth movement in rats. *Am. J. Orthod. Dentofacial Orthop*. 144, 523–532. doi: 10.1016/j.ajodo.2013.05.010

Li, T., Wang, H., Lv, C., Huang, L., Zhang, C., Zhou, C., et al. (2021). Intermittent parathyroid hormone promotes cementogenesis via ephrinB2-EPHB4 forward signaling. *J. Cell Physiol.* 236, 2070–2086. doi: 10.1002/jcp.29994

Li, X., Han, L., Nookaew, I., Mannen, E., Silva, M. J., Almeida, M., et al. (2019). Stimulation of Piezo1 by mechanical signals promotes bone anabolism. *Elife* 8:e49631. doi: 10.7554/eLife.49631

Liu, J., Zhao, X., Pei, D., Sun, G., Li, Y., Zhu, C., et al. (2018). The promotion function of Berberine for osteogenic differentiation of human periodontal ligament stem cells via ERK-FOS pathway mediated by EGFR. *Sci. Rep.* 8:2848. doi: 10.1038/s41598-018-21116-3

Maeda, H. (2020). Mass acquisition of human periodontal ligament stem cells. *World J. Stem Cells* 12, 1023–1031. doi: 10.4252/wjsc.v12.i9.1023

Römer, P., Köstler, J., Koretsi, V., and Proff, P. (2013). Endotoxins potentiate COX-2 and RANKL expression in compressed PDL cells. *Clin. Oral Investig.* 17, 2041–2048. doi: 10.1007/s00784-013-0928-0

Sachs, F. (2015). Mechanical transduction by ion channels: a cautionary tale. *World J. Neurol.* 5, 74–87. doi: 10.5316/wjn.v5.i3.74

Saleh, L. S., Carles-Carner, M., and Bryant, S. J. (2018). The in vitro effects of macrophages on the osteogenic capabilities of MC3T3-E1 cells encapsulated in a biomimetic poly(ethylene glycol) hydrogel. *Acta Biomater.* 71, 37–48. doi: 10.1016/j.actbio.2018.02.026

Schara, R., Skaleric, E., Seme, K., and Skaleric, U. (2013). Prevalence of periodontal pathogens and metabolic control of type 1 diabetes patients. *J. Int. Acad. Periodontol.* 15, 29–34.

Shen, Y., Pan, Y., Guo, S., Sun, L., Zhang, C., and Wang, L. (2020). The roles of mechanosensitive ion channels and associated downstream MAPK signaling pathways in PDLC mechanotransduction. *Mol. Med. Rep.* 21, 2113–2122. doi: 10.3892/mmr.2020.11006

Suchyna, T. M. (2017). Piezo channels and GsMTx4: two milestones in our understanding of excitatory mechanosensitive channels and their role in pathology. *Prog. Biophys. Mol. Biol.* 130, 244–253. doi: 10.1016/j.pbiomolbio.2017.07.011

Sugimoto, A., Miyazaki, A., Kawarabayashi, K., Shono, M., Akazawa, Y., Hasegawa, T., et al. (2017). Piezo type mechanosensitive ion channel component 1 functions as a regulator of the cell fate determination of mesenchymal stem cells. *Sci. Rep.* 7:17696. doi: 10.1038/s41598-017-18089-0

Sun, W., Chi, S., Li, Y., Ling, S., Tan, Y., Xu, Y., et al. (2019). The mechanosensitive Piezo1 channel is required for bone formation. *Elife* 8:e47454. doi: 10.7554/eLife.47454

Vansant, L., Cadenas De Llano-Pérula, M., Verdonck, A., and Willems, G. (2018). Expression of biological mediators during orthodontic tooth movement: a systematic review. *Arch. Oral Biol.* 95, 170–186. doi: 10.1016/j.archoralbio.2018.08.003

Wang, L., You, X., Lotinun, S., Zhang, L., Wu, N., and Zou, W. (2020b). Mechanical sensing protein PIEZO1 regulates bone homeostasis via osteoblast-osteoclast crosstalk. *Nat. Commun.* 11:282. doi: 10.1038/s41467-019-14146-6

Wang, L., Wang, X., Ji, N., Li, H. M., and Cai, S. X. (2020a). Mechanisms of the mechanically activated ion channel Piezo1 protein in mediating osteogenic differentiation of periodontal ligament stem cells via the Notch signaling pathway. *Hua Xi Kou Qiang Yi Xue Za Zhi* 38, 628–636. doi: 10.7518/hxkq.2020.06.004

Wang, Y., and Xiao, B. (2018). The mechanosensitive Piezo1 channel: structural features and molecular bases underlying its ion permeation and mechanotransduction. *J. Physiol.* 596, 969–978. doi: 10.1113/jp274404

Wu, J., Lewis, A. H., and Grandl, J. (2017). Touch, Tension, and Transduction - The Function and Regulation of Piezo Ion Channels. *Trends Biochem. Sci.* 42, 57–71. doi: 10.1016/j.tibs.2016.09.004

Wu, Y., Wang, W., and Liu, L. (2015). Effect of β-anhydroicaritin on the expression levels of tumor necrosis factor-α and matrix metalloproteinase-3 in periodontal tissue of diabetic rats. *Mol. Med. Rep.* 12, 1829–1837. doi: 10.3892/mmr.2015.3591

Yang, Y., Wang, B. K., Chang, M. L., Wan, Z. Q., and Han, G. L. (2018). Cyclic stretch enhances Osteogenic differentiation of human PDL cells via YAP activation. *Biomed. Res. Int.* 2018:2174824. doi: 10.1155/2018/2174824

Zhou, T., Gao, B., Fan, Y., Liu, Y., Feng, S., Cong, Q., et al. (2020). Piezo1/2 mediate mechanotransduction essential for bone formation through concerted activation of NFAT-YAP1-ß-catenin. *Elife* 9:e52779. doi: 10.7554/eLife.52779

Conflict of Interest: The authors declare that the research was conducted in the absence of any commercial or financial relationships that could be construed as a potential conflict of interest.

Publisher's Note: All claims expressed in this article are solely those of the authors and do not necessarily represent those of their affiliated organizations, or those of the publisher, the editors and the reviewers. Any product that may be evaluated in this article, or claim that may be made by its manufacturer, is not guaranteed or endorsed by the publisher.

frontiers in Physiology

ORIGINAL RESEARCH
published: 10 December 2021
doi: 10.3389/fphys.2021.773878

Facilitating Reparative Dentin Formation Using Apigenin Local Delivery in the Exposed Pulp Cavity

Yam Prasad Aryal[1†], Chang-Yeol Yeon[1†], Tae-Young Kim[1], Eui-Seon Lee[1], Shijin Sung[1], Elina Pokharel[1], Ji-Youn Kim[2], So-Young Choi[3], Hitoshi Yamamoto[4], Wern-Joo Sohn[5], Youngkyun Lee[1], Seo-Young An[6], Chang-Hyeon An[6], Jae-Kwang Jung[7], Jung-Hong Ha[8‡] and Jae-Young Kim[1*‡]*

[1] Department of Biochemistry, School of Dentistry, IHBR, Kyungpook National University, Daegu, South Korea, [2] Department of Dental Hygiene, College of Health Science, Gachon University, Incheon, South Korea, [3] Department of Oral and Maxillofacial Surgery, School of Dentistry, IHBR, Kyungpook National University, Daegu, South Korea, [4] Department of Histology and Developmental Biology, Tokyo Dental College, Tokyo, Japan, [5] Pre-major of Cosmetics and Pharmaceutics, Daegu Haany University, Gyeongsan, South Korea, [6] Department of Oral and Maxillofacial Radiology, School of Dentistry, IHBR, Kyungpook National University, Daegu, South Korea, [7] Department of Oral Medicine, School of Dentistry, IHBR, Kyungpook National University, Daegu, South Korea, [8] Department of Conservative Dentistry, School of Dentistry, IHBR, Kyungpook National University, Daegu, South Korea

Apigenin, a natural product belonging to the flavone class, affects various cell physiologies, such as cell signaling, inflammation, proliferation, migration, and protease production. In this study, apigenin was applied to mouse molar pulp after mechanically pulpal exposure to examine the detailed function of apigenin in regulating pulpal inflammation and tertiary dentin formation. *In vitro* cell cultivation using human dental pulp stem cells (hDPSCs) and *in vivo* mice model experiments were employed to examine the effect of apigenin in the pulp and dentin regeneration. *In vitro* cultivation of hDPSCs with apigenin treatment upregulated bone morphogenetic protein (BMP)- and osteogenesis-related signaling molecules such as BMP2, BMP4, BMP7, bone sialoprotein (BSP), runt-related transcription factor 2 (RUNX2), and osteocalcin (OCN) after 14 days. After apigenin local delivery in the mice pulpal cavity, histology and cellular physiology, such as the modulation of inflammation and differentiation, were examined using histology and immunostainings. Apigenin-treated specimens showed period-altered immunolocalization patterns of tumor necrosis factor (TNF)-α, myeloperoxidase (MPO), NESTIN, and transforming growth factor (TGF)-β1 at 3 and 5 days. Moreover, the apigenin-treated group showed a facilitated dentin-bridge formation with few irregular tubules after 42 days from pulpal cavity preparation. Micro-CT images confirmed obvious dentin-bridge structures in the apigenin-treated specimens compared with the control. Apigenin facilitated the reparative dentin formation through the modulation of inflammation and the activation of signaling regulations. Therefore, apigenin would be a potential therapeutic agent for regenerating dentin in exposed pulp caused by dental caries and traumatic injury.

Keywords: inflammation, osteodentin, pulp cavity, reparative dentin formation, signaling modulation

OPEN ACCESS

Edited by:
Guohua Yuan,
Wuhan University, China

Reviewed by:
Zhipeng Fan,
Capital Medical University, China
Michel Goldberg,
Institut National de la Santé et de la Recherche Médicale (INSERM), France

***Correspondence:**
Jung-Hong Ha
endoking@knu.ac.kr
orcid.org/0000-0002-0469-4324
Jae-Young Kim
jykim91@knu.ac.kr
orcid.org/0000-0002-6752-5683

†These authors have contributed equally to this work and share first authorship

‡These authors have contributed equally to this work and share last authorship

Specialty section:
This article was submitted to Craniofacial Biology and Dental Research, a section of the journal Frontiers in Physiology

Received: *10 September 2021*
Accepted: *08 November 2021*
Published: *10 December 2021*

Citation:
Aryal YP, Yeon C-Y, Kim T-Y, Lee E-S, Sung S, Pokharel E, Kim J-Y, Choi S-Y, Yamamoto H, Sohn W-J, Lee Y, An S-Y, An C-H, Jung J-K, Ha J-H and Kim J-Y (2021) Facilitating Reparative Dentin Formation Using Apigenin Local Delivery in the Exposed Pulp Cavity. Front. Physiol. 12:773878. doi: 10.3389/fphys.2021.773878

INTRODUCTION

Reparative dentinogenesis is the biological regeneration of dentin from new odontoblast-like cells when a dental injury is severe and reaches up to the dental pulp (Smith et al., 1995; Simon et al., 2012). A range of signaling molecules such as transcription, autocrine, and paracrine factors plays significant roles in dentin secretion and regeneration (Angelova Volponi et al., 2018; Baranova et al., 2020). Unlike enamel, dentin would be regenerated and modified by mature odontoblasts (Simon et al., 2012). During dental caries and lesions, dental pulp cells trigger a repair response to secrete dentin matrix to prevent spreading infection (Shah et al., 2020); and depending on the degree of severity, the secreted dentin is either tubular or osteodentin during reactionary and reparative dentinogenesis (Ricucci et al., 2014).

The restoration of the damaged pulpal tissue and the destroyed tooth structure has been still a challenge in the endodontic field. Recent studies are focused on using different growth factors and related signaling molecules before designing new drugs and biocapping materials (Bottino et al., 2017; Moussa and Aparicio, 2019). Previous reports highlighted different approaches such as mineral calcium phosphates, bioactive extracellular matrix, and stem cells for pulp healing and dentin regeneration (Goldberg et al., 2009; Lacerda-Pinheiro et al., 2012; Dimitrova-Nakov et al., 2014; Njeh et al., 2016). Particularly, most of the reports showed the effects of capping molecules in the reparative dentin formation (Accorinte et al., 2008; Huang, 2011; Smith et al., 2012; Tran et al., 2019). Besides these, (1) the protease inhibitor, bortezomib (Jung et al., 2017), (2) the transforming growth factor-β (TGF-β) family ligands, such as bone morphogenetic proteins (BMPs; Kwak and Lee, 2019), (3) glycogen synthase kinase (GSK-3) antagonists (Neves et al., 2017), (4) bone sialoprotein (BSP; Decup et al., 2000), (5) dentin phosphophoryn (DPP)/collagen composite (Koike et al., 2014), and (6) osteogenic protein-1 (OP-1), calcium hydroxide, and N-acetyl cysteine (NAC; Goldberg et al., 2001) have been incorporated in biomaterial scaffolds for dentin regeneration. For proper healing and regeneration of dentin, it is required to involve various signaling molecules and pathways. Specifically, previous reports emphasized the importance of Wnt and TGF-β signaling in the development of dental pulp and odontoblasts and the reparative dentin formation (Lim et al., 2014; Hunter et al., 2015; Jung et al., 2017; Niwa et al., 2018; Ali et al., 2019). Copious reports on detailed signaling molecules in dentin regeneration were prepared (Huang, 2011; Chmilewsky et al., 2014; Hunter et al., 2015; Karakida et al., 2019; Neves et al., 2020); however, it is still difficult to regenerate the dentin in the clinical field. These problems would result from the less focused study on controlling the inflammation in the early stage of tissue injury. During dentin-pulp regeneration, inflammation is the biggest hurdle for proper regeneration of pulp-dentin complex along with dental pulp tissue proliferation and remodeling (Shah et al., 2020). Inflammatory and immunological aspects of dental pulp repair should be taken into consideration during cavity treatment (Smith, 2002; Goldberg et al., 2008). The widely accepted paradigm both in the pulp and other bodily sites is that healing can only occur after removal of the infection, enabling a significant dampening of inflammation (Duncan and Cooper, 2020; Neves et al., 2020). Therefore, drugs that have both anti-inflammatory properties showing low cytokine stimulation levels and facilitating tissue regeneration can be considered as the supplementary agent to facilitate the reparative dentine formation (Julier et al., 2017).

Apigenin (4′,5,7-trihydroxyflavone), a natural flavonoid found in fruits and vegetables, has the effective anti-inflammatory, antioxidant, and anticancer properties (Shukla and Gupta, 2010; Ginwala et al., 2019; Zhou et al., 2019; Javed et al., 2021). The pharmacological value of apigenin now draws attention to be applied in different research fields, such as cardiology, neurology, and immunology (Shukla and Gupta, 2010; Li et al., 2017; Jiao et al., 2019). Several experiments reported apigenin in inflammation and disease control by modulating different signaling cascades (Shukla and Gupta, 2010; Ozbey et al., 2019); however, research involving apigenin in dental hard tissue regeneration, especially dentin regeneration, is lacking. Therefore, we evaluated the roles of apigenin in dentin-bridge formation and regeneration, with local delivery of apigenin after pulpal cavity access preparation in mice molar. In addition, we examined the signaling regulations and cellular physiology modulated by apigenin during human dental pulp stem cell (hDPSC) differentiation.

MATERIALS AND METHODS

Human Dental Pulp Stem Cells and Apigenin Treatment

The hDPSCs (cat# PT-5025, Lonza Bioscience, Basel, Switzerland) were cultured in DPSC SingleQuot Growth Medium (cat# PT-4516, Lonza Bioscience, Basel, Switzerland). For osteogenic differentiation, cells were seeded in collagen-coated 48-well plates at a density of 2×10^4 cells/well. After 24 h of seeding, the medium was changed with osteogenic medium [a-MEM, 2% fetal bovine serum (FBS), 10 mM b-glycerophosphate, 50 μg/ml ascorbic acid, 100 nM dexamethasone] with or without apigenin (cat# 520-36-5, Sigma Aldrich, Saint Louis, MO, United States). The hDPSCs were cultured with three different sets: osteogenic medium only (negative control), osteogenic medium with 0.05% dimethyl sulfoxide (DMSO; vehicle control), and osteogenic medium with various concentrations of apigenin (experimental). The culture medium was changed three times per week (**Figure 1A**).

Cell Viability Assay

Cell viability was evaluated by CellTiter 96® AQueous One Solution Cell Proliferation Assay (MTS) (cat# G3582, Promega, Madison, WI, United States) in accordance with the instruction of the manufacturer. In brief, hDPSCs were seeded in 96-well plates at a density of 1×10^4 cells/well with serum-free media, and apigenin treatments were performed 24 h after seeding. The MTS solution was added after 24, 48, and 72 h of apigenin treatment and incubated for 1 h at 37°C. Colorimetric

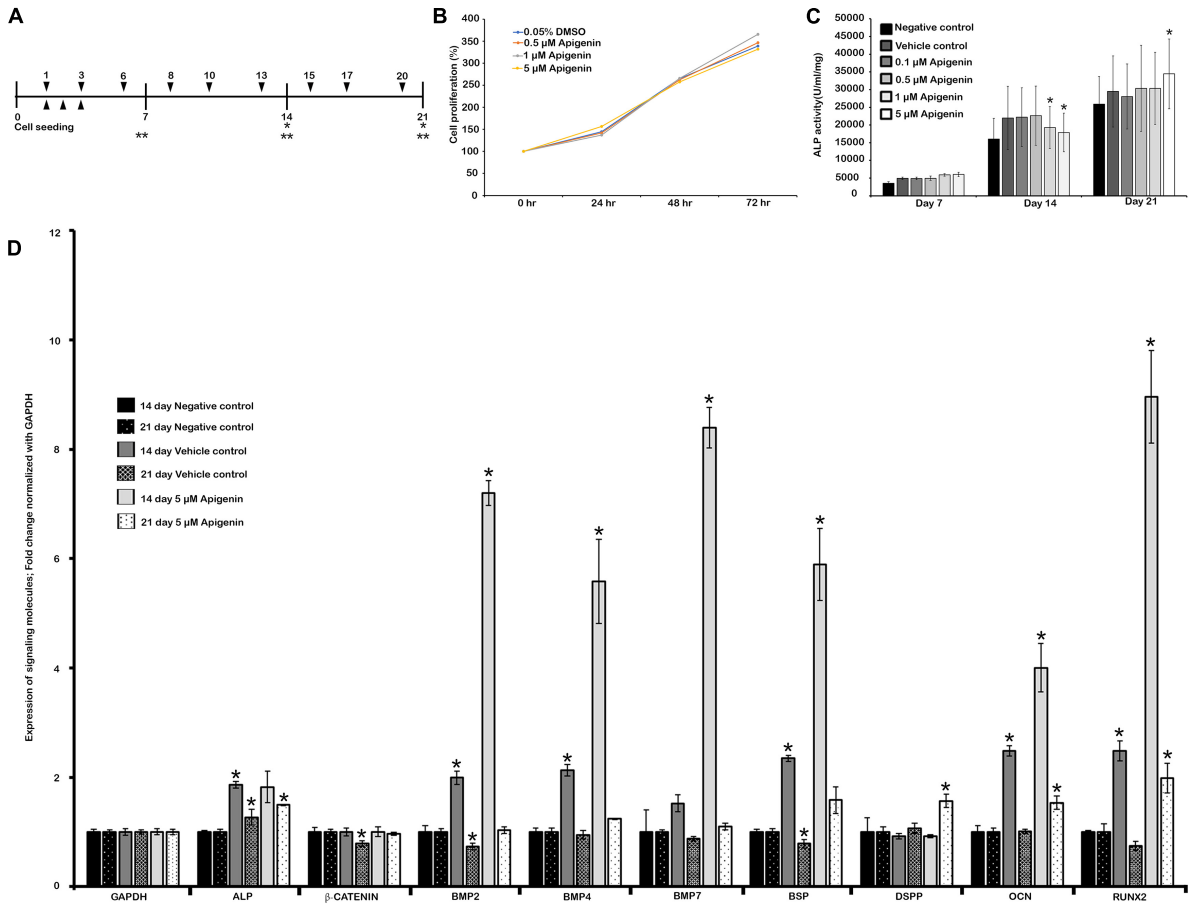

FIGURE 1 | Human dental pulp stem cells (hDPSCs) and apigenin treatment. Experimental design showing hDPSCs cultured with apigenin for 3 weeks **(A)**; MTS assay showing cell viability and proliferation **(B)**; the effect of apigenin on ALP activity in hDPSCs **(C)**; altered expression patterns of signaling molecules after 5 μM apigenin treatment on hDPSCs at days 14 and 21 **(D)**. The highest ALP activity is observed following treatment with 5 μM apigenin at day 21. Bone morphogenetic protein (BMP)-related and osteogenesis-related signaling molecules are significantly upregulated in the apigenin-treated hDPSCs after 2 weeks. ▼ indicates the change of osteogenic medium, ▲ indicates MTS assay, * indicates real-time quantitative PCR (RT-qPCR), ** indicates ALP Assay **(A)**. * indicates $p < 0.05$ **(C,D)**.

changes were measured at 490 nm using a SpectraMax ABS Microplate Reader, Molecular devices, CA, United States.

Alkaline Phosphatase Activity Assay

The effect of apigenin on alkaline phosphatase (ALP) activity in an osteoinductive environment was determined using ALP Assay Kit (cat # K412-500, BioVision, Milpitas, CA, United States). hDPSCs cultured in osteogenic medium for 7, 14, and 21 days were harvested and lysed with assay buffer. Then, the supernatant was treated with para-nitrophenyl phosphate (pNPP) solution for 1 h at room temperature. Finally, the reaction was terminated by adding a stop solution, and the absorbance was measured at 405 nm using a SpectraMax ABS Microplate Reader. Standard curve determination and ALP activity evaluations were performed according to the instructions of the manufacturer.

Animals

For the pulp cavity preparation, 8-week-old male Institute of Cancer Research (ICR) mice were used. At least 10 mice were euthanized for 3, 5, and 42 days after cavity preparation to be used as control ($N = 10$) and experimental ($N = 10$) groups. Adult mice were housed under the following conditions: 22 ± 2°C, 55 ± 5% humidity, and artificial illumination lit between 5 a.m. and 5 p.m. with free access to food and water. All experimental protocols involving animal care and handling were approved by the Kyungpook National University, School of Dentistry, Animal Care and Use Committee (KNU-2015-136).

Pulp Cavity Exposure and Drug Local Delivery

Mice were anesthetized by injecting Avertin (cat# T48402-5G, Sigma-Aldrich, MA, United States) intraperitoneally. The upper right first molar was ground using 0.6-mm round burr with a water spray immediately before pulp exposure. Subsequent pulpal exposure was conducted with ISO #15 K-file having 0.15 mm diameter (M-access, Dentsply Sirona, Ballaigues, Switzerland) to minimize heat stress under a dissecting microscope (S6, Leica, Wetzlar, Germany) as described previously (Jung et al., 2017).

After that, 50 μM apigenin (experimental) or 0.05% DMSO (control) with Pluronic F-127 were delivered through the Hamilton syringe into the pulp cavity. After treatment, the teeth with exposed pulp were doubly sealed with Dycal (Dentsply Caulk, Milford, DE, United States) and light-cured composite resin (Jung et al., 2017). At least 10 mice ($N = 10$) were used for each group.

Histology and Immunohistochemistry

The mice were sacrificed after 3, 5, and 42 days from local drug treatment, for which we have set up the experimental protocols in our laboratory (Jung et al., 2017). The sacrificed mice were fixed in 4% paraformaldehyde (PFA), washed with phosphate-buffered saline, decalcified by ethylenediaminetetraacetic acid (EDTA), and embedded in paraffin wax, after which 7-μm frontal sections were prepared for immunostaining and histological analysis. The histomorphological analyses were performed using H&E and Masson's trichrome (MTC) staining as described previously (Jung et al., 2017). For immunostaining, primary antibodies against TNF-α (cat# ab9739, Abcam, Cambridge, MA, United States); myeloperoxidase (MPO) (cat# bs-4943R, Bioss, Woburn, MA, United States); NESTIN (cat# ab11306, Abcam, Cambridge, MA, United States), and TGF-β (cat# ab92486, Abcam, Cambridge, MA, United States) were used. The secondary antibodies used were biotinylated anti-rabbit or anti-mouse immunoglobulin G (IgG). The primary antibody binding to the fragment was visualized using the diaminobenzidine tetrahydrochloride (DAB) reagent kit (cat# C09-12, GBI Labs, Bothell, WA, United States).

Real-Time PCR

After 14 and 21 days of hDPSCs cultured with apigenin, total RNA was isolated from cells and complementary DNA (cDNA) was synthesized. Then, a real-time PCR assay was performed to quantify the gene expression with Power SYBR^{TM} Green PCR Master Mix (cat# 4367659, Thermo Fisher Scientific, Waltham, MA, United States). The expressions of genes encoding ALP, β-CATENIN, BMP2, BMP4, BMP7, dentin sialophosphoprotein (DSPP), glyceraldehyde 3-phosphate dehydrogenase (GAPDH), osteocalcin (OCN), and RUNX2 were examined. Each sample was analyzed in triplicates. The results of the assays were normalized to the levels of an endogenous control gene (GAPDH). The primers used in this study are listed in **Supplementary Table 1**.

Micro-CT Evaluations

The maxilla after 6 weeks of treatment with apigenin was analyzed using micro-CT imaging (Skyscan 1272; Bruker, Kontich, Belgium), and the three-dimensional (3D) reconstructions were constructed using NRecon software for quantifying the volume of hard tissue formed as described previously (Jung et al., 2017).

Photography and Image Analysis

All histological and immunostaining slides were photographed using a DM2500 microscope (Leica, Wetzlar, Germany) and a digital CCD camera (DF310 FX, Leica, Wetzlar, Germany).

Statistical Analysis

The statistical data are expressed as mean ± SD. Comparisons were made between the experimental and control groups using Student's t-test, and p-values < 0.05 were considered significant.

RESULTS

Human Dental Pulp Stem Cells and Apigenin Treatment

The DPSCs or stem cells from the human exfoliated deciduous tooth (SHED) have important applications in regenerative therapies such as dentin regeneration (Potdar, 2015). In this study, hDPSCs were used as *in vitro* model to examine the effect of apigenin during pulp and dentin regeneration. To examine the cell viability and cytotoxicity, we employed an MTS assay to analyze the proliferation of hDPSCs after treatment of apigenin with various concentrations (**Figure 1B**). Our results showed that cellular proliferation was not affected in a range of concentrations between 0.1 μM and 5 μM of apigenin after 24, 48, and 72 h (**Figure 1B**). After ensuring the cell viability, the ALP activity of hDPSCs with various concentrations of apigenin was examined. The highest ALP activity was observed with 5 μM apigenin treatment at day 21 ($p < 0.05$). In contrast, the ALP activity was almost similar to 0.1, 0.5, 1, and 5 μM apigenin at days 7 and 14 (**Figure 1C**). Therefore, we selected 5 μM apigenin as a suitable concentration for *in vitro* cell cultivation. ALP is one of the earliest markers of osteoblastic cell differentiation (Wrobel et al., 2016), and therefore, we examined the expression patterns of some BMP- and osteogenesis-related signaling molecules on day 14 prior to higher ALP activity in the hDPSCs. Our results showed that both the Bmp- and the osteogenesis-related signaling molecules (i.e., BMP2, BMP4, BMP7, BSP, RUNX2, and OCN) were significantly upregulated in the apigenin-treated specimens compared to controls after 14 days (**Figure 1D** and **Supplementary Table 2**). Similarly, the expressions of ALP, BMP2, BMP4, BSP, OCN, and RUNX2 were also increased in the vehicle control compared to the negative control (**Figure 1D** and **Supplementary Table 2**). In addition, we also examined the expression patterns of these signaling molecules on day 21, in which, most of the signaling molecules were upregulated in the apigenin-treated hDPSCs (**Figure 1D**). Particularly, DSPP, one of the important proteins for the mineralization of tooth dentin (Yamakoshi, 2009), was significantly upregulated in the apigenin-treated hDPSCs (**Figure 1D**). Based on these *in vitro* examinations, we performed *in vivo* animal experiments using 50 μM apigenin as a suitable concentration, which is 10 times of *in vitro* cell cultivation as in the previous study (Kim et al., 2020).

Inflammatory Reaction Modulation by Apigenin Treatment

The histological examinations of dentin-pulp tissue were performed using H&E staining as described previously (Jung et al., 2017). After 3 days, more disintegrated cells were detected in the DMSO-control specimen compared with the apigenin-treated specimen (**Figures 2a,b**). Specifically, the

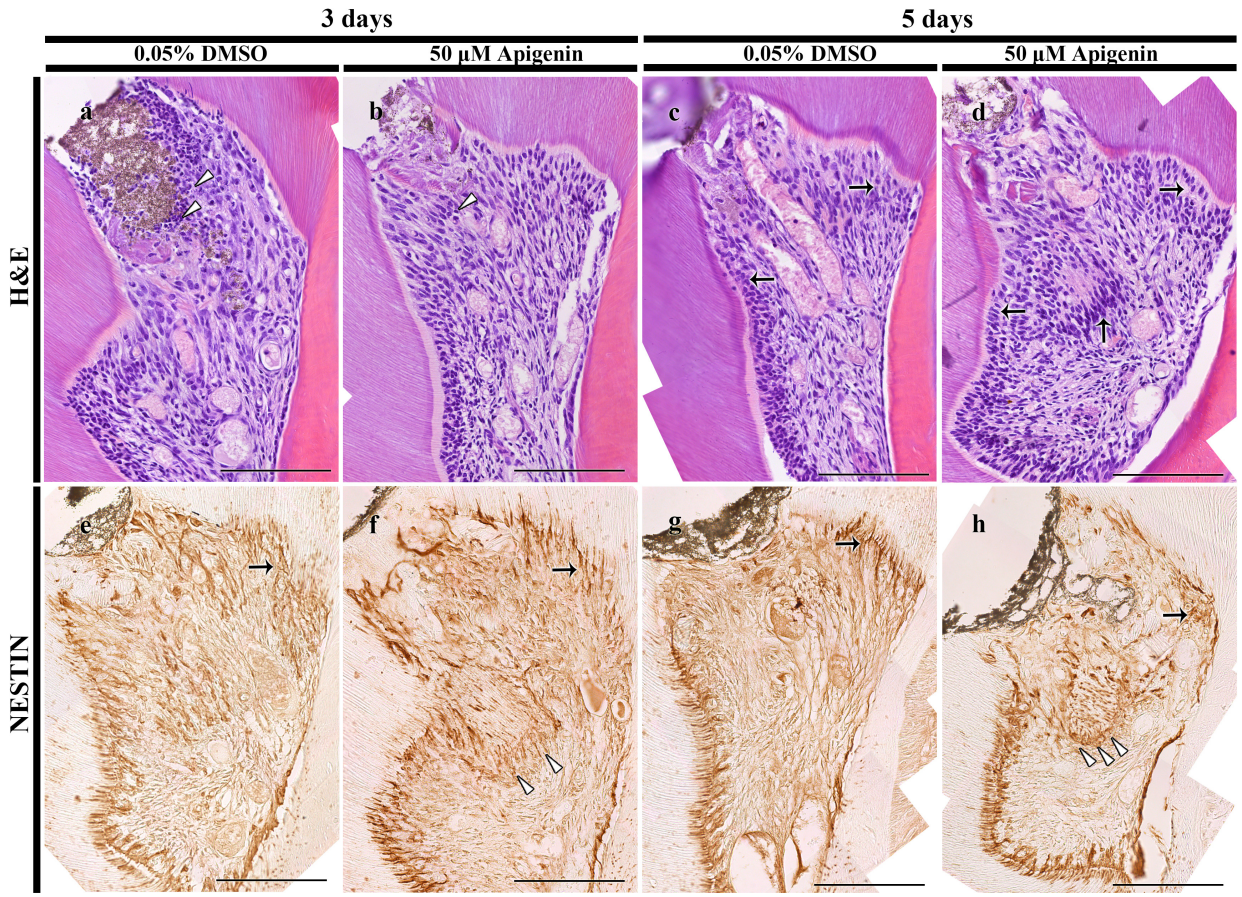

FIGURE 2 | H&E staining and immunolocalization of NESTIN. H&E staining showing more disintegrated cells in the DMSO-control than apigenin-treated pulp cavity after 3 days (arrowheads) **(a,b)**. Increased pulp and odontoblast cells are observed in the apigenin-treated specimen after 5 days (arrows) **(c,d)**. The intense immunolocalization of NESTIN is observed beneath the exposed pulp (arrowheads) and reactionary dentin-forming region (arrows) in the apigenin-treated pulp cavity in both 3- and 5-day specimens **(e–h)**. Scale bars: 50 μm **(a–h)**.

disintegrated cells were observed beneath the exposed pulp in the DMSO-control group compared with the coincided region of the apigenin-treated group (**Figures 2a,b**). After 5 days, more pulp and odontoblast cells were observed in the apigenin-treated specimen compared with DMSO-control (**Figures 2c,d**). In addition, the localization of active odontoblast differentiation marker, i.e., NESTIN, was intense in both 3- and 5-day apigenin-treated specimens compared with DMSO-control (**Figures 2e–h**).

The tissues were inflamed after the pulp cavity access preparation, and hence, to examine the role of apigenin in the inflammatory modulation in the exposed and inflamed pulp tissue, immunostainings were performed in 3- and 5-day specimens (**Figure 3**). The well-known anti-inflammatory markers, i.e., TNF-α and MPO, were examined to understand the apigenin function in exposed pulp inflammation control. After 3 days from pulp exposure, there was a decreased localization pattern of TNF-α in the apigenin-treated specimens (**Figures 3a,b**). Meanwhile, the intensity of immunostaining of TNF-α was very slightly decreased in the apigenin-treated specimens after 5 days (**Figures 3c,d**). Similarly, apigenin-treated specimens showed a decreased localization pattern of MPO after 3 days (**Figures 3e,f**), whereas no obvious differences were observed between the control and the apigenin-treated specimens after 5 days (**Figures 3g,h**). The *in vitro* experiment showed the upregulation of BMP- and osteogenesis-related signaling molecules after apigenin treatment; therefore, we sought to examine the immunolocalization of TGF-β1 in the *in vivo* animal experiment. Our result showed the stronger positive localization pattern of TGF-β1 in the apigenin-treated specimens compared to control in both 3- and 5-day specimens (**Figures 3i–l**). Specifically, the intense immunostainings were observed along the reparative and reactionary dentin-forming regions in the apigenin-treated specimens compared with the same region of DMSO-control (**Figures 3i–l**). Furthermore, the intensities of immunostainings were quantified as weak (+), mild (++), and strong (+++) and prepared as **Supplementary Table 3**.

Micro-CT and Dentin-Bridge Evaluations

After 42 days of apigenin treatment, MTC staining and micro-CT evaluation were employed to examine the dentin-bridge and

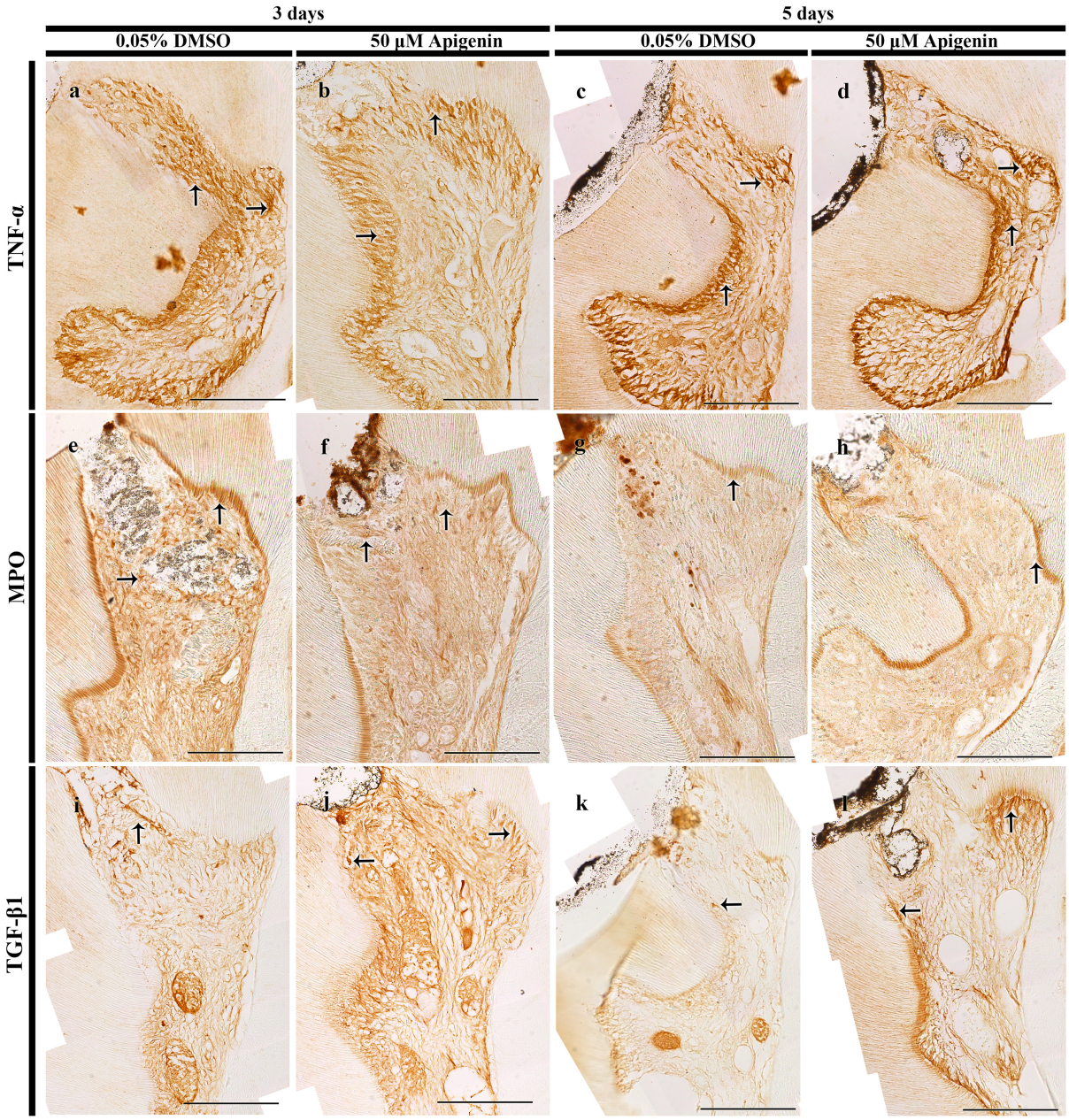

FIGURE 3 | Immunostainings of tumor necrosis factor (TNF)-α, myeloperoxidase (MPO), and transforming growth factor (TGF)-β1. The localization of TNF-α is decreased in both 3- and 5-day apigenin-treated specimens (arrows) when compared to control **(a–d)**. On day 3, the localization of MPO is decreased in the apigenin-treated specimens; however, the immunostaining of MPO is almost similar in both DMSO-control and apigenin-treated specimens (arrows) on day 5 **(e–h)**. In contrast, increased immunostaining of TGF-β1 is observed in both 3- and 5-day apigenin-treated specimens (arrows) when compared to control **(i–l)**. Scale bars: 50 μm **(a–l)**.

the percentage of newly regenerated tissue in the pulp cavity as described previously (**Figures 4a–e**; Jung et al., 2017). Compared with the DMSO-control, the apigenin-treated specimen showed dentin-bridge formation beneath the exposed area as reparative dentin (**Figures 4a,b**). The newly formed dentinal tubules were osteodentin-like rather than tubular reparative dentin (**Figures 4a,b**). Similarly, the percentage of hard tissue volume in the apigenin-treated specimen (81.5 ± 6.1%; N = 3) was significantly higher than the DMSO-control (62.4 ± 1.9%; N = 3) (**Figures 4c–e**).

DISCUSSION

Various procedures, such as tissue-engineered biomolecules and scaffolds are practiced in regenerative endodontics to restore the

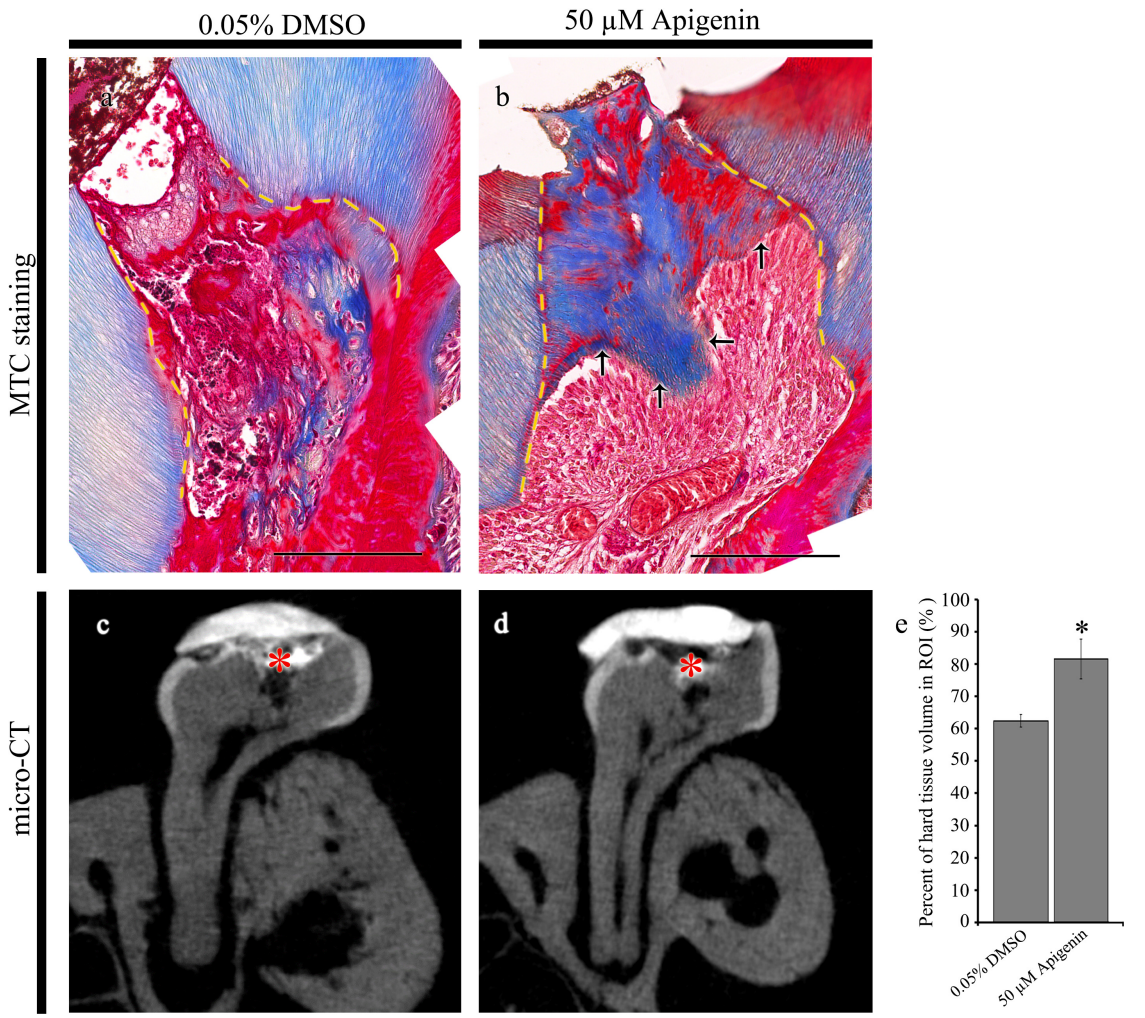

FIGURE 4 | Micro-CT examinations and Masson's trichrome (MTC) staining after 42 days from cavity preparation. MTC staining showing dentin-bridge (arrows) formation in the apigenin-treated specimen **(a,b)**. Micro-CT showing pulpal access preparation and dentin-bridge formation after 42 days of cavity preparation **(c,d)**. The percentage of hard tissue regenerated within the region of interest after 42 days of cavity preparation ($N = 3$) **(e)**. ROI, region of interest. Red * indicates the region of cavity preparation **(c,d)**. The yellow dotted line indicates the existing dentin in the cavity **(a,b)**. * indicates $p < 0.05$ **(e)**. Scale bars: 50 µm **(a,b)**.

biological properties of lost tooth structure (Decup et al., 2000; Goldberg et al., 2001, 2009; Dimitrova-Nakov et al., 2014; Njeh et al., 2016; Bottino et al., 2017). In dental caries, the restoration of the biological function of injured pulp and odontoblasts might be one of the plausible ways for tissue regeneration (Lesot et al., 1993). Mostly, the exposed dentin acts as a barrier for preventing further tooth damage; therefore, applying such drugs that facilitate the restoration of the biological function of pulp cells plays a pivotal role in cavity treatment and dentin regeneration (Karakida et al., 2019). Considering these, the local delivery of drug in the exposed pulp using a mouse model system was employed, which we had already established the experimental protocols (Jung et al., 2017). In this study, apigenin, a phytochemical molecule, was introduced into the pulp cavity of the mouse, and its biological role was evaluated through histology, immunohistochemistry, and micro-CT analysis. We selected apigenin, a well-known anti-inflammatory molecule, as one of the drugs for dentin regeneration because the management of inflammatory reaction is one of the key factors during wound healing and tissue regeneration (Eming et al., 2017; Serra et al., 2017).

The inflammatory response, i.e., a complex biological response, would be a hallmark to induce repair response for local tissue recovery (Slavich and Irwin, 2014; Serra et al., 2017), and therefore, the first step of tissue regeneration is the inflammation control, which otherwise can lead to either disease progression or cell death (Hunter, 2012). It is, therefore, the inflammatory and immunological aspects of the pulp cavity should be taken into consideration during cavity treatment (Smith, 2002; Goldberg et al., 2008). The neutrophils and macrophages are the primary innate cells involved in the cytokine pathway, and during tissue repair and the physiological wound healing process, the inflammation subsides after infectious agents are eliminated from the site of injury (Oishi and Manabe, 2018;

Goodman et al., 2019). The decreased localizations of TNF-α and MPO in the apigenin-treated specimens suggested that apigenin would modulate early inflammation in the exposed pulp (**Figure 3**; Goodman et al., 2019). It is proposed that anti-TNF-α therapies are a major treatment of inflammatory diseases (Parameswaran and Patial, 2010), and reducing inflammatory cytokines, such as TNF-α, is the first step for proper tissue regeneration (Goodman et al., 2019). In this study, the reduced level of TNF-α localization in a 3-day apigenin-treated specimen suggests its role in inflammation control toward the tissue repair process (**Figure 3**), coincided with previous findings (Ginwala et al., 2019; Zhou et al., 2019). In addition, the controlled release of MPO from the infective site indicates the progress of tissue recovery (Khan et al., 2018); however, the prolonged MPO production is not good for tissue recovery (Lee et al., 1995). The decreased localization of MPO in the apigenin-treated specimen suggests that the injured pulp and odontoblast cells subside their inflammation after 3 days; however, after 5 days, the inflammatory reaction recedes and the stage of tissue repair progress (**Figure 3**; Eming et al., 2017; Serra et al., 2017). Furthermore, various plant-derived compounds inhibit inflammation by reducing cytokine levels (Fürst and Zündorf, 2014), and apigenin, one of the natural flavonoids, also showed early inflammation control in the pulp cavity in this study.

After the pulp was exposed to the oral cavity, there was extensive cell death, and the repair response initiated surviving pulp cells rather than injured odontoblasts. Therefore, the exposed pulp response triggers pulp cells to secrete dentin, which has a bone-like characteristic, called osteodentin; however, if the injured odontoblasts secrete dentin, it has a tubular structure (Ricucci et al., 2014). In this study, apigenin showed elevated osteoblast differentiation-related genes such as RUNX2 and OCN, as well as the ALP activity as in the previous report (Jung, 2014). Apigenin is reported to be involved in regulating different signaling cascades (Ozbey et al., 2019). In this study, the upregulation of BMPs and osteogenesis-related genes in the apigenin-treated specimen showed its modulating roles in TGF signaling, especially during dentinogenesis (**Figures 1**, **3**). Several studies emphasized the importance of cross-talk between BMP and Wnt-/β-catenin during dentin formation and pulp repair (Handrigan and Richman, 2010; Silvério et al., 2012; Yang et al., 2015); however, apigenin showed an inhibitory effect in the Wnt/β-catenin pathway (Ozbey et al., 2019). Interestingly, our result showed that apigenin-treated hDPSCs did not show any changes in the expression of Wnt/β-catenin (**Figure 1**). These results suggest that apigenin modulates BMP/TGF-β signaling rather than Wnt-/β-catenin signaling during pulp repair and regeneration. The dentin-bridge thus formed would be osteodentin (**Figure 4**) rather than true dentin formed by the cross-talk between BMP and Wnt-/β-catenin signaling. In addition, the high ALP activity indicates the osteoblast differentiation in the apigenin-treated hDPSCs. Therefore, this study suggests that to recover the local tissue during pulp injury, the modulating role of apigenin in the BMP/TGF-β signaling pathway is remarkable (**Figures 1**, **3**; Niwa et al., 2018). Moreover, TGF-β1 regulates transcription and interacts with the major dentin proteins present in odontoblasts and dental pulp (Unterbrink et al., 2002; Niwa et al., 2018) and, therefore, plays a crucial role during tooth development and pulp repair (Nie et al., 2006). In this study, the modulating role of apigenin in BMPs and TGF-β signaling showed that apigenin applied in the exposed pulp would facilitate repair response initiation in the injured pulp and enhance calcified structure production as a dentin-bridge to prevent further tooth loss as in previous reports (Ricucci et al., 2014; Jung et al., 2017). Odontoblasts are directly injured after cavity preparation; however, a decreased number of disintegrated cells and increased NESTIN localization in the apigenin-treated tooth specimens showed that the injured odontoblasts during pulp cavity preparation are reexpressed, especially beneath the exposed pulp (**Figure 2**). Furthermore, the increased expression of DSPP in the hDPSCs suggests that apigenin modulates maintaining the secretory activity of injured odontoblasts and pulp vitality through the modulation of inflammation and the facilitation of BMP/TGF-β signaling after dental injury (**Figure 1**).

CONCLUSION

The fundamental process for dentin regeneration is the healing of exposed pulp through the modulation of signaling pathways during dentinogenesis (Chmilewsky et al., 2014; Angelova Volponi et al., 2018). The *in vitro* model that we employed in this study ensured the cell toxicity, viability, and osteogenic differentiation with apigenin treatment, while the *in vivo* model showed the modulating role of apigenin in inflammation control and dentin regeneration with sound dentin-bridge formation. Overall, this study showed that apigenin treatment resolves inflammation by regulating inflammatory cytokines and modulates TGF-β and BMP signaling, which finally facilitate the dentin-bridge formation. Therefore, apigenin could be used as a potential therapeutic agent for regenerating exposed pulp due to dental caries and traumatic injury.

DATA AVAILABILITY STATEMENT

The original contributions presented in the study are included in the article/**Supplementary Material**, further inquiries can be directed to the corresponding authors.

ETHICS STATEMENT

The animal study was reviewed and approved by the KNU-2015-136.

AUTHOR CONTRIBUTIONS

YA, C-YY, J-HH, and Ja-YK contributed to conception, design, and data interpretation, and critically revised the manuscript. T-YK, E-SL, SS, EP, Ji-YK, S-YC, HY, W-JS, YL, S-YA, C-HA, and J-KJ contributed to data analysis, interpretation, and critically

revised the manuscript. All authors gave final approval and agreed to be accountable for all aspects of the study.

FUNDING

This study was supported by the National Research Foundation of Korea (Grant Nos. NRF-2017R1A5A2015391, 2018R1A2A3075600, and NRF-2021R1F1A1062736) and funded by the Ministry of Education, Science and Technology, South Korea.

SUPPLEMENTARY MATERIAL

The Supplementary Material for this article can be found online at: https://www.frontiersin.org/articles/10.3389/fphys.2021.773878/full#supplementary-material

REFERENCES

Accorinte, M. L. R., Loguercio, A. D., Reis, A., Carneiro, E., Grande, R. H. M., Murata, S. S., et al. (2008). Response of human dental pulp capped with MTA and calcium hydroxide powder. *Oper. Dent.* 33, 488–495. doi: 10.2341/07-143

Ali, M., Okamoto, M., Komichi, S., Watanabe, M., Huang, H., Takahashi, Y., et al. (2019). Lithium-containing surface pre-reacted glass fillers enhance hDPSC functions and induce reparative dentin formation in a rat pulp capping model through activation of Wnt/β-catenin signaling. *Acta Biomater.* 96, 594–604. doi: 10.1016/j.actbio.2019.06.016

Angelova Volponi, A., Zaugg, L. K., Neves, V., Liu, Y., and Sharpe, P. T. (2018). Tooth repair and regeneration. *Curr. Oral Heal. Rep.* 5, 295–303. doi: 10.1007/s40496-018-0196-9

Baranova, J., Büchner, D., Götz, W., Schulze, M., and Tobiasch, E. (2020). Tooth formation: are the hardest tissues of human body hard to regenerate? *Int. J. Mol. Sci.* 21:4031. doi: 10.3390/ijms21114031

Bottino, M. C., Pankajakshan, D., and Nör, J. E. (2017). Advanced scaffolds for dental pulp and periodontal regeneration. *Dent. Clin. North Am.* 61, 689–711. doi: 10.1016/j.cden.2017.06.009

Chmilewsky, F., Jeanneau, C., Dejou, J., and About, I. (2014). Sources of dentin-pulp regeneration signals and their modulation by the local microenvironment. *J. Endod.* 40, 19–25. doi: 10.1016/j.joen.2014.01.012

Decup, F., Six, N., Palmier, B., Buch, D., Lasfargues, J. J., Salih, E., et al. (2000). Bone sialoprotein-induced reparative dentinogenesis in the pulp of rat's molar. *Clin. Oral Investig.* 4, 110–119. doi: 10.1007/s007840050126

Dimitrova-Nakov, S., Baudry, A., Harichane, Y., Kellermann, O., Goldberg, M., and Dr ès Sciences Naturelles. (2014). Pulp stem cells: implication in reparative dentin formation. *J. Endod.* 40, 13–18. doi: 10.1016/j.joen.2014.01.011

Duncan, H. F., and Cooper, P. R. (2020). Pulp innate immune defense: translational opportunities. *J. Endod.* 46, 10–18. doi: 10.1016/j.joen.2020.06.019

Eming, S. A., Wynn, T. A., and Martin, P. (2017). Inflammation and metabolism in tissue repair and regeneration. *Science* 356, 1026–1030.

Fürst, R., and Zündorf, I. (2014). Plant-derived anti-inflammatory compounds: hopes and disappointments regarding the translation of preclinical knowledge into clinical progress. *Mediators Inflamm.* 2014, 1–9. doi: 10.1155/2014/146832

Ginwala, R., Bhavsar, R., Chigbu, D. I., Jain, P., and Khan, Z. K. (2019). Potential role of flavonoids in treating chronic inflammatory diseases with a special focus on the anti-inflammatory activity of Apigenin. *Antioxidants* 8:35. doi: 10.3390/antiox8020035

Goldberg, M., Farges, J. C., Lacerda-Pinheiro, S., Six, N., Jegat, N., Decup, F., et al. (2008). Inflammatory and immunological aspects of dental pulp repair. *Pharmacol. Res.* 58, 137–147. doi: 10.1016/j.phrs.2008.05.013

Goldberg, M., Six, N., Chaussain, C., DenBesten, P., Veis, A., and Poliard, A. (2009). Dentin extracellular matrix molecules implanted into exposed pulps generate reparative dentin: a novel strategy in regenerative dentistry. *J. Dent. Res.* 88, 396–399. doi: 10.1177/0022034509337101

Goldberg, M., Six, N., Decup, F., Buch, D., Soheili-Majd, E., Lasfargues, J. J., et al. (2001). Application of bioactive molecules in pulp-capping situations. *Adv. Dent. Res.* 15, 91–95. doi: 10.1177/08959374010150012401

Goodman, S. B., Pajarinen, J., Yao, Z., and Lin, T. (2019). Inflammation and bone repair: from particle disease to tissue regeneration. *Front. Bioeng. Biotechnol.* 7:230. doi: 10.3389/fbioe.2019.00230

Handrigan, G. R., and Richman, J. M. (2010). A network of Wnt, hedgehog and BMP signaling pathways regulates tooth replacement in snakes. *Dev. Biol.* 348, 130–141. doi: 10.1016/j.ydbio.2010.09.003

Huang, G. T. J. (2011). Dental pulp and dentin tissue engineering and regeneration advancement and challenge. *Front. Biosci.* 3:788–800. doi: 10.2741/e286

Hunter, D. J., Bardet, C., Mouraret, S., Liu, B., Singh, G., Sadoine, J., et al. (2015). Wnt acts as a prosurvival signal to enhance dentin regeneration. *J. Bone Miner. Res.* 30, 1150–1159. doi: 10.1002/jbmr.2444

Hunter, P. (2012). The inflammation theory of disease. *EMBO Rep.* 13, 968–970. doi: 10.1038/embor.2012.142

Javed, Z., Sadia, H., Iqbal, M. J., Shamas, S., Malik, K., Ahmed, R., et al. (2021). Apigenin role as cell-signaling pathways modulator: implications in cancer prevention and treatment. *Cancer Cell Int.* 21:189. doi: 10.1186/s12935-021-01888-x

Jiao, R., Chen, H., Wan, Q., Zhang, X., Dai, J., Li, X., et al. (2019). Apigenin inhibits fibroblast proliferation and reduces epidural fibrosis by regulating Wnt3a/β-catenin signaling pathway. *J. Orthop. Surg. Res.* 14:258. doi: 10.1186/s13018-019-1305-8

Julier, Z., Park, A. J., Briquez, P. S., and Martino, M. M. (2017). Promoting tissue regeneration by modulating the immune system. *Acta Biomater.* 53, 13–28. doi: 10.1016/j.actbio.2017.01.056

Jung, J. K., Gwon, G. J., Neupane, S., Sohn, W. J., Kim, K. R., Kim, J. Y., et al. (2017). Bortezomib facilitates reparative dentin formation after pulp access cavity preparation in mouse molar. *J. Endod.* 43, 2041–2047. doi: 10.1016/j.joen.2017.07.018

Jung, W. W. (2014). Protective effect of apigenin against oxidative stress-induced damage in osteoblastic cells. *Int. J. Mol. Med.* 33, 1327–1334. doi: 10.3892/ijmm.2014.1666

Karakida, T., Onuma, K., Saito, M., Yamamoto, R., Chiba, T., Chiba, R., et al. (2019). Potential for drug repositioning of midazolam for dentin regeneration. *Int. J. Mol. Sci.* 20:670. doi: 10.3390/ijms20030670

Khan, A., Alsahli, M., and Rahmani, A. (2018). Myeloperoxidase as an active disease biomarker: recent biochemical and pathological perspectives. *Med. Sci.* 6:33. doi: 10.3390/medsci6020033

Kim, T. Y., Park, J. K., Aryal, Y. P., Lee, E. S., Neupane, S., Sung, S., et al. (2020). Facilitation of bone healing processes based on the developmental function of meox2 in tooth loss lesion. *Int. J. Mol. Sci.* 21:8701. doi: 10.3390/ijms21228701

Koike, T., Polan, M. A., Izumikawa, M., and Saito, T. (2014). Induction of reparative dentin formation on exposed dental pulp by dentin phosphophoryn/collagen composite. *Biomed. Res. Int* 2014:745139. doi: 10.1155/2014/745139

Kwak, E. A., and Lee, N. Y. (2019). Synergetic roles of TGF-β signaling in tissue engineering. *Cytokine* 115, 60–63. doi: 10.1016/j.cyto.2018.12.010

Lacerda-Pinheiro, S., Dimitrova-Nakov, S., Harichane, Y., Souyri, M., Petit-Cocault, L., Legrès, L., et al. (2012). Concomitant multipotent and unipotent dental pulp progenitors and their respective contribution to mineralised tissue formation. *Eur. Cell Mater.* 23, 371–386. doi: 10.22203/eCM.v023a29

Lee, W., Aitken, S., Sodek, J., and McCulloch, C. A. G. (1995). Evidence of a direct relationship between neutrophil collagenase activity and periodontal tissue destruction in vivo: role of active enzyme in human periodontitis. *J. Periodontal Res.* 30, 23–33. doi: 10.1111/j.1600-0765.1995.tb01249.x

Lesot, H., Begue-Kirn, C., Kubler, M. D., Meyer, J. M., Smith, A. J., Cassidy, N., et al. (1993). Experimental induction of odontoblast differentiation and stimulation during preparative processes. *Cells Mater.* 3:8.

Li, F., Lang, F., Zhang, H., Xu, L., Wang, Y., Zhai, C., et al. (2017). Apigenin alleviates endotoxin-induced myocardial toxicity by modulating inflammation, oxidative stress, and autophagy. *Oxid. Med. Cell. Longev.* 2017:2302896. doi: 10.1155/2017/2302896

Lim, W. H., Liu, B., Cheng, D., Hunter, D. J., Zhong, Z., Ramos, D. M., et al. (2014). Wnt signaling regulates pulp volume and dentin thickness. *J. Bone Miner. Res.* 29, 892–901. doi: 10.1002/jbmr.2088

Moussa, D. G., and Aparicio, C. (2019). Present and future of tissue engineering scaffolds for dentin-pulp complex regeneration. *J. Tissue Eng. Regen. Med.* 13, 58–75. doi: 10.1002/term.2769

Neves, V. C. M., Babb, R., Chandrasekaran, D., and Sharpe, P. T. (2017). Promotion of natural tooth repair by small molecule GSK3 antagonists. *Sci. Rep.* 7:39654. doi: 10.1038/srep39654

Neves, V. C. M., Yianni, V., and Sharpe, P. T. (2020). Macrophage modulation of dental pulp stem cell activity during tertiary dentinogenesis. *Sci. Rep.* 10:20216. doi: 10.1038/s41598-020-77161-4

Nie, X., Tian, W., Zhang, Y., Chen, X., Dong, R., Jiang, M., et al. (2006). Induction of transforming growth factor-beta 1 on dentine pulp cells in different culture patterns. *Cell Biol. Int.* 30, 295–300. doi: 10.1016/j.cellbi.2005.12.001

Niwa, T., Yamakoshi, Y., Yamazaki, H., Karakida, T., Chiba, R., Hu, J. C. C., et al. (2018). The dynamics of TGF-β in dental pulp, odontoblasts and dentin. *Sci. Rep.* 8:4450. doi: 10.1038/s41598-018-22823-7

Njeh, A., Uzunoğlu, E. M., Ardila-Osorio, H., Simon, S., Berdal, A., Kellermann, O., et al. (2016). Reactionary and reparative dentin formation after pulp capping: hydrogel vs. Dycal. *Evid. Based Endod.* 1:3. doi: 10.1186/s41121-016-0003-9

Oishi, Y., and Manabe, I. (2018). Macrophages in inflammation, repair and regeneration. *Int. Immunol.* 30, 511–528. doi: 10.1093/intimm/dxy054

Ozbey, U., Attar, R., Romero, M. A., Alhewairini, S. S., Afshar, B., Sabitaliyevich, U. Y., et al. (2019). Apigenin as an effective anticancer natural product: spotlight on TRAIL, WNT/β-catenin, JAK-STAT pathways, and microRNAs. *J. Cell. Biochem.* 120, 1060–1067. doi: 10.1002/jcb.27575

Parameswaran, N., and Patial, S. (2010). Tumor Necrosis Factor-α Signaling in Macrophages. *Crit. Rev. Eukaryot. Gene Expr.* 20, 87–103. doi: 10.1615/CritRevEukarGeneExpr.v20.i2.10

Potdar, P. D. (2015). Human dental pulp stem cells: applications in future regenerative medicine. *World J. Stem Cells* 7, 839–851. doi: 10.4252/wjsc.v7.i5.839

Ricucci, D., Loghin, S., Lin, L. M., Spångberg, L. S. W., and Tay, F. R. (2014). Is hard tissue formation in the dental pulp after the death of the primary odontoblasts a regenerative or a reparative process? *J. Dent.* 42, 1156–1170. doi: 10.1016/j.jdent.2014.06.012

Serra, M. B., Barroso, W. A., da Silva, N. N., Silva, S. D. N., Borges, A. C. R., Abreu, I. C., et al. (2017). From inflammation to current and alternative therapies involved in wound healing. *Int. J. Inflam.* 2017:3406215. doi: 10.1155/2017/3406215

Shah, D., Lynd, T., Ho, D., Chen, J., Vines, J., Jung, H. D., et al. (2020). Pulp–dentin tissue healing response: a discussion of current biomedical approaches. *J. Clin. Med.* 9:434. doi: 10.3390/jcm9020434

Shukla, S., and Gupta, S. (2010). Apigenin: a promising molecule for cancer prevention. *Pharm. Res.* 27, 962–978. doi: 10.1007/s11095-010-0089-7

Silvério, K. G., Davidson, K. C., James, R. G., Adams, A. M., Foster, B. L., Nociti, F. H., et al. (2012). Wnt/β-catenin pathway regulates bone morphogenetic protein (BMP2)-mediated differentiation of dental follicle cells. *J. Periodontal Res.* 47, 309–319. doi: 10.1111/j.1600-0765.2011.01433.x

Simon, S., Smith, A. J., Lumley, P. J., Cooper, P. R., and Berdal, A. (2012). The pulp healing process: from generation to regeneration. *Endod. Top.* 26, 41–56. doi: 10.1111/etp.12019

Slavich, G. M., and Irwin, M. R. (2014). From stress to inflammation and major depressive disorder: a social signal transduction theory of depression. *Psychol. Bull.* 140, 774–815. doi: 10.1037/a0035302

Smith, A. J. (2002). Pulpal responses to caries and dental repair. *Caries Res.* 36, 223–232. doi: 10.1159/000063930

Smith, A. J., Cassidy, N., Perry, H., Bègue-Kirn, C., Ruch, J. V., and Lesot, H. (1995). Reactionary dentinogenesis. *Int. J. Dev. Biol.* 39, 273–280.

Smith, J. G., Smith, A. J., Shelton, R. M., and Cooper, P. R. (2012). Recruitment of dental pulp cells by dentine and pulp extracellular matrix components. *Exp. Cell Res.* 318, 2397–2406. doi: 10.1016/j.yexcr.2012.07.008

Tran, X., Salehi, H., Truong, M., Sandra, M., Sadoine, J., Jacquot, B., et al. (2019). Reparative mineralized tissue characterization after direct pulp capping with calcium-silicate-based cements. *Materials (Basel).* 12:2102. doi: 10.3390/ma12132102

Unterbrink, A., O'Sullivan, M., Chen, S., and MacDougall, M. (2002). TGFβ-1 downregulates DMP-1 and DSPP in Odontoblasts. *Connect. Tissue Res.* 43, 354–358. doi: 10.1080/03008200290000565

Wrobel, E., Leszczynska, J., and Brzoska, E. (2016). The characteristics of human bone-derived cells (HBDCS) during osteogenesis in vitro. *Cell. Mol. Biol. Lett.* 21:26. doi: 10.1186/s11658-016-0027-8

Yamakoshi, Y. (2009). Dentinogenesis and dentin sialophosphoprotein (DSPP). *J. Oral Biosci.* 51, 134–142. doi: 10.2330/joralbiosci.51.134

Yang, J., Ye, L., Hui, T. Q., Yang, D. M., Huang, D. M., Zhou, X. D., et al. (2015). Bone morphogenetic protein 2-induced human dental pulp cell differentiation involves p38 mitogen-activated protein kinase-activated canonical WNT pathway. *Int. J. Oral Sci.* 7, 95–102. doi: 10.1038/ijos.2015.7

Zhou, Q., Xu, H., Yu, W., Li, E., and Wang, M. (2019). Anti-inflammatory effect of an apigenin-maillard reaction product in macrophages and macrophage-endothelial cocultures. *Oxid. Med. Cell. Longev.* 2019, 1–12. doi: 10.1155/2019/9026456

Conflict of Interest: The authors declare that the research was conducted in the absence of any commercial or financial relationships that could be construed as a potential conflict of interest.

Publisher's Note: All claims expressed in this article are solely those of the authors and do not necessarily represent those of their affiliated organizations, or those of the publisher, the editors and the reviewers. Any product that may be evaluated in this article, or claim that may be made by its manufacturer, is not guaranteed or endorsed by the publisher.

frontiers in Physiology

ORIGINAL RESEARCH
published: 08 February 2022
doi: 10.3389/fphys.2022.823275

Operation of the Atypical Canonical Bone Morphogenetic Protein Signaling Pathway During Early Human Odontogenesis

Xiaoxiao Hu, Chensheng Lin, Ningsheng Ruan, Zhen Huang, Yanding Zhang and Xuefeng Hu**

Center for Biomedical Research of South China, Fujian Key Laboratory of Developmental and Neural Biology, College of Life Science, Fujian Normal University, Fuzhou, China

Bone morphogenetic protein (BMP) signaling plays essential roles in the regulation of early tooth development. It is well acknowledged that extracellular BMP ligands bind to the type I and type II transmembrane serine/threonine kinase receptor complexes to trigger the BMP signaling pathway. Then, the receptor-activated Smad1/5/8 in cytoplasm binds to Smad4, the central mediator of the canonical BMP signaling pathway, to form transfer complexes for entering the nucleus and regulating target gene expression. However, a recent study revealed the functional operation of a novel BMP-mediated signaling pathway named the atypical BMP canonical signaling pathway in mouse developing tooth, which is Smad1/5/8 dependent but Smad4 independent. In this study, we investigated whether this atypical BMP canonical signaling is conserved in human odontogenesis. We showed that pSMAD1/5/8 is required for the expression of Msh homeobox 1 (*MSX1*), a well-defined BMP signaling target gene, in human dental mesenchyme, but the typical BMP canonical signaling is in fact not operating in the early human developing tooth, as evidenced by the absence of pSMAD1/5/8-SMAD4 complexes in the dental mesenchyme and translocation of pSMAD1/5/8, and the expression of *MSX1* induced by BMP4 is mothers against decapentaplegic homolog 4 (SMAD4)-independent in human dental mesenchymal cells. Moreover, integrative analysis of RNA-Seq data sets comparing the transcriptome profiles of human dental mesenchymal cells with and without *SMAD4* knockdown by siRNA displays unchanged expression profiles of pSMAD1/5/8 downstream target genes, further affirming the functional operation of the atypical canonical BMP signaling pathway in a SMAD1/5/8-dependent but SMAD4-independent manner in the dental mesenchyme during early odontogenesis in humans.

Keywords: tooth, development, Smad4-independent, atypical canonical BMP signaling, human dental mesenchymal cell

OPEN ACCESS

Edited by:
Guohua Yuan,
Wuhan University, China

Reviewed by:
Yi Liu,
Capital Medical University, China
Xiaoxing Kou,
Sun Yat-sen University, China

****Correspondence:***
Yanding Zhang
ydzhang@fjnu.edu.cn
Xuefeng Hu
bioxfh@fjnu.edu.cn

Specialty section:
This article was submitted to Craniofacial Biology and Dental Research, a section of the journal Frontiers in Physiology

Received: *27 November 2021*
Accepted: *10 January 2022*
Published: *08 February 2022*

Citation:
Hu X, Lin C, Ruan N, Huang Z, Zhang Y and Hu X (2022) Operation of the Atypical Canonical Bone Morphogenetic Protein Signaling Pathway During Early Human Odontogenesis. Front. Physiol. 13:823275. doi: 10.3389/fphys.2022.823275

INTRODUCTION

The mouse tooth has long served as an excellent model system to study the molecular mechanism underlying mammalian odontogenesis. Bone morphogenetic protein (BMP) signaling has been demonstrated to be a fundamental player in mouse tooth development. The major BMP ligands, including *Bmp2*, *Bmp4*, and *Bmp7*, are found to be expressed in the epithelium and mesenchyme

of the developing tooth germ in mice (Nie et al., 2006). Amid them, *Bmp4* is initially expressed in the dental epithelium at the laminar stage around E11 and subsequently induces the expression of *Msx1*, a well-known *Bmp4* downstream target gene, in the dental mesenchyme. At the following bud stage, the expression of *Bmp4* is shifted to the dental mesenchyme, which is activated by the mesenchymally expressed *Msx1* and is being maintained there until the late differentiation stage. This mesenchymal *Bmp4*, in turn, maintains *Msx1* expression by forming a positive regulatory loop with *Msx1*. Deletion of *Msx1* revealed a dramatic downregulation of Bmp4 in dental mesenchyme and exhibited an arrest of tooth development at the bud stage. Application of exogenous BMP4 to or ectopic expression of *Bmp4* in *Msx1* mutant dental mesenchyme can partially rescue tooth deficiency (Bei et al., 2000; Zhang et al., 2005). Meanwhile, mesenchymal BMP4 acts on the dental epithelium as a feedback signal to induce and maintain gene expression, such as *Shh* and *p21*, in the dental epithelium and is responsible for the formation of the enamel knot, a signaling center for tooth cusp patterning (Jernvall et al., 1998). In addition, *Bmp4*, together with *Bmp2* and *Bmp7*, is expressed in the enamel knot and responsible for apoptosis in the knot cell (Mitsiadis et al., 2010). Moreover, *Bmp4* also synergizes with *Msx1* to activate the mesenchymal odontogenic potential for sequential tooth formation by inhibiting the expression of *Dkk2* and *Osr2* (Jia et al., 2013). Taken together, BMP signaling is absolutely required for early tooth morphogenesis.

Activation of BMP signaling involves binding of BMP ligands to transmembrane type II and type I serine/threonine kinase receptors. Activated receptors transduce signals through canonical and non-canonical pathways (Nohe et al., 2004; Miyazono et al., 2010). In the canonical pathway, with binding of BMP ligands to receptors, the type II receptor phosphorylates the type I receptor and forms heterodimeric complexes, which in turn lead to phosphorylation of Smad1/5/8 (the receptor-regulated Smads, R-Smads) in the cytoplasm. pSmad1/5/8 then forms a complex with Smad4 (the common Smad, Co-Smad) and translocates to the nucleus to regulate target gene transcription (Nohe et al., 2004). In this currently accepted model, Smad4 has been regarded as the central mediator, playing an indispensable role for the nuclear translocation of pSmad1/5/8-Smad4 complex and the activation of downstream target gene expression during the signaling transduction (Lagna et al., 1996). However, previous studies also reported that the accumulation of Smad1/5 in the nucleus for the transduction of BMP signaling to trigger the expression of downstream target genes is independent of Smad4, and the deficiency in Smad4 causes no or mild defects in the development of several organs (Xu et al., 2008; Retting et al., 2009). Conditional knockout of *Smad4* in the dental mesenchyme does not reveal dental abnormality and alteration of *Msx1* expression in early tooth development (Li et al., 2011). These results obviously challenge the current model of the canonical BMP signaling pathway. Actually, a previous study in mice did demonstrate that this typical canonical signaling pathway is not, in fact, operating but a novel BMP signaling, named as the atypical canonical BMP signaling pathway, is functioning in developing mouse teeth, which is pSmad1/5/8-dependent but Smad4-independent (Yang et al., 2014).

Although the regulatory mechanism and function of BMP signaling have been studied and their importance has been established in the mouse model, it remains elusive whether this fundamental pathway is fully conserved or how it operated in humans. In this study, we aimed to further explore whether this atypical BMP/pSMAD1/5/8 canonical pathway is conserved in human tooth morphogenesis. We found that BMP-induced *MSX1* expression and pSMAD1/5/8 nuclear translocation is, in fact, SMAD4-independent in cap-stage human molar germs and human dental mesenchymal cells. In addition, unchanged expression profiles of genes downstream of pSMAD1/5/8 were confirmed by analysis of RNA-Seq data sets comparing the transcriptome profiles of human dental mesenchymal cells with and without *SMAD4* knockdown by siRNA. Our results demonstrate that the atypical canonical BMP signaling pathway is operating during early human odontogenesis.

MATERIALS AND METHODS

Collection of Human Embryonic Tissues

Human embryonic jaws isolated from chemically aborted human fetuses of 12-week gestations were provided by the Maternal and Children Health Care Hospital of Fujian Province. Informed consent forms of utilizing aborted embryos for scientific research were approved by the participants. Experiments of the human embryonic tissues were performed following the stipulations of the Ethics Committee of Fujian Normal University.

Organ Culture and Cell Culture

For organ culture, freshly separated human molar germs were cultured with the Trowell-type organ culture system in DMEM/10% fetal bovine serum (FBS) at 37°C and a 5% CO_2 incubator. Isolation of primary human dental mesenchymal cells (hDMCs) and culture of immortalized human dental mesenchymal cells (ihDMCs) was carried out as previously described (Huang et al., 2015b). BMP4 protein (R&D Systems, 314-BP-050) was added to the medium at the final concentration of 100 ng/ml. For small-molecule inhibition experiments, dorsomorphin (Sigma, P5499), SB203580 (CST, 5633), U0126 (CST, 9903), and SP600125 (Abcam, ab120065) were added into the medium at the final concentration of 20 μM. Dimethyl sulfoxide (DMSO) (Sigma, 76314) was used as the negative control. Immunofluorescence and Western blotting were used to verify the efficiency after 24 h.

RNA Interference, Immunocytochemical Staining, and Western Blotting

SMAD4 siRNA (Sigma, SASI_Hs01_00207794) or negative control siRNA were transfected into cells at a final concentration of 20 nM using Lipofectamine™ RNAiMAX Transfection Reagent (Thermo Fisher, 13778075) for 48 h. Transfections were performed when cells grow to 60–80% of the dishes. For immunofluorescence, tooth germs were fixed in 4%

paraformaldehyde (PFA), embedded in paraffin, and sectioned at 6 μm for immunohistochemical staining. After blocking in 5% bovine serum albumin (BSA), tissue sections and cell slides were then incubated with primary antibodies at 4°C overnight. Secondary antibodies were incubated at room temperature for 1 h followed by DAPI (Life, D1306) staining (sections for 2 min and cell slides for 1 min). For Western blot, cells were lysed using RIPA with protease inhibitor (Roche, 30559) followed by sonication of five cycles at 4°C. Proteins were separated with 12% SDS-PAGE gel and transferred to the nitrocellulose membrane. Subsequently, the membrane was blocked in 5% non-fat powdered milk at room temperature and then incubated with primary antibodies at 4°C overnight. Secondary antibodies were incubated at room temperature for 1 h, followed by visualizing. Semiquantitative analysis of Western blot and immunofluorescence mean values was carried out using Image J.[1]

The following primary antibodies were used: anti-pSMAD1/5/9 (CST, 13820), anti-SMAD4 (Abcam, ab40759), anti-MSX1 (R&D Systems, AF5045), anti-pSMAD2/3 (Santa Cruz, sc11769), anti-ERK1/2 (Sigma, M5670), anti-JNK (Santa Cruz, sc-6254), anti-pP38 (CST, 4511), and anti-ACTIN (Santa Cruz, sc58673). Secondary antibodies included donkey anti-mouse IgG (H + L) highly cross-adsorbed secondary antibody, Alexa Fluor 488 (Thermo, A-21202), Alexa Fluor 488 donkey anti-goat Ig (H + L) (Life, A11055), Alexa Fluor 594 donkey anti-goat Ig (H + L) (Life, A11058), donkey anti-rabbit IgG, Alexa Fluor 488 (Thermo, A-21206), Alexa Fluor 680 donkey anti-rabbit IgG (H + L) (Thermo, A10043), Alexa Fluor 680 donkey anti-goat Ig (H + L) (Life, A21084), and Alexa Fluor 790 donkey anti-mouse IgG (H + L) (Life, A11371). All the experiments were performed according to the instructions of the manufacturer and repeated at least three times.

In situ Proximity Ligation Assay

Tissue sections on glass slides were detected using Duolink® *in situ* Red Starter Kit (Sigma-Aldrich, DUO92101). Slides were blocked with Duolink blocking solution in a preheated humidity chamber for 30 min at 37°C and then incubated with anti-pSMAD1/5/9 (CST, 9511), anti-pSMAD2/3 (Santa Cruz, sc11769), and anti-SMAD4 (Invitrogen, MA5-15682) antibodies in the same chamber overnight at 4°C. Samples were incubated with proximity ligation assay (PLA) probe solution (anti-mouse PLA probe Minus and anti-rabbit PLA probe Plus or anti-goat PLA Plus) for 1 h at 37°C and then incubated with a ligation solution for 30 min followed by amplification reaction for 100 min at 37°C. Slides were mounted with a coverslip using a minimal volume of mounting medium containing DAPI.

RNA-Seq and Data Analysis

Total RNA of cultured hDMCs was extracted using the RNeasy Mini Kit (Qiagen, 74104). RNA samples were then used for quality control and library preparation. Illumilla HiSeq X Ten was used to perform sequencing using the 150-bp pair-end-read configuration. All the experiments were repeated three times. Data were analyzed using Galaxy. Reads were mapped to hg38 with HISAT2 (Kim et al., 2019) and were counted in genomic features using FeatureCounts software (Liao et al., 2014). DEseq2 was used to differ differential expressions (Love et al., 2014). TBtools was used to visualize Venn and for gene ontology (GO) enrichment analysis by default setting (Chen et al., 2020). Then, ggplot2 (Wickham, 2016) was used to visualize the GO enrichment result. The $\log_2$ transformed transcript level showed in the scatterplot was obtained using Seqmonk,[2] and the scatterplot was visualized using MATLAB.[3] The RNA-Seq data were deposited in the Gene Expression Omnibus (GEO) database (accession number: GSE179474).

RESULTS

Presence of Bone Morphogenetic Protein Intracellular Signal Transducers During Early Human Odontogenesis

To validate the functional operation of BMP signaling during human odontogenesis, based on our previous report on the expression patterns of BMP ligands, receptors, and antagonists in the human developing tooth germs (Dong et al., 2014), we first set out to further confirm the presence of BMP intracellular signal transducers during human tooth development using human cap-stage molar germs. Immunostaining showed that the major molecules that mediate canonical BMP signaling pathways including SMAD4 (**Figure 1A**) and pSMAD1/5/8 (**Figure 1B**) were abundantly present in the epithelium and mesenchyme of the tooth germs. We also detected an intense expression of SMAD2/3, the transducers involved in TGFβ signaling, that were overlapped with SMAD4 and pSMAD1/5/8 in the tooth germs (**Figure 1C**). Meanwhile, the expression of the central transducers of BMP/MAPK pathway pERK1/2, pP38, and pJNK was observed at a high level in the dental epithelium and mesenchyme, except for barely detectable pERK1/2 in the dental mesenchyme at this stage (**Figures 1D–F**). Thus, taken together with our previous report (Dong et al., 2014), all these observations indicate that BMP signaling, transduced both/either through SMADs and/or MAPK, is, in fact, operating during early human tooth development.

Expression of *MSX1* Is Regulated by Bone Morphogenetic Protein/SMAD1/5/8 Signaling in Early Human Tooth Germs

Msx1 has been demonstrated to be a BMP/Smad1/5/8 signaling target gene and is well known for its critical role in early tooth morphogenesis in mice (Jia et al., 2016). In humans, *MSX1* is also restricted to the dental mesenchyme as in mice (Lin et al., 2007) and is a crucial player in human odontogenesis as evidenced by the fact that mutation in *MSX1* results in Rieger syndrome, which exhibits severe tooth agenesis. To determine whether the regulation of *MSX1* expression by BMP/pSMAD1/5/8 is

[1] https://imagej.nih.gov/ij/index.html

[2] www.bioinformatics.babraham.ac.uk/projects/seqmonk/

[3] www.mathworks.com/products/matlab.html

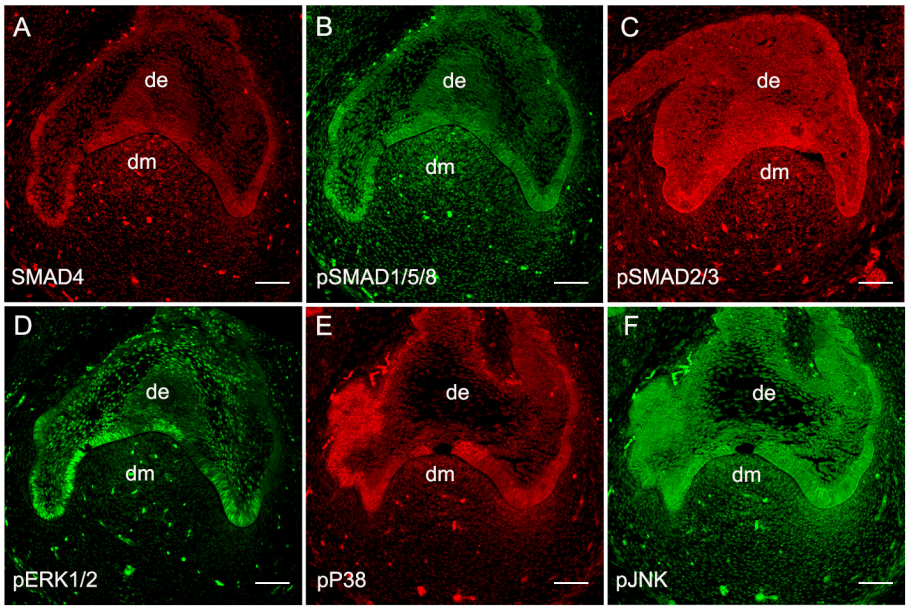

FIGURE 1 | Expression of BMP intracellular signal transducers at the human cap-stage tooth germ. **(A–C)** Expression of SMAD signal transducers: SMAD4 **(A)**, pSMAD1/5/8 **(B)**, and pSMAD2/3 **(C)**. **(D–F)** Expression of MAPK signal transducers: pERK1/2 **(D)**, pP38 **(E)**, and pJNK **(F)**. de, the dental epithelium; dm, the dental mesenchyme. Bar = 50 μm.

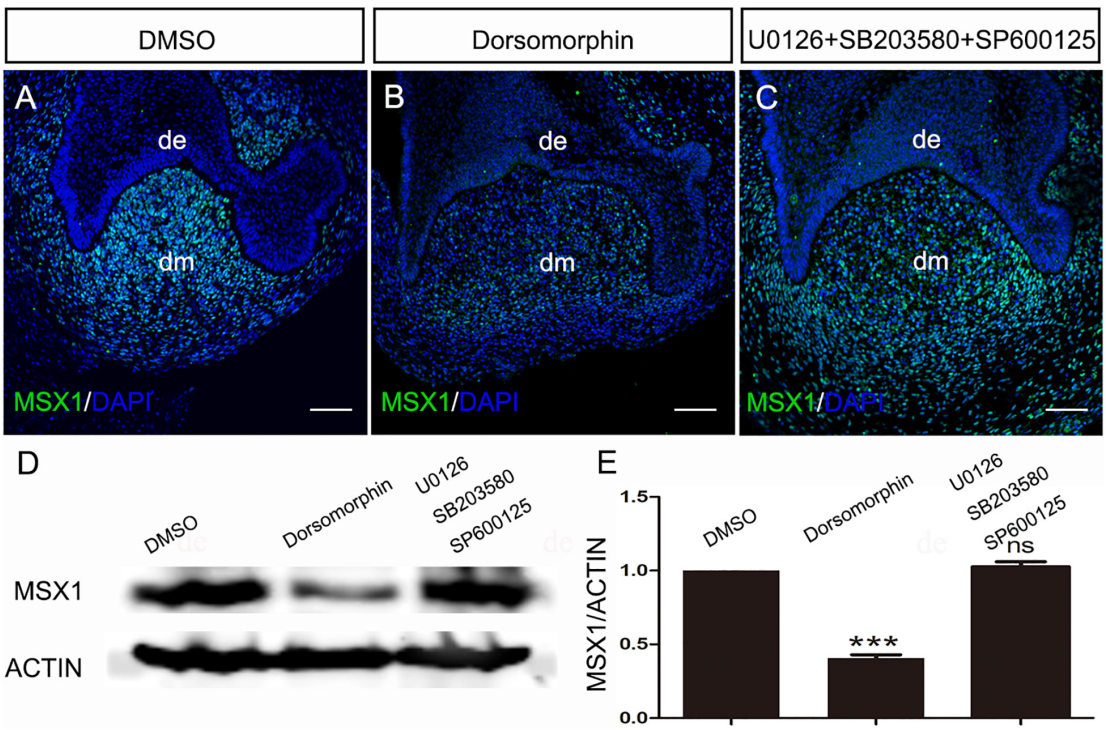

FIGURE 2 | Regulation of MSX1 expression is mediated by pSMAD1/5/8 in the human cap-stage tooth germs. **(A–C)** Immunostaining shows that MSX1 expression is abundant in dimethyl sulfoxide (DMSO)-treated human cap-stage tooth germs, dramatically reduced in dorsomorphin treated human cap-stage tooth germ, and unaltered in U0126 + SB203580 + SP600125 treated human cap-stage tooth germs. **(D)** A Western blot assay confirms the dramatically reduced expression of MSX1 in dorsomorphin treated human cap-stage tooth germs. Actin was used as the internal control. **(E)** Quantitative analysis of the Western blot assay. de, the dental epithelium; dm, the dental mesenchyme. Error bars represent SD. ***$p < 0.001$. Bar = 50 μm.

conserved during early human tooth development, we performed a small-molecule inhibition experiment using dorsomorphin (SMAD1/5/8 phosphorylation inhibitor) to specifically block transduction of BMP/pSMAD1/5/8 signaling pathway and combination of SB203508 (p38 MAPK inhibitor), U0126 (ERK1/2 inhibitor), and SP600125(JNK inhibitor) to specifically block BMP/MAPK signaling pathway (Xiao et al., 2017; Liu et al., 2018; Wang et al., 2019) in cap-stage human molar germs cultured *in vitro* with the Trowell-type organ culture system. Immunostaining showed that, after cultured for 24 h, the expression of *MSX1* was dramatically downregulated in dorsomorphin-treated molar tooth germs (**Figure 2B**), whereas it was hardly disturbed when treated with the combination of SB203508, U0126, and SP600125 (**Figure 2C**) as compared with that treated with DMSO (**Figure 2A**). This inhibition of *MSX1* expression by dorsomorphin but not SB203508, U0126, and SP600125 was further confirmed by Western blotting (**Figure 2D**), where more than 60% reduction in the *MSX1* expression level was quantified in dorsomorphin-treated human tooth germs compared with that in SB203508, U0126, and SP600125 co-treated human molar germs and DMSO-controls (**Figure 2E**). These results indicate that the regulation of *MSX1* expression is mediated by pSMAD1/5/8 signaling but not by MAPK in developing human dental mesenchyme.

SMAD4 Is Not Required for Bone Morphogenetic Protein4/pSMAD1/5/8-Induced *MSX1* Expression in the Human Dental Mesenchymal Cells

To elucidate whether *MSX1* expression regulated by BMP/pSMAD1/5/8 is also independent of SMAD4 in human dental mesenchyme as its mouse congener does, we then conducted SMAD4 siRNA knockdown experiments in hDMCs and ihDMCs that were isolated from bell-stage human molar germs and retains the expression of several tooth-specific markers including *MSX1* (Huang et al., 2015a). Approximately 60% knockdown efficiency of SMAD4 at the protein level was first verified by Western blotting in the hDMCs (**Figures 3A,B**) and ihDMCs (**Supplementary Figures 1A,B**) transfected with SMAD4 siRNA compared with that treated with control-siRNA for 48 h. Further RNAi experiments demonstrated that the nuclear translocation of pSMAD1/5/8 was SMAD4-independent as shown in **Figures 3C–N** and **Supplementary Figures 1C–K**. Weak nuclear staining of pSMAD1/5/8 was seen in the cultured hDMCs (**Figures 3C,I,L**) and ihDMCs (**Supplementary Figures 1C,F,I**), and this nuclear-located pSMAD1/5/8 became abundant after the addition of exogenous BMP4 and treated with control siRNA (**Figures 3D,J,M** and **Supplementary Figures 1D,G,J**), indicating that an active BMP-induced pSMAD1/5/8-translocation is operating in these cells. As expected, this nuclear translocation was not affected by *SMAD4* knockdown as evidenced by the presence of equally abundant nuclear pSMAD1/5/8 in these cultured cells when transfected with SMAD4 siRNA (**Figures 3E,K,N** and **Supplementary Figures 1E,H,K**) as compared with the control siRNA. Similarly, equally abundant MSX1 present in the nuclei of hDMCs (**Figures 3F–N**) and ihDMCs (**Supplementary Figures 2A–I**) treated with SMAD4 siRNA compared with that treated with control siRNA after induced with BMB4. The results were further confirmed by semiquantification (**Figures 3O,P**). Consistent with these findings, abundant pSMAD2/3-SMAD4 complexes (**Figure 4A**) but rare pSMAD1/5/8-SMAD4

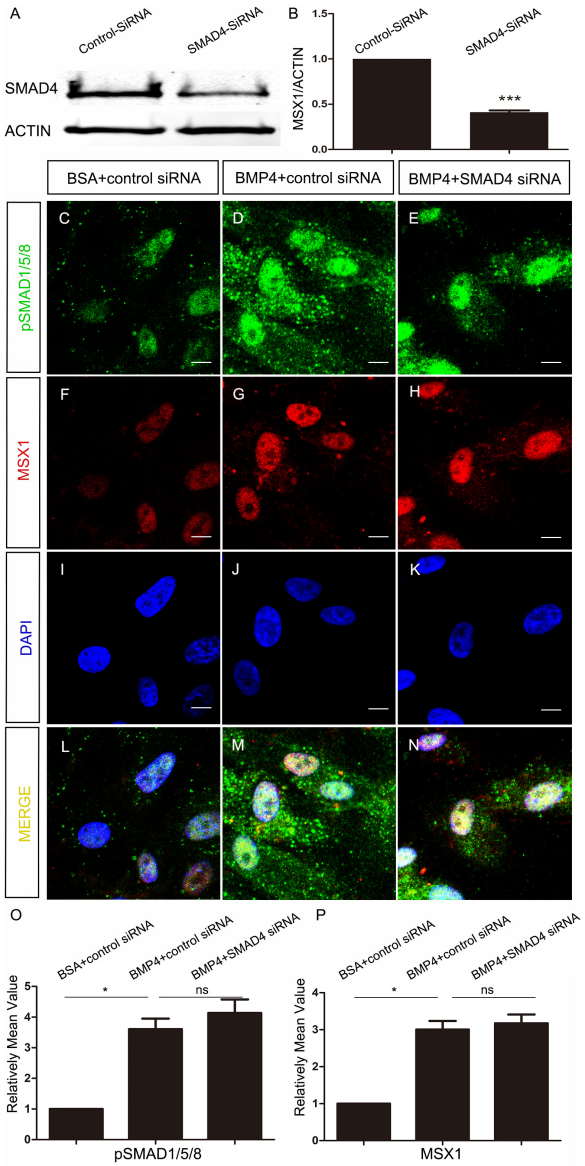

FIGURE 3 | SMAD4 is not required for BMP4-induced pSMAD1/5/8 nuclear translocation and MSX1 expression in the hDMCs. **(A,B)** Western blot shows approximately 60% knockdown efficiency of SMAD4 siRNA. **(C–N)** Co-immunostaining of MSX1 and pSMAD1/5/8 show that BMP4-induced pSMAD1/5/8 nuclear translocation and MSX1 expression are not affected by knockdown of SMAD4. **(O,P)** Quantitative analysis of relative mean fluorescence values shows that pSMAD1/5/8 and MSX1 expressions are not affected by the knockdown of SMAD4. Error bars represent SD. ns, $p > 0.05$; $^{*}p < 0.05$; and $^{***}p < 0.001$. Bar = 10 μm.

complexes (**Figure 4B**), visualized by PLA [an assay for detecting protein-protein interaction with high specificity and sensitivity, (Renfrow et al., 2011)], were found in the human cap-stage molar germs, suggesting that pSMAD2/3 possesses higher binding affinity with SMAD4 than pSMAD1/5/8 in the context of developing human teeth, and the absence of pSMAD1/5/8-SMAD4 complex could be the consequence of saturated SMAD4 by SMAD2/3. Together, our results provide compelling evidence that SMAD4 is dispensable for *MSX1* expression regulated by BMP/pSMAD1/5/8 signaling during early human tooth development.

Modulation of Bone Morphogenetic Protein/SMAD1/5/8 Signaling Cascade in a SMAD4-Independent Manner in the Human Dental Mesenchymal Cells

Nuclearly translocated pSMAD1/5/8 not only activates *MSX1* expression but also triggers a signaling cascade in association with other transcription factors and transcriptional coactivators or corepressors. To identify the gene set that is involved in the BMP/pSMAD1/5/8 signaling cascade, we compared the difference in the genome-wide transcriptome among hDMCs treated with BSA, BMP4, and BMP4 plus dorsomorphin, respectively, using RNA-Seq. Comparing of RNA-Seq data between BSA- and BMP4-treated hDMCs revealed that 794 genes are upregulated and 590 genes downregulated by BMP4 proteins (**Figures 5A,B**, blue oval). As expression alteration of these genes was triggered by BMP proteins, they are considered to be both involved in BMP canonical and non-canonical pathways. To distinguish genes involved in BMP/pSMAD1/5/8 signaling cascade from genes belonging to the entire BMP signaling cascade, we further conducted RNA-Seq on the hDMCs treated with BMP4 + DMSO and BMP4 + dorsomorphin (pSMAD1/5/8 inhibitor), respectively. Comparison of these two RNA-Seq data sets identified 2,551 downregulated genes and 2,666 upregulated genes (**Figures 5A,B**, pink oval). Since dorsomorphin exerts an inhibitive effect on pSMAD1/5/8 function and would restrain its downstream target gene activity, the downregulated and upregulated genes identified in the above inhibitive experiment would be in an opposing situation, i.e., the downregulated would be the upregulated and vice versa, in the normal physiological condition in the hDMCs (**Figures 5A,B**). Comparison of genes associated with BMP signaling cascade and genes with pSMAD1/5/8 signaling cascade identified 586 overlapped genes that are involved in BMP/pSMAD1/5/8 signaling cascade with 352 genes upregulated and 234 genes downregulated when treated with BMP4 in hDMCs (**Figures 5A,B** and **Supplementary Table 1**). GO analysis showed that these genes are primarily involved in development and morphogenesis (**Figure 5C**). Several studies demonstrated that ∼60% RNAi efficiency of critical upstream genes was capable of altering the expression pattern of downstream genes by RNA-Seq analysis (Brooks et al., 2011; Sun et al., 2018; Smekalova et al., 2020). Therefore, we further performed RNA-Seq on the hDMCs treated with BMP4 + control siRNA and BMP4 + SMAD4 siRNA, respectively, to test if the expression levels of these 586 genes involved in the BMP/pSMAD1/5/8 signaling cascade are altered by knockdown of *SMAD4*. Comparison of RNA-Seq data from 352 upregulated genes and 234 downregulated genes is plotted in **Figure 5D**. The dots are distributed along the diagonal line although there are genes, particularly the genes with lower expression levels, apparently deviated from the diagonal line. These deviations could be the consequence of indirect regulation of them by pSMAD1/5/8 and crosstalk/interaction among the signaling pathways that constitute the complex signal network of the cell. Actually, when chasing down the genes that have been demonstrated to play crucial roles in tooth development and are directly bound by pSMAD1/5/8 at their promoter domains (Genander et al., 2014), including *MSX1*, *MSX2*, *SP6*, *FGFR2*, *ID3*, *DLX1*, *DLX2,* and *DLX3* (Zhang et al., 2003; Choi et al., 2010; Nakamura et al., 2012; Huang et al., 2015a; Aurrekoetxea et al., 2016; Gong et al., 2020; Hu et al., 2020; **Figure 5D**, red dot), we found that they are closely situated along the diagonal line, indicating that *SMAD4* is not required for modulation of pSMAD1/5/8 direct target genes when triggered with BMP4.

DISCUSSION

In this study, we provided compelling evidence that, as in the mouse, the atypical canonical BMP signaling pathway is in fact operating during early human tooth development. We demonstrated that, in the human dental mesenchyme, pSMAD1/5/8 are able to transduce BMP signal to regulate the expression of downstream target gene *MSX1* in a *SMAD4* independent manner, as evidenced by the fact that *MSX1* expression is inhibited by dorsomorphin in the human cap stage tooth germ and that knockdown of *SMAD4* by siRNA exhibits no effect on BMP-induced pSMAD1/5/8 nuclear translocation and *MSX1* expression in hDMCs. This notion is further strengthened by the fact that the BMP-induced expression of genes involved in BMP/SMAD1/5/8 signaling cascade, such as *MSX1*, *MSX2*, *SP6*, *FGFR2*, *RSPO2*, *ID3*, *DLX1*, *DLX2,* and *DLX3*, which have been demonstrated to play critical roles in tooth development and to their promoters pSMAD1/5/8 directly bind, is *SMAD4*-independent, as estimated by *SMAD4* knockdown and RNA-Seq analysis. PLA shows that the cytoplasmic SMAD4 in human dental mesenchymal cells is saturated by pSMAD2/3 to form pSMAD2/3-SMAD4 complexes, a central signal transduction element for TGFβ/Smad2/3 signaling pathways, which also play important functions in tooth development (Ohta et al., 2018).

Since the partnership between SMAD4 and mothers against decapentaplegic homolog (SMAD) proteins in TGFβ signaling pathways was verified in *Xenopus* embryos and breast epithelial cells (Lagna et al., 1996), numerous studies have demonstrated that *SMAD4* functioning as a central mediator (common-partner SMAD) is indispensable in BMP/SMAD1/5/8 and TGFβ/activin/2/3 signaling pathways that exert essential functions during embryonic development and are also involved tissue homeostasis and regeneration in the adults (Nickel and Mueller, 2019). However, this widely accepted model that Smad4 is indispensable for SMAD signal transduction has been challenged by *Smad4* knockout studies in several developing

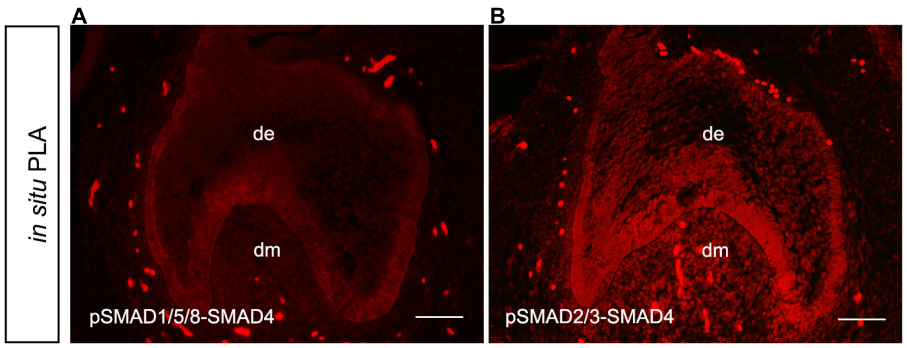

FIGURE 4 | Absence of pSMAD1/5/8-SMAD4 complex in the hDMCs. *In situ* proximity ligation assay (PLA) shows barely detectable pSMAD1/5/8-SMAD4 complexes **(A)** but abundant pSMAD2/3-SMAD4 complexes **(B)** in hDMCs. Bar = 50 μm.

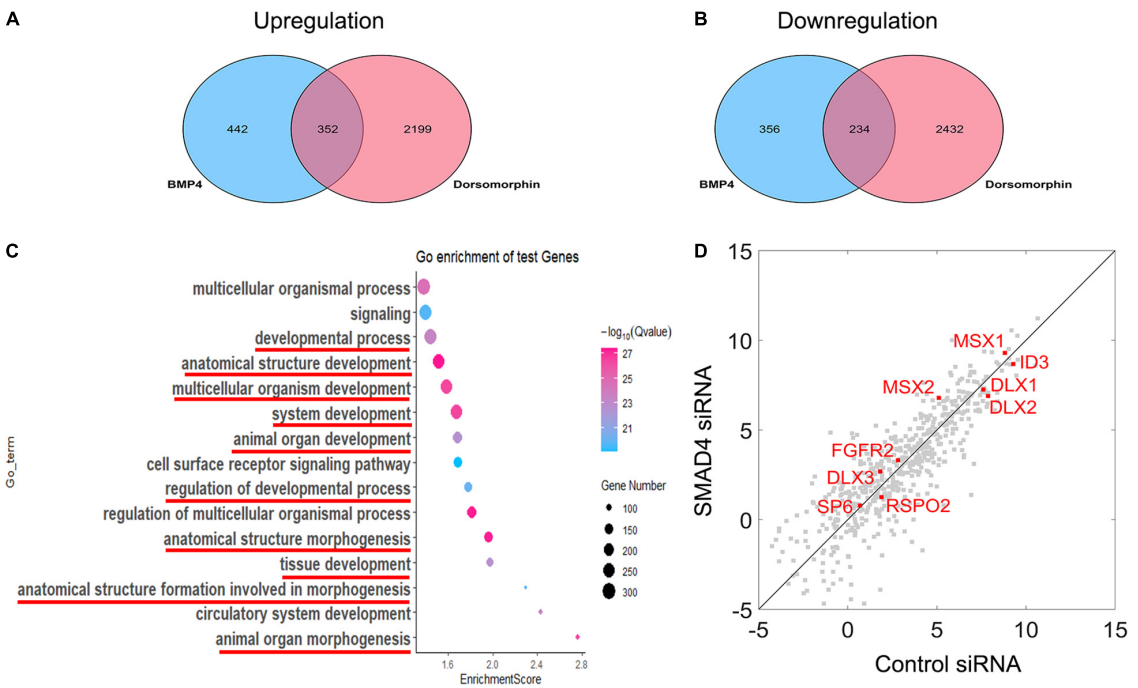

FIGURE 5 | RNA-Seq analysis reveals that the modulation of BMP/pSMAD1/5/8 is SMAD4-independent. **(A,B)** Venn diagram showing the overlap between BMP4-induced and dorsomorphin-inhibited mRNA transcripts and the mRNA ≥1 × changed in hDMCs. **(C)** Gene ontology analysis shows that the upregulated and downregulated genes are primarily involved in development and morphogenesis (red line). The scatterplot reveals differences in transcript abundance between control siRNA-treated hDMCs and SMAD4 siRNA-treated hDMCs. **(D)** Transcript levels are log2 transformed. The genes that have been demonstrated to be crucial in tooth development and their regulatory domains (promoters) are directly bound by pSMAD1/5/8 as well are indicated in red.

organs. Specific inactivation of Smad4 in the early mouse epiblast resulted in a profound failure to pattern derivatives of the anterior primitive streak, including prechordal plate, node, notochord, and definitive endoderm, whereas the TGFβ- and BMP-regulated processes involved in mesoderm formation and patterning are unaffected, which results in the normal formation of the allantois, a rudimentary heart, somite, and lateral plate mesoderm. These results suggest that *Smad4* is dispensable for some tissue and organ formation during early embryonic development (Chu et al., 2004). Conditional knockout of *Smad1* and *Smad5* introduced severe phenotypes including cerebellar hypoplasia, reduced granule cell numbers, and disorganized Purkinje neuron migration, whereas conditional inactivation of *Smad4* resulted in only very mild cerebellar defects during nervous system development (Tong and Kwan, 2013). *Smad4*-independent events were also found in TGFβ signaling pathways. For instance, TGFβ/Smad2/3-dependent Mad1 induction and keratinocyte differentiation are independent of *Smad4* during cell-cycle exit and differentiation of suprabasal epidermal keratinocytes. It is IκB kinase but not Smad4 serves as a nuclear cofactor for Smad2/3 recruitment to *Mad1* chromatin (Descargues et al., 2008). Yang et al. (2014) demonstrated

that the BMP canonical signaling pathway is operating in a Smad1/5/8-dependent but *Smad4*-independent manner in the dental mesenchyme during marine early odontogenesis, named as the atypical BMP canonical signaling pathway. The absence of pSmad1/5/8-Smad4 complexes is the consequence of the saturation of Smad4 by Smad2/3 in the dental mesenchymal cells. In this investigation, we provided compelling evidence that this atypical BMP canonical signaling pathway is fully conserved in humans.

According to the study by Nickel and Mueller, the dilemma for the SMAD study is that many growth factors but just two principal signaling pathways: "A hallmark of the TGF protein family is that all of the more than 30 growth factors identified to date signal by binding and hetero-oligomerization of a very limited set of transmembrane serine-threonine kinase receptors. [. . .] This discrepancy indicates that our current view of TGF signaling initiation just by hetero-oligomerization of two receptor subtypes and transduction *via* two main pathways in an on-off switch manner is too simplified" (Nickel and Mueller, 2019). The report by Yang et al. (2014) together with this study implies that tinkering of the SMAD signaling by weeding out extant components, such as SMAD4, and adding additional components, such as IκB kinase (Descargues et al., 2008), may allow diversification of signal transduction and downstream target gene activation at the cellular level. This certainly warrants further attention.

Although the human and mouse teeth share considerable homology throughout the developmental stages (Zhang et al., 2005), they do manifest heterodont dentition and apparently various morphologies including developmental phase, shape, and pattern. It is suggested that the diversity of tooth morphology resulted from the tinkering of the conserved signal pathway instead of creating novel ones during evolution (Tummers and Thesleff, 2009). Our recent studies revealed distinct expression patterns of genes involved in the major conserved signal pathways, such as SHH (Hu et al., 2013), WNT(Wang et al., 2014), FGF(Huang et al., 2015a), and BMP (Dong et al., 2014) signaling. For instance, our previous study showed that, as in the mouse, BMP ligands including BMP2, 3, 4, and 7 are also expressed in the cap and bell stages of human tooth germs (Dong et al., 2014). However, these genes are expressed in a broad and persistent pattern in both the dental epithelium and mesenchyme throughout the early cap to the late bell stage in humans, unlike in mice their expression is restricted to the limited region of the tooth germ, such as enamel knot, and appears in limited periods of time. We believe that this spatial-temporal difference in gene expression would confer engaged cells and/or tissues with specific biological behavior such as proliferation, apoptosis, and differentiation and result in characteristic tooth morphology of their own. In this study, we found that the central intracellular signal transducer involved in the BMP/MAPK signaling pathway, such as pERK1/2, pP38, and pJNK, and involved in SMAD signaling, including SMAD4, SMAD1/5/8, and SMAD2/3, are all present in the cap-stage human tooth germ, indicating operating and importance of BMP signaling during early human odontogenesis. We demonstrated that an intracellular BMP signal transduction pathway, the atypical canonical BMP signaling pathway, is fully conserved between humans and mice. Our results provide evidence that the diversity of tooth morphology in different species may be resulted from tinkering of the extracellular signal molecules with distinct distributing pattern instead of tinkering with intracellular signal transduction in mammal.

A large portion of the human population has congenitally missing teeth, and the probability of tooth loss increases with the age of a person. The pressing demand for replacement teeth in regenerative dental medicine has brought up a matter of great urgency to explore the molecular mechanisms that regulate tooth development in humans. However, the major bulk of our current knowledge on tooth development derives from studies on mice. Unveiling the molecular basis involved in human tooth morphogenesis will provide important insight for studying genetically related dental abnormalities and tooth regeneration in humans.

DATA AVAILABILITY STATEMENT

The datasets presented in this study can be found in online repositories. The names of the repository/repositories and accession number(s) can be found in the article/ **Supplementary Material**.

ETHICS STATEMENT

The studies involving human participants were reviewed and approved by Ethics Committee of Fujian Normal University. The patients/participants provided their written informed consent to participate in this study.

AUTHOR CONTRIBUTIONS

XXH contributed to the conception, experimental data acquisition and analysis, and draft. CL and NR contributed to experimental data acquisition. ZH contributed to data analysis. XFH and YZ contributed to conception and manuscript revision. All authors contributed to the article and approved the submitted version.

FUNDING

This study was supported by the National Natural Science Foundation of China (Grant Nos. 81870739, 81271102, 81771034, and 28170917) and the Natural Science Foundation of Fujian Province (Grant No. 2020J01180).

SUPPLEMENTARY MATERIAL

The Supplementary Material for this article can be found online at: https://www.frontiersin.org/articles/10.3389/fphys.2022.823275/full#supplementary-material

REFERENCES

Aurrekoetxea, M., Irastorza, I., Garcia-Gallastegui, P., Jimenez-Rojo, L., Nakamura, T., Yamada, Y., et al. (2016). Wnt/beta-catenin regulates the activity of epiprofin/Sp6, SHH, FGF, and BMP to coordinate the stages of odontogenesis. *Front. Cell Dev. Biol* 4:25. doi: 10.3389/fcell.2016.00025

Bei, M., Kratochwil, K., and Maas, R. L. (2000). BMP4 rescues a non-cell-autonomous function of Msx1 in tooth development. *Development* 127, 4711–4718.

Brooks, A. N., Yang, L., Duff, M. O., Hansen, K. D., Park, J. W., Dudoit, S., et al. (2011). Conservation of an RNA regulatory map between *Drosophila* and mammals. *Genome Res.* 21, 193–202. doi: 10.1101/gr.108662.110

Chen, C., Chen, H., Zhang, Y., Thomas, H. R., Frank, M. H., He, Y., et al. (2020). TBtools: an integrative toolkit developed for interactive analyses of big biological data. *Mol. Plant* 13, 1194–1202. doi: 10.1016/j.molp.2020.06.009

Choi, S. J., Song, I. S., Feng, J. Q., Gao, T., Haruyama, N., Gautam, P., et al. (2010). Mutant DLX 3 disrupts odontoblast polarization and dentin formation. *Dev. Biol.* 344, 682–692. doi: 10.1016/j.ydbio.2010.05.499

Chu, G. C., Dunn, N. R., Anderson, D. C., Oxburgh, L., and Robertson, E. J. (2004). Differential requirements for Smad4 in TGFbeta-dependent patterning of the early mouse embryo. *Development* 131, 3501–3512. doi: 10.1242/dev.01248

Descargues, P., Sil, A. K., Sano, Y., Korchynskyi, O., Han, G., Owens, P., et al. (2008). IKKalpha is a critical coregulator of a Smad4-independent TGFbeta-Smad2/3 signaling pathway that controls keratinocyte differentiation. *Proc. Natl. Acad. Sci. U.S.A.* 105, 2487–2492. doi: 10.1073/pnas.0712044105

Dong, X., Shen, B., Ruan, N., Guan, Z., Zhang, Y., Chen, Y., et al. (2014). Expression patterns of genes critical for BMP signaling pathway in developing human primary tooth germs. *Histochem. Cell Biol.* 142, 657–665. doi: 10.1007/s00418-014-1241-y

Genander, M., Cook, P. J., Ramskold, D., Keyes, B. E., Mertz, A. F., Sandberg, R., et al. (2014). BMP signaling and its pSMAD1/5 target genes differentially regulate hair follicle stem cell lineages. *Cell Stem. Cell* 15, 619–633. doi: 10.1016/j.stem.2014.09.009

Gong, Y., Yuan, S., Sun, J., Wang, Y., Liu, S., Guo, R., et al. (2020). R-spondin 2 induces odontogenic differentiation of dental pulp stem/progenitor cells via regulation of Wnt/beta-catenin signaling. *Front Physiol* 11:918. doi: 10.3389/fphys.2020.00918

Hu, L., Xu, J., Wu, T., Fan, Z., Sun, L., Liu, Y., et al. (2020). Depletion of ID3 enhances mesenchymal stem cells therapy by targeting BMP4 in Sjogren's syndrome. *Cell Death Dis.* 11:172. doi: 10.1038/s41419-020-2359-6

Hu, X., Zhang, S., Chen, G., Lin, C., Huang, Z., Chen, Y., et al. (2013). Expression of SHH signaling molecules in the developing human primary dentition. *BMC Dev. Biol.* 13:11. doi: 10.1186/1471-213X-13-11

Huang, Y., Yang, Y., Jiang, M., Lin, M., Li, S., and Lin, Y. (2015b). Immortalization and characterization of human dental mesenchymal cells. *J. Dent.* 43, 576–582. doi: 10.1016/j.jdent.2015.02.008

Huang, F., Hu, X., Fang, C., Liu, H., Lin, C., Zhang, Y., et al. (2015a). Expression profile of critical genes involved in FGF signaling pathway in the developing human primary dentition. *Histochem. Cell Biol.* 144, 457–469. doi: 10.1007/s00418-015-1358-7

Jernvall, J., Aberg, T., Kettunen, P., Keranen, S., and Thesleff, I. (1998). The life history of an embryonic signaling center: BMP-4 induces p21 and is associated with apoptosis in the mouse tooth enamel knot. *Development* 125, 161–169.

Jia, S., Kwon, H. E., Lan, Y., Zhou, J., Liu, H., and Jiang, R. (2016). Bmp4-Msx1 signaling and Osr2 control tooth organogenesis through antagonistic regulation of secreted Wnt antagonists. *Dev. Biol.* 420, 110–119. doi: 10.1016/j.ydbio.2016.10.001

Jia, S., Zhou, J., Gao, Y., Baek, J. A., Martin, J. F., Lan, Y., et al. (2013). Roles of Bmp4 during tooth morphogenesis and sequential tooth formation. *Development* 140, 423–432. doi: 10.1242/dev.081927

Kim, D., Paggi, J. M., Park, C., Bennett, C., and Salzberg, S. L. (2019). Graph-based genome alignment and genotyping with HISAT2 and HISAT-genotype. *Nat. Biotechnol.* 37, 907–915. doi: 10.1038/s41587-019-0201-4

Lagna, G., Hata, A., Hemmati-Brivanlou, A., and Massagué, J. (1996). Partnership between DPC4 and SMAD proteins in TGF-beta signalling pathways. *Nature* 383, 832–836. doi: 10.1038/383832a0

Li, J., Huang, X., Xu, X., Mayo, J., Bringas, P. Jr., Jiang, R., et al. (2011). SMAD4-mediated WNT signaling controls the fate of cranial neural crest cells during tooth morphogenesis. *Development* 138, 1977–1989. doi: 10.1242/dev.061341

Liao, Y., Smyth, G. K., and Shi, W. (2014). featureCounts: an efficient general purpose program for assigning sequence reads to genomic features. *Bioinformatics* 30, 923–930. doi: 10.1093/bioinformatics/btt656

Lin, D., Huang, Y., He, F., Gu, S., Zhang, G., Chen, Y., et al. (2007). Expression survey of genes critical for tooth development in the human embryonic tooth germ. *Dev. Dyn.* 236, 1307–1312. doi: 10.1002/dvdy.21127

Liu, F., Feng, X. X., Zhu, S. L., Huang, H. Y., Chen, Y. D., Pan, Y. F., et al. (2018). Sonic hedgehog signaling pathway mediates proliferation and migration of fibroblast-like synoviocytes in rheumatoid arthritis via MAPK/ERK signaling pathway. *Front. Immunol.* 9:2847. doi: 10.3389/fimmu.2018.02847

Love, M. I., Huber, W., and Anders, S. (2014). Moderated estimation of fold change and dispersion for RNA-seq data with DESeq2. *Genome Biol.* 15, 550. doi: 10.1186/s13059-014-0550-8

Mitsiadis, T. A., Graf, D., Luder, H., Gridley, T., and Bluteau, G. (2010). BMPs and FGFs target Notch signalling via jagged 2 to regulate tooth morphogenesis and cytodifferentiation. *Development* 137, 3025–3035. doi: 10.1242/dev.049528

Miyazono, K., Kamiya, Y., and Morikawa, M. (2010). Bone morphogenetic protein receptors and signal transduction. *J. Biochem.* 147, 35–51. doi: 10.1093/jb/mvp148

Nakamura, T., Yamada, Y., and Fukumoto, S. (2012). "Review: the regulation of tooth development and morphogenesis," in *Interface Oral Health Science 2011* eds K. Sasaki, O. Suzuki, and N. Takahashi (Tokyo: Springer). doi: 10.1007/978-4-431-54070-0_3

Nickel, J., and Mueller, T. D. (2019). Specification of BMP signaling. *Cells* 8:1579. doi: 10.3390/cells8121579

Nie, X., Luukko, K., and Kettunen, P. (2006). BMP signalling in craniofacial development. *Int. J. Dev. Biol.* 50, 511–521. doi: 10.1387/ijdb.052101xn

Nohe, A., Keating, E., Knaus, P., and Petersen, N. O. (2004). Signal transduction of bone morphogenetic protein receptors. *Cell Signal* 16, 291–299. doi: 10.1016/j.cellsig.2003.08.011

Ohta, M., Chosa, N., Kyakumoto, S., Yokota, S., Okubo, N., Nemoto, A., et al. (2018). IL1beta and TNFalpha suppress TGFbetapromoted NGF expression in periodontal ligamentderived fibroblasts through inactivation of TGFbetainduced Smad2/3 and p38 MAPKmediated signals. *Int. J. Mol. Med.* 42, 1484–1494. doi: 10.3892/ijmm.2018.3714

Renfrow, J. J., Scheck, A. C., Dhawan, N. S., Lukac, P. J., Vogel, H., Chandler, J. P., et al. (2011). Gene-protein correlation in single cells. *Neuro Oncol.* 13, 880–885. doi: 10.1093/neuonc/nor071

Retting, K. N., Song, B., Yoon, B. S., and Lyons, K. M. (2009). BMP canonical Smad signaling through Smad1 and Smad5 is required for endochondral bone formation. *Development* 136, 1093–1104. doi: 10.1242/dev.029926

Smekalova, E. M., Gerashchenko, M. V., O'Connor, P. B. F., Whittaker, C. A., Kauffman, K. J., Fefilova, A. S., et al. (2020). In Vivo RNAi-mediated eIF3m knockdown affects ribosome biogenesis and transcription but has limited impact on mRNA-specific translation. *Mol. Ther. Nucleic Acids* 19, 252–266. doi: 10.1016/j.omtn.2019.11.009

Sun, Y., Luo, G., Zhao, L., Huang, L., Qin, Y., Su, Y., et al. (2018). Integration of RNAi and RNA-seq reveals the immune responses of epinephelus coioides to sigX gene of *Pseudomonas* plecoglossicida. *Front. Immunol.* 9:1624. doi: 10.3389/fimmu.2018.01624

Tong, K. K., and Kwan, K. M. (2013). Common partner Smad-independent canonical bone morphogenetic protein signaling in the specification process of the anterior rhombic lip during cerebellum development. *Mol. Cell Biol.* 33, 1925–1937. doi: 10.1128/mcb.01143-12

Tummers, M., and Thesleff, I. (2009). The importance of signal pathway modulation in all aspects of tooth development. *J. Exp. Zool. B Mol. Dev. Evol.* 312B, 309–319. doi: 10.1002/jez.b.21280

Wang, B., Li, H., Liu, Y., Lin, X., Lin, Y., Wang, Y., et al. (2014). Expression patterns of WNT/beta-CATENIN signaling molecules during human tooth development. *J. Mol. Histol.* 45, 487–496. doi: 10.1007/s10735-014-9572-5

Wang, Q., Yuan, X., Li, B., Sun, D., Liu, J., Liu, T., et al. (2019). Roles of SP600125 in expression of JNK, RANKL and OPG in cultured dental follicle cells. *Mol. Biol. Rep.* 46, 3073–3081. doi: 10.1007/s11033-019-04745-3

Wickham, H. (2016). *ggplot2: Elegant Graphics for Data Analysis*. New York, NY: Springer-Verlag.

Xiao, Y. T., Yan, W. H., Cao, Y., Yan, J. K., and Cai, W. (2017). P38 MAPK pharmacological inhibitor SB203580 alleviates total parenteral nutrition-induced loss of intestinal barrier function but promotes hepatocyte lipoapoptosis. *Cell Physiol. Biochem.* 41, 623–634. doi: 10.1159/000457933

Xu, X., Han, J., Ito, Y., Bringas, P. Jr., Deng, C., and Chai, Y. (2008). Ectodermal Smad4 and p38 MAPK are functionally redundant in mediating TGF-beta/BMP signaling during tooth and palate development. *Dev. Cell* 15, 322–329. doi: 10.1016/j.devcel.2008.06.004

Yang, G., Yuan, G., Ye, W., Cho, K. W., and Chen, Y. (2014). An atypical canonical bone morphogenetic protein (BMP) signaling pathway regulates Msh homeobox 1 (Msx1) expression during odontogenesis. *J. Biol. Chem.* 289, 31492–31502. doi: 10.1074/jbc.M114.600064

Zhang, Y. D., Chen, Z., Song, Y. Q., Liu, C., and Chen, Y. P. (2005). Making a tooth: growth factors, transcription factors, and stem cells. *Cell Res.* 15, 301–316. doi: 10.1038/sj.cr.7290299

Zhang, Z., Zhang, X., Avniel, W. A., Song, Y., Jones, S. M., Jones, T. A., et al. (2003). Malleal processus brevis is dispensable for normal hearing in mice. *Dev. Dyn.* 227, 69–77. doi: 10.1002/dvdy.10288

Conflict of Interest: The authors declare that the research was conducted in the absence of any commercial or financial relationships that could be construed as a potential conflict of interest.

frontiers in Physiology

ORIGINAL RESEARCH
published: 09 February 2022
doi: 10.3389/fphys.2021.760223

circKLF4 Upregulates *Klf4* and *Endoglin* to Promote Odontoblastic Differentiation of Mouse Dental Papilla Cells *via* Sponging miRNA-1895 and miRNA-5046

*Yue Zhang†, Hao Zhang†, Guohua Yuan and Guobin Yang**

The State Key Laboratory Breeding Base of Basic Science of Stomatology and Key Laboratory of Oral Biomedicine of Ministry of Education, School and Hospital of Stomatology, Wuhan University, Wuhan, China

OPEN ACCESS

Edited by:
Jean-Pierre Saint-Jeannet, New York University, United States

Reviewed by:
Emi Shimizu, Rutgers School of Dental Medicine, The State University of New Jersey, United States
Joo Cheol Park, Seoul National University, South Korea

***Correspondence:**
Guobin Yang
guobin.yang@whu.edu.cn

† These authors have contributed equally to this work

Specialty section:
This article was submitted to Craniofacial Biology and Dental Research, a section of the journal Frontiers in Physiology

Received: *17 August 2021*
Accepted: *29 October 2021*
Published: *09 February 2022*

Citation:
Zhang Y, Zhang H, Yuan G and Yang G (2022) circKLF4 Upregulates Klf4 and Endoglin to Promote Odontoblastic Differentiation of Mouse Dental Papilla Cells via Sponging miRNA-1895 and miRNA-5046. Front. Physiol. 12:760223. doi: 10.3389/fphys.2021.760223

circular RNAs (circRNAs) is a broad and diverse endogenous subfamily of non-coding RNAs, regulating the gene expression by acting as a microRNA (miRNA) sponge. However, the biological functions of circRNAs in odontoblast differentiation remain largely unknown. Our preliminary study identified an unknown mouse circRNA by circRNA sequencing generated from mouse dental papilla and we termed it circKLF4. In this study, quantitative real-time PCR and *in situ* hybridization were used and demonstrated that circKLF4 was upregulated during odontoblastic differentiation. Gene knockdown and overexpression assays indicated that circKLF4 promoted odontoblastic differentiation of mouse dental papilla cells (mDPCs). Mechanistically, we found that circKLF4 increased the linear KLF4 expression in a microRNA-dependent manner. By mutating the binding sites of microRNA and circKLF4, we further confirmed that circKLF4 acted as sponge of miRNA-1895 and miRNA-5046 to promote the expression of KLF4. We then also found that ENDOGLIN was also up-regulated by circKLF4 by transfection of circKLF4 overexpression plasmids with or without microRNA inhibitor. In conclusion, circKLF4 increases the expression of KLF4 and ENDOGLIN to promote odontoblastic differentiation *via* sponging miRNA-1895 and miRNA-5046.

Keywords: circRNA, KLF4, dental papilla cells, odontoblasts, differentiation

INTRODUCTION

Neural crest derived dental papilla cells play pivotal role in odontoblast differentiation, during which multiple signaling molecules, receptors, and transcription factors have been implicated in mediating odontoblast differentiation (Zhang et al., 2005). Odontoblasts are differentiated cells that produce dentin and (Dassule et al., 2000) and dental papilla cells are usually used to investigate odontoblast differentiation mechanism *in vitro* (Thesleff et al., 1987). With the in-depth research on the odontoblast differentiation, the molecular research mechanism about non-coding RNAs (ncRNAs) was implicated in this differentiation processes (Sun et al., 2015).

ncRNAs play crucial roles in many biological processes. As a member of ncRNAs family, circular RNAs (circRNAs) have become new research hotspots with the rapid development of high-throughput sequencing (RNA-seq) and bioinformatics recently (Sun et al., 2020). Unlike the linear

RNAs with 5′ and 3′ termini, circRNAs is a new class of RNA composed of covalently single-stranded closed circular structure due to alternative splicing and back-splicing processes (Memczak et al., 2013; Ashwal-Fluss et al., 2014). Lacking 5′-caps and 3′-tails render circRNAs higher degrees of sequence conservation and stability (Capel et al., 1993; Pasman et al., 1996). circRNAs are ubiquitous across multiple species and the abundance of the circRNAs is approximately 5–10% of their linear counterparts for circular RNA isoforms of most genes. Furthermore, it is estimated that the circular transcript isoforms of some genes are more abundant than linear isoforms for some genes (Salzman et al., 2012, 2013). Besides, circRNAs exhibits tissue-specific and development stage-dependent patterns, which indicates its important role in regulating physiological activities (Memczak et al., 2013; Salzman et al., 2013; Szabo et al., 2015; Greene et al., 2017). Emerging evidence has revealed that circRNAs participate in osteogenesis of periodontal ligament stem cell (PDLSCs) by interacting with miRNA (Gu et al., 2017). Moreover, 154 differentially expressed circRNAs were found to associate with osteogenic differentiation in MC3T3-E1 cells (Qian et al., 2017). In our preliminary study, using circRNA sequencing, we detected the differential expression of circRNAs in mouse dental papilla cells (mDPCs) cultured in either growth medium or differentiation medium for 9 days. Based on these data, we found that 3,255 and 809 circRNAs were upregulated and downregulated after 9 days' induction of differentiation. These circRNAs profiles suggested that the differentially expressed circRNAs had specific functions during odontogenesis. We screened that the expression level of circRNA_ID:4:55530561-55530959 was 6.7 times more than that in the control group, which indicates its close relationship to odontoblast differentiation. According to its sequence, we confirmed that this circRNA was derived from the third exon of *Klf4*. As a newly discovered circRNA absent from circBase,[1] we term it circKLF4. Concerning the important function of its parental gene, *Klf4*, during odontoblastic differentiation (Lin et al., 2013; Tao et al., 2019), we supposed that circKLF4 might be closely related to the odontoblast differentiation.

In this study, we investigated the role circKLF4 plays during the odontoblastic differentiation of mDPCs and the underlying molecular mechanism during this process.

MATERIALS AND METHODS

The entire study satisfied the requirements of the Ethics Committee of the School of Stomotology, Wuhan University (protocol 00266935).

Cell/Tissue Isolation and Culture

The primary mDPCs were separated from Kunming mice (China) at embryonic day (E) 18.5, digested with 3 mg/mL trypsin and cultured in Dulbecco modified Eagle medium (DMEM; Hyclone) supplemented with 10% fetal bovine serum (FBS; Gibco) and 1% penicillin/streptomycin (Hyclone). mDPCs were seeded in a 12-well plate at an initial density of 1×10^5 cells/well. The culture medium was changed every 2–3 days as previously described (Lin et al., 2013). The dental pulp tissues were isolated from mandibular molar teeth of six Kunming mice (China) at postnatal day (PN) 21.

Odontoblastic Differentiation of mDPCs

For odontoblastic differentiation induction, mDPCs were incubated with 1 mL of DMEM supplemented with 10% FBS, 1% penicillin/streptomycin, 50 μg/mL ascorbic acid (Sigma-Aldrich), 10 mmol/L β-glycerophosphate (Sigma-Aldrich) and 10 nmol/L dexamethasone (Sigma-Aldrich) after the cells became confluent.

In situ Hybridization

Kunming mice were sacrificed for sample collection at PN 1. Tissues for *in situ* hybridizations were dissected and fixed in 4% paraformaldehyde. Samples were followed by paraffin embedding and sectioning. Digoxin-labeled specific targeting the mouse circKLF4 probe was prepared and the *in situ* hybridization procedures were performed as described earlier (Yuan et al., 2009). Briefly, hybridization was performed at 65–68°C overnight in a solution containing 50% formamide, 0.5 mM EDTA (pH 8), formamide (50%), 20 × SSC (pH 4.5), yeast RNA (50 mg/mL), heparin (10 mg/mL), 0.1% Tween 20, CHAPS (10%) and circKLF4 probe. After hybridization, add anti–digoxygenin (DIG)-alkaline phosphatase (AP) antibody at 4°C overnight. Wash the slides with freshly made NTMT buffer and then incubate them in BM purple and develop color in dark, humid environment at 4°C for several days. Stop reaction with washing in PBS and dehydrate slides, then mount with mounting medium and capture images.

circKLF4 and Dicer Knockdown, Plasmid Construction

The sequences of circKLF4 siRNA oligonucleotides (circKLF4-si) (GenePharma) are 5′-UGGGGGAAGUCGCUUGUUGTT-3′ (sense) and 5′-CAACAAGCGACUUCCCCCATT-3′ (antisense). Silencer select negative control siRNA (GenePharma) was used as the control. *Dicer* siRNA oligonucleotides were purchased from Thermo.

The circKLF4 sequence was cloned into the pcDNA 3.1 (+) circRNA Mini Vector (*P*-vector) to construct its overexpression plasmid (P-circKLF4). The mutated circKLF4 plasmids (P-circKLF4-Mut-1895 and P-circKLF4-Mut-5046) were created using the Fast Mutagenesis Kit (Vazyme).

After 3–4 days' culture of mDPCs, siRNA, miRNA inhibitor (30 pmol, GenePharma) and wild type or mutant circKLF4 plasmid were co-transfected into cells with Lipofectamine 2,000 (Invitrogen).

Real-Time RT-PCR

Total RNAs were isolated using the HP Total RNA Kit (Omega Bio-tech) according to the manufacturer's protocol and was transcribed into cDNA using the Revert Aid First

[1] http://www.circbase.org/

Strand cDNA Synthesis Kit (Thermo Scientific). The cDNA samples were then amplified using FastStart Universal SYBR Green Master (Rox) with primers (**Table 1**). Total microRNA was isolated using miRNeasy mini Kit (QIAGEN) and was transcribed into cDNA using the miSript Reverse Transcription Kit (QIAGEN). The cDNA samples were amplified using miSript SYBR Green PCR Kit (QIAGEN) with primers (**Table 1**). The cDNA samples were assayed using the CFX Connect Real Time PCR Detection System (Bio-Rad). The relative gene expression levels of circRNA and mRNA were normalized to GAPDH primers, and levels of microRNA were normalized to U6 primers using the $2^{-\Delta\Delta Ct}$ method. The gene expression ratio was determined from three independent experiments.

Western Blot

Cells were lysed in protein lysis buffer (Beyotime). The whole cell lysis products were analyzed with SDS-PAGE and then transferred to PVDF membrane (Millipore). The following primary antibodies were used: anti-KLF4 polyclonal antibody (ab106629, Abcam), anti-DMP1 polyclonal antibody (ab103203, Abcam), anti-DSP polyclonal antibody (NBP191612, NOVUS), and anti-β-ACTIN monoclonal antibody (660091Ig, Proteintech). After incubation with the corresponding antibodies, the membrane was washed 3 times for 5 min each with TBST. We used ImageJ software for further densitometric analysis. Bound primary antibodies were detected by incubating for 1 h with horseradish peroxidase conjugated goat anti-mouse or anti-rabbit IgG (Biofly, China) for analysis. The membrane was washed and developed by a chemiluminescence assay (GE Healthcare).

Statistical Analysis

All experiments were independently repeated at least 3 times and the results are presented as mean ± standard deviation (SD). Differences between two groups were analyzed with a 2-tailed *t*-test with *p*-values less than 0.05 indicated significant. Data analysis were performed by GraphPad Prism 5.0 software (San Diego, CA, United States).

TABLE 1 | Oligonucleotide primer sequences utilized in RT-qPCR.

Gene	Forward primer	Reverse primer
Gapdh	F: TGTGTCCGTCGTGGATCTGA	R: TTGCTGTTGAAGTCGCAGGAG
Alp	F: TCATTCCCACGTTTTCACATTC	R: GTTGTTGTGAGCGTAATCTACC
Dmp1	F: CTGTCATTCTCCTTGTGTT CCTTTG	R: CAAATCACCCGTCCTC TCTTCA
Dspp	F: ATCATCAGCCAGTCAGAA GCAT	R: TGCCTTTGTTGGGACC TTCA
Klf4	F: GGGAAGTCGCTTCATGTG AGAG	R: GCGGGAAGGGAGAAGA CACT
circKLF4	F: TCGCTTCATGTTGAAGGGGG	R: CCTGCAGCTTCAGCTATCCG
Dicer	F: AGCTCCGGCCAACACCTTTA	R:GTGTACCGCTATGAAATCATTGA
Endoglin	F: CACAGCTGCACTCTGGTACA	R: GGAGGCTTGGGATACTCACG

RESULTS

circKLF4 Promotes the Odontoblastic Differentiation of mDPCs

In order to determine whether circKLF4 is associated with odontoblast differentiation, the expression level of circKLF4 was detected in mDPCs cells during odontoblastic differentiation. Specific primers covering the head-to-tail splicing site of circKLF4 were designed. The specificity of the primers was confirmed by PCR, with cDNA and genomic DNA (gDNA) as the template. As expected, PCR products were only amplified in cDNA but not in gDNA (**Figure 1A**), which suggests that the primers are specific for circKLF4 but not for linear KLF4. qPCR results showed that circKLF4 was significantly upregulated on day 9 in primary mDPCs (**Figure 1B**). Furthermore, the mRNA and protein expression levels of odontoblastic-related genes (*Alp*, *Dmp1*, *Dspp*, and *Klf4*) were significantly upregulated on day 9, which confirmed the odontoblastic differentiation of the cells (**Figures 1B,C**). The expression level of circKLF4 in dental pulp cells of erupted molar of 3 weeks old was also investigated and we found that the expression levels of both circKLF4 and linear *Klf4* in mouse dental pulp cells were significantly up-regulated compared with that in the mDPCs (**Supplementary Figure 1A**). Then the expression pattern of circKLF4 in the mouse lower molar at PN1 was detected *in vivo*, using *in situ* hybridization. As showed in **Figure 1D**, circKLF4 displayed at a low level in the papilla but was expressed intensely and specifically in odontoblasts and ameloblasts.

To determine the biological function of circKLF4 in odontoblastic differentiation, a small interfering RNA specifically targeting the back-splicing junction site of circKLF4 (circKLF4-si) was designed to knock down circKLF4. circKLF4 was substantially decreased at 48 h after transfection with circKLF4-si (**Figure 1E**). The expressions of the odontoblast marker genes were also substantially down-regulated both in mRNA and protein levels (**Figures 1E,F**). Furthermore, these odontoblast marker genes were upregulated both in mRNA and protein levels with overexpression of circKLF4 (**Figures 1G,H**).

circKLF4 Increases the Linear *Klf4* Expression in a microRNA-Dependent Manner

Since KLF4 operates as a switch-triggering odontoblast differentiation (Feng et al., 2017), **Figure 1** showed circKLF4 was able to up-regulate linear KLF4 expression in the gain- and loss-of circKLF4 experiments, which indicates circKLF4 promotes odontoblastic differentiation of mDPCS *via* upregulation of linear KLF4. Then the mechanism of how circKLF4 regulates linear KLF4 was explored. As circRNAs can regulate gene expression by sponging microRNAs, to determine whether circKLF4 can increase the liner *Klf4* expression by sponging certain microRNAs, we knocked down Dicer, an enzyme required for cleavage of precursor miRNAs, to decrease mature miRNAs (Song and Rossi, 2017). qRT-PCR results showed that *Dicer* was significantly knocked down with *Dicer* siRNA (*Dicer*-si) transfection (**Figure 2A**). Overexpression of circKLF4

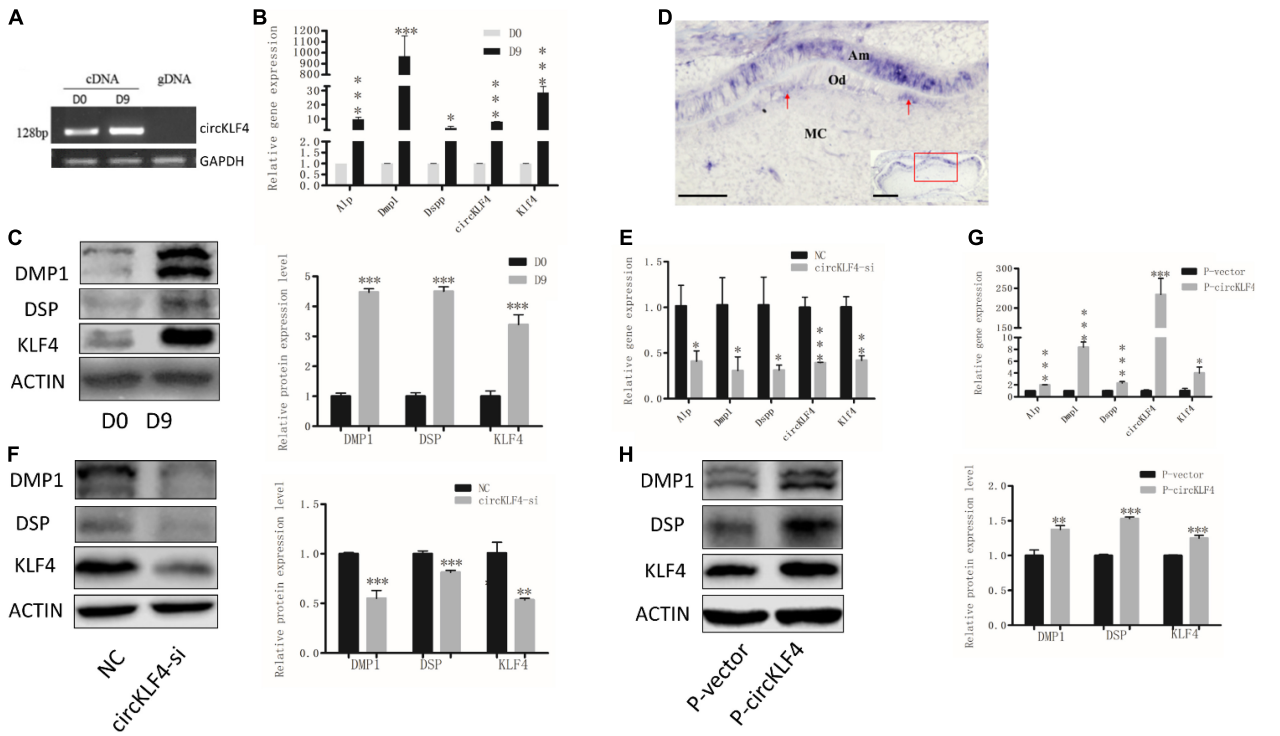

FIGURE 1 | circKLF4 promotes the odontoblastic differentiation of mDPCs. **(A)** The existence of circKLF4 was validated by gel electrophoresis using the products of quantitative real-time PCR. **(B)** mRNA levels of *Alp, Dmp1, Dspp,* circKLF4, and *Klf4* by real-time reverse transcription polymerase chain reaction in the mDPCs cultured in differentiation medium. **(C)** Western blot and quantification of the relative protein levels of DMP1, DSP, KLF4 cultured in differentiation medium. **(D)** *In situ* hybridization of circKLF4 in PN1 mouse molar. **(E)** mRNA levels of *Alp, Dmp1, Dspp,* circKLF4, and *Klf4* after transfection with circKLF4 siRNA (circKLF4-si) compared with the control group (NC). **(F)** DMP1, DSP, KLF4 levels and quantified density after circKLF4 was knocked down. **(G)** mRNA levels of *Alp, Dmp1, Dspp, Klf4,* and circKLF4 after transfected with circKLF4 overexpression plasmid (*P*-circKLF4) compared with the empty vector (*P*-vector). **(H)** The protein levels of DMP1, DSP, and KLF4 after overexpression of circKLF4. Right panel shows the quantified data. Significant difference vs. day 0, $^{*}P < 0.05$; $^{**}P < 0.01$; $^{***}P < 0.001$. Scale bars = 100 μm for **(D)**.

increased the expression of *Klf4* in mRNA and protein levels, but co-transfection with *Dicer* siRNA partially abolished this effect (**Figures 2B,C**), suggesting that the regulation of linear *Klf4* by circKLF4 is in a microRNAs-dependent manner.

To screen the certain microRNAs binding to circKLF4, 10 predicted miRNAs were acquired by mirBase[2] and listed in **Supplementary Table 1**. miRNA-1895 and miRNA-5046 were found to be among the top 2 miRNAs of the list. The binding sequences of miR-1895 and miR-5046 on linear *Klf4* were shown in **Supplementary Figure 1**. Given that these sequences are shared by both circKLF4 and linear *Klf4* in miR-1895 and miR-5046 (**Figure 3A** and **Supplementary Figure 1B**), we hypothesized that circKLF4 might promote liner *Klf4* expression by sponging miR-1895 or miR-5046.

The RT-PCR results showed that both miRNA-1895 and miRNA-5046 were down-regulated at day 9 (**Figure 2D**). To further elucidate the function of miR-1895 and miR-5046 during the regulation of linear KLF4 by circKLF4, the inhibitors of miR-1895 and miR-5046 were used and knock-down efficiency was confirmed by qPCR (**Figure 2E**). Furthermore, we transfected the miR-1895 inhibitor and/or miR-5046 inhibitor into mDPCs with or without overexpression of circKLF4. Overexpression of circKLF4 increased the mRNA and protein levels of linear *Klf4*, but co-transfection with miR-1895 inhibitor or miR-5046 inhibitor could abolished this effect (**Figures 2F,G**). These results indicated that circRNA circKLF4 upregulates linear KLF4 *via* miR-1895 and miR-5046.

circKLF4 Promotes Liner *Klf4* Level by Competitively Binding miR-1895 and miR-5046

To further confirm whether circKLF4 regulates linear *Klf4* level by competitively binding miR-1895 and miR-5046, we mutated the binding site of miR-1895 and miR-5046 in circKLF4 overexpression plasmid (**Figure 3A**) and transfected the mutants into mDPCs with/without co-transfection of miR-1895/miR-5046 inhibitor. The western blot results showed that transfection of either wild type circKLF4 expression plasmid or circKLF4-mut-1895 plasmid was able to upregulate KLF4 expression (**Figure 3B**, lane 2 and 4). Co-transfection of miR-1895 inhibitor was able to effectively abolish the upregulation effect of wild type circKLF4 expression plasmid to linear KLF4 expression (**Figure 3B**, compared lane 3 and 2), but was not so effective to

[2]http://www.mirbase.org/

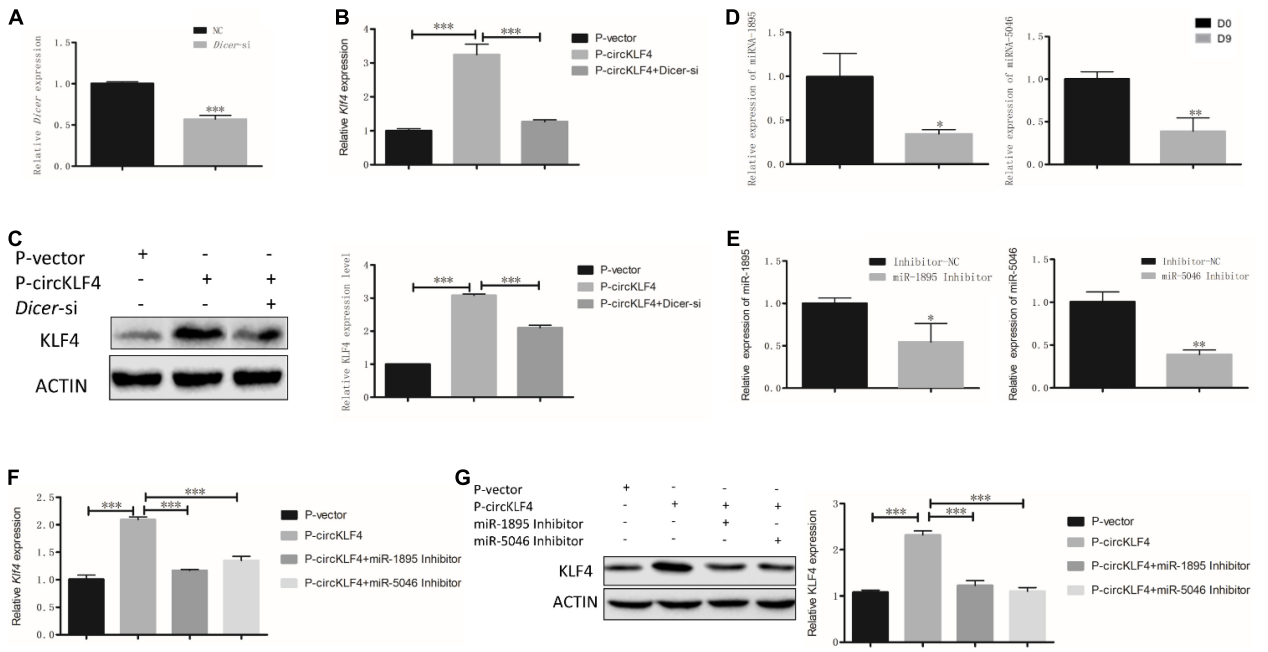

FIGURE 2 | circKLF4 up-regulates liner *Klf4* expression to promote Odontoblastic Differentiation in a microRNA-dependent manner. **(A)** mRNA level of *Dicer* was significantly down-regulated after *Dicer*-si was transfected. **(B,C)** Compared with overexpression of circKLF4 alone, mRNA and protein levels of *Klf4* were significantly down-regulated after co-transfected with *Dicer*-si. **(D,E)** miR-1895 and miR-5046 was analyzed by RT-PCR after 9 days' differentiation induction or using the inhibitors. **(F,G)** mRNA and protein levels of *Klf4* were significantly down-regulated after co-transfection of miR-1895/miR-5046 inhibitor with *P*-circKLF4. $^{*}P < 0.05$; $^{**}P < 0.01$; $^{***}P < 0.001$.

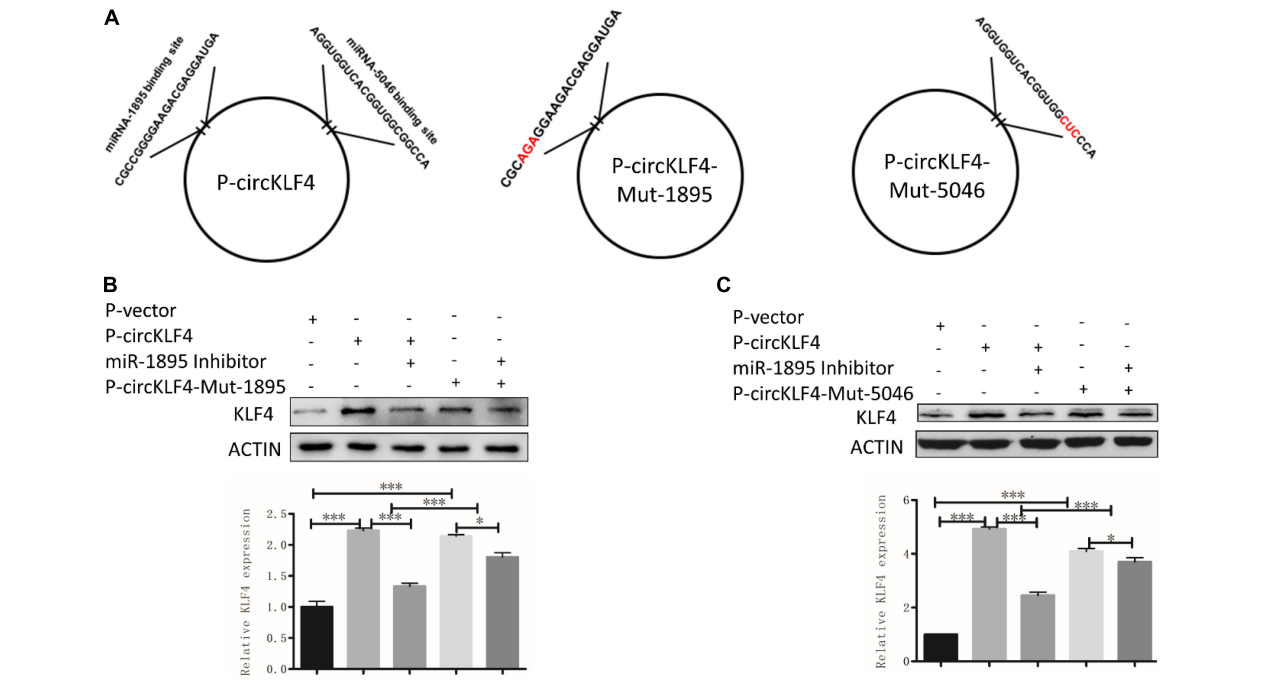

FIGURE 3 | circKLF4 promotes liner Klf4 expression by competitively binding miR-1895 and miR-5046. **(A)** The left scheme demonstrated the predicted binding sites of miR-1895 and miR-5046 in *P*-circKLF4. The right two diagrams showed the characteristics of mutant-type P-circKLF4 (*P*-circKLF4-Mut-1895 and *P*-circKLF4-Mut-5046). **(B,C)** Western blot and qPCR results showed the expression of KLF4 after transfected with or without P-circKLF4, miR-1895 or miR-5046 inhibitor, *P*-circKLF4-Mut-1895 or *P*-circKLF4-Mut-5046. $^{*}P < 0.05$; $^{***}P < 0.001$.

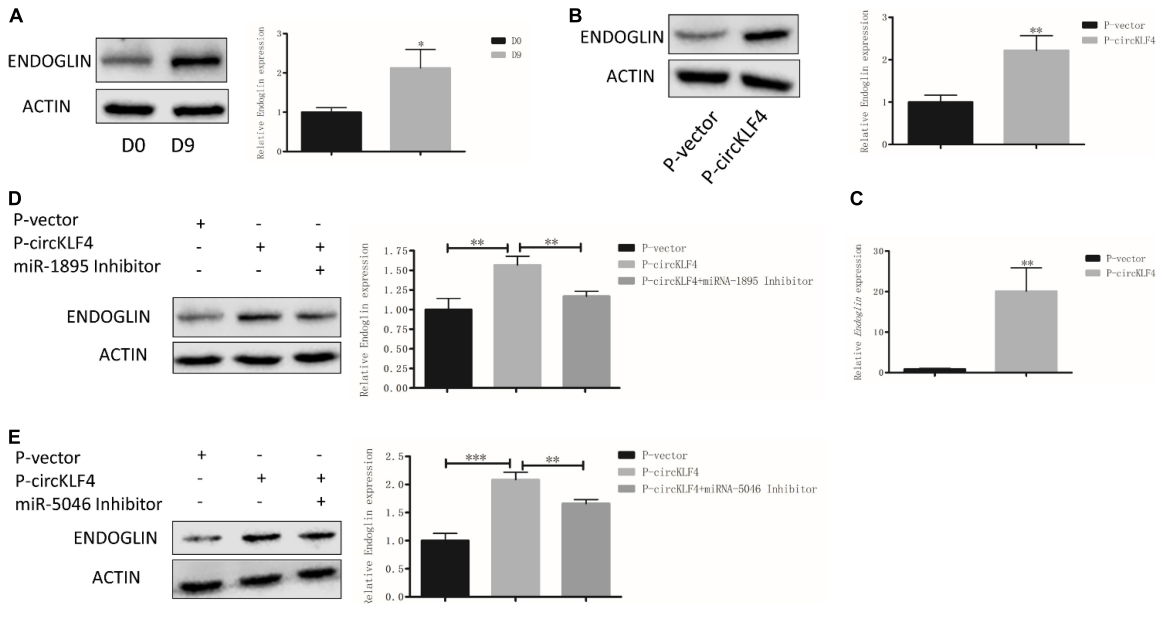

FIGURE 4 | circKLF4 also promotes Endoglin expression *via* sponging miR-1895 and miR-5046. **(A)** Protein level of ENDOGLIN was significantly up-regulated after 9 days' induction. **(B,C)** The protein and mRNA levels of ENDOGLIN were significantly up-regulated after transfected with *P*-circKLF4 compared with the *P*-vector group. **(D,E)** Western blot results showed the expression level of ENDOGLIN after co-transfected of miR-1895 or miR-5046 inhibitor with *P*-circKLF4. $^{*}P < 0.05$; $^{**}P < 0.01$; $^{***}P < 0.001$.

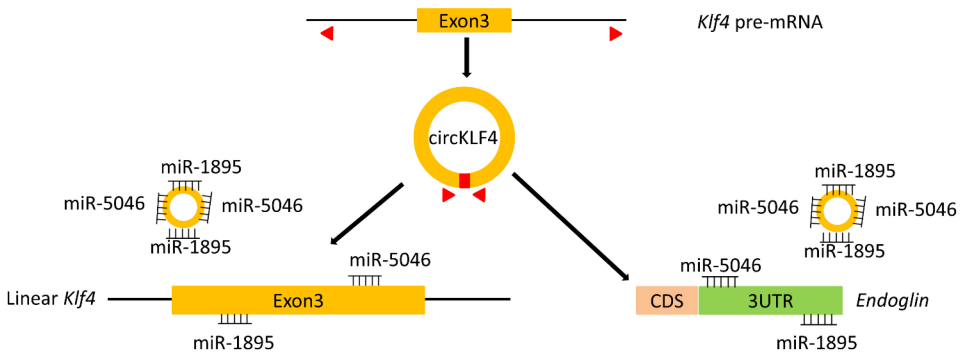

FIGURE 5 | A scheme indicates that circKLF4 upregulates *Klf4* and *Endoglin* to promote odontoblastic differentiation of mDPCs *via* sponging miRNA-1895 and miRNA-5046.

abolish the upregulation effect of circKLF4-mut-1895 plasmid to linear KLF4 expression (**Figure 3B**, compared lane 5 and 4). The similar results were found in the transfection of circKLF4-mut-5046 and miR-5046 inhibitor (**Figure 3C**). These results indicated that circKLF4 regulates linear KLF4 expression by competitively binding miR-1895 and miR-5046.

circKLF4 Also Promotes Endoglin Expression *via* Sponging miR-1895 and miR-5046

Since circKLF4 could competitively bind miR-1895 and miR-5046, furthermore, miRNA could regulate multiple genes' expression (Panda, 2018). Thus, we wondered if it is possible that circKLF4 can regulate odontoblastic differentiation by regulating other genes except for *Klf4* through miR-1895 and miR-5046. By querying the miRNA target gene prediction and functional analysis database TargetScan,[3] we found that both miRNA-1895 and miRNA-5046 have binding sites with *Endoglin* by binding its 3′ untranslated region (3′UTR) (**Supplementary Figure 1C**). Endoglin has been identified to participate in odontoblast differentiation in the previous studies. In our *in vitro* odontoblastic differentiation experiments, western blot results showed that ENDOGLIN was significantly increased on day 9 (**Figure 4A**). Overexpression of circKLF4 upregulated both the protein and mRNA levels of *Endoglin* (**Figures 4B,C**). However, co-transfection of miR-1895/miR-5046 inhibitor abolished this

[3]http://www.targetscan.org/

effect (**Figures 4D,E**). These results showed, besides KLF4, circKLF4 also promotes Endoglin expression *via* miR-1895 and miR-5046 to induce odontoblastic differentiation of mDPCs.

DISCUSSION

The study of odontoblastic differentiation is essential to understand the process of tooth development and to achieve tooth regeneration in the future. Emerging evidence has revealed that circRNAs participate in odontoblast differentiation (Li and Jiang, 2019). Here, we reported and elucidated the potential role of a circRNA termed circKLF4 during odontoblast differentiation. We demonstrated that circKLF4 modulated the expression of KLF4 and ENDOGLIN to promote odontoblastic differentiation by sponging miRNA-5046 and miRNA-1895 mechanistically (**Figure 5**).

As we know, the studies about circRNAs in odontoblast differentiation are still limited (Li and Jiang, 2019). A recent study demonstrated that 1,314 and 1,780 circRNAs were upregulated and downregulated in human dental pulp cells during odontogenic differentiation (Li and Jiang, 2019). In our preliminary circRNA sequencing data, we also found the differential expression of circRNAs in dental papilla cells after differentiation. In this study, we identified that circKLF4 was upregulated in differentiated odontoblasts with 9 days' induction of differentiation. Our *in situ* hybridization result showed that circKLF4 expression was intense in the odontoblasts and ameloblasts, but was at a low level in the mesenchyme cells. Similarly, as the parental gene of circKLF4, KLF4 was also detectable in polarizing odontoblasts and ameloblasts in the first molar at PN1 in the previous investigation (Chen et al., 2009). The similar expression patterns of circKLF4 and linear KLF4 indicated the possibility of regulation between circKLF4 and KLF4. Besides, KLF4 has been identified to promote odontoblast differentiation both *in vitro* and *in vivo* (Tao et al., 2019), which leads us to explore the role of circKLF4 during odontoblastic differentiation. In the present investigation, gain- and loss-of-circKLF4 confirmed that circKLF4 could up-regulate KLF4 expression and promote odontoblast differentiation.

Accumulating investigations have implied that circRNAs act as miRNA sponges to regulate gene expression. MicroRNA are predicted to regulate protein-coding genes (Berezikov et al., 2005). The miRNA genes are transcribed into primary miRNA (pri-miRNA) to generate pre-miRNA, which is then processed by Dicer to produce mature miRNA (Siomi and Siomi, 2010). As Dicer could inhibit the formation of miRNAs (Song and Rossi, 2017), with transfection of *Dicer* siRNA we revealed that known-down of Dicer abolished the upregulation of KLF4 by circKLF4, suggesting that circKLF4 modulated KLF4 expression in a miRNAs-dependent manner. The targeted microRNAs binding to circKLF4 were predicted by mirBase, miRNA-1895 and miRNA-5046 were found to be the top 2 miRNAs. Accumulating evidence indicates that miRNAs participate in odontoblast differentiation (Sun et al., 2015) and circRNAs are shown to regulate gene expression by inhibiting miRNA activity (Panda, 2018). Our previous study showed that miR-1895 inhibited the odontoblastic differentiation (Zhang and Yang, 2021), suggesting that circKLF4 might be a miR-1895 antagonist with a miR-1895-binding capacity. To our knowledge, the function of miR-5046 during odontoblast differentiation has not been studied. However, RT-PCR data demonstrated that miR-1895 and miR-5046 were both downregulated in the differentiated mDPCs. Several other assays, including gain- and loss-of-circKLF4, use of microRNAs inhibitor and mutation of the binding sites of the microRNAs in circKLF4 overexpression plasmid were also performed, which indicated that circKLF4 regulated KLF4 expression *via* sponging miR-1895 and miR-5046.

As miRNA could target the 3′ UTRs of specific mRNA targets (Pillai, 2005) and regulate multiple genes' stability and/or translation (Panda, 2018). By querying the miRNA target gene prediction and functional analysis database TargetScan (see text footnote 3), we found that both miR-1895 and miR-5046 have binding sites with the 3′ UTR region of the gene *Endoglin*. So it is predicted that circKLF4 could also regulate *Endoglin* expression *via* miR-1895 and miR-5046. Endoglin, also called CD105, which is ubiquitously expressed in mesenchymal stem cells. Besides, the Endoglin positive selection has been proposed for the isolation of DPSC (dental pulp stem cells) and Endoglin expression was detected in odontoblasts of human (Huang et al., 2010). A previous study showed that, *Endoglin* was found to be upregulated in DPSCs during the induction of DPSCs into dentin-secreting odontoblast-like cells (Liu et al., 2007) and involved in osteogenic differentiation of periodontal ligament cells (Ishibashi et al., 2010). Consistent with our study, we also identified that *Endoglin* was significantly increased with odontoblastic differentiation in mDPCs and overexpression of circKLF4 increased the expression levels of *Endoglin*. Besides, co-transfection with miR-1895 or miR-5046 could inhibited the up-regulation of ENDOGLIN by overexpression of circKLF4, indicating the potential role of miRNA during the regulation of ENDOGLIN by circKLF4.

To summarize, we identified that circKLF4 was up-regulated in differentiated mDPCs and promoted odontoblast differentiation through up-regulation of KLF4 and ENDOGLIN by sponging miR-1895 and miR-5046.

DATA AVAILABILITY STATEMENT

The original contributions presented in the study are included in the article/**Supplementary Material**, further inquiries can be directed to the corresponding author/s.

ETHICS STATEMENT

The animal study was reviewed and approved by the Ethics Committee of the School of Stomotology, Wuhan University.

AUTHOR CONTRIBUTIONS

YZ made contributions to data acquisition, analysis, draft, and critical revision of the manuscript. HZ contributed to advice, analysis, and discussions. GHY conceived, analyzed the experiments, and critically revised the manuscript.

GBY contributed to conception, design, analysis, and critically revised the manuscript. All authors approved the manuscript and agreed to be accountable for the work.

FUNDING

This work was supported by the National Natural Science Foundation of China (Grant/Award No. 81570942).

REFERENCES

Ashwal-Fluss, R., Meyer, M., Pamudurti, N. R., Ivanov, A., Bartok, O., and Hanan, M. (2014). circRNA biogenesis competes with pre-mRNA splicing. *Mol. Cell* 56, 55–66.

Berezikov, E., Guryev, V., van de Belt, J., Wienholds, E., Plasterk, R. H., and Cuppen, E. (2005). Phylogenetic shadowing and computational identification of human microRNA genes. *Cell* 120, 21–24. doi: 10.1016/j.cell.2004.12.031

Capel, B., Swain, A., Nicolis, S., Hacker, A., Walter, M., and Koopman, P. (1993). Circular transcripts of the testis-determining gene Sry in adult mouse testis. *Cell* 73, 1019–1030. doi: 10.1016/0092-8674(93)90279-y

Chen, Z., Couble, M. L., Mouterfi, N., Magloire, H., Chen, Z., and Bleicher, F. (2009). Spatial and temporal expression of KLF4 and KLF5 during murine tooth development. *Arch. Oral Biol.* 54, 403–411. doi: 10.1016/j.archoralbio.2009.02.003

Dassule, H. R., Lewis, P., Bei, M., Maas, R., and McMahon, A. P. (2000). Sonic hedgehog regulates growth and morphogenesis of the tooth. *Development* 127, 4775–4785.

Feng, J., Jing, J., Li, J., Zhao, H., Punj, V., and Zhang, T. (2017). BMP signaling orchestrates a transcriptional network to control the fate of mesenchymal stem cells in mice. *Development* 144, 2560–2569. doi: 10.1242/dev.150136

Greene, J., Baird, A. M., Brady, L., Lim, M., Gray, S. G., and McDermott, R. (2017). Circular RNAs: biogenesis, function and role in human diseases. *Front. Mol. Biosci.* 4:38. doi: 10.3389/fmolb.2017.00038

Gu, X., Li, M., Jin, Y., Liu, D., and Wei, F. (2017). Identification and integrated analysis of differentially expressed lncRNAs and circRNAs reveal the potential ceRNA networks during PDLSC osteogenic differentiation. *BMC Genet.* 18:100. doi: 10.1186/s12863-017-0569-4

Huang, G. T., Yamaza, T., Shea, L. D., Djouad, F., Kuhn, N. Z., and Tuan, R. S. (2010). Stem/progenitor cell-mediated de novo regeneration of dental pulp with newly deposited continuous layer of dentin in an in vivo model. *Tissue Eng. Part A* 16, 605–615. doi: 10.1089/ten.TEA.2009.0518

Ishibashi, O., Ikegame, M., Takizawa, F., Yoshizawa, T., Moksed, M. A., and Iizawa, F. (2010). Endoglin is involved in BMP-2-induced osteogenic differentiation of periodontal ligament cells through a pathway independent of Smad-1/5/8 phosphorylation. *J. Cell. Physiol.* 222, 465–473. doi: 10.1002/jcp.21968

Li, C., and Jiang, H. (2019). Altered expression of circular RNA in human dental pulp cells during odontogenic differentiation. *Mol. Med. Rep.* 20, 871–878. doi: 10.3892/mmr.2019.10359

Lin, H., Liu, H., Sun, Q., Yuan, G., Zhang, L., and Chen, Z. (2013). KLF4 promoted odontoblastic differentiation of mouse dental papilla cells via regulation of DMP1. *J. Cell. Physiol.* 228, 2076–2085. doi: 10.1002/jcp.24377

Liu, J., Jin, T., Chang, S., Ritchie, H. H., Smith, A. J., and Clarkson, B. H. (2007). Matrix and TGF-beta-related gene expression during human dental pulp stem cell (DPSC) mineralization. *In Vitro Cell. Dev. Biol. Anim.* 43, 120–128. doi: 10.1007/s11626-007-9022-8

Memczak, S., Jens, M., Elefsinioti, A., Torti, F., Krueger, J., and Rybak, A. (2013). Circular RNAs are a large class of animal RNAs with regulatory potency. *Nature* 495, 333–338. doi: 10.1038/nature11928

Panda, A. C. (2018). Circular RNAs Act as miRNA Sponges. *Adv. Exp. Med. Biol.* 1087, 67–79. doi: 10.1007/978-981-13-1426-1_6

Pasman, Z., Been, M. D., and Garcia-Blanco, M. A. (1996). Exon circularization in mammalian nuclear extracts. *RNA* 2, 603–610.

Pillai, R. S. (2005). MicroRNA function: multiple mechanisms for a tiny RNA? *RNA* 11, 1753–1761. doi: 10.1261/rna.2248605

Qian, D. Y., Yan, G. B., Bai, B., Chen, Y., Zhang, S. J., and Yao, Y. C. (2017). Differential circRNA expression profiles during the BMP2-induced osteogenic differentiation of MC3T3-E1 cells. *Biomed. Pharmacother.* 90, 492–499. doi: 10.1016/j.biopha.2017.03.051

Salzman, J., Chen, R. E., Olsen, M. N., Wang, P. L., and Brown, P. O. (2013). Cell-type specific features of circular RNA expression. *PLoS Genet.* 9:e1003777. doi: 10.1371/journal.pgen.1003777

Salzman, J., Gawad, C., Wang, P. L., Lacayo, N., and Brown, P. O. (2012). Circular RNAs are the predominant transcript isoform from hundreds of human genes in diverse cell types. *PLoS One* 7:e30733. doi: 10.1371/journal.pone.0030733

Siomi, H., and Siomi, M. C. (2010). Posttranscriptional regulation of microRNA biogenesis in animals. *Mol. Cell* 38, 323–332. doi: 10.1016/j.molcel.2010.03.013

Song, M. S., and Rossi, J. J. (2017). Molecular mechanisms of Dicer: endonuclease and enzymatic activity. *Biochem. J.* 474, 1603–1618. doi: 10.1042/BCJ20160759

Sun, J., Li, B., Shu, C., Ma, Q., and Wang, J. (2020). Functions and clinical significance of circular RNAs in glioma. *Mol. Cancer* 19:34. doi: 10.1186/s12943-019-1121-0

Sun, Q., Liu, H., and Chen, Z. (2015). The fine tuning role of microRNA-RNA interaction in odontoblast differentiation and disease. *Oral Dis.* 21, 142–148.

Szabo, L., Morey, R., Palpant, N. J., Wang, P. L., Afari, N., and Jiang, C. (2015). Statistically based splicing detection reveals neural enrichment and tissue-specific induction of circular RNA during human fetal development. *Genome Biol.* 16:126. doi: 10.1186/s13059-015-0690-5

Tao, H., Lin, H., Sun, Z., Pei, F., Zhang, J., and Chen, S. (2019). Klf4 promotes dentinogenesis and odontoblastic differentiation *via* modulation of TGF-beta signaling pathway and interaction with histone acetylation. *J. Bone Miner. Res.* 34, 1502–1516. doi: 10.1002/jbmr.3716

Thesleff, I., Partanen, A. M., Kuusela, P., and Lehtonen, E. (1987). Dental papilla cells synthesize but do not deposit fibronectin in culture. *J. Dent. Res.* 66, 1107–1115. doi: 10.1177/00220345870660060401

Yuan, G., Wang, Y., Gluhak-Heinrich, J., Yang, G., Chen, L., and Li, T. (2009). Tissue-specific expression of dentin sialophosphoprotein (DSPP) and its polymorphisms in mouse tissues. *Cell Biol. Int.* 33, 816–829. doi: 10.1016/j.cellbi.2009.05.001

Zhang, H., and Yang, G. (2021). Regulation of odontoblastic differentiation by miR-1895 in mouse dental papilla cells. *J. Oral Sci. Res.* 37, 28–32. doi: 10.13701/j.cnki.kqyxyj.2021.01.007

Zhang, Y. D., Chen, Z., Song, Y. Q., Liu, C., and Chen, Y. P. (2005). Making a tooth: growth factors, transcription factors, and stem cells. *Cell Res.* 15, 301–316.

Conflict of Interest: The authors declare that the research was conducted in the absence of any commercial or financial relationships that could be construed as a potential conflict of interest.

Publisher's Note: All claims expressed in this article are solely those of the authors and do not necessarily represent those of their affiliated organizations, or those of the publisher, the editors and the reviewers. Any product that may be evaluated in this article, or claim that may be made by its manufacturer, is not guaranteed or endorsed by the publisher.

SUPPLEMENTARY MATERIAL

The Supplementary Material for this article can be found online at: https://www.frontiersin.org/articles/10.3389/fphys.2021.760223/full#supplementary-material

Supplementary Figure 1 | (A) mRNA levels of *circKLF4 and Klf4* were significantly up-regulated in mouse dental pulp of PN21, compared with those in mouse dental papilla cells of PN1. **(B,C)** A scheme shows the potential binding sites between miR-1895 or miR-5046 and the *Klf4* or *Endoglin*.

frontiers | Frontiers in Physiology

REVIEW
published: 19 April 2022
doi: 10.3389/fphys.2022.827470

Odontogenic MSC Heterogeneity: Challenges and Opportunities for Regenerative Medicine

Yuan Chen[1†], *Zhaoyichun Zhang*[2†], *Xiaoxue Yang*[1], *Anqi Liu*[1], *Shiyu Liu*[1], *Jianying Feng*[2] *and Kun Xuan*[1*]

[1]State Key Laboratory of Military Stomatology, National Clinical Research Center for Oral Diseases, Department of Preventive Dentistry, School of Stomatology, The Fourth Military Medical University, Xi'an, China, [2]School of Stomatology, Zhejiang Chinese Medical University, Hangzhou, China

Cellular heterogeneity refers to the genetic and phenotypic differences among cells, which reflect their various fate choices, including viability, proliferation, self-renewal probability, and differentiation into different lineages. In recent years, research on the heterogeneity of mesenchymal stem cells has made some progress. Odontogenic mesenchymal stem cells share the characteristics of mesenchymal stem cells, namely, good accessibility, low immunogenicity and high stemness. In addition, they also exhibit the characteristics of vasculogenesis and neurogenesis, making them attractive for tissue engineering and regenerative medicine. However, the usage of mesenchymal stem cell subgroups differs in different diseases. Furthermore, because of the heterogeneity of odontogenic mesenchymal stem cells, their application in tissue regeneration and disease management is restricted. Findings related to the heterogeneity of odontogenic mesenchymal stem cells urgently need to be summarized, thus, we reviewed studies on odontogenic mesenchymal stem cells and their specific subpopulations, in order to provide indications for further research on the stem cell regenerative therapy.

Keywords: heterogeneity, mesenchymal stem cells, odontogenic, development, regeneration

OPEN ACCESS

Edited by:
Guohua Yuan,
Wuhan University, China

Reviewed by:
Marco Tatullo,
University of Bari Medical School, Italy
Xiaoxing Kou,
Sun Yat-sen University, China

***Correspondence:**
Kun Xuan
xuankun@fmmu.edu.cn

[†]*These authors have contributed equally to this work*

Specialty section:
This article was submitted to Craniofacial Biology and Dental Research, a section of the journal Frontiers in Physiology

Received: *02 December 2021*
Accepted: *30 March 2022*
Published: *19 April 2022*

Citation:
Chen Y, Zhang Z, Yang X, Liu A, Liu S, Feng J and Xuan K (2022) Odontogenic MSC Heterogeneity: Challenges and Opportunities for Regenerative Medicine. Front. Physiol. 13:827470. doi: 10.3389/fphys.2022.827470

INTRODUCTION

Cellular heterogeneity was first discovered in tumor cells, and the term is used to describe the differences in genes and phenotypes between different tumor cells (Ono et al., 2021; Pe'er et al., 2021). In terms of pluripotency, self-renewal ability, and other traits, mesenchymal stem cells (MSCs), as undifferentiated cells, show similar behaviors to tumor cells, as mentioned in many studies; in contrast, the heterogeneity of MSCs has rarely been reported (Hayashi et al., 2019). Initially, it was found that alkaline phosphatase (ALP) is highly expressed in somes but not other individual colony cultures of MSCs, and there is also a third type that has intermediate expression; in

Abbreviations: 2D, two-dimensional; ALP, alkaline phosphatase; BMSCs, bone marrow stromal cells; DFSCs, dental follicle stem cells; DP, dermal papilla; DPSCs, dental pulp stem cells; GDNF, glial cell-line derived neurotrophic factor; GMSCs, gingival mesenchymal stem cells; Hh, hedgehog signaling; hDPSCs, the human deciduous pulp stem cells; hPCy-MSCs, human periapical cyst-mesenchymal stem cells; MSC, mesenchymal stem cell; PA-MSC, plastic adherence isolated MSC; PDL, periodontal ligament; PDLSCs, periodontal ligament stem cells; SCAPs, stem cells of the apical papilla; SCF, stem cell factor; scRNA-seq, single-cell RNA sequencing; SDF-1, stromal cell-derived factor; SHED, Stem cells from exfoliated deciduous teeth; Th17, T helper 17; Tregs, regulatory T cells; VEGF, vascular endothelial growth factor.

addition, this factor is not expressed in the periphery (Friedenstein et al., 1982). Further research showed that the expression patterns of markers such as CD90 and CD45 in several types and subpopulations of MSCs are quite different (Abe et al., 2008; Li et al., 2012; Mabuchi et al., 2021). With the help of new technologies, such as single-cell RNA sequencing (scRNA-seq) and its derivative technologies, a better approach for studying cell heterogeneity has been developed (Chen S et al., 2020; Lei et al., 2021). Using single-cell sequencing, it was found that even within an MSC subpopulation, due to changes in the internal and the external factors, the gene expression also differs among cells (Bianco et al., 2001; Mabuchi et al., 2021). Overall, heterogeneity of the MSC phenotype is likely to exist among cell lines, among cells within a line, and among temporal states of a single cell.

Odontogenic MSCs have been isolated from dental tissue, including dental pulp (Gronthos et al., 2000), exfoliated deciduous teeth (Miura et al., 2003), periodontal ligaments (Seo et al., 2004), dental follicles (Morsczeck et al., 2005), apical papillae (Sonoyama et al., 2006), papillae (Tziafas and Kodonas, 2010) and periapical cysts (Marrelli et al., 2013). Odontogenic MSCs have become an attractive source of autologous MSCs because they exhibit the characteristics of vasculogenesis and neurogenesis (Liu et al., 2015), along with their good accessibility, low immunogenicity and high stemness (Merimi et al., 2021). There has been some clinical evidence verifying the therapeutic effect of odontogenic MSCs in tissue regeneration. For example, implantation of human deciduous pulp stem cells (hDPSCs) into injuried incisors can promote pulp regeneration and partial tooth recovery (Xuan et al., 2018). However, the effect of odontogenic MSCs on tissue regeneration and disease management remains unclear (Levy et al., 2020). It is generally accepted that the extracellular environment affects the therapeutic efficacy of engrafted odontogenic MSCs. A chronic inflammatory environment interferes with odontogenic MSC osteogenesis, resulting in osteolysis (Bressan et al., 2019).

Recently, the heterogeneity of odontogenic MSCs has attracted attention. To date, the sudy and application of human MSCs are mostly based on the hybrid effect, and only a small part of the hybrid may play a pivotal role in regeneration and immunoregulation (Huang et al., 2019). In this review, the characteristics and application prospects of odontogenic MSCs are summarized according to their specific subpopulations, with the aim of obtaining a better understanding the opportunities and challenges generated by the heterogeneity of stem cells in the context of regenerative medicine and providing ideas for further research on the stem cell regenerative therapy.

MSC HETEROGENEITY DURING DEVELOPMENT AND REGENERATION

MSCs, which can alternatively be defined as multipotent MSCs, are a series of premature stromal cells with multilineage differentiation potential. They can be amplified *in vitro* and differentiate into specific tissues (such as bone, cartilage, adipose tissue, etc.) under diverse conditions (Uccelli et al., 2008). From almost every type of connective tissue, specific MSCs can be isolated, which explains the importance of MSCs in tissue regeneration research. However, researchers have suggested that there are differences within a single type of MSCs derived from different individuals (Lv et al., 2014); either different cultivation conditions or different numbers of cell passages can determine gene or protein expression profiles, which directly reflects the phenotype of the colony. This is currently called MSC heterogeneity.

For example, in skin tissue, there are many specialized mesenchymal cells called dermal papillae (DPs) located at the base of the hair follicles, which are essential for hair regeneration (Driskell et al., 2011; Morgan, 2014). Freshly isolated DPs or in vitro-cultured DP cells can induce *de novo* hair follicle formation when implanted elsewhere, with the hair type determined by the source of the DPs (Jahoda et al., 1984). This indicates that DP cells are intrinsically heterogeneous and contain hard-wired positional memory that in turn instructs the overlaying epithelial cell activity. Furthermore, the same holds for bone marrow MSCs; only a fraction of colony-forming units from plastic adherence isolated MSCs(PA-MSCs) exhibited multipotency, indicating that PA-MSCs comprise a heterogeneous population of cells with different lineage commitments, which may be relate to their *in vivo* environments (Lv et al., 2014). This is reflected in the differences in the protein expression profiles, cytokine profiles, and differentiation potency of MSCs from various source. In addition, the oral cavity is a source of MSCs, but the heterogeneity of these MSCs has not been systematically reviewed.

ODONTOGENIC MSC HETEROGENEITY

The mesoderm and neural crest are currently considered to be the main sources of MSCs (Takashima et al., 2007). Mesoderm-derived MSCs mainly give rise to bone and connective tissue. When cultured *in vitro*, they show potential for chondrogenic, osteogenic and adipogenic differentiation (Vodyanik et al., 2010). Neural crest-derived MSCs are considered to generate the craniofacial bones. Notably, they show neurogenic potential compared to mesoderm-derived MSCs (Isern et al., 2014).

Odontogenic MSCs are considered to be derived from the neural crest (Thesleff and Nieminen, 1996) and have become a remarkable source of autologous MSCs. They have been isolated and identified from various sites in dental tissues, including apical papillae, exfoliated deciduous teeth, dental follicles, periodontal ligaments, dental pulp, dental papillae and periapical cysts. In 2000, Gronthos et al. isolated a clonogenic group of dental pulp cells that have similar capabilities as bone marrow stromal cells (BMSCs), including self-renewal ability and multidirectional differentiation potential (Gronthos et al., 2000). Since then, an increasing number of MSCs have been isolated from dental pulp, apical papillae, dental follicles, periodontal ligaments, periapical cysts and even the gingiva (Zhang et al., 2009). These odontogenic MSCs have been widely used in various tissue regeneration studies, including studies of bone, nerve and liver

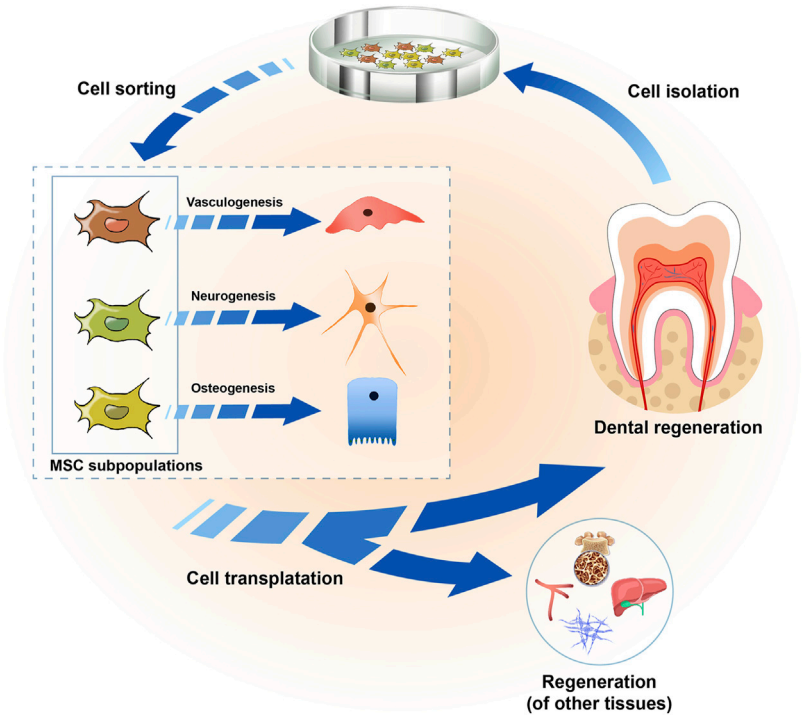

FIGURE 1 | Strategies for utilizing the odontogenic MSC heterogeneity in tissue regeneration. Odontogenic MSCs were isolated from dental tissue, including dental pulp, periodontal ligaments, dental follicles, apical papillae, and the gingiva, and they showed heterogeneity in terms of their pluripotency *in vitro* culture. They could be sorted into several cell subpopulations according to their characteristics, with enhanced vasculogenic, neurogenic and osteogenic differentiation abilities. In the regeneration of teeth or other tissues, such as bone, liver, nerves and blood vessels, the selection of one or more cell subpopulations according to different needs might improve the outcomes of regenerative medicine.

regeneration. Several studies have found that in animal calvarial bone defect models, odontogenic MSCs promote new bone formation and play an important role in bone regeneration (Yang H et al., 2019). In the context of neural restoration, odontogenic MSCs can differentiate into neuron-like cells and achieve neuro-regeneration, and their effectiveness in the treatment of ischemic vascular diseases has been validated (Zhang et al., 2018; Gonmanee et al., 2020). Moreover, odontogenic MSCs have the potential to differentiate into hepatocyte-like cells. Transplantation of stem cells from exfoliated deciduous teeth (SHED) has been reported to significantly reduce rat liver fibrosis and normalize the disordered liver structure (Yokoyama et al., 2019). Notably, compared with MSCs from other sources, odontogenic MSCs exhibit several unique advantages.

Interestingly, there seem to be location-related differences in the regenerative potential of these cells. For example, stem cells from periodontal ligaments can differentiate into cementoblasts (J. W. Yang et al., 2020) and concentrate collagen fibers similar to Sharpey fibers (Hasegawa et al., 2005), whereas stem cells from dental pulp show the ability to produce calcified nodules, the components of which are similar to dentin (Zhang et al., 2005; Feng et al., 2011). In this regard, the functional heterogeneity of MSCs makes the application of MSCs more challenging, as different cells may show different therapeutic effects for different therapeutic purposes. However, this heterogeneity also raises the opportunity that dividing MSCs into different subgroups according to their different functions may improve the outcomes of stem cell therapy (**Figure 1**). A study proved that after the transplantation of dental pulp stem cells (DPSCs) *in situ*, the vascularized pulp tissue of canine teeth was successfully repaired (Iohara et al., 2013). Similarly, stem cells of the apical papillae (SCAPs) have been shown to exhibit the ability to support tooth root formation (Abe et al., 2008). On the other hand, gingival mesenchymal stem cells (GMSCs) injected through the tail vein could accurately locate periodontal injury sites and participate in periodontal tissue regeneration (Sun et al., 2019), whereas DPSCs could hardly repair periodontal tissue defects (Park et al., 2011). Nevertheless, some studies suggested that DPSCs might be able to accomplish periodontal tissue repair and regeneration (Liu et al., 2011). These results suggest that investigations of the role of different odontogenic MSC subpopulations in tissue repair and regeneration should be carried out more systematically.

The cellular environment required for growth and development is highly dynamic and heterogeneous. The cellular origin of the tooth can be shown by using lineage tracking, which helps to better explore the cellular environment required for tooth development. In mouse incisors, the population of peripheral glial MSCs originates trom the teeth, and these cells can differentiate into odontoblasts and dental pulp cells (Kaukua et al., 2014;

Krivanek et al., 2020). In addition, non-glial-derived dental MSCs have been reported in mouse incisors, and these cells are found in the neurovascular bundle and responsive to Shh (Zhao et al., 2014). Lineage tracing of these cells using Ng2-Cre showed that they are derived from pericytes and mainly act on the vascular system. They are also responsible for the continuous generation of odontoblasts, especially after odontoblasts are damaged (Feng et al., 2011; Zhao et al., 2014; Pang et al., 2016). Taken together, these findings indicate that more than one type of MSC is involved in tooth development, and different cells perform different functions.

ADVANTAGES OF ODONTOGENIC MSCS IN TISSUE REGENERATION

Better Accessibility

Although MSCs can be isolated from connective tissue throughout the body, the invasiveness of the collection process often limits their clinical application. In contrast, odontogenic MSCs, which can be isolated from discarded teeth and periodontal tissue, are easier to obtain from the body (J. Yang et al., 2020). Teeth extracted due to impaction, trauma or severe periodontitis and exfoliated deciduous teeth that have fallen out naturally, which are often abandoned, can be a rich source of odontogenic MSCs (Chen et al., 2012). In addition, gingiva that was removed for aesthetic or pathological reasons can also be an attractive source of MSCs. In comparison to the difficulty of obtaining stem cells from other organs or tissues in the human body, not only is it easy to access to the collection site of odontogenic MSCs but also the extraction of stem cells from dental tissue is highly efficient.

Lower Immunogenicity

Low immunogenicity has been reported to be a common characteristic among different MSC populations, including odontogenic MSCs (Laing et al., 2018). This is mainly because they do not express immune costimulatory factors, such as major histocompatibility complex class II antigen, as well as CD40, CD80 and CD86 (Wada et al., 2013). In this regard, the low immunogenicity of odontogenic MSCs solves the problem of transplant rejection caused by immune incompatibility between the donor and the recipient. Transplant rejection usually occurs after transplantation of allogeneic cells, tissues or organs, which is one of the critical issues in tissue engineering. Of note, odontogenic MSCs have immunomodulatory properties that inhibit immune responses and make them suitable for the treatment of autoimmune and inflammation-related diseases (Le Blanc, 2006). For example, PDLSCs can induce macrophages to polarize toward the M2 phenotype that supports tissue repair, thereby changing the immune microenvironment and promoting periodontal regeneration (Liu et al., 2019). *In vitro* experiments showd that DPSCs could reduce the viability of natural killer cells and inhibit their cytotoxic activity. Moreover, SHEDs increase the ratio of regulatory T cells (Tregs) to T helper 17 (Th17) cells *in vivo* by restraining the differentiation of Th17 cells (Yamaza et al., 2010). In conclusion, the immunomodulatory properties of odontogenic MSCs allow them to support allotransplantation for tissue-engineering applications, addressing the problem of failure to generate sufficient cells from a single donor for cell transplantation therapy.

Higher Stemness

Odontogenic MSCs show higher stemness because tooth development continues until the permanent teeth replace the deciduous teeth after birth. DPSCs and SHEDs have been reported to have superior proliferative capability to BMSCs and to express some pluripotent markers, such as Sox-2, Nanog and Oct-3/4 (Monterubbianesi et al., 2019; Yang X et al., 2019). GMSCs have also been shown to maintain long-term proliferation with a faster population doubling time than BMSCs (Al Bahrawy et al., 2020). In terms of osteogenic differentiation, DPSCs showed higher odontogenic capacity than BMSCs (Monterubbianesi et al., 2019). After tooth damage occurs, DPSCs are quickly activated, and then proliferate, migrate and differentiate into odontoblasts, replacing apoptotic odontoblasts (Chen et al., 2016). Moreover, from a developmental point of view, teeth and periodontal tissue are produced by the continuous interaction between ectodermal epithelial cells and ectodermal mesenchymal cells from the neural crest and mesoderm (Kota et al., 2016). All subpopulations of odontogenic MSCs not only have the general characteristics of other MSCs but also have neurogenic abilities similar to those of neural crest-derived stem cells (Liu et al., 2015). Several odontogenic MSC subpopulations have been shown to be able to differentiate into nerve cells, including SHEDs (Rosa et al., 2016), dental follicle stem cells (DFSCs) and SCAPs (De Berdt et al., 2015) and human periapical cyst-mesenchymal stem cells (hPCy-MSCs) (Tatullo et al., 2020). Notably, SCAPs can express nestin, GAD, βIII tubulin and neurofilament M and other neuronal cell-associated markers, as well as some neurotrophic factors or neuroprotective factors, to promote neurogenesis and regeneration (de Almeida et al., 2014). Overall, odontogenic MSCs show higher stemness than BMSCs, suggesting that they might play key roles in periodontal regeneration and tooth homeostasis.

Although odontogenic MSCs exhibit many advantages, as described above, they are heterogeneous. The phenotype and genotype of each cell determine its functions. Therefore, studying cell heterogeneity will enable accurate targeting and improved effects on tissue regeneration.

CHARACTERISTICS OF SEVERAL ODONTOGENIC MSC SUBPOPULATIONS

Odontogenic MSC Subpopulations

With the improving understanding of the heterogeneity of MSCs, an increasing number of odontogenic MSC subpopulations have been isolated (**Figure 2**). $CD24^+$ cells were isolated from apical papilla and identified as undifferentiated SCAPs with greater dentine regeneration capacity (Sonoyama et al., 2006). A group of $Gli1^+$ MSCs were also isolated from the periodontal ligaments of

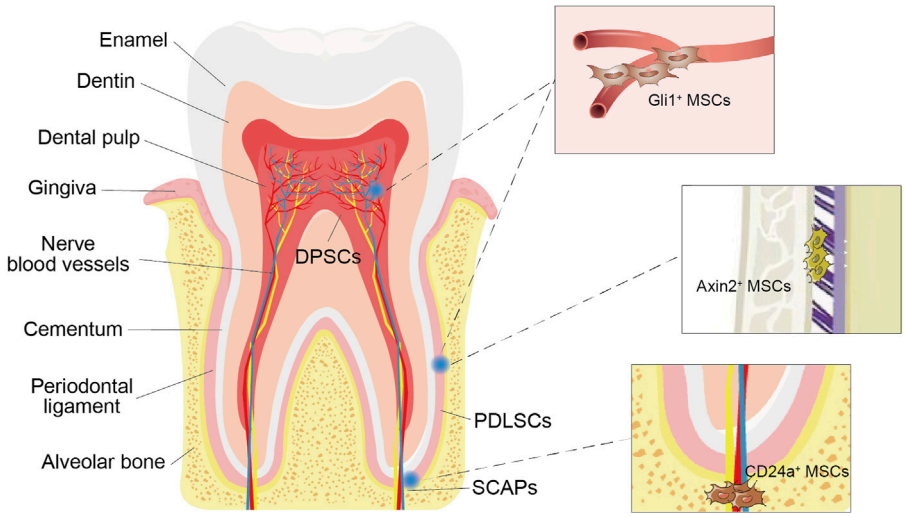

FIGURE 2 | Odontogenic MSCs and their subpopulations. Various types of stem cells, such as dental pulp stem cells (DPSCs), periodontal ligament stem cells (PDLSCs) and stem cells from the root apical papilla (SCAPs), can be found in the dental pulp and periodontal ligament around the tooth root. Gli1$^+$ MSCs surround the vasculature exclusively. Axin2$^+$ MSCs were identified in the periodontal ligament (PDL). CD24a + MSCs were present in human dental papilla tissues.

TABLE 1 | Summary of main characteristics and therapeutic efficacy of MSC subpopulations.

MSC Subpopulations	Tissue Sources	Primary Function	Main characteristics	Therapeutic Efficacy
Gli1$^+$ MSC	Mouse incisor	Tooth support	Strong mobilization in response to tissue injury	Periodontal bone regeneration ↑
		Dentin formation	Generating bone matrix *in vivo*	Fracture repair ↑
Axin2$^+$ MSC	Periodontal ligament	Tooth support Cementum formation	Give rise to cementoblasts and cementocytes *in vivo* Express transcription factors for controlling cementum formation	Cementum regeneration ↑
CD24a$^+$ MSC	Apical papilla	Tooth support Wound healing	Higher proliferation capacity than BM-MSCs Enhanced osteogenic/odontogenic differentiation capabilities	Dental pulp regeneration ↑
CD146$^+$ MSC	Periodontium and pulpal tissue of deciduous teeth	Dentin formation	Express neurogenic markers	Periodontal bone regeneration ↑
			Form dentin-like structures *in vivo*	Dental pulp regeneration ↑
			Higher proliferation capacity than DPSCs and BM-MSCs	
Stro-1$^+$ MSC	Dental pulp of permanent teeth	Dentin formation	Generate the cementum-PDL structure *in vivo*	Periodontal tissue regeneration ↑
			Higher proliferation capacity than DPSCs and BM-MSCs	Alveolar bone regeneration ↑
CD105$^+$ MSC	Dental pulp of permanent teeth	Dentin formation	Express neurogenic markers	Dental tissue inflammation ↓
			Higher proliferation capacity and odontogenic capacity than BM-MSCs	Dentin regeneration ↑
				Dental pulp regeneration ↑
				Alveolar bone regeneration ↑
				Osteogenic potential ↑

mouse molars, surrounding the neurovascular bundle and forming the PDL, cementum, and alveolar bone (Men et al., 2020). In addition, cell lineage tracing studies have shown that the rapid proliferation of Axin2$^+$ MSCs and their progeny can directly contribute to the cellular cementum and the postnatal acellular cementum (Xie et al., 2019). Overall, these subgroups have distinct characteristics and biological activity and enhance the regenerative potential of certain tooth structures. Therefore, it is necessary to further subdivide odontogenic stem cells, clarify their differences in differentiation potential, proliferation rate,

immunosuppression ability and other biological functions, and conduct comparative studies to standardize treatment methods (**Table 1**).

Gli1$^+$ MSCs and Their Role in Odontogenic Regeneration

Gli1 is one of three GLI family transcription effectors at the terminal end of the hedgehog signaling (Hh) pathway, which participate in the progression of cell differentiation and development. Gli1 was first identified in human glioblastoma (Kinzler et al., 1987). Later, in the heart, lung, kidney and other tissues, it was found to have different functions and to participate in injury repair (Kramann et al., 2015). Gli1$^+$ cells surround the vasculature exclusively and are negative for the expression markers of neural or glial cells (b3-tubulin, S100), endothelium (GS-IB4), smooth muscle cells (aSMA), or pericytes (NG2, LepR) (Zhao et al., 2014; Men et al., 2020). Therefore, Gli1$^+$ cell sorting can improve the purity of MSCs and reduce the impact of impurities on clinical applications.

Gli1$^+$ cells have been identified as the stem cells of the mouse long bone, craniofacial bones, and incisor (Pang et al., 2015; Zhao et al., 2015; Shi et al., 2017). It was found that inhibition of Gli1$^+$ cells in the mouse incisor can result in alveolar bone resorption and wider PDL gaps in the periodontium of mice (Chen S et al., 2020), suggesting that the activation of Gli1$^+$ cells may be related to periodontal development and repair in mice.

A large body of work has indicated that Hh critically regulates osteoblast differentiation and is implicated in alveolar bone development and remodeling. As a transcription effector at the terminal end of the Hh signaling pathway, Gli1 may be a marker of a specific MSC subpopulation with enhanced osteogenic capacity (Shi et al., 2017). Several studies have investigated the distribution characteristics and physiological functions of Gli1$^+$ cells *in vivo*. Gli1 expression was detected by using Gli1-LacZ mice, and it was found that there was a large number of stem cells in the periodontal membrane of young mice, especially in 1/3 of the root tip. Gli1$^+$ cells differentiate and mature during the development of the periodontal membrane, and some fusiform or polygonal fibroblasts develop into long fusiform cells, which account for a large proportion of the total number of periodontal ligament cells (Men et al., 2020). Of note, Gli1$^+$ cells in the periodontal membrane can gradually differentiate and proliferate into osteocytes around alveolar bone, and their numbers increase gradually, with the secretion of bone matrix and the formation bone (Hosoya et al., 2020; Liu et al., 2020). Taken together, these findings indicate that Gli1$^+$ cells may be the main cell source for the periodontal membrane and alveolar bone and participate in growth and development during the peak period.

Gli1$^+$ cells exhibit strong mobilization in response to tissue injury. These cells proliferated massively and migrated to the damaged area 24 h after tooth injury and formed repaired dentin later (Zhao et al., 2014). Consistently, 10 days after fracture, Gli1$^+$ cells were detected in the whole fracture callus, indicating that Gli1$^+$ cells, as progenitors of osteoblasts, are responsible for normal bone formation as well as fracture repair (Shi et al., 2017). The ability of Gli1$^+$ cells to respond quickly to injury of multiple tissues and organs suggests that they are a specific MSC subpopulation with potential for morphologic development and repair and regeneration.

Although Gli1$^+$ cells are negative for markers of neural or glial cells (b3-tubulin, S100), endothelium (GS-IB4), smooth muscle cells (aSMA), and pericytes (NG2, LepR) and surround the vasculature (Zhao et al., 2014; Men et al., 2020), they are also heterogeneous, which reflects the complex functions of MSCs in promoting tissue repair and maintaining tissue homeostasis. ScRNA-seq analysis of mouse incisors showed that Gli1$^+$ cells consisted of nine distinct clusters (Chen S et al., 2020). Runx2$^+$ cells in the Gli1$^+$ MSC subpopulation are not MSCs, and they have been identified as niche cells. These niche cells can regulate the proliferation and differentiation of TACs through IGF signaling (Chen S et al., 2020). In this regard, the role of heterogeneous MSCs in tissue regeneration needs to be reconsidered.

Axin2$^+$ MSCs and Their Role in Odontogenic Regeneration

Axin2, which is expressed in the periosteum and osteogenic Frontier of developing sutures, is a negative regulator of the canonical Wnt pathway (Yu et al., 2005; Di Pietro et al., 2020). Targeted destruction of Axin2 in mice leads to structural malformations of the skull (Yu et al., 2005), suggesting that Axin2 may influence osteoblast proliferation and differentiation.

Axin2$^+$ cells were identified in the mouse PDL (Yuan et al., 2018). Severe cementum hypoplasia appeared after the cell ablation of Axin2$^+$ cells *in vivo* (Xie et al., 2019), indicating that Axin2$^+$ mesenchymal PDL cells may be related to cementum growth.

During the development of alveolar bone, Axin2$^+$ cells are activated to form the cementum. After tracing the fate of Axin2$^+$ PDL cells in transgenic mice, these cells were found to give rise to the majority of cementoblasts and cementocytes, and the expression of Axin2 in PDL cells was consistent with postnatal cementum growth (Xie et al., 2019; Zhao et al., 2021). Consistently, cell ablation assays showed a significant decrease in the cellular cementum area and acellular cementum thickness of the mandibular molar distal roots after Axin2$^+$ cell ablation. In addition, immunostaining revealed that Axin2$^+$ cells expressed OSX, a transcription factor in MSCs essential for controlling cementum formation (Cao et al., 2012). Taken together, these findings indicate that Axin2$^+$ PDL cells are the major progenitor cell source for both cellular and acellular cementum growth.

Axin2$^+$ cells respond to Wnt signaling to promote cementum regeneration. Several studies have suggested that Axin2 is a key target of Wnt/β-catenin signaling, which is a fundamental pathway in many stem cell/regenerative/repair contexts (Lohi et al., 2010; Babb et al., 2017). During the development of the periodontium, both cellular and acellular cementum expanded rapidly, while the level of Wnt signaling decreased gradually (Xie et al., 2019; Men et al., 2020). When roots are fully formed, appropriate Wnt signaling activates Axin2$^+$ cells to form cementoblasts to replenish those lost through apoptosis. Thus,

maintaining the characteristics of acellular cementum requires low Wnt activity in Axin2$^+$ cells.

However, Axin2$^+$ cells did not exhibit strong regenerative function after physical injury or infection of periodontal tissue. A likely explanation is that in normally occurring periodontitis the bacteria inhibit the remobilization of Axin2$^+$ cells. Moreover, the heterogeneity of Axin2$^+$ cells is not well understood. Further research should focus on the mechanism by which Axin2$^+$ cells are activated and repressed and the heterogeneity of this specific MSC population to improve clinical treatment outcomes.

CD24a$^+$ MSCs and Their Role in Odontogenic Regeneration

CD24a, also known as heat-stable antigen, is a highly glycosylated molecule with a protein core of only 27 amino acids and is expressed mainly in hamatopoietic and neural cells (Sammar et al., 1997). During development, the expression of CD24a in progenitor cells and metabolically active cells is higher than that in terminally differentiated cells, which reveals that CD24a$^+$ cells show cellular pluripotency and have a strong correlation with the self-renewal state (Shakiba et al., 2015). In cancer-related research, it has been proven that CD24a is associated with aggressive tumor behavior, can enhance the tendency of cells to renew, differentiate and metastasize, and can increase the expression levels of enriched Sox2 and Oct4 (Lee et al., 2011).

CD24a + cells were present in both mouse tooth germs and human dental papilla tissues. The CD24a$^+$ cell population in human dental papillae is an undifferentiated SCAP population. In response to osteogenic induction conditions *in vitro* culture, the number of CD24a$^+$ cells decreased gradually, while the expression of ALP was observed, indicating that CD24a$^+$ stem cells may be related to osteogenic differentiation (Sonoyama et al., 2006).

To further study the osteogenic differentiation ability of CD24a$^+$ cells, Chen et al. developed a 3D spheroid culture system for tooth-derived stem cells to dissect their lineage commitment and characterize their tissue regenerative potential, which can make up for the deficiency of the traditional two-dimensional (2D) adherent culture system. The results showed that 3D spheroid cultured CD24a$^+$ cells maintained their self-renewal state over multiple passages and exhibited enhanced osteogenic/odontogenic differentiation capabilities (Chen H et al., 2020). When transplanted into the renal capsule, these cells could further develop to form regenerative dentin and neurovascular-like structures that mimicked those of native teeth. Therefore, the CD24a$^+$ cell population is an excellent alternative cell source for potential translational use in the clinical management of pulpitis and pulp necrosis.

There have been several studies on the mechanisms by which CD24a improves cell proliferation. CD24a has been shown to trigger downstream SRC-family tyrosine kinases, mediating self-renewal and epithelial-to-mesenchymal transition (Sammar et al., 1997; Lee et al., 2011; Lee et al., 2012). Notably, overexpression of CD24a may cause functional inactivation of the tumor-suppressor genes TP53 and ARF, thereby promoting cell proliferation, which provides a link between CD24a and cell growth (Wang et al., 2015). In addition, knockdown of Sp7 was found to strongly abolish the proliferation of CD24a$^+$ cells. In this regard, Sp7 may be the key transcription factor driving the self-renewal of CD24a$^+$ cells.

However, there have been no *in vivo* trails using the CD24a$^+$ cell subpopulation for pulp regeneration to verify its potential for therapy, which was only observed in the renal capsule. In the future, single-cell sequencing will be required to further clarify the composition of the CD24a$^+$ cell population and verify its ability to regenerate dental pulp *in vivo*.

CD146$^+$ MSCs and Their Role in Odontogenic Regeneration

CD146, also known as Mel-CAM, MUC18, A32 antigen, and S-Endo-1, is a membrane glycoprotein that functions as a Ca^{2+}-independent cell adhesion molecule involved in heterophilic cell–cell interactions (Shih, 1999). CD146 is usually coexpressed with CD73, CD90, CD105, and CD44 on pericytes located outside of capillaries and microvessels in various tissues, such as the muscles, adipose tissue, BM and placenta (Crisan et al., 2008). Several studies suggest that CD146 identifies MSCs with multidirectional differentiation potential (Ma et al., 2021). Compared with CD146$^-$ cells, CD146$^+$ cells showed the potential to differentiate into adipocytes, chondrocytes, and osteoblasts, while CD146$^-$ cells did not (Baksh et al., 2007).

CD146$^+$ cells from dental pulp have the ability to generate dentin/pulp-like structures. The coexpression of CD146 and STRO-1 has been shown to be a prerequisite for enhanced stem cell phenotypes, including higher CFU efficiency, expression of embryonic SC markers and enhanced odontogenic differentiation potential (Bakopoulou et al., 2013). In human dental pulp tissue, CD146 and STRO-1 are coexpressed on the cellular membranes of blood vessels (Shi & Gronthos, 2003; Tavangar et al., 2017), indicating that these cells may be a population with enhanced stem cell phenotypes. *In vitro* alizarin red staining and qRT-PCR showed that CD146$^+$ cells from dental pulp presented higher mineralization ability than nonseparated cells (Xuan et al., 2018). CD146$^+$ cells transplanted into immunocompromised mice also demonstrated their ability to generate dentin/pulp-like structures, compared with CD146$^-$ cells and CD146$^{+/-}$ cells (Matsui et al., 2018). Therefore, CD146$^+$ cells from dental pulp have the ability to perform mineralization *in vitro*, and to form dentin-like structures *in vivo*. Notably, this characteristic of the CD146$^+$ cell subpopulation may be related to the microenvironment required for pulp regeneration. CD146 is a membrane glycoprotein that functions as a Ca^{2+}-independent cell adhesion molecule involved in heterophilic cell–cell interactions (Shih, 1999). Several studies have indicated that CD146$^+$ cells maintain the hematopoietic microenvironment through the release of paracrine factors, such as vascular endothelial growth factor (VEGF), stem cell factor (SCF), Ang-1 and stromal cell-derived factor (SDF)-1 (Sorrentino et al., 2008), and through cell-to-cell contact mechanisms, such as Notch signaling (Corselli et al., 2013). However, it is not clear whether all or only some

$CD146^+$ cells are involved in the maintenance of microenvironmental homeostasis. Further subdivision of $CD146^+$ cells is needed to clarify their role in pulp regeneration.

In addition, $CD146^+$ cells in the PDL also have the capacity to generate a cementum/PDL-like structure and contribute to periodontal tissue repair. Seo et al. isolated $STRO\text{-}1^+/CD146^+$ cells from PDLSCs for the first time, showing their capacity to develop into cementoblast-like cells, adipocytes *in vitro*, and cementum/PDL-like tissue *in vivo* (Seo et al., 2004). Impressively, PDLSCs also showed the capacity to form collagen fibers, similar to Sharpey's fibers, connected to the cementum-like tissue, suggesting their potential to regenerate PDL attachment. However, the limited number of the PDLSCs in extracted teeth limits their application in periodontal tissue regeneration. To obtain sufficient cell numbers, expansion of PDLSCs by cell culture with growth factors such as FGF-2 is essential (Hidaka et al., 2012).

Taken together, these findings reflect the fact that $CD146^+$ cells exhibit a remarkable capacity for regeneration. However, *in vitro* culture for amplification may increase the heterogeneity of the $CD146^+$ cell population, which may affect clinical application. Further research needs to be done to investigate the respective roles of different subpopulations of $CD146^+$ cells in tissue regeneration, and to explore how to increase the number of cells on a large scale without affecting their functions.

STRO-1$^+$ MSCs and Their Role in Odontogenic Regeneration

STRO-1 is considered the best-known marker used to identify MSCs (Kolf et al., 2007). STRO-1 is a 75 kDa endothelial antigen that is localized to the endothelium of some arterioles and capillaries in some tested tissues, such as adipose tissue, muscle, liver, lungs and kidneys (Lin et al., 2011; Ning et al., 2011). STRO-1-negative cell populations have been reported to be unable to form colonies (Simmons and Torok-Storb, 1991). Only cells expressing the STRO-1 antigen are capable of becoming hematopoiesis-supportive stromal cells with a vascular smooth muscle-like phenotype, adipocytes, osteoblasts and chondrocytes (Dennis et al., 2002), which is consistent with the functional role of MSCs.

$STRO\text{-}1^+$ cells isolated from human adult dental pulp were located in the perivascular region (Shi and Gronthos, 2003). It was reported that sorted $STRO\text{-}1^+$ dental pulp cells demonstrated the capacity to form multiple layers and mineralized nodules when cultured in conditioned medium, whereas the $STRO\text{-}1^-$ population showed a lack of the capability to form mineralized nodules *in vitro* (Yang et al., 2007). Thus, $STRO\text{-}1^+$ cells might represent a better source of cells for therapeutic purposes than unsorted heterogeneous cells.

$STRO\text{-}1^+$ cells exhibit greater clonogenicity, proliferative capacity and multilineage differentiation potential than $STRO\text{-}1^-$ or the nonsorted cell population (Simmons and Torok-Storb, 1991; Gronthos et al., 2001; Psaltis et al., 2010). $STRO\text{-}1^+$ cells were observed to achieve approximately 20% more population doublings than nonsorted cell populations *in vitro* culture, ultimately resulting in higher cumulative population expansion *in vitro* (Gronthos et al., 2003; Psaltis et al., 2010). In addition, $STRO\text{-}1^+$ cells consistently exhibited higher mRNA transcript levels, which have been associated with early mesenchymal development and/or proliferative capacity (Psaltis et al., 2010). This may explain the high cloning efficiency of $STRO\text{-}1^+$ cells. Notably, it was suggested that the telomerase activity of $STRO\text{-}1^+$ cells was greatly enhanced (Simonsen et al., 2002), whereas the telomerase activity of normal somatic cells was lost during proliferation and differentiation (Fuchs and Segre, 2000). Telomerase activity is a key factor oin the proliferative lifespan and osteogenic potential of human BM mesenchymal cells in culture. Therefore, the enhanced telomerase activity of $STRO\text{-}1^+$ cells also greatly enhanced their proliferative and osteogenic potential.

$STRO\text{-}1^+$ cell sorting improves the purity of MSCs, which may affect their odontogenic differentiation capacity. However, it was recently found that although the proportion of $STRO\text{-}1^+$ cells expanded during osteogenic differentiation (Perczel-Kovach et al., 2021), they did not show a better performance than $STRO\text{-}1^-$ or unsorted heterogeneous cells in osteogenesis (Gurel Pekozer et al., 2018). This is probably because STRO-1 simply distinguishes a subpopulation of MSCs that are unique in terms of adherence, proliferation and multilineage differentiation potential, but these cells are still heterogeneous. Therefore, further studies are needed to determine the composition of $STRO\text{-}1^+$ cells and to determine which subpopulation has stronger odontogenic differentiation ability.

CD105$^+$ MSCs and Their Role in Odontogenic Regeneration

CD105 (Endoglin, SH2), a 180 kDa homodimeric glycoprotein, is a component of the TGF-β receptor complex and is mainly found on circulating vascular endothelial cells in regenerating, inflamed tissues or tumors with active angiogenesis (Cheifetz et al., 1992). Nakashima et al. isolated a $CD105^+$ cell population from human adult dental pulp tissue for the first time by flow cytometry and demonstrated colony formation activity of these cells (Nakashima et al., 2009).

Compared with total pulp cells, $CD105^+$ pulp cells showed high proliferation and migration activities and expressed higher levels of glial cell line-derived neurotrophic factor (GDNF) and VEGF-A *in vitro*, suggesting that they appear to have good cell properties for pulp regeneration.

The $CD105^+$ cell subpopulation may be involved in nerve and vascular development. CD105 has been associated with active angiogenesis (Cheifetz et al., 1992). $CD105^+$ cells showed multilineage differentiation potential, including adipogenesis, dentinogenesis, angiogenesis and neurogenesis potential, *in vitro* (Iohara et al., 2011). In an experimental model of tooth autogenous transplantation of $CD105^+$ cells together with type I and type III collagen as a scaffold, pulp tissue achieved complete regeneration of capillaries and neuronal processes, whereas unsorted DPSCs were preferable for differentiation into odontoblasts to mineralize and form dentin in the pulp chamber and root canal (Nakashima et al., 2009). Thus, compared with total pulp cells, the pulp $CD105^+$ cell

subpopulation may be a candidate cell resource for the induction of pulp regeneration by cell therapy.

Moreover, $CD105^+$ cells are capable of trophic effects on endothelial cells. It was reported that the transplanted $CD105^+$ cells were likely to be located near the newly formed vasculature and expressed proangiogenic factors, implying their nutritional effect on the formation of new blood vessels (Iohara et al., 2011).

However, the $CD105^+$ cell subpopulation is inherently heterogeneous, and some fractions, such as the $CD105^+$/STRO-1^- population, may have a negative effect on the differentiation potential of the whole population (Gothard et al., 2014). Further subdivision of the $CD105^+$ cell population is needed in the future to achieve a stable therapeutic effect in the context of pulp regeneration.

CONCLUSION AND PERSPECTIVE

The body of work outlined in this review highlights the biological characteristics of several odontogenic MSC subpopulations. Recent studies suggest that odontogenic MSCs have enormous potential in the regeneration of pulp, periodontium and alveolar bone. However, the phenotypic and genetic differences among cell subpopulations affect the function of MSCs. There are also differences in proliferation and differentiation potential among stem cells isolated from the same site, which makes their role in tissue regeneration and disease management unclear, posing a challenge for the development of regenerative medicine. In addition, different cell subpopulations also provide different treatment approaches for diseases. It is essential to further clarify the biological differences between odontogenic MSC subpopulations and evaluate their therapeutic benefits in specific tissue regeneration contexts in the field of regenerative medicine. It may be important to improve the outcomes of regenerative therapy via cell sorting, which aims to divide cells into subpopulations according to their functional characteristics, and subsequent application of one or more subpopulation for different needs. To achieve this, larger patient-donor cohorts need to be included, and lineages of MSC subsets with different proliferation and differentiation characteristics need to be studied more extensively using extensive genomic and proteomic sequencing to explore more reliable gene, protein and metabolic markers.

AUTHOR CONTRIBUTIONS

YC, ZZ, AL and KX contributed to the design, review, and proofreading of the manuscript. XY and JF contributed to the material collections and analysis. YC and SL contributed to the design of the figures. All authors agreed with the submission of the final version of the manuscript.

FUNDING

This work was supported by the National Natural Science Foundation of China (Nos. 82071075, 8210031832).

REFERENCES

Abe, S., Yamaguchi, S., Watanabe, A., Hamada, K., and Amagasa, T. (2008). Hard Tissue Regeneration Capacity of Apical Pulp Derived Cells (APDCs) from Human Tooth with Immature apex. *Biochem. biophysical Res. Commun.* 371 (1), 90–93. doi:10.1016/j.bbrc.2008.04.016

Al Bahrawy, M., Ghaffar, K., Gamal, A., El-Sayed, K., and Iacono, V. (2020). Effect of Inflammation on Gingival Mesenchymal Stem/Progenitor Cells' Proliferation and Migration through Microperforated Membranes: An *In Vitro* Study. *Stem Cell Int.* 2020, 1–10. doi:10.1155/2020/5373418

Babb, R., Chandrasekaran, D., Carvalho Moreno Neves, V., and Sharpe, P. T. (2017). Axin2-expressing Cells Differentiate into Reparative Odontoblasts via Autocrine Wnt/β-Catenin Signaling in Response to Tooth Damage. *Sci. Rep.* 7 (1), 3102. doi:10.1038/s41598-017-03145-6

Bakopoulou, A., Leyhausen, G., Volk, J., Koidis, P., and Geurtsen, W. (2013). Comparative Characterization of STRO-1(neg)/CD146(pos) and STRO-1(pos)/CD146(pos) Apical Papilla Stem Cells Enriched with Flow Cytometry. *Arch. Oral Biol.* 58 (10), 1556–1568. doi:10.1016/j.archoralbio.2013.06.018

Baksh, D., Yao, R., and Tuan, R. S. (2007). Comparison of Proliferative and Multilineage Differentiation Potential of Human Mesenchymal Stem Cells Derived from Umbilical Cord and Bone Marrow. *Stem Cells* 25 (6), 1384–1392. doi:10.1634/stemcells.2006-0709

Bianco, P., Riminucci, M., Gronthos, S., and Robey, P. G. (2001). Bone Marrow Stromal Stem Cells: Nature, Biology, and Potential Applications. *Stem Cells* 19 (3), 180–192. doi:10.1634/stemcells.19-3-180

Bressan, E., Ferroni, L., Gardin, C., Bellin, G., Sbricoli, L., Sivolella, S., et al. (2019). Metal Nanoparticles Released from Dental Implant Surfaces: Potential Contribution to Chronic Inflammation and Peri-Implant Bone Loss. *Materials* 12 (12), 2036. doi:10.3390/ma12122036

Cao, Z., Zhang, H., Zhou, X., Han, X., Ren, Y., Gao, T., et al. (2012). Genetic Evidence for the Vital Function of Osterix in Cementogenesis. *J. Bone Miner Res.* 27 (5), 1080–1092. doi:10.1002/jbmr.1552

Cheifetz, S., Bellón, T., Calés, C., Vera, S., Bernabeu, C., Massagué, J., et al. (1992). Endoglin Is a Component of the Transforming Growth Factor-Beta Receptor System in Human Endothelial Cells. *J. Biol. Chem.* 267, 19027–19030. doi:10.1016/s0021-9258(18)41732-2

Chen, F.-M., Sun, H.-H., Lu, H., and Yu, Q. (2012). Stem Cell-Delivery Therapeutics for Periodontal Tissue Regeneration. *Biomaterials* 33 (27), 6320–6344. doi:10.1016/j.biomaterials.2012.05.048

Chen, H., Fu, H., Wu, X., Duan, Y., Zhang, S., Hu, H., et al. (2020). Regeneration of Pulpo-dentinal-like Complex by a Group of Unique Multipotent CD24a + Stem Cells. *Sci. Adv.* 6 (15), eaay1514. doi:10.1126/sciadv.aay1514

Chen, S., Jing, J., Yuan, Y., Feng, J., Han, X., Wen, Q., et al. (2020). Runx2+ Niche Cells Maintain Incisor Mesenchymal Tissue Homeostasis through IGF Signaling. *Cel Rep.* 32 (6), 108007. doi:10.1016/j.celrep.2020.108007

Chen, Y.-Y., He, S.-T., Yan, F.-H., Zhou, P.-F., Luo, K., Zhang, Y.-D., et al. (2016). Dental Pulp Stem Cells Express Tendon Markers under Mechanical Loading and Are a Potential Cell Source for Tissue Engineering of Tendon-like Tissue. *Int. J. Oral Sci.* 8 (4), 213–222. doi:10.1038/ijos.2016.33

Corselli, M., Chin, C. J., Parekh, C., Sahaghian, A., Wang, W., Ge, S., et al. (2013). Perivascular Support of Human Hematopoietic Stem/progenitor Cells. *Blood* 121 (15), 2891–2901. doi:10.1182/blood-2012-08-451864

Crisan, M., Yap, S., Casteilla, L., Chen, C.-W., Corselli, M., Park, T. S., et al. (2008). A Perivascular Origin for Mesenchymal Stem Cells in Multiple Human Organs. *Cell Stem Cell* 3 (3), 301–313. doi:10.1016/j.stem.2008.07.003

de Almeida, J. F. A., Chen, P., Henry, M. A., and Diogenes, A. (2014). Stem Cells of the Apical Papilla Regulate Trigeminal Neurite Outgrowth and Targeting through a BDNF-dependent Mechanism. *Tissue Engineering. Part. A.* 20, 3089–3100. doi:10.1089/ten.TEA.2013.0347

De Berdt, P., Vanacker, J., Ucakar, B., Elens, L., Diogenes, A., Leprince, J. G., et al. (2015). Dental Apical Papilla as Therapy for Spinal Cord Injury. *J. Dent Res.* 94 (11), 1575–1581. doi:10.1177/0022034515604612

Dennis, J. E., Carbillet, J.-P., Caplan, A. I., and Charbord, P. (2002). The STRO-1+ Marrow Cell Population Is Multipotential. *Cells Tissues Organs* 170, 73–82. doi:10.1159/000046182

Di Pietro, L., Barba, M., Prampolini, C., Ceccariglia, S., Frassanito, P., Vita, A., et al. (2020). GLI1 and AXIN2 Are Distinctive Markers of Human Calvarial Mesenchymal Stromal Cells in Nonsyndromic Craniosynostosis. *Ijms* 21 (12), 4356. doi:10.3390/ijms21124356

Driskell, R. R., Clavel, C., Rendl, M., and Watt, F. M. (2011). Hair Follicle Dermal Papilla Cells at a Glance. *J. Cel. Sci.* 124, 1179–1182. doi:10.1242/jcs.082446

Feng, J., Mantesso, A., De Bari, C., Nishiyama, A., and Sharpe, P. T. (2011). Dual Origin of Mesenchymal Stem Cells Contributing to Organ Growth and Repair. *Proc. Natl. Acad. Sci. U.S.A.* 108 (16), 6503–6508. doi:10.1073/pnas.1015449108

Friedenstein, A. J., Latzinik, N. W., Grosheva, A. G., and Gorskaya, U. F. (1982). Marrow Microenvironment Transfer by Heterotopic Transplantation of Freshly Isolated and Cultured Cells in Porous Sponges. *Exp. Hematol.* 10, 217–227.

Fuchs, E., and Segre, J. A. (2000). Stem Cells: a New Lease on Life. *Cell* 100 (1), 143–155. doi:10.1016/s0092-8674(00)81691-8

Gonmanee, T., Sritanaudomchai, H., Vongsavan, K., Faisaikarm, T., Songsaad, A., White, K. L., et al. (2020). Neuronal Differentiation of Dental Pulp Stem Cells from Human Permanent and Deciduous Teeth Following Coculture with Rat Auditory Brainstem Slices. *Anatomical Rec.* 303 (11), 2931–2946. doi:10.1002/ar.24368

Gothard, D., Greenhough, J., Ralph, E., and Oreffo, R. O. (2014). Prospective Isolation of Human Bone Marrow Stromal Cell Subsets: A Comparative Study between Stro-1-, CD146- and CD105-Enriched Populations. *J. Tissue Eng.* 5, 204173141455176. doi:10.1177/2041731414551763

Gronthos, S., Mankani, M., Brahim, J., Robey, P. G., and Shi, S. (2000). Postnatal Human Dental Pulp Stem Cells (DPSCs) *In Vitro* and *In Vivo*. *Proc. Natl. Acad. Sci. U.S.A.* 97 (25), 13625–13630. doi:10.1073/pnas.240309797

Gronthos, S., Simmons, P. J., Graves, S. E., and G. Robey, P. (2001). Integrin-mediated Interactions between Human Bone Marrow Stromal Precursor Cells and the Extracellular Matrix. *Bone* 28 (2), 174–181. doi:10.1016/s8756-3282(00)00424-5

Gronthos, S., Zannettino, A. C. W., Hay, S. J., Shi, S., Graves, S. E., Kortesidis, A., et al. (2003). Molecular and Cellular Characterisation of Highly Purified Stromal Stem Cells Derived from Human Bone Marrow. *J. Cel Sci* 116 (Pt 9), 1827–1835. doi:10.1242/jcs.00369

Gurel Pekozer, G., Ramazanoglu, M., Schlegel, K. A., Kok, F. N., and Torun Kose, G. (2018). Role of STRO-1 Sorting of Porcine Dental Germ Stem Cells in Dental Stem Cell-Mediated Bone Tissue Engineering. *Artif. Cell Nanomedicine, Biotechnol.* 46 (3), 607–618. doi:10.1080/21691401.2017.1332637

Hasegawa, M., Yamato, M., Kikuchi, A., Okano, T., and Ishikawa, I. (2005). Human Periodontal Ligament Cell Sheets Can Regenerate Periodontal Ligament Tissue in an Athymic Rat Model. *Tissue Eng.* 11, 469–478. doi:10.1089/ten.2005.11.469

Hayashi, Y., Ohnuma, K., and Furue, M. K. (2019). Pluripotent Stem Cell Heterogeneity. *Adv. Exp. Med. Biol.* 1123, 71–94. doi:10.1007/978-3-030-11096-3_6

Hidaka, T., Nagasawa, T., Shirai, K., Kado, T., and Furuichi, Y. (2012). FGF-2 Induces Proliferation of Human Periodontal Ligament Cells and Maintains Differentiation Potentials of STRO-1(+)/CD146(+) Periodontal Ligament Cells. *Arch. Oral Biol.* 57 (6), 830–840. doi:10.1016/j.archoralbio.2011.12.003

Hosoya, A., Shalehin, N., Takebe, H., Shimo, T., and Irie, K. (2020). Sonic Hedgehog Signaling and Tooth Development. *Ijms* 21 (5), 1587. doi:10.3390/ijms21051587

Huang, Y., Li, Q., Zhang, K., Hu, M., Wang, Y., Du, L., et al. (2019). Single Cell Transcriptomic Analysis of Human Mesenchymal Stem Cells Reveals Limited Heterogeneity. *Cell Death Dis* 10 (5), 368. doi:10.1038/s41419-019-1583-4

Iohara, K., Imabayashi, K., Ishizaka, R., Watanabe, A., Nabekura, J., Ito, M., et al. (2011). Complete Pulp Regeneration after Pulpectomy by Transplantation of CD105+ Stem Cells with Stromal Cell-Derived Factor-1. *Tissue Eng. A* 17 (15-16), 1911–1920. doi:10.1089/ten.TEA.2010.0615

Iohara, K., Murakami, M., Takeuchi, N., Osako, Y., Ito, M., Ishizaka, R., et al. (2013). A Novel Combinatorial Therapy with Pulp Stem Cells and Granulocyte colony-stimulating Factor for Total Pulp Regeneration. *Stem Cell translational Med.* 2 (7), 521–533. doi:10.5966/sctm.2012-0132

Isern, J., García-García, A., Martín, A. M., Arranz, L., Martín-Pérez, D., Torroja, C., et al. (2014). The Neural Crest Is a Source of Mesenchymal Stem Cells with Specialized Hematopoietic Stem Cell Niche Function. *Elife* 3, e03696. doi:10.7554/eLife.03696

Jahoda, C. A. B., Horne, K. A., and Oliver, R. F. (1984). Induction of Hair Growth by Implantation of Cultured Dermal Papilla Cells. *Nature* 311 (5986), 560–562. doi:10.1038/311560a0

Kaukua, N., Shahidi, M. K., Konstantinidou, C., Dyachuk, V., Kaucka, M., Furlan, A., et al. (2014). Glial Origin of Mesenchymal Stem Cells in a Tooth Model System. *Nature* 513 (7519), 551–554. doi:10.1038/nature13536

Kinzler, K. W., Bigner, S. H., Bigner, D. D., Trent, J. M., Law, M. L., O'Brien, S. J., et al. (1987). Identification of an Amplified, Highly Expressed Gene in a Human Glioma. *Science* 236 (4797), 70–73. doi:10.1126/science.3563490

Kolf, C. M., Cho, E., and Tuan, R. S. (2007). Mesenchymal Stromal Cells. Biology of Adult Mesenchymal Stem Cells: Regulation of Niche, Self-Renewal and Differentiation. *Arthritis Res. Ther.* 9 (1), 204. doi:10.1186/ar2116

Kota, K., Kota, K., Chakkarayan, R., Chakkarayan, J., and Thodiyil, A. (2016). Epithelial - Mesenchymal Interactions in Tooth Development and the Significant Role of Growth Factors and Genes with Emphasis on Mesenchyme - A Review. *Jcdr* 10 (9), ZE05–ZE09. doi:10.7860/jcdr/2016/21719.8502

Kramann, R., Schneider, R. K., DiRocco, D. P., Machado, F., Fleig, S., Bondzie, P. A., et al. (2015). Perivascular Gli1+ Progenitors Are Key Contributors to Injury-Induced Organ Fibrosis. *Cell Stem Cell* 16 (1), 51–66. doi:10.1016/j.stem.2014.11.004

Krivanek, J., Soldatov, R. A., Kastriti, M. E., Chontorotzea, T., Herdina, A. N., Petersen, J., et al. (2020). Dental Cell Type Atlas Reveals Stem and Differentiated Cell Types in Mouse and Human Teeth. *Nat. Commun.* 11 (1), 4816. doi:10.1038/s41467-020-18512-7

Laing, A. G., Riffo-Vasquez, Y., Sharif-Paghaleh, E., Lombardi, G., and Sharpe, P. T. (2018). Immune Modulation by Apoptotic Dental Pulp Stem Cells *In Vivo*. *Immunotherapy* 10 (3), 201–211. doi:10.2217/imt-2017-0117

Le Blanc, K. (2006). Mesenchymal Stromal Cells: Tissue Repair and Immune Modulation. *Cytotherapy* 8 (6), 559–561. doi:10.1080/14653240601045399

Lee, K.-m., Ju, J.-h., Jang, K., Yang, W., Yi, J. Y., Noh, D. Y., et al. (2012). CD24 Regulates Cell Proliferation and Transforming Growth Factor β-induced Epithelial to Mesenchymal Transition through Modulation of Integrin β1 Stability. *Cell Signal.* 24 (11), 2132–2142. doi:10.1016/j.cellsig.2012.07.005

Lee, T. K. W., Castilho, A., Cheung, V. C. H., Tang, K. H., Ma, S., and Ng, I. O. L. (2011). CD24(+) Liver Tumor-Initiating Cells Drive Self-Renewal and Tumor Initiation through STAT3-Mediated NANOG Regulation. *Cell Stem Cell* 9 (1), 50–63. doi:10.1016/j.stem.2011.06.005

Lei, Y., Tang, R., Xu, J., Wang, W., Zhang, B., Liu, J., et al. (2021). Applications of Single-Cell Sequencing in Cancer Research: Progress and Perspectives. *J. Hematol. Oncol.* 14 (1), 91. doi:10.1186/s13045-021-01105-2

Levy, O., Kuai, R., Siren, E. M. J., Bhere, D., Milton, Y., Nissar, N., et al. (2020). Shattering Barriers toward Clinically Meaningful MSC Therapies. *Sci. Adv.* 6 (30), eaba6884. doi:10.1126/sciadv.aba6884

Li, T.-S., Cheng, K., Malliaras, K., Smith, R. R., Zhang, Y., Sun, B., et al. (2012). Direct Comparison of Different Stem Cell Types and Subpopulations Reveals superior Paracrine Potency and Myocardial Repair Efficacy with Cardiosphere-Derived Cells. *J. Am. Coll. Cardiol.* 59 (10), 942–953. doi:10.1016/j.jacc.2011.11.029

Lin, G., Liu, G., Banie, L., Wang, G., Ning, H., Lue, T. F., et al. (2011). Tissue Distribution of Mesenchymal Stem Cell Marker Stro-1. *Stem Cell Dev.* 20 (10), 1747–1752. doi:10.1089/scd.2010.0564

Liu, A. Q., Zhang, L. S., Chen, J., Sui, B. D., Liu, J., Zhai, Q. M., et al. (2020). Mechanosensing by Gli1 + Cells Contributes to the Orthodontic Force-induced Bone Remodelling. *Cell Prolif* 53 (5), e12810. doi:10.1111/cpr.12810

Liu, H.-C., E, L.-L., Wang, D.-S., Su, F., Wu, X., Shi, Z.-P., et al. (2011). Reconstruction of Alveolar Bone Defects Using Bone Morphogenetic Protein 2 Mediated Rabbit Dental Pulp Stem Cells Seeded on Nano-hydroxyapatite/collagen/poly(L-Lactide). *Tissue Engineering. Part. A.* 17, 2417–2433. doi:10.1089/ten.TEA.2010.0620

Liu, J., Chen, B., Bao, J., Zhang, Y., Lei, L., and Yan, F. (2019). Macrophage Polarization in Periodontal Ligament Stem Cells Enhanced Periodontal Regeneration. *Stem Cel Res Ther* 10 (1), 320. doi:10.1186/s13287-019-1409-4

Liu, J., Yu, F., Sun, Y., Jiang, B., Zhang, W., Yang, J., et al. (2015). Concise Reviews: Characteristics and Potential Applications of Human Dental Tissue-Derived Mesenchymal Stem Cells. *Stem cells (Dayton, Ohio)* 33 (3), 627–638. doi:10.1002/stem.1909

Lohi, M., Tucker, A. S., and Sharpe, P. T. (2009). Expression of Axin2 Indicates a Role for Canonical Wnt Signaling in Development of the crown and Root during Pre- and Postnatal Tooth Development. *Dev. Dyn.* 239 (1), NA. doi:10.1002/dvdy.22047

Lv, F.-J., Tuan, R. S., Cheung, K. M. C., and Leung, V. Y. L. (2014). Concise Review: the Surface Markers and Identity of Human Mesenchymal Stem Cells. *Stem cells (Dayton, Ohio)* 32 (6), 1408–1419. doi:10.1002/stem.1681

Ma, L., Huang, Z., Wu, D., Kou, X., Mao, X., and Shi, S. (2021). CD146 Controls the Quality of Clinical Grade Mesenchymal Stem Cells from Human Dental Pulp. *Stem Cel Res Ther* 12 (1), 488. doi:10.1186/s13287-021-02559-4

Mabuchi, Y., Okawara, C., Méndez-Ferrer, S., and Akazawa, C. (2021). Cellular Heterogeneity of Mesenchymal Stem/Stromal Cells in the Bone Marrow. *Front. Cel Dev. Biol.* 9, 689366. doi:10.3389/fcell.2021.689366

Marrelli, M., Paduano, F., and Tatullo, M. (2013). Cells Isolated from Human Periapical Cysts Express Mesenchymal Stem Cell-like Properties. *Int. J. Biol. Sci.* 9 (10), 1070–1078. doi:10.7150/ijbs.6662

Matsui, M., Kobayashi, T., and Tsutsui, T. W. (2018). CD146 Positive Human Dental Pulp Stem Cells Promote Regeneration of Dentin/pulp-like Structures. *Hum. Cel* 31 (2), 127–138. doi:10.1007/s13577-017-0198-2

Men, Y., Wang, Y., Yi, Y., Jing, D., Luo, W., Shen, B., et al. (2020). Gli1+ Periodontium Stem Cells Are Regulated by Osteocytes and Occlusal Force. *Dev. Cel* 54 (5), 639–654. doi:10.1016/j.devcel.2020.06.006

Merimi, M., El-Majzoub, R., Lagneaux, L., Moussa Agha, D., Bouhtit, F., Meuleman, N., et al. (2021). The Therapeutic Potential of Mesenchymal Stromal Cells for Regenerative Medicine: Current Knowledge and Future Understandings. *Front. Cel Dev. Biol.* 9, 661532. doi:10.3389/fcell.2021.661532

Miura, M., Gronthos, S., Zhao, M., Lu, B., Fisher, L. W., Robey, P. G., et al. (2003). SHED: Stem Cells from Human Exfoliated Deciduous Teeth. *Proc. Natl. Acad. Sci. U.S.A.* 100 (10), 5807–5812. doi:10.1073/pnas.0937635100

Monterubbianesi, R., Bencun, M., Pagella, P., Woloszyk, A., Orsini, G., and Mitsiadis, T. A. (2019). A Comparative *In Vitro* Study of the Osteogenic and Adipogenic Potential of Human Dental Pulp Stem Cells, Gingival Fibroblasts and Foreskin Fibroblasts. *Sci. Rep.* 9 (1), 1761. doi:10.1038/s41598-018-37981-x

Morgan, B. A. (2014). The Dermal Papilla: an Instructive Niche for Epithelial Stem and Progenitor Cells in Development and Regeneration of the Hair Follicle. *Cold Spring Harbor Perspect. Med.* 4 (7), a015180. doi:10.1101/cshperspect.a015180

Morsczeck, C., Götz, W., Schierholz, J., Zeilhofer, F., Kühn, U., Möhl, C., et al. (2005). Isolation of Precursor Cells (PCs) from Human Dental Follicle of Wisdom Teeth. *Matrix Biol.* 24 (2), 155–165. doi:10.1016/j.matbio.2004.12.004

Nakashima, M., Iohara, K., and Sugiyama, M. (2009). Human Dental Pulp Stem Cells with Highly Angiogenic and Neurogenic Potential for Possible Use in Pulp Regeneration. *Cytokine Growth Factor. Rev.* 20 (5-6), 435–440. doi:10.1016/j.cytogfr.2009.10.012

Ning, H., Lin, G., Lue, T. F., and Lin, C.-S. (2011). Mesenchymal Stem Cell Marker Stro-1 Is a 75kd Endothelial Antigen. *Biochem. Biophysical Res. Commun.* 413 (2), 353–357. doi:10.1016/j.bbrc.2011.08.104

Ono, H., Arai, Y., Furukawa, E., Narushima, D., Matsuura, T., Nakamura, H., et al. (2021). Single-cell DNA and RNA Sequencing Reveals the Dynamics of Intra-tumor Heterogeneity in a Colorectal Cancer Model. *BMC Biol.* 19 (1), 207. doi:10.1186/s12915-021-01147-5

Pang, P., Shimo, T., Takada, H., Matsumoto, K., Yoshioka, N., Ibaragi, S., et al. (2015). Expression Pattern of Sonic Hedgehog Signaling and Calcitonin Gene-Related Peptide in the Socket Healing Process after Tooth Extraction. *Biochem. Biophysical Res. Commun.* 467 (1), 21–26. doi:10.1016/j.bbrc.2015.09.139

Pang, Y. W., Feng, J., Daltoe, F., Fatscher, R., Gentleman, E., Gentleman, M. M., et al. (2016). Perivascular Stem Cells at the Tip of Mouse Incisors Regulate Tissue Regeneration. *J. Bone Miner Res.* 31 (3), 514–523. doi:10.1002/jbmr.2717

Park, J.-Y., Jeon, S. H., and Choung, P.-H. (2011). Efficacy of Periodontal Stem Cell Transplantation in the Treatment of Advanced Periodontitis. *Cel Transpl.* 20 (2), 271–286. doi:10.3727/096368910x519292

Pe'er, D., Ogawa, S., Elhanani, O., Keren, L., Oliver, T. G., and Wedge, D. (2021). Tumor Heterogeneity. *Cancer cell* 39 (8), 1015–1017. doi:10.1016/j.ccell.2021.07.009

Perczel-Kovách, K., Hegedűs, O., Földes, A., Sangngoen, T., Kálló, K., Steward, M. C., et al. (2021). STRO-1 Positive Cell Expansion during Osteogenic Differentiation: A Comparative Study of Three Mesenchymal Stem Cell Types of Dental Origin. *Arch. Oral Biol.* 122, 104995. doi:10.1016/j.archoralbio.2020.104995

Psaltis, P. J., Paton, S., See, F., Arthur, A., Martin, S., Itescu, S., et al. (2010). Enrichment for STRO-1 Expression Enhances the Cardiovascular Paracrine Activity of Human Bone Marrow-Derived Mesenchymal Cell Populations. *J. Cel. Physiol.* 223 (2), 530. doi:10.1002/jcp.22081

Rosa, V., Dubey, N., Islam, I., Min, K.-S., and Nör, J. E. (2016). Pluripotency of Stem Cells from Human Exfoliated Deciduous Teeth for Tissue Engineering. *Stem Cell Int.* 2016, 1–6. doi:10.1155/2016/5957806

Sammar, M., Gulbins, E., Hilbert, K., Lang, F., and Altevogt, P. (1997). Mouse CD24 as a Signaling Molecule for Integrin-Mediated Cell Binding: Functional and Physical Association with Src-Kinases. *Biochem. biophysical Res. Commun.* 234 (2), 330–334. doi:10.1006/bbrc.1997.6639

Seo, B.-M., Miura, M., Gronthos, S., Mark Bartold, P., Batouli, S., Brahim, J., et al. (2004). Investigation of Multipotent Postnatal Stem Cells from Human Periodontal Ligament. *The Lancet* 364 (9429), 149–155. doi:10.1016/s0140-6736(04)16627-0

Shakiba, N., White, C. A., Lipsitz, Y. Y., Yachie-Kinoshita, A., Tonge, P. D., Hussein, S. M. I., et al. (2015). CD24 Tracks Divergent Pluripotent States in Mouse and Human Cells. *Nat. Commun.* 6, 7329. doi:10.1038/ncomms8329

Shi, S., and Gronthos, S. (2003). Perivascular Niche of Postnatal Mesenchymal Stem Cells in Human Bone Marrow and Dental Pulp. *J. Bone Miner Res.* 18 (4), 696–704. doi:10.1359/jbmr.2003.18.4.696

Shi, Y., He, G., Lee, W.-C., McKenzie, J. A., Silva, M. J., and Long, F. (2017). Gli1 Identifies Osteogenic Progenitors for Bone Formation and Fracture Repair. *Nat. Commun.* 8 (1), 2043. doi:10.1038/s41467-017-02171-2

Shih, I.-M. (1999). The Role of CD146 (Mel-CAM) in Biology and Pathology. *J. Pathol.* 189 (1), 4–11. doi:10.1002/(sici)1096-9896(199909)189:1<4::aid-path332>3.0.co;2-p

Simmons, P., and Torok-Storb, B. (1991). Identification of Stromal Cell Precursors in Human Bone Marrow by a Novel Monoclonal Antibody, STRO-1. *Blood* 78 (1), 55–62. doi:10.1182/blood.v78.1.55.bloodjournal78155

Simonsen, J. L., Rosada, C., Serakinci, N., Justesen, J., Stenderup, K., Rattan, S. I. S., et al. (2002). Telomerase Expression Extends the Proliferative Life-Span and Maintains the Osteogenic Potential of Human Bone Marrow Stromal Cells. *Nat. Biotechnol.* 20 (6), 592–596. doi:10.1038/nbt0602-592

Sonoyama, W., Liu, Y., Fang, D., Yamaza, T., Seo, B.-M., Zhang, C., et al. (2006). Mesenchymal Stem Cell-Mediated Functional Tooth Regeneration in Swine. *PLoS One* 1, e79. doi:10.1371/journal.pone.0000079

Sorrentino, A., Ferracin, M., Castelli, G., Biffoni, M., Tomaselli, G., Baiocchi, M., et al. (2008). Isolation and Characterization of CD146+ Multipotent Mesenchymal Stromal Cells. *Exp. Hematol.* 36 (8), 1035–1046. doi:10.1016/j.exphem.2008.03.004

Sun, W., Wang, Z., Xu, Q., Sun, H., Liu, X., Yang, J., et al. (2019). The Treatment of Systematically Transplanted Gingival Mesenchymal Stem Cells in Periodontitis in Mice. *Exp. Ther. Med.* 17 (3), 2199–2205. doi:10.3892/etm.2019.7165

Takashima, Y., Era, T., Nakao, K., Kondo, S., Kasuga, M., Smith, A. G., et al. (2007). Neuroepithelial Cells Supply an Initial Transient Wave of MSC Differentiation. *Cell* 129 (7), 1377–1388. doi:10.1016/j.cell.2007.04.028

Tatullo, M., Marrelli, B., Zullo, M. J., Codispoti, B., Paduano, F., Benincasa, C., et al. (2020). Exosomes from Human Periapical Cyst-MSCs: Theranostic Application in Parkinson's Disease. *Int. J. Med. Sci.* 17 (5), 657–663. doi:10.7150/ijms.41515

Tavangar, M. S., Hosseini, S. M., Dehghani-Nazhvani, A., and Monabati, A. (2017). Role of CD146 Enrichment in Purification of Stem Cells Derived from Dental Pulp Polyp. *Iran Endod. J.* 12 (1), 92–97. doi:10.22037/iej.2017.19

Thesleff, I., and Nieminen, P. (1996). Tooth Morphogenesis and Cell Differentiation. *Curr. Opin. Cel. Biol.* 8 (6), 844–850. doi:10.1016/s0955-0674(96)80086-x

Tziafas, D., and Kodonas, K. (2010). Differentiation Potential of Dental Papilla, Dental Pulp, and Apical Papilla Progenitor Cells. *J. Endodontics* 36 (5), 781–789. doi:10.1016/j.joen.2010.02.006

Uccelli, A., Moretta, L., and Pistoia, V. (2008). Mesenchymal Stem Cells in Health and Disease. *Nat. Rev. Immunol.* 8 (9), 726–736. doi:10.1038/nri2395

Vodyanik, M. A., Yu, J., Zhang, X., Tian, S., Stewart, R., Thomson, J. A., et al. (2010). A Mesoderm-Derived Precursor for Mesenchymal Stem and Endothelial Cells. *Cell Stem Cell* 7 (6), 718–729. doi:10.1016/j.stem.2010.11.011

Wada, N., Gronthos, S., and Bartold, P. M. (2013). Immunomodulatory Effects of Stem Cells. *Periodontol. 2000* 63 (1), 198–216. doi:10.1111/prd.12024

Wang, L., Liu, R., Ye, P., Wong, C., Chen, G.-Y., Zhou, P., et al. (2015). Intracellular CD24 Disrupts the ARF-NPM Interaction and Enables Mutational and Viral Oncogene-Mediated P53 Inactivation. *Nat. Commun.* 6, 5909. doi:10.1038/ncomms6909

Xie, X., Wang, J., Wang, K., Li, C., Zhang, S., Jing, D., et al. (2019). Axin2+-Mesenchymal PDL Cells, Instead of K14+ Epithelial Cells, Play a Key Role in Rapid Cementum Growth. *J. Dent Res.* 98 (11), 1262–1270. doi:10.1177/0022034519871021

Xuan, K., Li, B., Guo, H., Sun, W., Kou, X., He, X., et al. (2018). Deciduous Autologous Tooth Stem Cells Regenerate Dental Pulp after Implantation into Injured Teeth. *Sci. Transl. Med.* 10 (455), eaaf3227. doi:10.1126/scitranslmed.aaf3227

Yamaza, T., Kentaro, A., Chen, C., Liu, Y., Shi, Y., Gronthos, S., et al. (2010). Immunomodulatory Properties of Stem Cells from Human Exfoliated Deciduous Teeth. *Stem Cel Res Ther* 1 (1), 5. doi:10.1186/scrt5

Yang, H., Li, J., Hu, Y., Sun, J., Guo, W., Li, H., et al. (2019). Treated Dentin Matrix Particles Combined with Dental Follicle Cell Sheet Stimulate Periodontal Regeneration. *Dental Mater.* 35 (9), 1238–1253. doi:10.1016/j.dental.2019.05.016

Yang, J. W., Shin, Y. Y., Seo, Y., and Kim, H.-S. (2020). Therapeutic Functions of Stem Cells from Oral Cavity: An Update. *Ijms* 21 (12), 4389. doi:10.3390/ijms21124389

Yang, X., Ma, Y., Guo, W., Yang, B., and Tian, W. (2019). Stem Cells from Human Exfoliated Deciduous Teeth as an Alternative Cell Source in Bio-Root Regeneration. *Theranostics* 9 (9), 2694–2711. doi:10.7150/thno.31801

Yang, X., van den Dolder, J., Walboomers, X. F., Zhang, W., Bian, Z., Fan, M., et al. (2007). The Odontogenic Potential of STRO-1 Sorted Rat Dental Pulp Stem Cellsin Vitro. *J. Tissue Eng. Regen. Med.* 1 (1), 66–73. doi:10.1002/term.16

Yokoyama, T., Yagi Mendoza, H., Tanaka, T., Ii, H., Takano, R., Yaegaki, K., et al. (2019). Regulation of CCl4-Induced Liver Cirrhosis by Hepatically Differentiated Human Dental Pulp Stem Cells. *Hum. Cel.* 32 (2), 125–140. doi:10.1007/s13577-018-00234-0

Yu, H.-M. I., Jerchow, B., Sheu, T.-J., Liu, B., Costantini, F., Puzas, J. E., et al. (2005). The Role of Axin2 in Calvarial Morphogenesis and Craniosynostosis. *Development* 132 (8), 1995–2005. doi:10.1242/dev.01786

Yuan, X., Pei, X., Zhao, Y., Tulu, U. S., Liu, B., and Helms, J. A. (2018). A Wnt-Responsive PDL Population Effectuates Extraction Socket Healing. *J. Dent Res.* 97 (7), 803–809. doi:10.1177/0022034518755719

Zhang, Q., Nguyen, P. D., Shi, S., Burrell, J. C., Xu, Q., Cullen, K. D., et al. (2018). Neural Crest Stem-like Cells Non-genetically Induced from Human Gingiva-Derived Mesenchymal Stem Cells Promote Facial Nerve Regeneration in Rats. *Mol. Neurobiol.* 55 (8), 6965–6983. doi:10.1007/s12035-018-0913-3

Zhang, Q., Shi, S., Liu, Y., Uyanne, J., Shi, Y., Shi, S., et al. (2009). Mesenchymal Stem Cells Derived from Human Gingiva Are Capable of Immunomodulatory Functions and Ameliorate Inflammation-Related Tissue Destruction in Experimental Colitis. *J. Immunol.* 183 (12), 7787–7798. doi:10.4049/jimmunol.0902318

Zhang, W., Walboomers, X. F., Wolke, J. G. C., Bian, Z., Fan, M. W., and Jansen, J. A. (2005). Differentiation Ability of Rat Postnatal Dental Pulp Cellsin Vitro. *Tissue Eng.* 11, 357–368. doi:10.1089/ten.2005.11.357

Zhao, H., Feng, J., Ho, T.-V., Grimes, W., Urata, M., and Chai, Y. (2015). The Suture Provides a Niche for Mesenchymal Stem Cells of Craniofacial Bones. *Nat. Cel Biol* 17 (4), 386–396. doi:10.1038/ncb3139

Zhao, H., Feng, J., Seidel, K., Shi, S., Klein, O., Sharpe, P., et al. (2014). Secretion of Shh by a Neurovascular Bundle Niche Supports Mesenchymal Stem Cell Homeostasis in the Adult Mouse Incisor. *Cell Stem Cell* 14 (2), 160–173. doi:10.1016/j.stem.2013.12.013

Zhao, J., Faure, L., Adameyko, I., and Sharpe, P. T. (2021). Stem Cell Contributions to Cementoblast Differentiation in Healthy Periodontal Ligament and Periodontitis. *Stem Cells* 39 (1), 92–102. doi:10.1002/stem.3288

Conflict of Interest: The authors declare that the research was conducted in the absence of any commercial or financial relationships that could be construed as a potential conflict of interest.

Publisher's Note: All claims expressed in this article are solely those of the authors and do not necessarily represent those of their affiliated organizations, or those of the publisher, the editors, and the reviewers. Any product that may be evaluated in this article, or claim that may be made by its manufacturer, is not guaranteed or endorsed by the publisher.

Frontiers in Physiology

Understanding how an organism's components work together to maintain a healthy state The second most-cited physiology journal, promoting a multidisciplinary approach to the physiology of living systems - from the subcellular and molecular domains to the intact organism and its interaction with the environment.

Discover the latest Research Topics

See more →

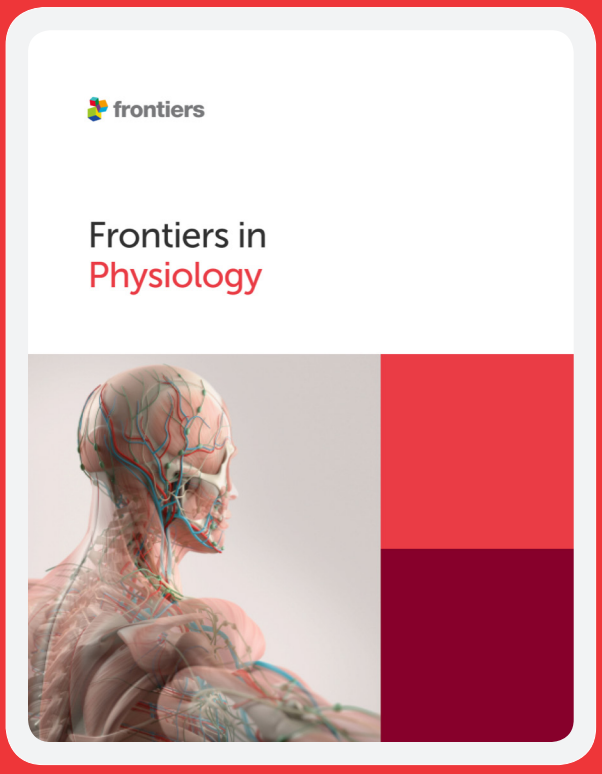

Frontiers

Avenue du Tribunal-Fédéral 34
1005 Lausanne, Switzerland
frontiersin.org

Contact us

+41 (0)21 510 17 00
frontiersin.org/about/contact